frontiers | Research Topics

The endless quest for optimal pacing support in failing hearts

Edited by
Maciej M. Sterlinski and Hans Henrik Odland

Published in
Frontiers in Physiology
Frontiers in Cardiovascular Medicine

ISSN 1664-8714
ISBN 978-2-8325-2252-3
DOI 10.3389/978-2-8325-2252-3

About Frontiers

Frontiers is more than just an open access publisher of scholarly articles: it is a pioneering approach to the world of academia, radically improving the way scholarly research is managed. The grand vision of Frontiers is a world where all people have an equal opportunity to seek, share and generate knowledge. Frontiers provides immediate and permanent online open access to all its publications, but this alone is not enough to realize our grand goals.

Frontiers journal series

The Frontiers journal series is a multi-tier and interdisciplinary set of open-access, online journals, promising a paradigm shift from the current review, selection and dissemination processes in academic publishing. All Frontiers journals are driven by researchers for researchers; therefore, they constitute a service to the scholarly community. At the same time, the *Frontiers journal series* operates on a revolutionary invention, the tiered publishing system, initially addressing specific communities of scholars, and gradually climbing up to broader public understanding, thus serving the interests of the lay society, too.

Dedication to quality

Each Frontiers article is a landmark of the highest quality, thanks to genuinely collaborative interactions between authors and review editors, who include some of the world's best academicians. Research must be certified by peers before entering a stream of knowledge that may eventually reach the public - and shape society; therefore, Frontiers only applies the most rigorous and unbiased reviews. Frontiers revolutionizes research publishing by freely delivering the most outstanding research, evaluated with no bias from both the academic and social point of view. By applying the most advanced information technologies, Frontiers is catapulting scholarly publishing into a new generation.

What are Frontiers Research Topics?

Frontiers Research Topics are very popular trademarks of the *Frontiers journals series*: they are collections of at least ten articles, all centered on a particular subject. With their unique mix of varied contributions from Original Research to Review Articles, Frontiers Research Topics unify the most influential researchers, the latest key findings and historical advances in a hot research area.

Find out more on how to host your own Frontiers Research Topic or contribute to one as an author by contacting the Frontiers editorial office: frontiersin.org/about/contact

The endless quest for optimal pacing support in failing hearts

Topic editors

Maciej M. Sterlinski — National Institute of Cardiology, Poland

Hans Henrik Odland — Oslo University Hospital, Norway

Citation

Sterlinski, M. M., Odland, H. H., eds. (2023). *The endless quest for optimal pacing support in failing hearts*. Lausanne: Frontiers Media SA.

doi: 10.3389/978-2-8325-2252-3

Table of contents

frontiers | Frontiers in Cardiovascular Medicine

ORIGINAL RESEARCH
published: 06 May 2022
doi: 10.3389/fcvm.2022.824194

Short QRS Duration After His-Purkinje Conduction System Pacing Predicts Left Ventricular Complete Reverse Remodeling in Patients With True Left Bundle Branch Block and Heart Failure

Xu-Min Guan†, Dan-Na Li†, Fu-Lu Zhao, Yan-Ni Zhao, Yi-Heng Yang, Bai-Ling Dai, Shi-Yu Dai, Lian-Jun Gao, Yun-Long Xia and Ying-Xue Dong**

Department of Cardiology, The First Affiliated Hospital of Dalian Medical University, Dalian, China

Objective: This study aimed to explore the outcomes of His-Purkinje conduction system pacing (HPCSP) and to screen the predictors of left ventricular (LV) complete reverse remodeling in patients with true left bundle branch block (LBBB) and heart failure with reduced ejection fraction (HFrEF).

Methods: Patients who underwent HPCSP for true LBBB and HFrEF from April 2018 to August 2020 were consecutively enrolled. All participants were followed up for at least 1 year. Thrombosis, infection, lead dislodgement, perforation, and other complications were observed after HPCSP. Clinical data, including echocardiographic parameters, electrocardiogram measurements, and cardiac function, were assessed before and after the procedure.

Results: A total of 46 patients were enrolled. HPCSP was successfully deployed in 42 cases (91.30%), which included 37 cases with His bundle pacing (HBP) and 5 cases with left bundle branch pacing (LBBP). The QRS duration decreased significantly (169.88 ± 19.17 ms vs. 113.67 ± 20.68 ms, $P < 0.001$). Left ventricular end-systolic volume (LVESV) (167.67 ± 73.20 ml vs. 85.97 ± 62.24 ml, $P < 0.001$), left ventricular end-diastolic diameter (LVEDD) (63.57 ± 8.19 mm vs. 55.46 ± 9.63 mm, $P = 0.003$) and left ventricular ejection fraction (LVEF) (26.52 ± 5.60% vs. 41.86 ± 11.56%, $P < 0.001$) improved dramatically. Complete reverse remodeling of the LV with normalized LVEF and LVEDD was found in nearly half of the patients (45.24%). A short QRS duration after HPCSP was a strong predictor of normalized LVEF and LVEDD ($P < 0.001$). The thresholds increased markedly in two patients approximately 6 months after HBP. No patients died during the total follow-up period of 20.07 ± 6.45 months.

Conclusion: Complete reverse remodeling of the LV could be found in nearly half of the patients with HFrEF and true LBBB after HPCSP, and the short QRS duration after HPCSP was a strong predictor.

Keywords: His-Purkinje conduction system pacing, left bundle branch block, heart failure, QRS duration, predictors

OPEN ACCESS

Edited by:
Dragos Cretoiu, Carol Davila University of Medicine and Pharmacy, Romania

Reviewed by:
Hui Li, Anesthesia Center, Fuwai Hospital, Chinese Academy of Medical Sciences and Peking Union Medical College, China
Giuseppe Damiano Sanna, Azienda Ospedaliero Universitaria Sassari, Italy
Xiaohan Fan, Fuwai Hospital, Chinese Academy of Medical Sciences and Peking Union Medical College, China

****Correspondence:***
Yun-Long Xia
yunlong_xia@126.com
Ying-Xue Dong
dlsusan@126.com

† These authors have contributed equally to this work and share first authorship

Specialty section:
This article was submitted to General Cardiovascular Medicine, a section of the journal Frontiers in Cardiovascular Medicine

Received: *29 November 2021*
Accepted: *08 April 2022*
Published: *06 May 2022*

Citation:
Guan XM, Li DN, Zhao FL, Zhao YN, Yang YH, Dai BL, Dai SY, Gao LJ, Xia YL and Dong YX (2022) Short QRS Duration After His-Purkinje Conduction System Pacing Predicts Left Ventricular Complete Reverse Remodeling in Patients With True Left Bundle Branch Block and Heart Failure. Front. Cardiovasc. Med. 9:824194. doi: 10.3389/fcvm.2022.824194

INTRODUCTION

Approximately 30% of patients with heart failure and left ventricular (LV) desynchronization showed no response to cardiac resynchronization therapy (CRT) *via* conventional biventricular pacing (BiVP) (1, 2). A greater response to BiVP was found in patients with true left bundle branch block (LBBB) (3).

Several studies have illustrated that His-Purkinje conduction system pacing (HPCSP), including His bundle pacing (HBP) and left bundle branch pacing (LBBP), could be a better option for CRT (4–8). Singh et al. demonstrated that normalized LVEF was found in 71.43% of patients with LBBB-induced cardiomyopathy after HPCSP (9). How can the proportion of LV complete reverse remodeling with normalized LVEF and LV end-diastolic diameter (LVEDD) be maximized? Obviously, the predictors are still unclear. This study aimed to evaluate the efficacy of the HPCSP and explore the predictors of LV complete reverse remodeling in patients with true LBBB and heart failure with reduced ejection fraction (HFrEF).

MATERIALS AND METHODS

Patient Enrollment and Follow-Up

Patients with true LBBB and HFrEF who underwent HPCSP from April 2018 to August 2020 were consecutively enrolled in our center. The exclusion criteria were recent myocardial infarction or cardiac surgery (<3 months). All patients consented to their treatment, which was approved by the hospital ethics board. LBBP would be the alternative therapy for those patients whose first choice of HBP failed, and BiVP would be the rescue therapy if HPCSP failed. All patients received guideline-directed medical therapy for at least 3 months before implantation.

Regular follow-up was conducted 1, 3, 6, 12, 18, and 24 months after the operation. During the follow-up, the 12-lead electrocardiogram (ECG), echocardiography, postoperative complications, and pacemaker parameters were monitored. The events of thrombosis, infection, lead dislodgement, perforation, stroke, rehospitalization due to heart failure, or death were recorded.

The left ventricular end-systolic volume (LVESV), LVEDD, and left atrial diameter (LAD) were measured following the guidelines of the American Society of Echocardiography. LVEF was measured using the biplane Simpson's method, and the maximum mitral regurgitation (MR) and tricuspid regurgitation (TR) were measured by the vena contracta width with color-flow Doppler.

Criteria and Definition

True LBBB was defined as QRS duration > 140 ms in men (>130 ms in women) and the presence of at least 2 mid-QRS notches or slurs in leads I, aVL, V_1, V_2, V_5, and V_6 (10). An LVEF higher than 50% and an LVEDD less than 50 mm were considered LV complete reverse remodeling.

His bundle pacing usually had two independent capture thresholds, including a His-bundle capture threshold and an LBBB correcting threshold in those patients. An abrupt decrease in the Stim-LV active time (LVAT) of more than 10 ms and the morphologies of Qr, qR, or rSR' in lead V_1 were the simple criteria for left bundle branch capture.

Implantation Procedure and Device Programme

The HBP and LBBP were performed using the Select Secure pacing lead (Model 3830, 69 cm, Medtronic Inc., Minneapolis, MN, United States) and a fixed-curve sheath (C315 HIS, Medtronic Inc., Dublin, Ireland). His bundle electrograms were mapped in a unipolar configuration and recorded in the system (Prucka Cardiolab, GE Healthcare, Waukesha, WI, United States). As described in our previous publications, LBBB correcting thresholds lower than 3.0 V/0.4 ms were accepted (11).

The LBBP was further performed when HBP failed to correct LBBB or when the corrected threshold was above 3.0 V/0.4 ms. The sheath and lead were advanced approximately 1–2 cm from the His bundle region. The unipolar-tip paced QRS configuration and pacing impedance were monitored along with the measurement of peak LV activation times in lead V_5 for LBBP. All patients accepted a CRT defibrillator (D) or CRT pacemaker (P) device according to the guidelines. The leads were then connected to the left atrium (LA), right ventricle (RV), and LV ports. The LV-RV delay was programmed to ensure the shortest QRS duration. The 3,830 lead was connected to the LV port, and the longer interventricular delay was programmed to ensure ventricular activation *via* conduction system pacing.

If HPCSP was unsuccessful, an LV lead was implanted *via* the traditional coronary venous approach. The LV lead was positioned with a standard technique in the lateral or posterolateral LV vein on patients with BiVP if possible. The RV lead was implanted in the right ventricular septum.

Statistical Analysis

Statistical analyses were performed using SPSS 23.0. Continuous variables were expressed as the mean ± SD or median and were compared with independent two-samples, paired *t*-test, or Wilcoxon test. Categorical variables were expressed as numbers (%) and were compared using the Fisher's exact test. Univariate and multivariate analyses were performed using logistic regression to determine the independent predictors of LV complete reverse remodeling after HPCSP. The optimal cutoff of QRS duration was shown on the receiver operator characteristic (ROC) curve with the maximized sensitivity and specificity. $P < 0.05$ (two-tailed) was considered to be statistically significant.

RESULTS

Baseline Patient Characteristics and Clinical Events

A total of 46 patients were enrolled in this study. The HPCSP was successfully deployed in 42 cases (91.30%), which included 37 cases (80.43%) with HBP and 5 cases (10.87%) with LBBP, and the other 4 patients for whom HPCSP failed accepted BiVP. All patients were implanted with CRT defibrillator (D) (30, 65.22%)

or CRT pacemaker (P) devices. All patients were followed up for at least 12 months, and the follow-up duration was 20.07 ± 6.45 months. The LBBB was corrected in all 42 patients after HBCSP with a correcting threshold of 2.13 ± 0.65 V/0.4 ms, and the His-bundle capture threshold was 1.71 ± 0.87.

The baseline characteristics of the patients are shown in **Table 1**. The average age of the patients was 70.21 ± 9.20 years, the average LVEF value was 26.52 ± 5.60%, and the average QRS duration was 169.88 ± 19.17 ms. During the follow-up, one patient was rehospitalized due to heart failure, and no patients died. Complications such as thrombosis, infection, lead dislodgement, perforation, and stroke were not found in any of the patients. The thresholds increased markedly (3.0 V/1.0 ms) in two patients approximately 6 months after HBP, and then the thresholds decreased to 1.5 V/0.4 ms after resetting the lead.

Lead Outcome of His-Purkinje Conduction System Pacing

There was a slight trend of increment in the correct threshold after follow-up in patients with HBCSP (from 2.13 ± 0.65 V/0.4 ms to 2.52 ± 0.42 V/0.4 ms, $P = 0.051$). The impedance decreased slightly after the follow-up (from 621.82 ± 135.80 Ω to 462.46 ± 109.95 Ω, $P = 0.022$). The correct threshold of the LBBB in patients with HPCSP was not different from that in patients with BiVP (2.13 V ± 0.65/0.4 ms vs. 2.36 V ± 0.45/0.4 ms, $P = 0.351$). All the changes are shown in **Table 2**. The pacing percentage at the final follow-up was 95.14 ± 4.17%.

Clinical Outcomes of His-Purkinje Conduction System Pacing

Complete LV reverse remodeling was found in nearly half of the patients (45.24%) approximately 6.03 ± 3.50 months after the operation. Approximately 97.62% of patients responded to HPCSP. The LVEF value was higher than 50% in 23 patients (54.76%) soon after the operation (5.21 ± 3.10 months), and the LVEDD decreased to less than 50 mm in 21 patients (50.00%) approximately 6.84 ± 3.72 months after the operation. The changes in values such as QRS duration, cardiac structure, and cardiac function are shown in **Table 3**. The continuous changes in LVEF, LVESV, and LVEDD after HPCSP are shown in **Figure 1**.

Clinical Features of Patients With Left Ventricular Complete Reverse Remodeling

Univariate analysis showed that a short course of heart failure ($P = 0.022$), small LVESV before HPCSP ($P = 0.008$), and short QRS duration after pacing ($P = 0.003$) were related to LV complete reverse remodeling. Further multivariate regression analysis demonstrated that a short QRS duration was an independent predictor of normalized LVEF and LVEDD in patients with true LBBB and heart failure after HPCSP (OR 0.90, 95% CI: 0.84–0.97, $P = 0.008$), which is shown in **Table 4**. The area under the ROC curve was 0.819. The cutoff point was 107 ms with a sensitivity of 78.3% and a specificity of 77.9%.

TABLE 1 | Baseline characteristics of patients.

	All patients ($n = 42$)
Male (n,%)	22(52.38)
Age (years)	70.21 ± 9.20
Course of heart failure (years)	5.24 ± 3.21
NYHA classification (level)	3.31 ± 0.60
LVEF (%)	26.52 ± 5.60
HBP (n,%)	37(88.10%)
BMI (kg/m2)	25.09 ± 3.47
BNP (ng/L)	438.00(222.50, 1287.50)
Crea (μ mol/L)	72.00(60.00, 89.25)
QRS duration (ms)	169.88 ± 19.17
QRS duration after HPCSP (ms)	113.67 ± 20.68
MR grade	
Mild (n,%)	12(28.6)
Moderate (n,%)	25(59.5)
Severe (n,%)	5(11.9)
TR grade	
Mild (n,%)	7(16.7)
Moderate (n,%)	23(54.8)
Severe (n,%)	12(28.6)
LVESV (ml)	167.67 ± 73.20
LVEDD (mm)	63.57 ± 8.19
LAD (mm)	44.59 ± 4.12
Diabetes mellitus (n,%)	12(28.57)
Hypertension (n,%)	21(50.00)
Chronic kidney disease (n,%)	2(4.76)
Coronary heart disease (n,%)	13(31.0)
Ventricular tachycardia/fibrillation (n,%)	8(19.0)
Atrial fibrillation (n,%)	8(19.0)
β -blockers (n,%)	39(92.9)
ARNI/ACEI/ARB	40(95.2)
Diuretics (n,%)	40(95.2)
Spirolactone (n,%)	39(92.9)
Statins (n,%)	26(61.9)
Aspirin (n,%)	10(23.8)
Nitrates (n,%)	17(40.5)

NYHA, New York Heart Association; LVEF, left ventricular ejection fraction; BMI, body mass index; BNP, B-type natriuretic peptide; MR, mitral regurgitation; TR, tricuspid regurgitation; LVESV, left ventricular end-systolic volume; LVEDD, left ventricular end-diastolic diameter; LAD, left atrial dimension; ARNi, angiotensin receptor-neprilysin inhibitors; ACEI, angiotensin-converting enzyme inhibitors; ARB, angiotensin receptor blockers; HBP, His-bundle pacing.

TABLE 2 | Changes in pacemaker parameters after HPCSP.

Parameters	During operation	Final follow-up	*P*-value
Capture threshold (V/0.4 ms)	1.87 ± 0.84	1.83 ± 0.96	0.895
Correct threshold (V/0.4 ms)	2.13 ± 0.65	2.52 ± 0.42	0.051
Impedance(Ω)	621.82 ± 135.80	462.46 ± 109.95	0.022

DISCUSSION

We proved that HBP and LBBP could dramatically improve heart function, and complete LV reverse remodeling was demonstrated in nearly half of the patients (45.24%) with true CLBBB and

TABLE 3 | Changes in QRS duration, cardiac structure, and cardiac function.

	Baseline	Follow up	*P*-value
QRS duration (ms)	169.88 ± 19.17	113.67 ± 20.68	<0.001
LVEF (%)	26.52 ± 5.60	41.86 ± 11.56	<0.001
LVESV (ml)	167.67 ± 73.20	85.97 ± 62.24	<0.001
LVEDD (mm)	63.57 ± 8.19	55.46 ± 9.63	<0.001
LAD (mm)	44.59 ± 4.12	40.64 ± 4.68	<0.001
MRgrade			
Mild (n,%)	12(28.6)	20(47.6)	0.072
Moderate (n,%)	25(59.5)	18(42.9)	0.127
Severe (n,%)	5(11.9)	4(9.5)	0.724
TR grade			
Mild (n,%)	7(16.7)	23(54.8)	<0.001
Moderate (n,%)	23(54.8)	14(33.3)	0.048
Severe (n,%)	12(28.6)	5(11.9)	0.057
NYHA classification	3.31 ± 0.60	2.33 ± 0.75	<0.001

LVEF, left ventricular ejection fraction; LVESV, left ventricular end-systolic volume; LVEDD, left ventricular end-diastolic diameter; LAD, left atrial dimension; MR, mitral regurgitation; TR, tricuspid regurgitation; NYHA, New York Heart Association.

HFrEF. To the best of our knowledge, this was the first study to demonstrate that a short QRS duration after HPCSP was a strong independent predictor of LV complete reverse remodeling.

Feasibility and Safety of His-Purkinje Conduction System Pacing

Although the report showed that the failure rate of BiVP was only 3.6%, it was unfortunate that the suboptimal position was accepted in approximately 20% of patients, which might impair the performance of CRT (12). We proved that the success rate of permanent HPCSP, including LBBP, reached approximately 90% in this study, which might be related to the combined application of HBP and LBBP (13, 14).

Complications such as thrombosis, infection, lead dislodgement and perforation, and other implant-related events were not found. Recently, Bhatt et al. reported that 8% of 101 patients with successful HBP implantation required electrode adjustment (15). In our study, the thresholds in most patients remained stable, with only two patients undergoing electrode adjustment 6 months after the operation. Consistent with our previous study, this study also demonstrated acceptable and stable thresholds for HBP 1 year after the operation (16).

The distal HBP lead helix, by virtue of being in the septal myocardium, played an important role in the favorable capture threshold and amplitude of the R wave (17). However, the failure of HBP was sometimes shown to be a non-negligible issue (18). For patients with a high threshold or failure of HBP, LBBP worked as a promising alternative for delivering physiological pacing to achieve electrical and mechanical synchrony.

Clinical Performance After His-Purkinje Conduction System Pacing

Although BiVP was effective in reducing desynchronization, it was difficult to achieve complete reverse remodeling for the impaired conduction defect (19). This dilemma was somewhat circumvented with HPCSP (20). A series of publications suggested that HPCSP was a favorable choice for patients with CRT indications (21, 22). Li et al. reported that the response rate and super response rate in heart failure patients with LBBB were 88.9 and 44.4%, respectively, which were greater than those of BiVP (66.7 and 16.7%) (23). We showed that the response ratio was 97.62%, and the LV complete reverse remodeling ratio was 45.24% after HPCSP. For those patients with a CRT indication, would HPCSP be the best choice? We hope that an increasing number of studies will explore this issue in the future.

Huang et al. found that HBP obviously improved LVEF, LVESV, and NYHA classification in 74 patients with heart failure and LBBB (24). In our study, we also found that the LVESV, LVEDD, MR, and TR significantly improved after HPCSP. Furthermore, an improvement in LA remodeling after HPCSP was shown, which might predict the possibility of rhythm management in patients with atrial fibrillation during long-term follow-up.

The dramatic shortening of QRS duration after HPCSP was also demonstrated in our study (169.88 ± 19.17 ms vs. 113.67 ± 20.68 ms, $P < 0.001$). It has been proved that the shortening of QRS duration after HPCSP was more obvious compared to BiVP (mean QRS reduction of 20 ms) (25). But the shortening of QRS duration by LBBP was not as obvious as that by HBP (56 vs. 69 ms, $P = 0.007$) (26). It suggests that we should distinguish LV septal myocardial pacing (LVSP) from HPCSP due to its limited value on LV synchronization

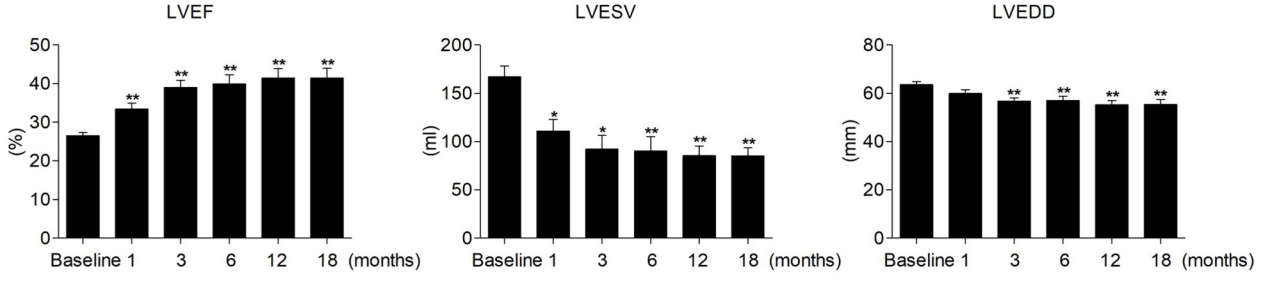

FIGURE 1 | Continuous changes in LVEF, LVESV, and LVEDD after HPCSP. LVEF, left ventricular ejection fraction; LVESV, left ventricular end-systolic volume; LVEDD, left ventricular end-diastolic diameter. *vs baseline $P < 0.05$, **vs baseline $P < 0.001$.

TABLE 4 | Predictors of LV complete reverse remodeling by univariate and multivariate analyses.

	Patients with LV complete reverse-remodeling (*n* = 19)	Patients with LV incomplete reverse-remodeling (*n* = 23)	Univariate			Multivariate		
			P-value	OR	95%CI	*P*-value	OR	95%CI
Male(n,%)	8(42.11)	14(60.87)	0.228					
Age(years)	68.95 ± 8.67	71.26 ± 9.68	0.414					
course of heart failure(years)	3.95 ± 2.89	6.32 ± 3.12	0.022	0.77	0.61–0.96	0.109	0.70	0.45–1.08
NYHA classification(level)	3.37 ± 0.50	3.26 ± 0.69	0.879					
LVEF(%)	27.58 ± 5.84	25.65 ± 5.37	0.267					
HBP (n,%)	(17, 89.47%)	(20, 86.96%)	0.670					
BMI(kg/m2)	25.24 ± 3.86	24.97 ± 3.20	0.810					
BNP(ng/L)	407.50(167.00, 2350.25)	541.00(230.00, 2683.50)	0.391					
Crea(μ mol/L)	71.00(60.21, 94.72)	82.00(62.31, 98.87)	0.697					
QRS duration(ms)	169.89 ± 16.47	169.87 ± 21.51	0.997					
QRS duration after HPCSP(ms)	102.21 ± 16.47	119.48 ± 21.73	0.003	0.94	0.90–0.98	0.008	0.90	0.84–0.97
MR grade			0.094					
Mild (n,%)	7(36.8)	5(21.7)						
Moderate (n,%)	11(57.9)	14(60.9)						
Severe (n,%)	1(5.3)	4(17.4)						
TR grade			0.717					
Mild (n,%)	3(15.8)	4(17.4)						
Moderate (n,%)	10(52.6)	13(56.5)						
Severe (n,%)	6(31.6)	6(26.1)						
LVESV(ml)	126.67 ± 51.38	201.83 ± 72.06	0.008	0.98	0.96–0.99	0.083	0.98	0.96–1.00
LVEDD(mm)	61.53 ± 7.40	65.26 ± 8.59	0.149					
LAD(mm)	43.39 ± 4.41	45.52 ± 3.70	0.109					
Diabetes mellitus (n,%)	7(36.84)	5(21.74)	0.285					
Hypertension (n,%)	11(57.89)	10(43.48)	0.354					
Chronic kidney disease (n,%)	1(5.26)	1(4.35)	1.000					
Coronary heart disease (n,%)	6(31.58)	8(34.78)	0.987					
Ventricular tachycardia/fibrillation (n,%)	3(15.79)	5(21.74)	0.626					
Atrial fibrillation (n,%)	3(15.79)	5(21.74)	0.243					
β -blockers (n,%)	18(94.74)	21(91.30)	0.915					
ARNI/ACEI/ARB	12(63.16)	14(60.87)	0.975					
Diuretics (n,%)	19(100.00)	21(91.30)	1.000					
Spirolactone (n,%)	19(100.00)	20(86.96)	0.999					
Statins (n,%)	11(57.89)	15(65.22)	0.496					
Aspirin (n,%)	4(21.05)	6(26.09)	0.644					
Nitrates (n,%)	6(31.58)	11(47.83)	0.236					

NYHA, New York Heart Association; LVEF, left ventricular ejection fraction; BMI, body mass index; BNP, B-type natriuretic peptide; MR, mitral regurgitation; TR, tricuspid regurgitation; LVESV, left ventricular end-systolic volume; LVEDD, left ventricular end-diastolic diameter; LAD, left atrial dimension; ARNi, angiotensin receptor-neprilysin inhibitors; ACEI, angiotensin-converting enzyme inhibitors; ARB, angiotensin receptor blockers; HBP, His-bundle pacing.

and physiological conduction system pacing (27). One of the differences is that LBBP can be fused with intrinsic RV activation for normal ventricular synchronization, whereas LVSP cannot.

Patient Characteristics of Left Ventricular Complete Reverse Remodeling

Quite different from BiVP, HPCSP completely corrected the LBBB and resulted in super electrical resynchronization. This means that all heart failures originating from LBBB without other heart troubles would be cured. However, approximately 30% of the patients still suffered from heart failure, indicating that some other factor plays a role in LV reverse remodeling.

The course of heart failure was an important factor for LV reverse remodeling (28, 29). Similar to those studies, we also found that a longer course of heart failure was more common in patients with LV incomplete reverse remodeling, even though it was not an independent predictor in our study. This result suggests that the early correction of LBBB might be necessary to halt the progression of the cardiomyopathic process.

Current trials demonstrate that factors such as non-ischemic etiology, QRS duration, and morphology can predict BiVP response (30). It was also found that not all the cardiac complete

reverse remodeling could be detected in patients with corrected LBBB in our study, which indicated that other etiologies might play a role in heart failure in one patient. Some patients' conduction bundle lesions were not located at the proximal end of the trunk, which played a role in the normalized cardiac function. Some patients might be complicated by more myocardial lesions, and some patients might suffer from more scar burden.

One of the reasons for the failure of CRT *via* classical technology might be that too many "true LBBB" cases were contained, which did not meet the strict physiology-based criteria for "true LBBB" after all. It was reasonable to critically evaluate the definition of "true LBBB" and the physiology behind its ECG signature (31). However, QRS shortening plays a central role in the CRT response (32). In our study, we also proved that the short QRS duration after HPCSP was a strong independent predictor of LV complete reverse remodeling. The more synchrony there is after HPCSP, the higher the likelihood of a favorable outcome (33). Whether the difference between HBP and LBBP resulted in different QRS duration and cardiac functions will require further exploration in future studies. QRS duration and morphology reflect the electrical timing and activation sequence of the ventricles; thus, reversal of the electrical pathology indicates a potentially favorable effect of the therapy (34).

Limitations

This was a single-center retrospective study with small sample size. More large-sample and randomized control multicenter studies might be necessary to confirm these results.

CONCLUSION

His-Purkinje conduction system pacing dramatically reversed cardiac remodeling and cardiac function in patients suffering from HFrEF and true LBBB. To the best of our knowledge, this is the first study to prove that a short QRS duration after HPCSP is a powerful predictor of LV complete reverse remodeling after HPCSP.

DATA AVAILABILITY STATEMENT

The original contributions presented in the study are included in the article/supplementary material, further inquiries can be directed to the corresponding authors.

AUTHOR CONTRIBUTIONS

X-MG, D-NL, and F-LZ contributed to the conception and design of the study. F-LZ organized the database. D-NL, Y-NZ, and Y-HY performed the statistical analysis. B-LD and S-YD followed up with the patients. X-MG and D-NL wrote the first draft of the manuscript. L-JG, Y-XD, and Y-LX wrote the sections and proofread the manuscript. All authors contributed to manuscript revision and read and approved the submitted version.

FUNDING

This study was supported by the Scientific and Technological Innovation Foundation of Dalian City (2020JJ26SN055).

ACKNOWLEDGMENTS

We greatly appreciate all of the participants in the study.

REFERENCES

1. Curtis AB. Will His bundle pacing make cardiac resynchronization therapy obsolete? *Circulation.* (2018) 137:1546–8. doi: 10.1161/CIRCULATIONAHA.117.031787
2. Daubert C, Behar N, Martins RP, Mabo P, Leclercq C. Avoiding non-responders to cardiac resynchronization therapy: a practical guide. *Eur Heart J.* (2016) 38:1463. doi: 10.1093/eurheartj/ehw270
3. Perrin MJ, Green MS, Redpath CJ, Nery PB, Keren A, Beanlands RS. Greater response to cardiac resynchronization therapy in patients with true complete left bundle branch block: a PREDICT substudy. *Europace.* (2012) 14:690–5. doi: 10.1093/europace/eur381
4. Wang Z, Wu Y, Zhang J. Cardiac resynchronization therapy in heart failure patients: tough road but clear future. *Heart Fail Rev.* (2021) 26:735–45. doi: 10.1007/s10741-020-10040-2
5. Sharma PS, Dandamudi G, Herweg B, Wilson D, Singh R, Naperkowski A, et al. Permanent His-bundle pacing as an alternative to biventricular pacing for cardiac resynchronization therapy: a multicenter experience. *Heart Rhythm.* (2018) 15:413–20. doi: 10.1016/j.hrthm.2017.10.014
6. Upadhyay GA, Vijayaraman P, Nayak HM, Verma N, Dandamudi G, Sharma PS, et al. His corrective pacing or biventricular pacing for cardiac resynchronization inheart failure. *J Am Coll Cardiol.* (2019) 74:157–9. doi: 10.1016/j.jacc.2019.04.026
7. Barba-Pichardo R, Manovel Sánchez A, Fernández-Gómez JM, Moriña-Vázquez P, Venegas-Gamero J, Herrera-Carranza M. Ventricular resynchronization therapy by direct His-bundle pacing using an internal cardioverter defibrillator. *Europace.* (2013) 15:83–8. doi: 10.1093/europace/eus228
8. Arnold A, Shun-Shin M, Keene D, Howard J, Sohaib S, Wright I, et al. His resynchronization versus biventricular pacing in patients with heart failure and left bundle branch block. *J Am Coll Cardiol.* (2018) 72:3112–22. doi: 10.1016/j.jacc.2018.09.073
9. Singh R, Devabhaktuni S, Ezzeddine F, Simon J, Khaira K, Dandamudi G. His-bundle pacing: a novel treatment for left bundle branch block-mediated cardiomyopathy. *J Cardiovasc Electrophysiol.* (2020) 31:2730–6. doi: 10.1111/jce.14692
10. Strauss DG, Selvester RH, Wagner GS. Defining left bundle branch block in the era of cardiac resynchronization therapy. *Rev Portuguesa De Cardiol.* (2011) 107:927. doi: 10.1016/j.amjcard.2010.11.010
11. Yang Y, Wang K, Ma P, Zhang R, Waleed K, Yin X, et al. His-purkinje system pacing upgrade improve the heart performances in patients suffering from pacing-induced cardiomyopathy with or without permanent atrial fibrillation. *Int J Cardiol.* (2021) 335:47–51. doi: 10.1016/j.ijcard.2021.04.012
12. Gamble J, Herring N, Ginks M, Rajappan K, Bashir Y, Betts T. Procedural Success of left ventricular lead placement for cardiac resynchronization therapy: a meta-analysis. *JACC Clin Electrophysiol.* (2016) 2:69–77. doi: 10.1016/j.jacep.2015.08.009

13. Moriña-Vázquez P, Moraleda-Salas M, Manovel-Sánchez A, Fernández-Gómez J, Arce-Léon Á, Venegas-Gamero J, et al. Early improvement of left ventricular ejection fraction by cardiac resynchronization through His bundle pacing in patients with heart failure. *Europace.* (2020) 22:125–32. doi: 10.1093/europace/euz296
14. Ponnusamy S, Vijayaraman P. Left bundle branch block-induced cardiomyopathy: insights from left bundle branch pacing. *JACC Clin Electrophysiol.* (2021) 7:1155–65. doi: 10.1016/j.jacep.2021.02.004
15. Bhatt A, Musat D, Milstein N, Pimienta J, Flynn L, Sichrovsky T, et al. The Efficacy of His bundle pacing: lessons learned from implementation for the first time at an experienced electrophysiology center. *JACC Clin Electrophysiol.* (2018) 4:1397–406. doi: 10.1016/j.jacep.2018.07.013
16. Ma P, Yang Y, Dai B, Zhang R, Wang N, Li D, et al. Brady-arrhythmias in patients with atrial fibrillation and heart failure of reduced ejection fraction: is his-bundle pacing superior to biventricular pacing? *Pacing Clin Electrophysiol PACE.* (2021) 44:1193–9. doi: 10.1111/pace.14289
17. Muthumala A, Vijayaraman P. Clinical outcomes of His-Purkinje conduction system pacing. *Pacing Clin Electrophysiol PACE.* (2021) 44:5–14. doi: 10.1111/pace.14050
18. Vijayaraman P, Chung M, Dandamudi G, Upadhyay G, Krishnan K, Crossley G, et al. His bundle pacing. *J Am Coll Cardiol.* (2018) 72:927–47.
19. Hawkins N, Petrie M, MacDonald M, Hogg K, McMurray J. Selecting patients for cardiac resynchronization therapy: electrical or mechanical dyssynchrony? *Eur Heart J.* (2006) 27:1270–81. doi: 10.1093/eurheartj/ehi826
20. Vijayaraman P, Bordachar P, Ellenbogen K. The continued search for physiological pacing: where are we now? *J Am Coll Cardiol.* (2017) 69:3099–114. doi: 10.1016/j.jacc.2017.05.005
21. Shan P, Su L, Zhou X, Wu S, Xu L, Xiao F, et al. Beneficial effects of upgrading to His bundle pacing in chronically paced patients with left ventricular ejection fraction <50. *Heart Rhythm.* (2018) 15:405–12. doi: 10.1016/j.hrthm.2017.10.031
22. Upadhyay G, Vijayaraman P, Nayak H, Verma N, Dandamudi G, Sharma P, et al. On-treatment comparison between corrective His bundle pacing and biventricular pacing for cardiac resynchronization: a secondary analysis of the His-SYNC Pilot trial. *Heart Rhythm.* (2019) 16:1797–807. doi: 10.1016/j.hrthm.2019.05.009
23. Li X, Qiu C, Xie R, Ma W, Wang Z, Li H, et al. Left bundle branch area pacing delivery of cardiac resynchronization therapy and comparison with biventricular pacing. *ESC Heart Fail.* (2020) 7:1711–22. doi: 10.1002/ehf2.12731
24. Huang W, Su L, Wu S, Xu L, Xiao F, Zhou X, et al. Long-term outcomes of His bundle pacing in patients with heart failure with left bundle branch block. *Heart.* (2019) 105:137–43. doi: 10.1136/heartjnl-2018-313415
25. Adamson P, Abraham W. Cardiac resynchronization therapy for advanced heart failure. *Curr Treat Options Cardiovasc Med.* (2003) 5:301–9.
26. Wu S, Su L, Vijayaraman P, Zheng R, Cai M, Xu L, et al. Left bundle branch pacing for cardiac resynchronization therapy: nonrandomized on-treatment comparison with His bundle pacing and biventricular pacing. *Can J Cardiol.* (2021) 37:319–28. doi: 10.1016/j.cjca.2020.04.037
27. Huang W, Zhou X, Ellenbogen K. Pursue physiological pacing therapy: A better understanding of left bundle branch pacing and left ventricular septal myocardial pacing. *Heart Rhythm.* (2021) 18:1290–1. doi: 10.1016/j.hrthm.2021.05.013
28. Sze E, Samad Z, Dunning A, Campbell K, Loring Z, Atwater B, et al. Impaired Recovery of left ventricular function in patients with cardiomyopathy and left bundle branch block. *J Am Coll Cardiol.* (2018) 71:306–17. doi: 10.1016/j.jacc.2017.11.020
29. Wang N, Hussain A, Adelstein E, Althouse A, Sharbaugh M, Jain S, et al. Myocardial recovery after cardiac resynchronization therapy in left bundle branch block-associated idiopathic nonischemic cardiomyopathy: A NEOLITH II substudy. *Ann Noninvas Electrocardiol.* (2019) 24:e12603. doi: 10.1111/anec.12603
30. Kandala J, Altman R, Park M, Singh J. Clinical, laboratory, and pacing predictors of CRT response. *J Cardiovasc Transl Res.* (2012) 5:196–212. doi: 10.1007/s12265-012-9352-0
31. Calle S, Kamoen V, De Buyzere M, De Pooter J, Timmermans FA. Strain-based staging classification of left bundle branch block-induced cardiac remodeling. *JACC Cardiovasc Imaging.* (2021) 14:1691–702. doi: 10.1016/j.jcmg.2021.02.019
32. Bazoukis G, Naka K, Alsheikh-Ali A, Tse G, Letsas K, Korantzopoulos P, et al. Association of QRS narrowing with response to cardiac resynchronization therapy-a systematic review and meta-analysis of observational studies. *Heart Fail Rev.* (2020) 25:745–56. doi: 10.1007/s10741-019-09839-5
33. Ajijola O, Upadhyay G, Macias C, Shivkumar K, Tung R. Permanent His-bundle pacing for cardiac resynchronization therapy: Initial feasibility study in lieu of left ventricular lead. *Heart Rhythm.* (2017) 14:1353–61. doi: 10.1016/j.hrthm.2017.04.003
34. Wu S, Cai M, Zheng R, Wang S, Jiang L, Xu L, et al. Impact of QRS morphology on response to conduction system pacing after atrioventricular junction ablation. *ESC Heart Fail.* (2021) 8:1195–203. doi: 10.1002/ehf2.13181

Conflict of Interest: The authors declare that the research was conducted in the absence of any commercial or financial relationships that could be construed as a potential conflict of interest.

frontiers | Frontiers in Cardiovascular Medicine

ORIGINAL RESEARCH
published: 12 May 2022
doi: 10.3389/fcvm.2022.901267

Acute Hemodynamic Effects of Simultaneous and Sequential Multi-Point Pacing in Heart Failure Patients With an Expected Higher Rate of Sub-response to Cardiac Resynchronization Therapy: Results of Multicenter SYNSEQ Study

Maciej Sterliński[1†], *Joanna Zakrzewska-Koperska*[1*†], *Aleksander Maciąg*[2], *Adam Sokal*[3], *Joaquin Osca-Asensi*[4], *Lingwei Wang*[5], *Vasiliki Spyropoulou*[6], *Baerbel Maus*[6], *Francesca Lemme*[6], *Osita Okafor*[7], *Berthold Stegemann*[8], *Richard Cornelussen*[6] *and Francisco Leyva*[8]

[1] *First Department of Arrhythmia, National Institute of Cardiology, Warsaw, Poland,* [2] *Second Department of Arrhythmia, National Institute of Cardiology, Warsaw, Poland,* [3] *Department of Cardiology, Congenital Heart Diseases and Electrotherapy, Silesian Center of Heart Disease, Zabrze, Poland,* [4] *Cardiology Department, University and Polytechnic Hospital la Fe, Valencia, Spain,* [5] *Section of Arrhythmias, Department of Cardiology, Clinical Sciences, Skåne University Hospital, Lund University, Lund, Sweden,* [6] *Bakken Research Center, Medtronic plc, Maastricht, Netherlands,* [7] *Queen Elisabeth Hospital, Birmingham University, Birmingham, United Kingdom,* [8] *Aston Medical School, Aston Medical Research Institute, Aston University, Birmingham, United Kingdom*

OPEN ACCESS

Edited by:
Laurens F. Tops, Leiden University Medical Center, Netherlands

Reviewed by:
Bert Vandenberk, University of Calgary, Canada
Giuseppe Mascia, San Martino Hospital (IRCCS), Italy

***Correspondence:**
Joanna Zakrzewska-Koperska
jzakrzewska@ikard.pl

[†] *These authors have contributed equally to this work and share first authorship*

Specialty section:
This article was submitted to Heart Failure and Transplantation, a section of the journal Frontiers in Cardiovascular Medicine

Received: *21 March 2022*
Accepted: *19 April 2022*
Published: *12 May 2022*

Citation:
Sterliński M, Zakrzewska-Koperska J, Maciąg A, Sokal A, Osca-Asensi J, Wang L, Spyropoulou V, Maus B, Lemme F, Okafor O, Stegemann B, Cornelussen R and Leyva F (2022) Acute Hemodynamic Effects of Simultaneous and Sequential Multi-Point Pacing in Heart Failure Patients With an Expected Higher Rate of Sub-response to Cardiac Resynchronization Therapy: Results of Multicenter SYNSEQ Study. Front. Cardiovasc. Med. 9:901267. doi: 10.3389/fcvm.2022.901267

The aim of the SYNSEQ (Left Ventricular Synchronous vs. Sequential MultiSpot Pacing for CRT) study was to evaluate the acute hemodynamic response (AHR) of simultaneous (3P-MPP $_{syn}$) or sequential (3P-MPP $_{seq}$) multi-3-point-left-ventricular (LV) pacing vs. single point pacing (SPP) in a group of patients at risk of a suboptimal response to cardiac resynchronization therapy (CRT). Twenty five patients with myocardial scar or QRS $\leq$ 150 or the absence of LBBB (age: 66 $\pm$ 12 years, QRS: 159 $\pm$ 12 ms, NYHA class II/III, LVEF $\leq$ 35%) underwent acute hemodynamic assessment by LV + dP/dt$_{max}$ with a variety of LV pacing configurations at an optimized AV delay. The change in LV + dP/dt $_{max}$ (%ΔLV + dP/dt $_{max}$) with 3P-MPP $_{syn}$ (15.6%, 95% CI: 8.8%-22.5%) was neither statistically significantly different to 3P-MPP $_{seq}$ (11.8%, 95% CI: 7.6-16.0%) nor to SPP $_{basal}$ (11.5%, 95% CI:7.1-15.9%) or SPP $_{mid}$ (12.2%, 95% CI:7.9-16.5%), but higher than SPP $_{apical}$ (10.6%, 95% CI:5.3-15.9%, $p = 0.03$). AHR (defined as a %ΔLV + dP/dt $_{max}$ $\geq$ 10%) varied between pacing configurations: 36% (9/25) for SPP $_{apical}$, 44% (11/25) for SPP $_{basal}$, 54% (13/24) for SPP $_{mid}$, 56% (14/25) for 3P-MPP $_{syn}$ and 48% (11/23) for 3P-MPP $_{seq.Fifteen}$ patients (15/25, 60%) had an AHR in at least one pacing configuration. AHR was observed in 10/13 (77%) patients with a LBBB but only in 5/12 (42%) patients with a non-LBBB ($p = 0.11$). To conclude, simultaneous or sequential multipoint pacing

compared to single point pacing did not improve the acute hemodynamic effect in a suboptimal CRT response population.

Clinical Trial Registration: ClinicalTrials.gov, identifier: NCT02914457.

Keywords: heart failure, biventricular pacing, quadripolar lead for left ventricle pacing, multipoint pacing, acute hemodynamic effect, cardiac resynchronization therapy

INTRODUCTION

Cardiac resynchronization therapy (CRT) has transformed the treatment of patients with heart failure, impaired left ventricular (LV) function and a wide QRS complex (1). It is well accepted, however, that the response to CRT delivered using bipolar and unipolar leads is variable. Quadripolar LV leads are associated with higher implant success rates, lower rates of re-interventions for LV lead displacement or phrenic nerve stimulation (2–4) and better clinical outcomes (3, 4).

Intuitively, the wide LV activation front provided by simultaneous, multipoint pacing (MPP_{syn}) could achieve a more rapid and uniform LV activation than single point pacing (SPP). A better acute hemodynamic response (AHR) to CRT with MPP compared to SPP has been reported by some studies (5, 6), but not others (7, 8). It has also been shown that MPP confers a better LV reverse remodeling response to CRT compared to SPP (9). With respect to clinical outcomes, some studies showed a superiority of MPP over SPP (2), but this was not supported by a recent randomized, controlled trial (10). Physiologically, sequential MPP from apex to base (MPP_{seq}) could also provide a physiological pattern of LV activation (11, 12). In this respect, a favorable response to CRT delivered using apical LV pacing is consistent with the notion that CRT, delivered using LV sequential activation from apex to base may be more physiological and therefore, more advantageous (13–15).

Response to CRT still raises many questions and there is a large population of subjects in which CRT brings moderate or even no benefit (16). Ischemic cardiomyopathy (17, 18), a relatively narrow QRS complex (19) and an non-LBBB morphology are associated with a higher risk of incomplete or poor/absent clinical improvement due to CRT ("sub-response") (20). In this experimental, interventional study, we compare the acute hemodynamic effect in presumed sub-responders to CRT delivered using SPP as well as 3-point, simultaneous (3P-MPP_{syn}) or sequential (3P-MPP_{seq}) MPP pacing. Recent data show that acute hemodynamic response measured by LV dP/dtmax is correlated with better clinical outcome and reverse remodeling, expressed as reduction of LVESV and LVEF improvement (21). Therefore, our work is part of the search for more effective resynchronizing stimulation techniques in a "sub-response" group. At the same time it offers new perspectives on this topic.

METHODS

Study Design

The SYNSEQ (Left Ventricular Synchronous versus Sequential MultiSpot Pacing for CRT) study (NCT02914457) was an acute hemodynamic study with prospective enrolment, conducted across five European centers. All patients provided written informed consent. The study was approved by the Local Ethics Committees and complied with the Declaration of Helsinki.

Study Population

LBBB morphology on ECG was defined using the Strauss criteria (22). Patients diagnosed with LBBB with QRS $>$ 150 ms together with absence of scar or patients having pure RBBB were not allowed in the study. Deviations from the above morphology in more than two surface ECG leads were classified as non-LBBB. ECG morphology was assessed independently by two blinded investigators. The etiology of heart failure was confirmed on basis of clinical history, and the echocardiographic examination. In addition, transmural/subendocardial myocardial scar was accessed by late-gadolinium enhancement cardiac magnetic resonance (23). All inclusion and exclusion criteria are listed in **Table 1**. This specific population was chosen based upon the (a) the relatively low-response acutely and chronic and therefore represent an opportunity for an experimental LV stimulation model, and (b) that typical-LBBB patients with relatively wide QRS and no scar do in general respond very well to conventional CRT-therapy.

Lead Implantation

This was undertaken using standard transvenous techniques with cephalic, axillary or subclavian access. Right atrial and right ventricular leads were first deployed into typical locations (preferred right atrium appendage if possibly and right ventricular apex or low septum, respectively), followed by deployment of a quadripolar LV lead within the vein chosen by implanters, who were instructed to deploy the LV lead tip as apical as possible within the vein of choice (an example of lead placement is shown in **Figure 1**). If the apex could not be reached with a transvenous LV lead, a 0.14" pacing wire (VisionWire, Biotronik, Berlin) was used for apical pacing. Apical position was defined by 30° RAO fluoroscopy as the lowest quartile in the longitudinal direction and was achieved in 100% of the patients. Acceptable LV lead position was either lateral or posterolateral (**Figure 1**).

Lead Positions

Anteroposterior, left anterior oblique (30°) and right anterior oblique (30°) fluoroscopic views were used to localize lead positions, as previously described (12). Briefly, the position of pacing poles was determined by measuring the distance from the coronary sinus to the apex, using 30° right anterior oblique fluoroscopic view. The circumferential position over the LV free wall was determined using the o'clock method, assuming that the anterior interventricular vein was at a 12 o'clock position and

the inferior vein at a 6 o'clock position. Thus, the LV pacing pole position (basal, mid, and apical) refers to the subtended myocardial segments, rather than the position of the pacing poles on the lead.

Pacing Protocol

The acute hemodynamic study was undertaken during implantation of a CRT device. The CRT implantation was performed as per standard practice after completion of the acute study. Four external pacemakers (Medtronic Model 5388, Medtronic, MN), synchronized by a central master pacemaker (Analyzer Medtronic 2290, Medtronic, MN) and a custom-made switch box, were used for each pacing site to ensure capture. The atrial channel of the central master was used for right atrial pacing. Throughout the acute study, cardiac electrograms, surface ECGs, invasive arterial blood pressure (femoral artery) and LV pressure (MicroCath Millar instruments, TX, USA) were acquired with a 32-channel recording system (Porti TMSi, Oldenzaal, Netherlands) and recorded on a laptop computer using customized software. Beat-to-beat raw signals were visualized and checked in real time to ensure appropriate signal quality and to confirm capture. Experimental lead configurations and atrioventricular (AV) delay settings were digitally annotated for off-line analysis.

The reference for calculation of $\%\Delta LV + dP/dt_{max}$ was AAI pacing 10 bpm above the intrinsic rate. For AV optimization, LV $+ dP/dt_{max}$ was measured at five different AV delays, namely the AV delay determined by the CardioSync algorithm (Medtronic, MN) and AV delays of ± 30 and ± 60 ms around this AV delay. All measurements were repeated 4 times over 20 beats for each pacing configuration and AV delay, interspersed with AAI pacing, to minimize sampling error (24). The inter-ventricular (VV) pacing delay was set to zero for all configurations except for the 3-P MPP_{seq} (VV-delay = 20ms between LV_{apex} and LV_{mid} and between LV_{mid} and LV_{basal}). The tested LV pacing configurations were RV and SPP_{apex}, RV and SPP_{mid}, RV and SPP_{basal}, RV and 3P-MPP_{syn}, RV and MPP_{seq}. For analysis, up to eight beats prior and eight beats immediately after each pacing change from a pacing configuration to AAI pacing were used to calculate percentage change in LV $+ dP/dt_{max}$.

TABLE 1 | Study inclusion and exclusion criteria.

Inclusion criteria	Exclusion criteria
CRT indication according to the present ESC/AHA guidelines and: a. Presence of myocardial scar or b. QRS duration $\leq$ 150 ms or c. Non-LBBB • Sinus rhythm • Oral optimal medical treatment • Voluntary participation in the study and signing of informed consent • $\geq$18 year old	• Permanent atrial fibrillation/flutter or other supraventricular tachycardia • Pure right bundle branch block (with no additional left ventricular conduction delays) • Myocardial infarction or valve surgery within 40 or, respectively, 90 days prior to enrollment • Severe aortic stenosis with area < 1.0 cm^2 or significant valve disease expected to be operated within the study period • Mechanical heart valves • Congenital heart disease • HT or active on the transplantation list • LVAD • Severe renal disease (up to physician's discretion) • Continuous or uninterrupted infusion (inotropic) therapy for heart failure ($\geq$2 stable infusions per week) • Pregnant or breastfeeding woman • Participation in another study that confound the results of this study, without documented pre-approval.

LBBB, left bundle branch block; non-LBBB, deviations from the LBBB morphology, according the Strauss criteria, in more than two surface ECG leads; MRI, Magnetic Resonance Imaging; LVAD, left ventricular assist device; HT, heart transplant.

Hemodynamic Endpoint

Acute hemodynamic effect (AHE) was assessed as the percentage change in LV $+ dP/dt_{max}$ ($\%\Delta LV + dP/dt_{max}$) from pacing on to pacing off (AAI). The acute hemodynamic response (AHR) was defined as $\geq$10% increase in the acute hemodynamic effect ($\%\Delta LV + dP/dt_{max}$).

Data Analysis

Beat-to-beat LV intraventricular pressure, 12 lead surface ECG and endocardial (RA, RV, and LV) electrograms were acquired simultaneously using a 32-channel physiological recording

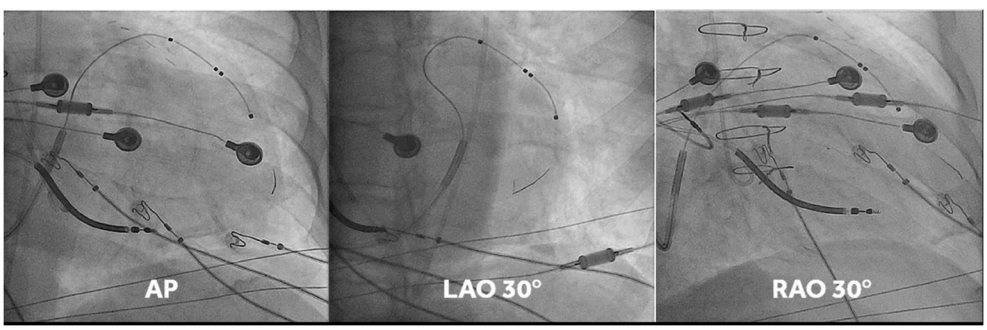

FIGURE 1 | Fluoro-images at AP, LAO 30° and RAO 30° displaying position of the different CRT leads. Note that in this case the vision wire administered through the lumen of the quadripolar was used to obtain true apical position. MPP was delivered on the vision wire, and on the distal and most proximal electrodes of the short bipole of the quadripolar lead.

system (Porti, TMSi, Twente, The Netherlands). Data analysis was undertaken offline. The Raschlab v0.3.0 software package (Raphael Schneider, Medtronic Inc.) was used for data review and annotation. Non-captured beats and ventricular ectopic beats plus the subsequent two beats were identified visually and excluded from further analyses. The dataset was then converted to Matlab (The Mathworks Inc., Massachusetts) compatible format for further analysis.

The AHE for each configuration was calculated with the median LV + dP/dt_{max} for up to eight cardiac beats before and after the experimental transition from pacing on to pacing off. We then calculated ΔLV + dP/dt_{max} for each of the eight transitions.

The paced QRS duration was measured from the ventricular pacing spike to the end of the QRS complex in surface ECGs. The Q-LV interval was defined as the interval from the onset of the intrinsic QRS on the surface ECG to the first large positive or negative peak of the LV electrogram. Q-LV-timing data are expressed as Q-LV/QRS. The electrical delay from RV or LV pacing spike to the different LV activations was also measured.

Statistical Analysis

Statistical analysis was performed using SAS 9.4 (SAS Institute, Cary, NC) and R (versions up to 3.6.1). Primary objectives: For comparison between pacing configurations, the following approach was performed. Firstly, the maximal average %ΔLV + dP/dt_{max} was calculated for each subject and each configuration by a regression analysis constructing a quadratic curve through all AV-delays (25, 26). Secondly, two-sided (except for non-inferiority which is one-sided per definition) weighted paired *t*-tests were performed to compare the pacing configurations to each other. Subjects were inversely weighted per comparison based on the model estimated variability of their maximal average %ΔLV + dP/dt_{max} for the compared configurations. Sensitivity analyses were performed comparing analysis results between a non-parametric Wilcoxon signed-rank test, unweighted *t*-test and weighted *t*-test. Two-tailed *p*-values smaller than 0.05 and one-tailed *p*-values smaller than 0.025 were considered significant. *P*-values are presented as two-sided unless indicated otherwise. For the comparison between 3P-MPP_{seq} and 3P-MPP_{syn}, non-inferiority testing was performed using a margin of −3% and a significance level of 0.025. If non-inferiority testing was significant, a test for superiority at a significance level of 0.05 was performed. Categorical variables were compared using Fisher's exact test. Binomial sample proportions were compared to expected percentages using a one-sided Wald test to see whether one configuration was more often the best one than would be expected by chance. Secondary objectives: Linear multiple regression analysis was used to assess correlation between %ΔLV + dP/dt_{max} and Q-LV/QRS ratio or ΔQRS duration.

Continuous variables are expressed as mean ± SD (unless indicated otherwise). No correction for multiple testing was performed because of the exploratory nature of this study.

RESULTS

Thirty-one patients were enrolled in the study. Complete datasets were available for analysis for 25 patients (study flowchart is shown in **Figure 2**). For comparison of typical LBBB vs. non-LBBB the groups size was only 13 and 12 patients, respectively,

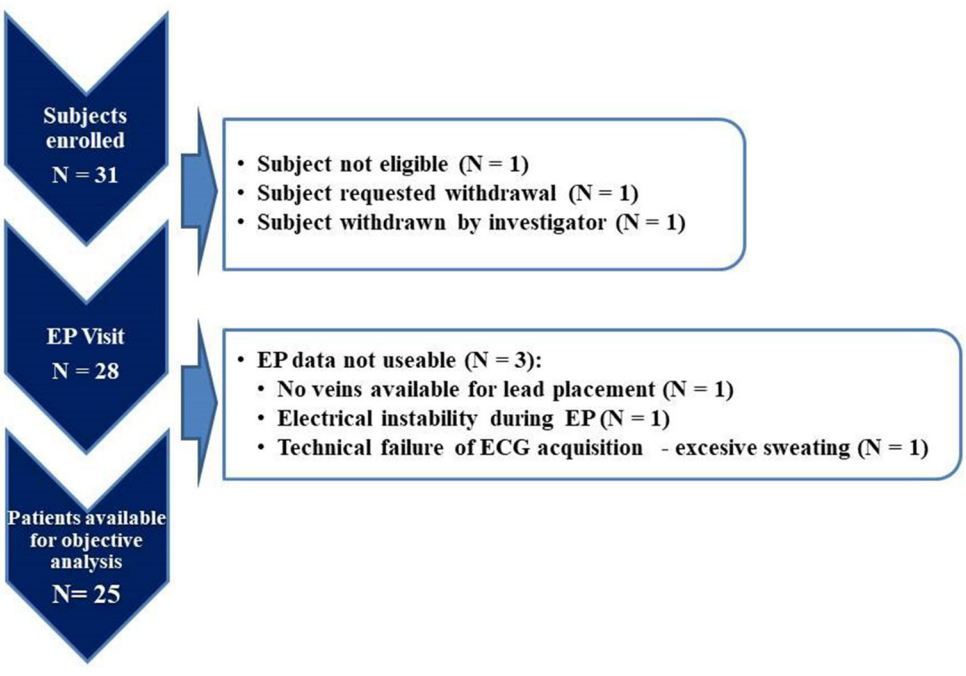

FIGURE 2 | SYNSEQ study flowchart.

indicating only a proof-of-principle (see also Limitations in the Discussion).

Baseline Characteristics of Patients With Complete Datasets

There were 25 subjects, (age: 66 ± 12 yrs [mean ± SD], 80% male), 12 of whom (12/25, 48%) showed no typical LBBB pattern on ECG. Twenty patients presented with myocardial scar (20/25, 80%), and 10 had a QRS-duration ≤ 150 (10/25, 40%). Patients received maximally tolerated pharmacological therapy for heart failure prior to the CRT implant. Patients' demographics are summarized in **Table 2**. No arrhythmias were induced during any of the pacing protocols. Data on the duration of the electrophysiological measurements determined by the protocol are included in **Supplementary Table 1**.

Effect of Simultaneous and Sequential Pacing Configurations

We observed an increase in %ΔLV + dP/dt_{max} for all pacing configurations at the optimized AV delay: 3P-MPP_{syn} (15.6%, 95% CI: 8.8-22.5%), 3P-MPP_{seq} (11.8%, 95% CI: 7.6-16.0%), SPP_{basal} (11.5%, 95% CI: 7.1-15.9%), SPP_{mid} (12.2%, 95% CI: 7.9-16.5%), and SPP_{apical} (10.6%, 95% CI: 5.3-15.9%). Comparisons between 3P-MPP_{syn} and SPP configurations, 3PP-MPP_{seq} and SPP configurations as well as between 3P-MPP_{syn} and 3P-MPP_{seq} based on the weighted within-patient differences were not statistically significant except for comparison between 3P-MPP_{syn} and SPP_{apical} (3.2%, 95% CI: 0.3-6.0%, $p = 0.03$) as well as 3P-MPP_{seq} and SPP_{apical} (3.3%, 95% CI: 0.3-6.4%, $p = 0.04$) (%ΔLV + $dPdt_{max}$ boxplot at best AV-delay is shown in **Figure 3**). The sensitivity analysis seemed to indicate that different results between weighted *t*-test, unweighted *t*-test and Wilcoxon signed-rank test were mainly due to the weighting of individual subjects rather than strong violation of the assumption of normality for the *t*-tests.

Fifteen patients (15/25; 60%) showed an acute hemodynamic response in at least one pacing configuration. Acute hemodynamic responder rates (i.e., AHR) varied between pacing configurations: 36% (9/25) for SPP_{apical}, 44% (11/25) for SPP_{basal}, 54% (13/24) for SPP_{mid}, 56% (14/25) for 3P-MPP_{syn} and 48% (11/23) for 3P-$MPP_{seq.}$ Overall, AHR was similar for MPP configurations and SPP configurations.

TABLE 2 | Characteristics of the study group.

Subjects characteristics	All (*N* = 25)	LBBB (*N* = 13)	Non-LBBB (*N* = 12)
Sex (male), *n* (%)	20 (80.0%)	9 (69.2%)	11 (91.7%)
Age, years	66.2 (11.9)	64.8 (14.1)	67.7 (9.5)
NYHA class II, *n* (%)	12 (48.0%)	7 (53.8%)	5 (41.7%)
NYHA class III, *n* (%)	13 (52.0%)	6 (46.2%)	7 (58.3%)
LVEF, %	26.0 (5.0)	27.4 (5.2)	24.4 (4.4)
Myocardial infarction, *n* (%)	17 (68.0%)	7 (53.8%)	10 (83.3%)
Scar (LGE), *n* (%)*	20 (80.0%)	11 (84.6%)	9 (75.0%)
Comorbidity, *n* (%)			
Diabetes	9 (36.0%)	3 (23.1%)	6 (50.0%)
Hypertension	17 (68.0%)	7 (53.8%)	10 (83.3%)
CABG	6 (24.0%)	2 (15.4%)	4 (33.3%)
ECG variables			
PR interval, ms	190.2 (32.9)	191.7 (37.4)	188.5 (28.8)
QRS duration, ms	158.7 (11.9)	160.0 (9.8)	157.3 (14.2)
Medications, *n* (%)			
Diuretics	20 (80.0%)	10 (76.9%)	10 (83.3%)
ACEIs/ARBs	22 (88.0%)	11 (84.6%)	11 (91.7%)
Beta-blockers	23 (92.0%)	11 (84.6%)	12 (100.0%)
Aldosterone antagonists	24 (96.0%)	12 (92.3%)	12 (100.0%)

**Two Non-LBBB subjects did not have MRI scan performed.*

Effect of LBBB Morphology

Patients had a mean QRS-duration of 158.7 ± 11.9 ms, and 52% (13/25) of patients presented with typical LBBB pattern on ECG. As shown in **Figure 4**, the acute hemodynamic effect (%ΔLV + dP/dt_{max}) trended higher for all pacing configuration in patients with a LBBB. The AHR in at least one pacing configuration was (77%, 10/13) for patients with a typical LBBB compared to patients with a non-LBBB (42%, 5/12) ($p = 0.11$).

Effect of QRS Duration

Percentage change QRS duration (%ΔQRS duration) increased by 3-9% for most pacing configurations [SPP_{basal} (4.9% ± 16.5), SPP_{mid} (3.2 ± 14.9%), SPP_{apical} (8.7% ± 18.0), and MPP_{seq} (8.5% ± 19.7)], but decreased by 4.3% with 3P-MPP_{syn} (−4.3% ± 14.3). No significant correlation emerged between %ΔQRS duration and %ΔLV + dP/dt_{max} ($N = 24$, $\rho = -0.28$, 95% CI: −0.44-0.10).

Effect of QLV-Delay

The Q-LV/QRS timings ranged from 0.46 ± 0.21 on the apical electrode to 0.55 ± 0.23 and 0.56 ± 0.24 on the mid and basal electrode, respectively. No significant correlation was found between the Q-LV/QRS ratio and the acute hemodynamic effect (%ΔLV + dP/dt_{max}) for the whole study group with available data ($N = 20$, $\rho = 0.20$, 95% CI: −0.06-0.44). However, Q-LV/QRS ratio correlated more strongly with %ΔLV + dP/dt_{max} for patients with non-LBBB ($N = 9$, $\rho = 0.41$, 95% CI: 0.04-0.69), but not with LBBB. Q-LV/QRS ratio correlation with %ΔLV + dP/dt_{max} was lower ($N = 11$, $\rho = 0.03$, 95% CI: −0.33-0.37, $p = 0.13$) in LBBB patients for all LV electrodes.

DISCUSSION

The current study was designed to search for potential solutions to increase the effectiveness of CRT, in a group of patients initially at risk of non- or sub-response. Factors affecting suboptimal or even non-response phenomenon are well known and have been previously described (27). They have been listed in **Supplementary Table 2**. Nevertheless current expert opinions (28, 29) indicate that majority of those factors might be easily modifiable and managed by systematic and methodological algorithms of care. LV lead location and LV pacing modes

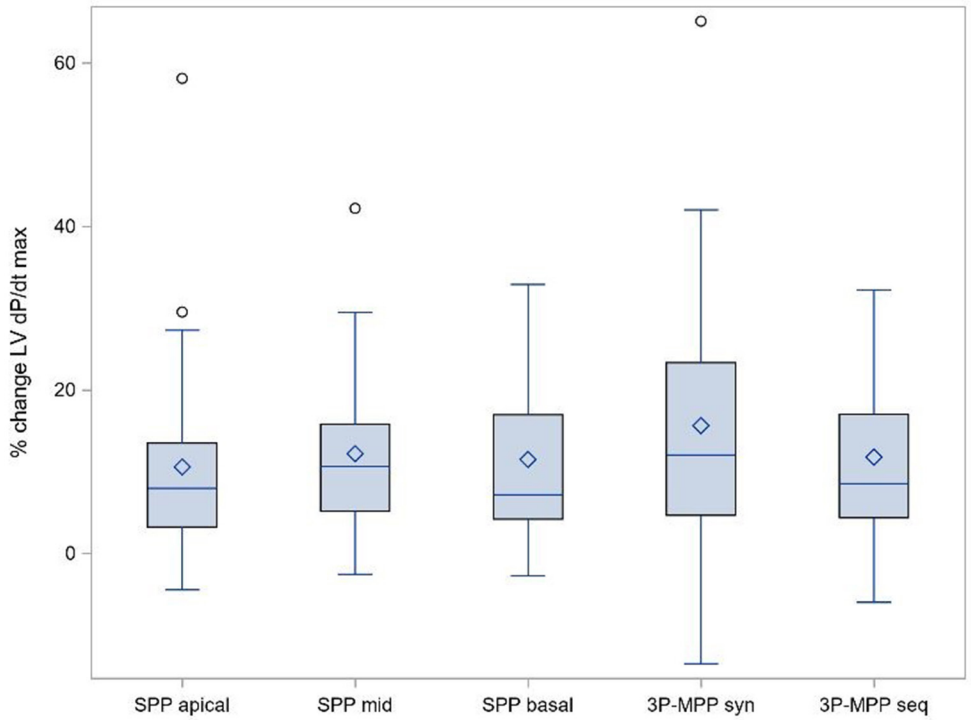

FIGURE 3 | Primary objective: % ΔLV + $dPdt_{max}$ boxplot at best AV-delay. SPP, RV-LV Single-point pacing and MPP, RV-LV Multi-point pacing. MPP_{seq}, Sequential MPP; MPP_{syn}, Synchronous (simultaneous) MPP; $SPP_{basal,mid,apical}$, SPP from base, mid, apical LV electrode. Solid line depicts the median value, and boxes are 25th and 75th percentile. Whiskers represent the most extreme data point within 1.5x interquartile range from the boxes. Diamonds represent mean value, and dots are outliers.

and types—in case of inadequate dyssynchrony correction—remain one of main reason of non-satisfying response and are challenging.

In this acute hemodynamic study, we explored whether CRT, delivered using 3P-MPP_{syn} or 3P-MPP_{seq} is superior to SPP in patients who are likely sub-responders using low-variance measurement of the acute hemodynamic response (8, 30). Several findings have emerged. **First**, 3P-MPP_{syn} and 3P-MPP_{seq} were not superior to SPP. **Second**, a trend toward an AHR in at least one pacing configuration was observed in patients with a typical LBBB morphology, but in less than half of patients without.

Acute Hemodynamic Response

The AHR rate for our population of patients with myocardial scar, or QRS $\leq$ 150 or the absence of LBBB was indeed low (∼44%). This was considerably lower than the response rate of 96% (23/24) observed in the iSPOT study [in patients with CRT indication and presence of LBBB using the 4 pacing configurations and otherwise a completely comparable protocol: (8)]. Our study confirms the necessity for tailored patient selection for CRT and multipoint LV pacing as proposed by authors (15).

The range of the hemodynamic effect within an individual patient is large (data shown in **Supplementary Figure 1**). In this study this is especially obvious because of the small standard error for each individual patient configuration, as enforced by the specific measurement protocol applied. This allows within patient assessment, which would otherwise not be possible. In 40% of the patients we find no response (%ΔLV + dP/dt_{max} < 10%) for any configuration (*consistent hemodynamic non-responders*). In 24% patients we find an acute hemodynamic response (%ΔLV + dP/dt_{max} $\geq$ 10%) independent of the configuration (*consistent hemodynamic responders*). And finally, in the remaining 36% patients we find an acute hemodynamic response only in some of the tested configurations. This last group is clinically the most relevant one, as choosing the right configuration will make the difference between acute hemodynamic response and non-response and thus result in reversed remodeling of LV and long-term patient benefit (31). However, identifying the LV lead position to obtain the maximal possible hemodynamic effect is beyond today's clinical practice, and new non-invasive approaches are clinically needed. QLV/QRSd was not strongly associated with acute hemodynamic response at group level (32). Optimization of the pacing configuration of CRT (with a quadripolar LV lead) is best to rely on functional assessment of cardiac function, instead of local electric delay (32).

Multi-Point Pacing

In the present study, 3P-MPP_{syn} was the optimal configuration in 36% of all patients which was almost statistically significantly higher than the value of 20% expected by chance (one sided

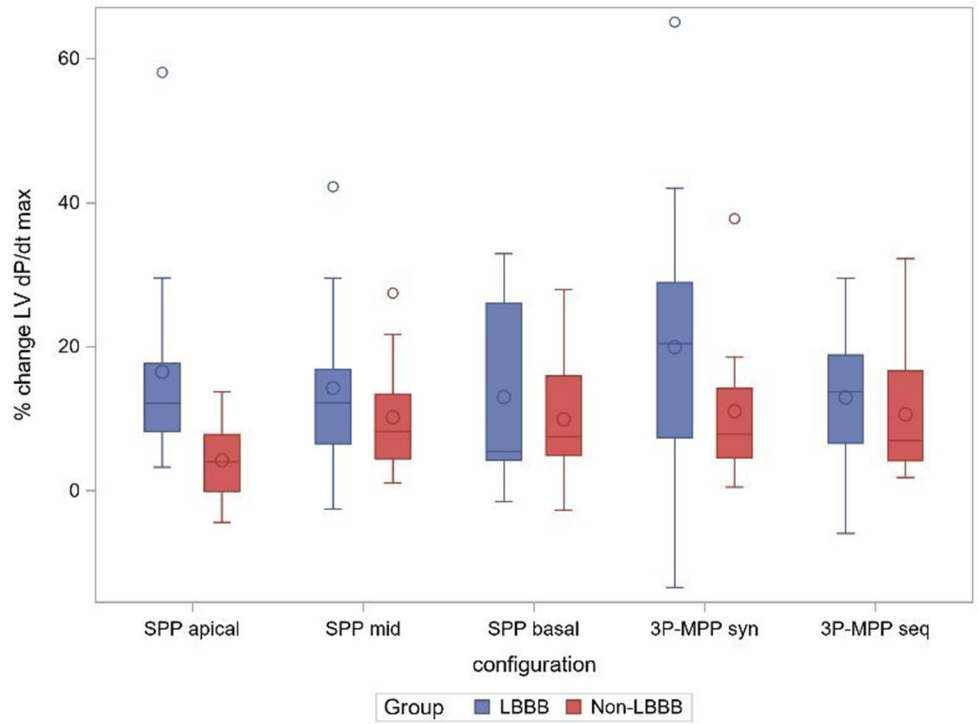

FIGURE 4 | % change ΔLV + $dPdt_{max}$ boxplot at best AV-delay in the subgroups LBBB and non-LBBB. SPP, RV-LV Single-point pacing and MPP, RV-LV Multi-point pacing. MPP_{seq}, Sequential MPP; MPP_{syn}, Synchronous (simultaneous) MPP; $SPP_{basal,mid,apical}$, SPP from base, mid, apical LV electrode. Solid line depicts the median value, and boxes are 25th and 75th percentile. Whiskers represent the most extreme data point within 1.5x interquartile range from the boxes. Diamonds represent mean value, and dots are outliers.

p-value = 0.03). At the same time 3P-MPP_{syn} demonstrated the highest acute hemodynamic benefit. Moreover, 3P-MPP_{syn} was the optimal configuration in 47% of those 15 patients who demonstrated an AHR in at least one configuration which was significantly higher than the proportion 21% expected by chance (one sided *p*-value $p < 0.01$). This indicates that MPP appears to consistently display better hemodynamic response.

In an pressure-volume loop study of 44 patients, Pappone et al. (6) showed that the best MPP vector configuration was associated with a greater ΔLV + dP/dt_{max}, stroke work, stroke volume and LVEF, compared with the best SPP vector configuration. Thibault et al. also showed that MPP_{syn} was associated with a higher ΔLV + dP/dt_{max} than AAI pacing and that MPP was superior to SPP in 72% patients (33). These data however, maybe confounded by their experimental setup favoring positive outcomes in MPP attributed to multiple MPP configurations vs. one BiV setting using the distal electrode.

In the present study, 3P-MPP_{seq} was the optimal configuration in 28% of all patients which was not significantly higher than the value of 20% expected by chance (one sided $p = 0.17$). 3P-MPP_{seq} had similar mean AHE as SPP_{mid} and SPP_{basal}. An acute hemodynamic effect emerged compared to SPP-apical, which must however be attributed to the relatively lesser effect of SPP-apical stimulation. In normal sinus rhythm, electrical impulses travel through the rapid conduction system from the His bundle toward the apex. Thereafter, LV activation spreads from apex to base as impulses exit the Purkinje system into the slower-conducting working myocardium (34). Accordingly, pacing at the apex would thus be expected to provide a physiological sequence of activation. Indeed, computer-modeling studies suggest that LV pacing guided by what is closest to normal activation is superior to pacing the latest activated region (35). In canine LBBB models, the highest hemodynamic response to CRT is observed with LV apical positions, rather than with basal and mid positions (36). This is consistent with our previous publication of a better hemodynamic response from LV apical pacing compared to basal LV pacing in patients with ischemic cardiomyopathy and a LBBB (37). Kandala et al. (38) showed that in patients with a LBBB a longer Q-LV in apically positioned LV leads was associated with more favorable LV reverse remodeling and better outcomes, compared to apically positioned LV leads with shorter Q-LV. Lercher et al. showed that a greater AHE (%ΔLV + dP/dt_{max}) could be achieved by synchronizing pacing to the earliest activated segment (39). They found that the AHR (i.e., change in systolic blood pressure) was highest when pacing from with distal to basal poles. Together, these findings suggest that mimicking physiological activation by using interpole electrical separation, from apex to base, could be beneficial. In the present study, however, no advantage of 3P-MPP_{seq} was observed.

Collectively the two MPP configurations achieved the highest acute hemodynamic response in 16/25 (64%) patients which was significantly higher than the value (39.2%) expected by chance (one sided $p < 0.01$).

LBBB Morphology

Sub-analyses of both REVERSE (40) and MADIT-CRT (41) suggested a reduced benefit in patients with non-LBBB QRS morphology. In the present study, we found that a typical LBBB morphology, even in patients with a QRS ≤ 150 ms or myocardial scar, trended toward a higher AHR (albeit small sample size in the current study). This is consistent with the importance placed on LBBB morphology by clinical guidelines (42).

According to recent studies, sequential His bundle pacing (HBP) followed by left ventricular (LV) pacing [His-Optimized CRT (HOT-CRT)] improves ventricular electrical synchrony beyond BiV and MPP (43, 44). In Vijayaraman et al. study (43) clinical response in HOT—CRT patients was also observed in CRT non-responders and non-LBBB patients. Similarly, Jastrzebski et al. (45) showed the best effect of electrical resynchronization and a higher percentage of clinical improvement in the left bundle branch area pacing—optimized CRT (LOT—CRT) group. On the other hand, Senes at al. (46) showed a better ECG effect in patients with HBP or HOT-CRT, but no clinical improvement compared to the conventional BIV pacing. However, large and randomized trials we needed.

Electrical Evaluation

A metanalysis of individual patient data from randomized, controlled trials suggested that the survival benefit from CRT starts at a QRS > 140 ms, with less clear benefit between 120 and 140 ms (47). We found that QRS duration increased by 3-9% in most pacing protocols, with the exception of 3P-MPP_{syn}, which led to a reduction. As in other studies (32, 48) we have observed no correlation between intrinsic QRS duration and $\Delta LV + dP/dt_{max}$ nor between ΔQRS duration and $\Delta LV + dP/dt_{max}$. In this study, Q-LV/QRS were lower (0.46-0.56) than observed in patients with LBBB and greater QRS durations (typically around 0.80) (8). In this respect, a low Q-LV/QRS has been shown to relate to worse clinical outcomes (48, 49).

Clinical Implications

This study shows that even in patients with a reduced likelihood of response to, a typical LBBB morphology seems still associated with an improved acute hemodynamics. Our findings indicate that tailoring of pacing configurations (i.e., pacing electrode and optimizing the program) is required to achieve an acute hemodynamic effect in individual patients on the borderline of an clinically relevant hemodynamic response. Whilst our findings support the use of MPP as an option in some patients, it has no clear general benefit in the entire potentially predisposed group.

Limitations

The small sample size is an important limitation, especially for the comparison between LBBB and non-LBBB patients. Therefore, other group comparisons like scar and no-scar or QRS < or > than 150 ms were not performed. The current study was a relatively small, but multicenter, non-randomized study. Furthermore, only acute hemodynamic measurements were used to define the optimal CRT device setting resulting in the best CRT-response. The results observed in this study should be tested in a larger cohort including besides acute hemodynamic measurements also longer term echocardiographic and clinical outcomes (50).

CONCLUSIONS

No acute hemodynamic advantage emerged for 3P-MPP_{syn} or 3P-MPP_{seq} compared to SPP pacing configuration in patients with higher likelihood of CRT sub-response, except when compared to LVapical pacing.

DATA AVAILABILITY STATEMENT

The original contributions presented in the study are included in the article/**Supplementary Material**, further inquiries can be directed to the corresponding author.

ETHICS STATEMENT

Study has been approved for all participating sites by Local Ethics Committees and all participants signed informed consent forms: 1. Komisja Bioetyczna Śląskiego Uniwersytetu Medycznego w Katowicach, Katowice, Poland. 2. Eticka Komisia NUSCH Pod Krasnou Horkou 1 83348 Bratislava Slovakia (Slovak Republic). 3. Comité Ético de Investigación Clínica (Instituto de Investigación Sanitaria La Fe), Valencia, Spain. 4. West Midlands - Edgbaston Research Ethics Committee The Old Chapel Royal Standard Place Nottingham NG1 6FS. 5. Regionala Etikprövningsn ämden Afdelning 1 Sandgatan 1 22350 Lund Sweden. The patients/participants provided their written informed consent to participate in this study.

AUTHOR CONTRIBUTIONS

All authors listed have made a substantial, direct, and intellectual contribution to the work and approved it for publication.

FUNDING

The authors declare that this study received funding from Medtronic, Inc., Bakken Research Center (BRC), Maastricht, The Netherlands. The funder had the following involvement in the study: a role in study design, data collection and analysis (including statistician and database management), decision to publish, preparation of the manuscript and submission process.

SUPPLEMENTARY MATERIAL

The Supplementary Material for this article can be found online at: https://www.frontiersin.org/articles/10.3389/fcvm.2022.901267/full#supplementary-material

REFERENCES

1. Leyva F, Nisam S, Auricchio A. 20 years of cardiac resynchronization therapy. *J Am Coll Cardiol.* (2014) 64:1047–58. doi: 10.1016/j.jacc.2014.06.1178
2. Forleo GB, Mantica M, Di Biase L, Panattoni G, Della Rocca DG, Papavasileiou LP, et al. Clinical and procedural outcome of patients implanted with a quadripolar left ventricular lead: early results of a prospective multicenter study. *Heart Rhythm.* (2012) 9:1822–8. doi: 10.1016/j.hrthm.2012.07.021
3. Leyva F, Zegard A, Qiu T, Acquaye E, Ferrante G, Walton J, et al. Cardiac resynchronization therapy using quadripolar versus non-quadripolar left ventricular leads programmed to biventricular pacing with single-site left ventricular pacing: impact on survival and heart failure hospitalization. *J Am Heart Assoc.* (2017) 6:e007026. doi: 10.1161/JAHA.117.007026
4. Behar JM, Bostock J, Zhu Li AP, Chin HM, Jubb S, Lent E, et al. Cardiac Resynchronization therapy delivered *via* a multipolar left ventricular lead is associated with reduced mortality and elimination of phrenic nerve stimulation: long-term follow-up from a multicenter registry. *J Cardiovasc Electrophysiol.* (2015) 26:540–6. doi: 10.1111/jce.12625
5. Rinaldi CA, Kranig W, Leclercq C, Kacet S, Betts T, Bordachar P, et al. Acute effects of multisite left ventricular pacing on mechanical dyssynchrony in patients receiving cardiac resynchronization therapy. *J Card Fail.* (2013) 19:731–8. doi: 10.1016/j.cardfail.2013.10.003
6. Pappone C, Calović ž, Vicedomini G, Cuko A, McSpadden LC, Ryu K, et al. Multipoint left ventricular pacing improves acute hemodynamic response assessed with pressure-volume loops in cardiac resynchronization therapy patients. *Heart Rhythm.* (2014) 11:394–401. doi: 10.1016/j.hrthm.2013.11.023
7. Leyva F, Umar F, Taylor RJ, Steeds RP, Frenneaux MP. The clinical outcome of cardiac resynchronization therapy in post-surgical valvular cardiomyopathy. *Europace.* (2016) 18:732–8. doi: 10.1093/europace/euv287
8. Sterliński M, Sokal A, Lenarczyk R, Van Heuverswyn F, Rinaldi CA, Vanderheyden M, et al. In heart failure patients with left bundle branch block single lead multispot left ventricular pacing does not improve acute hemodynamic response to conventional biventricular pacing. A multicenter prospective, interventional, non-randomized study. *PLoS ONE.* (2016) 11:e0154024. doi: 10.1371/journal.pone.0154024
9. Pappone C, Calović Ž, Vicedomini G, Cuko A, McSpadden LC, Ryu K, et al. Multipoint left ventricular pacing in a single coronary sinus branch improves mid-term echocardiographic and clinical response to cardiac resynchronization therapy. *J Cardiovasc Electrophysiol.* (2015) 26:58–63. doi: 10.1111/jce.12513
10. Leclercq C, Burri H, Curnis A, Delnoy PP, Rinaldi CA, Sperzel J, et al. Cardiac resynchronization therapy non-responder to responder conversion rate in the more response to cardiac resynchronization therapy with MultiPoint Pacing (MORE-CRT MPP) study: results from Phase I. *Eur Heart J.* (2019) 40:2979–87. doi: 10.1093/eurheartj/ehz109
11. Vanagt WY, Prinzen FW, Delhaas T. Reversal of pacing-induced heart failure by left ventricular apical pacing. *N Engl J Med.* (2007) 357:2637–8. doi: 10.1056/NEJMc072317
12. Leyva F, Zegard A, Taylor RJ, Foley PWX, Umar F, Patel K, et al. Long-term outcomes of cardiac resynchronization therapy using apical versus nonapical left ventricular pacing. *J Am Heart Assoc.* (2018) 7:e008508. doi: 10.1161/JAHA.117.008508
13. Rüssel IK, Götte MJ, Bronzwaer JG, Knaapen P, Paulus WJ, van Rossum AC. Left ventricular torsion: an expanding role in the analysis of myocardial dysfunction. *JACC Cardiovasc Imaging.* (2009) 2:648–55. doi: 10.1016/j.jcmg.2009.03.001
14. Pedrizzetti G, La Canna G, Alfieri O, Tonti G. The vortex–an early predictor of cardiovascular outcome? *Nat Rev Cardiol.* (2014) 11:545–53. doi: 10.1038/nrcardio.2014.75
15. Leyva F, Zegard A, Umar F, Taylor RJ, Acquaye E, Gubran C, et al. Long-term clinical outcomes of cardiac resynchronization therapy with or without defibrillation: impact of the aetiology of cardiomyopathy. *Europace.* (2018) 20:1804–12. doi: 10.1093/europace/eux357
16. Świerżyńska E, Mitkowski P, Zakrzewska-Koperska J, Oręziak A, Baranowski R, Bilińska M, Sterliński M. Spatial separation of left and right ventricular leads adjusted to the left ventricular end-diastolic dimension does not affect the change of the paced QRS complex duration in resynchronization therapy. *Kardiol Pol.* (2020) 78:1159–61. doi: 10.33963/KP.15595
17. Ginks MR, Shetty AK, Lambiase PD, Duckett SG, Bostock J, Peacock JL, et al. Benefits of endocardial and multisite pacing are dependent on the type of left ventricular electric activation pattern and presence of ischemic heart disease: insights from electroanatomic mapping. *Circ Arrhythm Electrophysiol.* (2012) 5:889–97. doi: 10.1161/CIRCEP.111.967505
18. Hussain MA, Bhamra-Ariza P, Jacques A, Wilkinson P, Odemuyiwa O, Fluck D, et al. Benefits of a quadripolar left ventricular lead in patients undergoing cardiac resynchronization therapy with underlying myocardial scar. *Pacing Clin Electrophysiol.* (2013) 36:e45–47. doi: 10.1111/j.1540-8159.2011.03065.x
19. Bordachar P, Ploux S, Ritter P. Three left ventricular leads required for improved haemodynamic and clinical status of a patient with very severe heart failure and a narrow QRS duration. *Europace.* (2011) 13:439. doi: 10.1093/europace/euq370
20. Henin M, Ragy H, Mannion J, David S, Refila B, Boles U. Indications of cardiac resynchronization in non-left bundle branch block: clinical review of available evidence. *Cardiol Res.* (2020) 11:1–8. doi: 10.14740/cr989
21. Sohal M, Hamid S, Perego G, Della Bella P, Adhya S, Paisey J, et al. A multicenter prospective randomized controlled trial of cardiac resynchronization therapy guided by invasive dP/dt. *Heart Rhythm.* (2021) 2:19–27. doi: 10.1016/j.hroo.2021.01.005
22. Strauss DG, Selvester RH. The QRS complex–a biomarker that "images" the heart: QRS scores to quantify myocardial scar in the presence of normal and abnormal ventricular conduction. *J Electrocardiol.* (2009) 42:85–96. doi: 10.1016/j.jelectrocard.2008.07.011
23. McCrohon JA, Moon JCC, Prasad SK, McKenna WJ, Lorenz CH, Coats AJS, et al. Differentiation of heart failure related to dilated cardiomyopathy and coronary artery disease using gadolinium-enhanced cardiovascular magnetic resonance. *Circulation.* (2003) 108:54–9. doi: 10.1161/01.CIR.0000078641.19365.4C
24. Stegemann B, Francis DP. Atrioventricular and interventricular delay optimization and response quantification in biventricular pacing: arrival of reliable clinical algorithms and research protocols, and how to distinguish them from unreliable counterparts. *Europace.* (2012) 14:1679–83. doi: 10.1093/europace/eus242
25. Whinnett ZI, Davies JE, Willson K, Manisty CH, Chow AW, Foale RA, et al. Haemodynamic effects of changes in atrioventricular and interventricular delay in cardiac resynchronisation therapy show a consistent pattern: analysis of shape, magnitude and relative importance of atrioventricular and interventricular delay. *Heart.* (2006) 92:1628–34. doi: 10.1136/hrt.2005.080721
26. Whinnett ZI, Francis DP, Denis A, Willson K, Pascale P, van Geldorp I, et al. Comparison of different invasive hemodynamic methods for AV delay optimization in patients with cardiac resynchronization therapy: implications for clinical trial design and clinical practice. *Int J Cardiol.* (2013) 168:2228–37. doi: 10.1016/j.ijcard.2013.01.216
27. Mullens W, Nijst P. Leadless left ventricular pacing: another step toward improved CRT response. *J Am Coll Cardiol.* (2017) 69:2130–3. doi: 10.1016/j.jacc.2017.03.534
28. Mullens W, Auricchio A, Martens P, Witte K, Cowie MR, Delgado V, et al. Optimized implementation of cardiac resynchronization therapy: a call for action for referral and optimization of care: a joint position statement from the Heart Failure Association (HFA), European Heart Rhythm Association (EHRA), and European Association of Cardiovascular Imaging (EACVI) of the European Society of Cardiology. *Eur J Heart Fail.* (2020) 22:2349–69. doi: 10.1002/ejhf.2046
29. Puvrez A, Duchenne J, Gorcsan J, Marwick TH, Smiseth OA, Voigt JU. Why mechanical dyssynchrony remains relevant to cardiac resynchronization therapy. Letter regarding the article 'Optimized implementation of cardiac resynchronization therapy: a call for action for referral and optimization of care: a joint position statement from the Heart Failure Association (HFA), European Heart Rhythm Association (EHRA), and European Association of Cardiovascular Imaging (EACVI) of the European Society of Cardiology'. *Eur J Heart Fail.* (2021) 23:843–4. doi: 10.1002/ejhf.2150
30. Shun-Shin MJ, Miyazawa AA, Keene D, Sterliński M, Sokal A, Van Heuverswyn F, et al. How to deliver personalized cardiac resynchronization therapy through the precise measurement of the acute hemodynamic

response: Insights from the iSpot trial. *J Cardiovasc Electrophysiol.* (2019) 30:1610–9. doi: 10.1111/jce.14001
31. Duckett SG, Ginks M, Shetty AK, Bostock J, Gill JS, Hamid S, et al. Invasive acute hemodynamic response to guide left ventricular lead implantation predicts chronic remodeling in patients undergoing cardiac resynchronization therapy. *J Am Coll Cardiol.* (2011) 58:1128–36. doi: 10.1016/j.jacc.2011.04.042
32. van Everdingen WM, Zweerink A, Cramer MJ, Doevendans PA, Nguyên UC, van Rossum AC, et al. Can we use the intrinsic left ventricular delay (QLV) to optimize the pacing configuration for cardiac resynchronization therapy with a quadripolar left ventricular lead? *Circ Arrhythm Electrophysiol.* (2018) 11:e005912. doi: 10.1161/CIRCEP.117.005912
33. Thibault B, Dubuc M, Khairy P, Guerra PG, Macle L, Rivard L, et al. Acute haemodynamic comparison of multisite and biventricular pacing with a quadripolar left ventricular lead. *Europace.* (2013) 15:984–91. doi: 10.1093/europace/eus435
34. Durrer D, van Dam RT, Freud GE, Janse MJ, Meijler FL, Arzbaecher RC. Total excitation of the isolated human heart. *Circulation.* (1970) 41:899–912. doi: 10.1161/01.CIR.41.6.899
35. Pluijmert M, Bovendeerd PH, Lumens J, Vernooy K, Prinzen FW, Delhaas T. New insights from a computational model on the relation between pacing site and CRT response. *Europace.* (2016) 18(suppl 4):iv94–103. doi: 10.1093/europace/euw355
36. van Deursen C, van Geldorp IE, Rademakers LM, van Hunnik A, Kuiper M, Klersy C, et al. Left ventricular endocardial pacing improves resynchronization therapy in canine left bundle-branch hearts. *Circ Arrhythm Electrophysiol.* (2009) 2:580–7. doi: 10.1161/CIRCEP.108.846022
37. Umar F, Taylor RJ, Stegemann B, Marshall H, Flannigan S, Lencioni M, et al. Haemodynamic effects of cardiac resynchronization therapy using single-vein, three-pole, multipoint left ventricular pacing in patients with ischaemic cardiomyopathy and a left ventricular free wall scar: the MAESTRO study. *Europace.* (2016) 18:1227–34. doi: 10.1093/europace/euv396
38. Kandala J, Upadhyay GA, Altman RK, Bose A, Heist EK, Mela T, et al. Electrical delay in apically positioned left ventricular leads and clinical outcome after cardiac resynchronization therapy. *J Cardiovasc Electrophysiol.* (2013) 24:182–7. doi: 10.1111/j.1540-8167.2012.02428.x
39. Lercher P, Lunati M, Rordorf R, Landolina M, Badie N, Qu F, et al. Long-term reverse remodeling by cardiac resynchronization therapy with MultiPoint Pacing: a feasibility study of noninvasive hemodynamics-guided device programming. *Heart Rhythm.* (2018) 15:1766–74. doi: 10.1016/j.hrthm.2018.06.032
40. Gold MR, Thebault C, Linde C, Abraham WT, Gerritse B, Ghio S, et al. Effect of QRS duration and morphology on cardiac resynchronization therapy outcomes in mild heart failure: results from the Resynchronization Reverses Remodeling in Systolic Left Ventricular Dysfunction (REVERSE) study. *Circulation.* (2012) 126:822–9. doi: 10.1161/CIRCULATIONAHA.112.097709
41. Zareba W, Klein H, Cygankiewicz I, Hall WJ, McNitt S, Brown M, et al. Effectiveness of cardiac resynchronization therapy by QRS morphology in the multicenter automatic defibrillator implantation trial-cardiac resynchronization therapy (MADIT-CRT). *Circulation.* (2011) 123:1061–72. doi: 10.1161/CIRCULATIONAHA.110.960898
42. Glikson M, Nielsen JC, Kronborg MB, Michowitz Y, Auricchio A, Barbash IM, et al. 2021 ESC Guidelines on cardiac pacing and cardiac resynchronization therapy. *Eur Heart J.* (2021) 42:3427–520. doi: 10.1093/eurheartj/ehab364
43. Vijayaraman P, Herweg B, Ellenbogen KA, Gajek J. His-optimized cardiac resynchronization therapy to maximize electrical resynchronization: a feasibility study. *Circ Arrhythm Electrophysiol.* (2019) 12:e006934. doi: 10.1161/CIRCEP.118.006934
44. Zweerink A, Zubarev S, Bakelants E, Potyagaylo D, Stettler C, Chmelevsky M, et al. His-optimized cardiac resynchronization therapy with ventricular fusion pacing for electrical resynchronization in heart failure. *JACC Clin Electrophysiol.* (2021) 7:881–92. doi: 10.1016/j.jacep.2020.11.029
45. Jastrzebski M, Moskal P, Huybrechts W, Curila K, Sreekumar P, Rademakers LM, et al. Left bundle branch-optimized cardiac resynchronization therapy (LOT-CRT): Results from an international LBBAP collaborative study group. *Heart Rhythm.* (2022) 19:13–21. doi: 10.1016/j.hrthm.2021.07.057
46. Senes J, Mascia G, Bottoni N, Oddone D, Donateo P, Grimaldi T, et al. Is His-optimized superior to conventional cardiac resynchronization therapy in improving heart failure? Results from a propensity-matched study. *Pacing Clin Electrophysiol.* (2021) 44:1532–9. doi: 10.1111/pace.14336
47. Cleland JG, Abraham WT, Linde C, Gold MR, Young JB, Claude Daubert J, et al. An individual patient meta-analysis of five randomized trials assessing the effects of cardiac resynchronization therapy on morbidity and mortality in patients with symptomatic heart failure. *Eur Heart J.* (2013) 34:3547–56. doi: 10.1093/eurheartj/eht290
48. Engels EB, Mafi-Rad M, van Stipdonk AM, Vernooy K, Prinzen FW. Why QRS Duration should be replaced by better measures of electrical activation to improve patient selection for cardiac resynchronization therapy. *J Cardiovasc Transl Res.* (2016) 9:257–65. doi: 10.1007/s12265-016-9693-1
49. Gold MR, Birgersdotter-Green U, Singh JP, Ellenbogen KA, Yu Y, Meyer TE, et al. The relationship between ventricular electrical delay and left ventricular remodelling with cardiac resynchronization therapy. *Eur Heart J.* (2011) 32:2516–24. doi: 10.1093/eurheartj/ehr329
50. Suzuki H, Shimano M, Yoshida Y, Inden Y, Muramatsu T, Tsuji Y, et al. Maximum derivative of left ventricular pressure predicts cardiac mortality after cardiac resynchronization therapy. *Clin Cardiol.* (2010) 33:E18–23. doi: 10.1002/clc.20683

Conflict of Interest: VS, FLem, and BS were employed by the company Medtronic Inc. BM and RC were an employee of Medtronic and holds Medtronic stocks. MS, AM, AS, and FLey they received fees from commercial companies.

The remaining authors declare that the research was conducted in the absence of any commercial or financial relationships that could be construed as a potential conflict of interest.

Publisher's Note: All claims expressed in this article are solely those of the authors and do not necessarily represent those of their affiliated organizations, or those of the publisher, the editors and the reviewers. Any product that may be evaluated in this article, or claim that may be made by its manufacturer, is not guaranteed or endorsed by the publisher.

frontiers | Frontiers in Physiology

ORIGINAL RESEARCH
published: 02 June 2022
doi: 10.3389/fphys.2022.903784

Tracking Early Systolic Motion for Assessing Acute Response to Cardiac Resynchronization Therapy in Real Time

Manuel Villegas-Martinez[1,2], *Magnus Reinsfelt Krogh*[1,3], *Øyvind S. Andersen*[4], *Ole Jakob Sletten*[2,4,5], *Ali Wajdan*[1,3], *Hans Henrik Odland*[5], *Ole Jakob Elle*[1,3] *and Espen W. Remme*[1,4]*

[1]The Intervention Centre, Oslo University Hospital, Oslo, Norway, [2]Institute of Clinical Medicine, University of Oslo, Oslo, Norway, [3]Department of Informatics, University of Oslo, Oslo, Norway, [4]Institute for Surgical Research, Oslo University Hospital, Oslo, Norway, [5]Department of Cardiology and Pediatric Cardiology, Oslo University Hospital, Oslo, Norway

An abnormal systolic motion is frequently observed in patients with left bundle branch block (LBBB), and it has been proposed as a predictor of response to cardiac resynchronization therapy (CRT). Our goal was to investigate if this motion can be monitored with miniaturized sensors feasible for clinical use to identify response to CRT in real time. Motion sensors were attached to the septum and the left ventricular (LV) lateral wall of eighteen anesthetized dogs. Recordings were performed during baseline, after induction of LBBB, and during biventricular pacing. The abnormal contraction pattern in LBBB was quantified by the septal flash index (SFI) equal to the early systolic shortening of the LV septal-to-lateral wall diameter divided by the maximum shortening achieved during ejection. In baseline, with normal electrical activation, there was limited early-systolic shortening and SFI was low (9 ± 8%). After induction of LBBB, this shortening and the SFI significantly increased (88 ± 34%, $p < 0.001$). Subsequently, CRT reduced it approximately back to baseline values (13 ± 13%, $p < 0.001$ vs. LBBB). The study showed the feasibility of using miniaturized sensors for continuous monitoring of the abnormal systolic motion of the LV in LBBB and how such sensors can be used to assess response to pacing in real time to guide CRT implantation.

Keywords: cardiac resynchonization therapy, left bundle branch block (LBBB), dyssynchronous wall motion, heart failure, response prediction

OPEN ACCESS

Edited by:
Mark Potse,
UMR5251 Institut de mathématiques de Bordeaux (IMB), France

Reviewed by:
Frits W. Prinzen,
Maastricht University, Netherlands
Uyen Chau Nguyen,
Maastricht University Medical Centre, Netherlands
Marc Strik,
Université de Bordeaux, France

***Correspondence:**
Espen W. Remme
espen.remme@medisin.uio.no

Specialty section:
This article was submitted to Cardiac Electrophysiology, a section of the journal Frontiers in Physiology

Received: *24 March 2022*
Accepted: *13 May 2022*
Published: *02 June 2022*

Citation:
Villegas-Martinez M, Krogh MR, Andersen ØS, Sletten OJ, Wajdan A, Odland HH, Elle OJ and Remme EW (2022) Tracking Early Systolic Motion for Assessing Acute Response to Cardiac Resynchronization Therapy in Real Time. Front. Physiol. 13:903784. doi: 10.3389/fphys.2022.903784

1 INTRODUCTION

Left bundle branch block (LBBB) causes asynchronous electrical activation of the ventricular myocardium, resulting in discoordinated contraction and inefficient pump function (Vernooy et al., 2005). Cardiac resynchronization therapy (CRT) is a widely used and effective therapy for patients with heart failure and LBBB. However, about one third of patients who receive CRT, do not benefit from the treatment and in some subgroups function may worsen after implantation (Cleland et al., 2004). Inappropriate device function may burden the patient and accrue costs to society. Ideally, identification of responders to CRT should be performed prior to implantation, and much research is focused on improving those methods. However, a method to assess acute response during the implantation of the CRT device may also have significant benefits. Acute, real-time feedback that shows how the pacing

improves cardiac function will be of interest, and if no improvement is demonstrated, different locations of pacing can be tested to see if cardiac function improves. This will potentially reduce the number of non-responders due to sub-optimal lead placement. Ultimately, if the method shows no improvement of cardiac function, the implantation may be aborted. This will avoid leaving pacing wires prone to infection and clotting in the patient's body, and as an external pacemaker is used during testing, it could save the cost of the pacemaker device and of the CRT follow-up controls that will not be needed.

However, there is yet no consensus on which hemodynamic parameter should be used to evaluate acute response (Achilli et al., 2006; Chung et al., 2008; Van Bommel et al., 2009), although promising methods exists (Odland et al., 2021). There have also been several studies testing different imaging-based criteria and although some show promising results, none have proven to add clinical value so far (Doltra et al., 2014). LV pressure measurements are a gold standard for evaluation of cardiac function and may currently be the best method for assessing response to CRT, with parameters such as maximum LV dP/dt. However, there are conflicting results regarding use of pressure as an acute response parameter (Suzuki et al., 2010; Bogaard et al., 2011). This could potentially be explained by our observation that CRT acutely reduces both end systolic and end diastolic volume (Boe et al., 2019). The reduced end diastolic volume is effectively a reduction of preload which will reduce preload dependent functional indices. An increase of an index by CRT may therefore be counteracted by a reduction by the lower preload, and the effect of CRT will be masked. There is therefore a need for a preload independent hemodynamic marker of acute response to CRT.

A commonly observed feature of LBBB is an abnormal early systolic left-right motion of the septum referred to as septal beaking or septal flash (SF) (Dillon et al., 1974). SF occurs during the isovolumic contraction period in certain heart failure patients with LBBB and is associated with reduced left ventricular (LV) pump function (Grines et al., 1989). The leftward septal motion occurs as the right ventricular free wall and septum are activated and start shortening unopposed by the late activated LV lateral wall, which in contrast passively stretches. The stretching of the lateral region increases the number of myofilament cross-bridges once activated according to the Frank-Starling effect, and hence, when it subsequently is activated, it contracts with a higher force, thus opposing the septal contraction and ultimately pushing the septum rightwards again (septal rebound stretch) (Gjesdal et al., 2011; Walmsley et al., 2015). This septal pre-ejection deformation is a complex phenomenon influenced by passive and active forces, regional contractility, electrical events and valve closure. The motion may be small or absent in the presence of septal scar, impaired global or right ventricular (RV) contractility or RV volume overload (Remme et al., 2016). However, SF assessed by echocardiography or other imaging technologies has been shown to be a reliable predictor of CRT response (De Boeck et al., 2009; Sohal et al., 2014; Risum et al., 2015; Aalen et al., 2019). The correction of this abnormal septal motion by CRT indicates an increased likelihood of LV volumetric reverse remodeling (Jansen et al., 2007; Parsai et al., 2009; Stankovic et al., 2016) and some studies have shown ability to predict long term response (Menet et al., 2017). While SF may be a clinical indicator for stratification of patients prior to CRT device implantation, there is currently no response confirmation during the intervention. This creates an uncertainty regarding response that may lead to excessive CRT implantation which burdens patients and health care systems. There is therefore a need to develop a method that improves response prediction. SF and its correction can potentially be measured during CRT implantation for acute assessment of CRT efficacy. Thus, such measurements can be used to identify in real time the patients that will benefit from the therapy and aid in the lead placement and device programming.

In this proof-of-concept study we investigated if the SF motion could be used as a measure of acute response to CRT and propose a method for real-time measurement of the motion that can be shown on a monitor during implantation. The first hypothesis of the study was that SF would be reduced or totally abolished with optimal CRT. A second hypothesis was that this method could also identify optimal LV lead placement. Finally, the third hypothesis was that these measurements could be performed using miniaturized electromagnetic (EM) tracking sensors. EM sensors are commonly used in humans for tracking catheter positions in the body (Nafis and Jensen, 2008; Boutaleb et al., 2015; Beaulieu et al., 2017), and these coil sensors are very small and can be potentially incorporated in the CRT pacing leads or guiding wires. This combination of lead and sensor has already been proven possible with devices such as SonRtip^{TM} which consists on an accelerometer embedded in the atrial lead. The sensor then measures mechanical vibrations to optimize the CRT timings (Brugada et al., 2017). Thus, EM tracking sensors could be integrated in the pacing leads in a similar way, giving a continuous measurement of displacement. Alternatively, temporary insertion of EM sensors on the right side of the septum and in a coronary vein on the LV lateral wall during implantation by incorporating EM sensors in the guide-wires or using EM-catheters, could be used to track the septum and LV lateral wall positions for measurements of SF during implantation. There are already other invasive methods that similarly use catheters to study CRT response by electro-mechanical mapping of the heart and studying the electrical activation pattern in the ventricle (Gyöngyösi and Dib, 2011; Grace et al., 2019). The study was done in a canine model with LBBB comparing responses to different pacing configurations and lead placement during CRT. Implanted sonomicrometry crystals were used as gold standard to measure SF and test the first two hypotheses. As a proof of concept, we also attached EM sensors in the septum and on the LV lateral wall to mimic a clinical setup and test the third hypothesis if this sensor system could be used for acute assessment of SF, comparing it to the gold standard sonomicrometric measurements.

2 MATERIALS AND METHODS

2.1 Animal Preparation

Our group has performed several studies on LBBB and CRT where sonomicrometric crystals have been implanted which

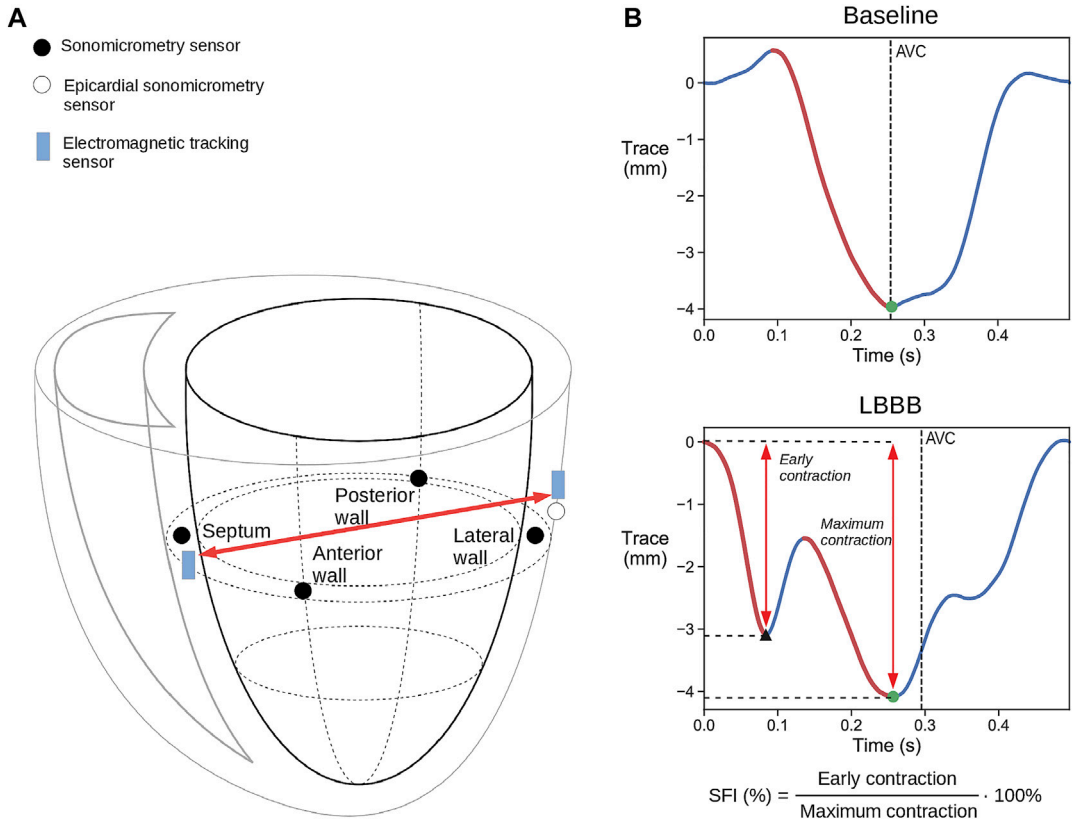

FIGURE 1 | (A) Schematic illustration of placement of the combined sonomicrometry crystals and IM-EMG sensors and the electromagnetic tracking (EM) sensors. The red arrow indicates the change in the distance that was measured between the sensors. Only one of the three epicardial LV free wall EM and sonomicrometry sensor pairs are shown for simplicity. **(B)** Representative displacement traces measured with EM tracking sensors during baseline and LBBB. The red traces mark the contraction during systole. The black triangle marks the end of the early contraction, while the black dots mark the point where full contraction is achieved which is then used to calculate SFI. AVC = aortic valve closure.

allows analysis of SF (Gjesdal et al., 2011; Aalen et al., 2019; Andersen et al., 2021). This study was therefore a combination of retrospective analysis of previously performed experiments (n = 4) and a prospective study where EM tracking sensors were implanted (n = 22). Thus, a total of 26 mongrel canines (8 female) of average weight 32 kg (±3 kg SD) were used in acute experiments for validation of the measurement of motion during pre-ejection period with sonomicrometry and EM tracking sensors. The study was conducted according to the guidelines of the Declaration of Helsinki, and approved by the Institutional Review Board (or Ethics Committee) of The Norwegian Food Safety Authority (FOTS ID: 8628, date of approval: 03.10.2018). The animals were supplied by the Center for Comparative Medicine (Oslo University Hospital, Rikshospitalet, Oslo, Norway). The animals were ventilated, anesthetized by propofol/opioids and surgically prepared as previously described (Andersen et al., 2021), including partial splitting of the pericardium from apex to base and loose re-suturing of the pericardial edges after completed instrumentation. LV pressure was measured with a calibrated micromanometer-tipped catheter (MPC-500, Millar Instruments Inc., Houston, TX) which was drift adjusted using a fluid-filled catheter in the left atrium (Andersen et al., 2021). LV volume was measured by sonometric crystals (Sonometrics, London, Ontario, Canada). Crystals were implanted subendocardially in a long axis diameter pair (apex to base), and two short axis diameter pairs in the LV equator (posterior to anterior wall and septum to lateral wall) (**Figure 1**). From these three diameter pairs the continuous volume was estimated using the formula (Mercier et al., 1982):

$$V = \pi/6 \cdot (longaxisdiameter \cdot shortaxisdiameter_1 \cdot shortaxisdiameter_2)$$

Stroke work was then calculated as the area of the LV pressure–volume loop. The four crystals placed in the equatorial plane were equipped with electrodes for measuring intramyocardial electromyograms (IM-EMG) to assess regional electrical activation times of the LV.

An epicardial pacemaker lead was attached to the right atrium, allowing measurements at a fixed heart rate. RV and LV pacing leads were placed to facilitate CRT by biventricular pacing. The endocardial RV lead was placed on the septum in the RV apex, while three epicardial pacing leads were placed on the LV free

wall: in a lateral position, in an apical position and close to the base on the anterior wall. The reason for placing three LV leads was to allow biventricular pacing from different LV locations to vary the degree of improvement. One EM tracking sensor (3DGuidance trakSTAR 2, NDI, Waterloo, ON) was inserted into the septum near the septal sonomicrometric crystal. Additionally, another pair of sonomicrometric and EM tracking sensors where sutured to the LV lateral wall. This allowed measurements of the diameter between the septum and the LV free wall with both sensors (**Figure 1**). A Mid-Range Transmitter used as reference for the EM tracking system was placed next to the animal and its x-axis was aligned with the longitudinal axis of the heart.

2.2 Experimental Protocol

Data were obtained at a fixed heart rate by atrial pacing (AP) at 120 beats per minute in all settings to avoid alterations in hemodynamic response parameters from differences in heart rate alone. After baseline recordings, LBBB was induced by radio-frequency ablation (Celsius Catheter, Biosense Webster, Inc.), with confirmation of successful induction by QRS widening, limb lead R wave notching and LV contraction patterns. When applying CRT, different pacing locations were tested. As CRT decreases both end-systolic and end-diastolic volumes, effectively reducing preload (Boe et al., 2019), it may mask the improvement by CRT. To correct for the acute changes in preload, we calculated the hemodynamic indices at identical end diastolic volume (EDV) for the different settings in each animal. Heart beats with identical EDV were found from transient vena cava constrictions that were performed in all settings. The preload corrected stroke work, SW_{EDV}, was obtained from the beats with the highest common EDV values from baseline, LBBB and CRT recordings. SW_{EDV} was then used as an index of global cardiac performance. All pressures, sonomicrometry, and EM tracking data were recorded simultaneously; EM data at 250 S/s and the other data at 200 S/s.

2.3 Signal Processing and Analysis

We used the Python programming language [version 3.7, Python Software Foundation (Van Rossum, 1995)] for all signal processing. All recordings were done with the respirator switched off to ensure that the values were unaffected by changes due to respiration. The raw EM signals were filtered using a second order Savitzky-Golay filter with a window size of 51 samples, to smooth them and remove high frequency noise.

2.4 Cardiac Function Estimation

The SF index (SFI) which was used to examine if CRT was able to correct the dyssynchrony, was calculated as the early systolic shortening of the LV septal-to-lateral wall diameter divided by the maximum shortening achieved after the early systolic motion during the cycle (**Figure 1B**). This diameter was measured by sonomicrometry from the septal crystal to the epicardial crystal next to the LV lateral wall pacing electrode, as shown in **Figure 1A**. Similarly, the spatial coordinates of the EM sensor in the septum and the EM sensor next to the LV lateral wall pacing electrode were used to calculate the equivalent diameter between the EM sensors.

2.5 Electromagnetic Sensor Validation

To check the accuracy of the EM tracking sensors and study its ability to measure the SFI, we compared the diameter trace and the derived SFI with the ones obtained with sonomicrometry.

2.6 Statistical Analyses

All statistical analyses were computed with SPSS software (version 28; SPSS Inc., Chicago, Ill). No statistical power calculation was conducted prior to the study as it was intended as a proof of concept. The sample size in this study is therefore relatively low and the statistical tests must therefore be considered with caution. Normality of distributions was determined using Shapiro-Wilks test. To test for significant effects of the interventions we used two-tailed Student's paired sample *t*-test on those with normal distribution and Wilcoxon signed-ranks test for the rest. Statistical significance was determined as $p < 0.05$. All values represent the mean of five consecutive heart cycles except data collected during transient caval constriction where only one beat was used. Values are reported as mean ± SD. No outliers have been excluded from the statistical tests.

A total of 26 experiments were conducted. Out of all of them, a total of 8 were excluded due to failure to induce LBBB or due to equipment malfunction. The protocol of each experiment varied slightly, so that only 14 out of the remaining 18 experiments included caval occlusions that allowed for preload adjustment of volumetric measurements, i.e. SW_{EDV}. Only 12 of these experiments had EM tracking sensors connected.

3 RESULTS

3.1 Cardiac Function Estimation

Hemodynamic values from baseline, LBBB, and the three CRT positions of all 18 experiments are shown in **Table 1**. Notably, there was a significant, acute reduction in EDV when CRT was turned on, regardless of the position of the lateral lead. Maximum LV dP/dt was increased for all three CRT positions. There was no significant change in stroke work, while stroke volume, cardiac output and ejection fraction were only significantly improved for CRT with apical position. On the other hand, when acute changes in preload were corrected for by measurements at similar EDV, there was a significant improvement with all CRT positions for all indices including stroke work (SW_{EDV}).

At baseline, with normal electrical activation, there was limited early-systolic shortening, and SFI by sonomicrometry was low (**Table 1**). After induction of LBBB, this shortening and the SFI significantly increased. Subsequently, CRT reduced SFI close to baseline values. There were no statistical significant difference in degree of improvement between the three CRT positions. However, as seen in **Table 1**, the trend was that apical position generated the highest preload corrected stroke work ($p = 0.096$ vs. lateral position) which was reflected also by a trend of lowest SFI value at this position ($p = 0.06$ vs. lateral position).

TABLE 1 | Hemodynamic values at baseline, LBBB, and all biventricular pacing sites (CRT) for all animals.

	Baseline	LBBB	CRT—lateral wall	CRT—apex	CRT—base	*n*
LV end-diastolic volume (ml)	71 ± 24	76 ± 26‡	72 ± 25*	73 ± 28§	72 ± 29§	18
Sensor indices						
Septal flash index (%)	9 ± 8	88 ± 34†	21 ± 20*	13 ± 13*	24 ± 22‡*	18
Septal flash index from EM tracking sensors (%)	9 ± 11	68 ± 49‡	9 ± 15§	6 ± 10§	18 ± 23§	12
Hemodynamic functional indices						
Stroke work (mmHg·ml)	1,020 ± 317	911 ± 283	796 ± 332‡	963 ± 331	873 ± 335‡	18
Stroke volume (ml)	13 ± 4	11 ± 3	11 ± 4‡	13 ± 3§	12 ± 4	18
Cardiac output (ml/min)	1,534 ± 408	1,414 ± 388	1,302 ± 448‡	1,581 ± 457§	1,428 ± 548	18
Ejection fraction (%)	19 ± 4	16 ± 5‡	16 ± 6‡	19 ± 5§	17 ± 4‡	18
LV dP/dt_{max} (mmHg/s)	1,568 ± 363	1,374 ± 276‡	1744 ± 744§	1,694 ± 705§	1711 ± 614§	18
Preload corrected hemodynamic functional indices						
Stroke work (mmHg·ml)	917 ± 279	541 ± 204†	748 ± 345‡§	848 ± 331*	792 ± 324§	14
Stroke volume (ml)	11 ± 3	7 ± 2†	9 ± 4§	11 ± 3*	10 ± 3§	14
Cardiac output (ml/min)	1,327 ± 316	810 ± 262†	1,073 ± 456‡§	1,300 ± 408*	1,195 ± 388§	14
Ejection fraction (%)	17 ± 3	10 ± 3†	14 ± 6‡§	17 ± 4*	16 ± 5§	14
LV dP/dt_{max} (mmHg/s)	1,639 ± 383	1,319 ± 234‡	1871 ± 712§	1758 ± 566§	1854 ± 496§	14

*Values are mean ± SD. †p < 0.001 compared to baseline, ‡p < 0.05 compared to baseline, *p < 0.001 compared to LBBB, §p < 0.05 compared to LBBB., Abbreviations; LBBB, left bundle branch block; CRT, cardiac resynchronization therapy; LV, left ventricle; LV dP/dtmax–maximum time derivative of left ventricular pressure; EM, electromagnetic.*

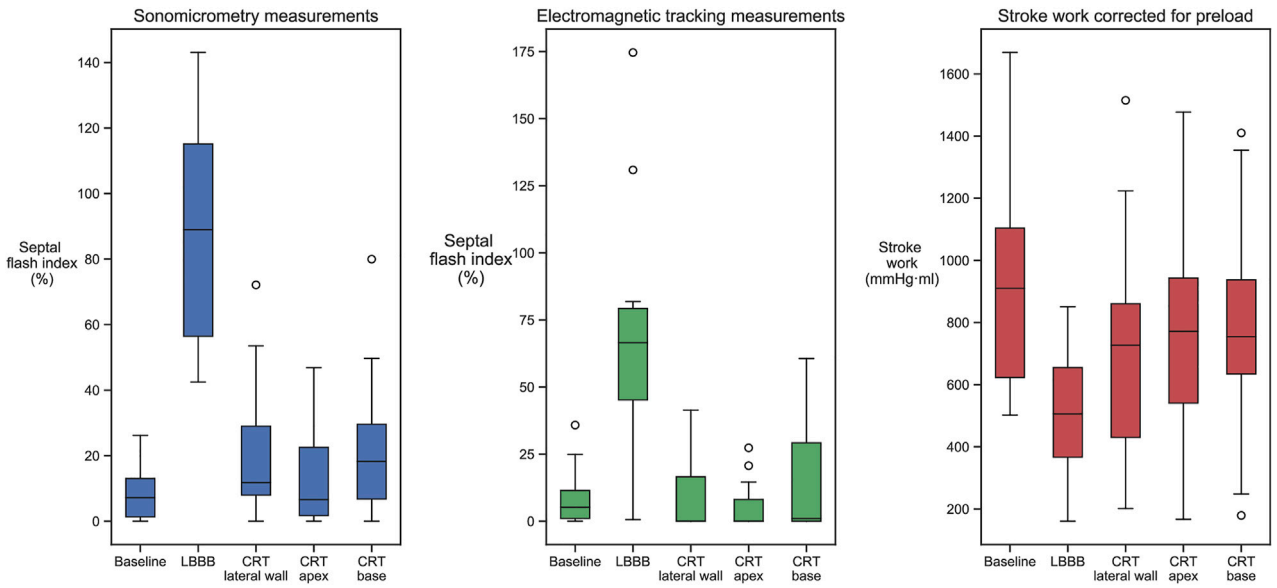

FIGURE 2 | Septal flash index, measured by sonomicrometry and EM sensors, and SW_{EDV} values measured in baseline, LBBB, and all three biventricular pacing sites. Induction of LBBB changed all measurements from baseline, while CRT returned them closer to baseline values.

The SFI measured by the EM sensors showed qualitatively a similar pattern as measured using sonomicrometry and furthermore, reflected the corresponding changes in cardiac function by SW_{EDV} (**Table 1**; **Figure 2**).

3.2 Electromagnetic Sensor Validation

The correspondence between the LV septum-to-lateral wall diameter trace measured using sonomicrometry and the one measured using EM sensors varied substantially between cases. In some cases, there were excellent correspondence (**Figure 3A**), where the SFI measured by the two methods were practically identical. However, there were cases with varying discrepancies where the EM measurements did not capture the rapid motions of the SF very well (**Figure 3B**). We noticed that the EM sensors were not properly sutured to the heart in some cases, and therefore was displaced or did not follow the motion of the heart correctly. The EM sensors we used were not designed for this purpose as they are intended to be embedded into medical instruments such as catheters, endoscopes, guide wires, and needle tips in order to help localize the instrument while

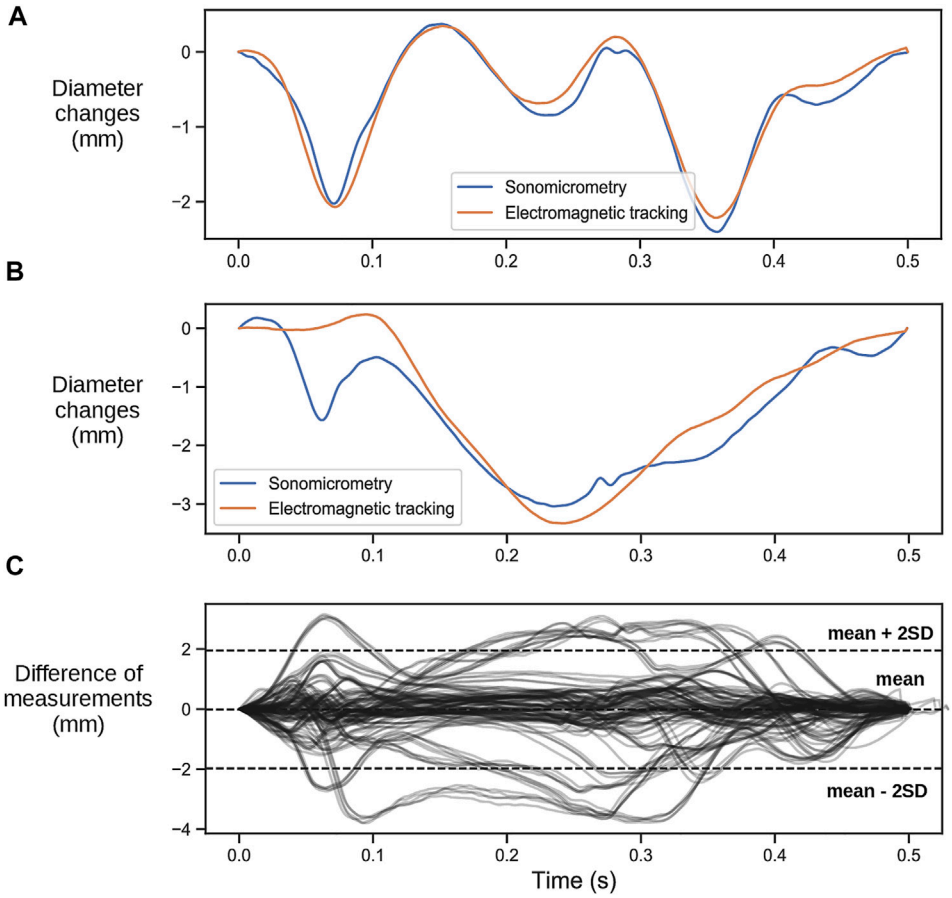

FIGURE 3 | (A) Representative case of a heartbeat comparing the change in the left ventricular septal-to-lateral wall diameter measured with the two different sensors where the measurements of the EM tracking sensors align with the ones obtained with sonomicrometry. **(B)** Representative case where the EM tracking sensors did not capture the rapid early contraction. **(C)** Difference between diameter changes measured with sonomicrometry and EM sensors for all recordings.

navigating through anatomical tracts. For this purpose, they are made with a thin and stiff wire. Two sutures approximately 1 cm apart were used to attach the wire to the epicardium. However, the stiffness of the wire and lack of proper attachment points resulted in dislocation of the wire during some experiments. This resulted in improper contact of the sensor to the point it was initially sutured to the heart and hence improper tracking of the motion. The difference between the measured diameter trace by sonomicrometry and the EM sensor for all the 12 animals with EM sensors are shown in **Figure 3C**.

4 DISCUSSION

In this study we have shown that acute changes in LV function during CRT implantation can be measured with sensors attached to the myocardium by assessing the degree of abnormal systolic motion. A hallmark of LBBB is the large pre-ejection shortening in the early activated septum and the resulting shortening of the LV septum-to-lateral wall diameter. Despite mechanical measurements not being currently recognized as relevant for the selection of patients for CRT, correction of electrical dyssynchrony should result in improved mechanical function for a meaningful response to occur. Successful CRT will synchronize the LV and remove or reduce this abnormal pre-ejection shortening. Additionally, patients with a greater septal to lateral wall delay present a more evident mechanical dyssynchrony (Andersson et al., 2013), which supports the notion that a mechanical index could be used as marker of dyssynchrony and monitor the effect of CRT. This is also supported by the notion that presence of SF is a statistically significant independent predictor of CRT response and that its correction by CRT is associated with significant acute and chronic benefits (Gabrielli et al., 2014; Walmsley et al., 2015). We therefore believe a mechanical measurement should be of potential use. In addition to this, SF is a relatively well defined and distinctive contraction pattern that is easily recognizable, so we believe that presence of SF and its abolishment or reduction would be a good marker of response to CRT. Hence, we studied if two sensors placed on the septum and on the LV free wall could measure this abnormal motion and if it would be able to monitor the response to CRT. We assessed this by calculating SFI as the proportion of the early systolic shortening relative to maximum shortening during ejection. The results of our study showed a reduction of this index with an improvement in LV function, which agrees with clinical

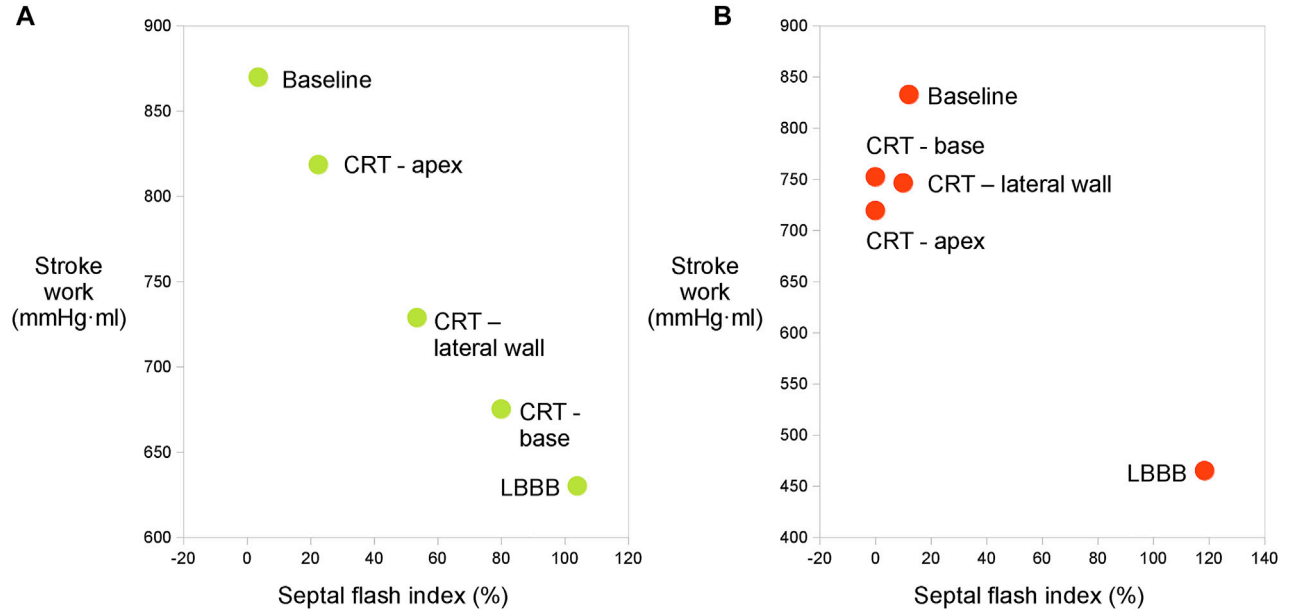

FIGURE 4 | (A) Relation between SW_{EDV} and SFI calculated with sonomicrometry from one experiment where different ranges of response were measured from different LV lead placements. There is a clear trend towards a reduction of SFI with improvement of LV function. **(B)** Relation between SW_{EDV} and SFI calculated with sonomicrometry from one experiment where the points obtained through different lead placements are clustered together.

data showing that more synchronous contraction during the pre-ejection period is associated with a better long-term clinical outcome (Odland et al., 2021). Note that as we extracted this index from the entire diameter, it is not strictly a pure septal motion as the originally proposed SF.

While the measurements showed a distinct and significant improvement in function from LBBB to CRT, we were not able to produce significant difference in the degree of improvement between the three LV lead positions. There was a smaller difference in most of the hemodynamic values, such as maximum dP/dt than we initially expected. We can only speculate as to causes of this, which could be due to differences in heart size or in the electrical conduction system between canines and humans, or short distance between the alternative lead positions. Humans who are treated with CRT, are usually in heart failure with enlargement of the heart size and may also have impaired conduction within the left ventricle, hence, different lead positioning is expected to broadly impact resynchronization. The lack of difference in response prevented us from investigating the ability of the method to identify optimal lead placement or the correlation between SW_{EDV} and SFI. This is showcased in **Figure 4** where we show the data from an experiment where different pacing positions gave different ranges of response (**Figure 4A**) and another in which similar values were obtained for all lead placements (**Figure 4B**).

As this was a proof-of-concept study, the intention was not to report the actual diagnostic accuracy, but rather show the potential of this method. Sensors for this purpose need to be custom made for it; small and robust enough to be added to the equipment that is routinely used in CRT implantation without adding complexity to the implantation procedure. For this purpose we chose to study EM tracking sensors, which can be miniaturized and are already used in different clinical setups where they can be visualized as they are navigated through different anatomical tracts in real time. However, the commercially available sensors we used, were not designed for our purpose, and the challenges when attaching them and recording data affected the accuracy and reliability of the measurements in some experiments. As a result, while the distance measured between the EM tracking sensors showed agreement with the reference in most cases, there were cases where the two technologies showed differences. Despite this, as we are aware of the limitations of the technology we used, we argue that by solving these issues with a custom design, the measurements would agree fully with those of sonomicrometry and the method would therefore work as well. Importantly, the EM sensor needs a higher sampling rate for this purpose than what may be typical for other clinical use of EM sensors. In two pilot experiments, we used a different EM tracking system, Aurora™ (NDI, Waterloo, Ontario, Canada). Those sensors had a sampling rate of 40 S/s, which did not allow an accurate tracking of the rapid motions during septal pre-ejection deformation. Data from those experiments could therefore not be used for the study, and the EM tracking system was changed to the one described in **section 2.1**.

4.1 Clinical Implications

The proposed SF index in this study, is able to act as an indicator for acute changes in LV function during CRT. This index could become a simple and reproducible tool for clinicians to assess baseline contraction characteristics and acute effects from CRT. The change in SFI could furthermore inform clinician about optimization strategies when testing capture and response to pacing. By measuring the reduction of SFI in real time, a clinician can determine whether the therapy is having the desired effect. If there is no reduction, or if it is a minor one, other pacing

settings or lead positions should be tested. Ultimately, the baseline SFI characteristic or the SFI response to pacing could provide necessary information for the operator to avoid implantations associated with poor clinical outcomes (Ross et al., 2020). If the EM tracking sensors are permanently placed with the pacemaker by incorporating them in the pacing leads, the system could assist in follow-up assessment to potentially optimize the programming of the pacemaker. This will also have the benefit of requiring no additional invasive procedure to insert them into the patients. However, in this case the pacemaker will have to be more complex to incorporate the extra wiring. Alternatively, the sensors may be introduced independently during CRT implantation only. This will then represent an extra invasive burden for the patient, though potentially this burden may be reduced if the sensors are incorporated in guidewires that will anyhow be introduced in the patients during the procedure.

Nowadays, SF can be reliably assessed by echocardiography, which is a non-invasive and harmless alternative. However, it seems less practical for use during CRT implantation as it requires extra personnel, time to obtain images and time for post-processing the images to quantify the desired indices as well as extra space in the operating-room for the ultrasound equipment. Another limitation when measuring SF by echocardiography, is the inter- and intra-observer variability. By using standardized mechanical devices, such as EM tracking sensors, this variability could be largely omitted. Hence, an automated sensor system for real-time analysis of the SF pattern seems a more attractive alternative which may become an important tool during CRT implantation.

4.2 Limitations

The present study used data from long interventions performed on heavily instrumented animals under anesthesia, hence heart function was depressed also at baseline. Furthermore, sonometric crystals were used to calculate LV volume. These crystals were not placed on the endocardium but somewhere in the wall and hence the LV cavity volume calculations were exaggerated as it included some myocardial mass and as a result the derived ejection fraction values were underestimated. We were not able to obtain statistically significant different responses from different pacing sites in our animal model. Hence, we were only able to evaluate correct capture and response to CRT, while the method's ability to guide optimal lead placement needs to be further investigated. As previously discussed, the EM sensors used in this study presented some limitations and did not always reflect accurately the heart wall motion. Hence, different sensors should be tested in future studies to find more suitable ones for this purpose.

5 CONCLUSION

This study showed first that measurements of the septal flash index in the LV septal-to-lateral wall diameter can be used to evaluate the acute improvements in LV function by CRT, and secondly that electromagnetic tracking sensors can be used for measuring this index. Such technology could thus have a role for assessing acute response to CRT and guide implantation.

DATA AVAILABILITY STATEMENT

The raw data supporting the conclusion of this article will be made available by the authors, without undue reservation.

ETHICS STATEMENT

The animal study was reviewed and approved by the Norwegian Food safety Authority.

AUTHOR CONTRIBUTIONS

Conceptualization, MK, HO, and ER; methodology, MV-M, MK, and ER; software, MV-M and MK; validation, MV-M, MK, and ER; formal analysis, MV-M; investigation, MV-M, MK, OA, OS, AW, HO, ER; data curation, MV-M and MK; writing—original draft preparation, MV-M; writing—review and editing, all authors; visualization, MV-M; supervision, OE and ER; project administration, OE and ER; funding acquisition, ER. All authors have read and agreed to the published version of the manuscript.

FUNDING

This project has received funding from the European Union's Horizon 2020 research and Innovation program under the Marie Skłodowska-Curie grant agreement No 764738, and from South-Eastern Norway Regional Health Authority (project number 16-00528-9).

ACKNOWLEDGMENTS

The authors thank Surgical Nurse Aurora Pamplona for her contribution to the animal experiments.

REFERENCES

Aalen, J. M., Remme, E. W., Larsen, C. K., Andersen, O. S., Krogh, M. R., and Smiseth, O. A. (2019). Mechanism of Abnormal Septal Motion in Left Bundle Branch Block. *JACC Cardiovasc. Imaging* 12 (12), 2402–2413. doi:10.1016/j.jcmg.2018.11.030

Achilli, A., Peraldo, C., Sassara, M., Orazi, S., Bianchi, S., Laurenzi, F., et al. (2006). Prediction of Response to Cardiac Resynchronization Therapy : The Selection of Candidates for CRT (SCART) Study. *Pacing Clin. Electrophysiol.* 29, 11–19. doi:10.1111/j.1540-8159.2006.00486.x

Andersen, Ø. S., Krogh, M. R., Boe, E., Storsten, P., Aalen, J. M., Larsen, C. K., et al. (2021). Left Bundle Branch Block Increases Left Ventricular Diastolic Pressure during Tachycardia Due to Incomplete Relaxation. *J. Appl. Physiol. (1985)* 128 (4), 729–738. doi:10.1152/japplphysiol.01002.2018

Andersson, L. G., Wu, K. C., Wieslander, B., Loring, Z., Frank, T. F., Maynard, C., et al. (2013). Left Ventricular Mechanical Dyssynchrony by Cardiac Magnetic Resonance Is Greater in Patients with Strict vs Nonstrict Electrocardiogram Criteria for Left Bundle-Branch Block. *Am. Heart J.* 165 (6), 956–963. doi:10.1016/j.ahj.2013.03.013

Beaulieu, L., Racine, E., Han, D. Y., Vigneault, E., Hsu, I., and Cunha, J. A. M. (2017). Real-time electromagnetic tracking e based treatment platform for high-

dose-rate prostate brachytherapy : Clinical workflows and end-to-end validation. *Brachytherapy* 17 (1), 103–110. doi:10.1016/j.brachy.2017.04.247

Boe, E., Smiseth, O. A., Storsten, P., Andersen, O. S., Aalen, J., Eriksen, M., et al. (2019). Left Ventricular End-Systolic Volume Is a More Sensitive Marker of Acute Response to Cardiac Resynchronization Therapy Than Contractility Indices: Insights from an Experimental Study. *Europace* 21, 347–355. doi:10.1093/europace/euy221

Bogaard, M. D., Houthuizen, P., Bracke, F. A., Doevendans, P. A., Prinzen, F. W., Meine, M., et al. (2011). Baseline Left Ventricular dP/dt Max rather Than the Acute Improvement in dP/dt Max Predicts Clinical Outcome in Patients with Cardiac Resynchronization Therapy. *Eur. J. Heart Fail.* 13, 1126–1132. doi:10.1093/eurjhf/hfr094

Boutaleb, S., Racine, E., Fillion, O., Bonillas, A., Hautvast, G., Binnekamp, D., et al. (2015). Performance and Suitability Assessment of a Real-Time 3D Electromagnetic Needle Tracking System for Interstitial Brachytherapy. *J. Contemp. Brachytherapy* 7 (4), 280–289. doi:10.5114/jcb.2015.54062

Brugada, J., Delnoy, P. P., Brachmann, J., Reynolds, D., Padeletti, L., Noelker, G., et al. (2017). Contractility Sensor-Guided Optimization of Cardiac Resynchronization Therapy: Results from the RESPOND-CRT Trial. *Eur. Heart J.* 38, 730–738. doi:10.1093/eurheartj/ehw526

Chung, E. S., Leon, A. R., Tavazzi, L., Sun, J.-P., Nihoyannopoulos, P., Merlino, J., et al. (2008). Results of the Predictors of Response to CRT (PROSPECT) Trial. *Circulation* 117, 2608–2616. doi:10.1161/circulationaha.107.743120

Cleland, J. G., Daubert, J. C., Erdmann, E., Freemantle, N., Gras, D., Kappenberger, L., et al. (2004). The Effect of Cardiac Resynchronization on Morbidity and Mortality in Heart Failure. *N. Engl. J. Med.* 352 (15), 1539–1549. doi:10.1056/NEJMoa050496

De Boeck, B. W. L., Teske, A. J., Meine, M., Leenders, G. E., Cramer, M. J., Prinzen, F. W., et al. (2009). Septal Rebound Stretch Reflects the Functional Substrate to Cardiac Resynchronization Therapy and Predicts Volumetric and Neurohormonal Response. *Eur. J. Heart Fail.* 11, 863–871. doi:10.1093/eurjhf/hfp107

Dillon, J. C., Chang, S., and Feigenbaum, H. (1974). Echocardiographic Manifestations of Left Bundle Branch Block. *Circulation*, 49. 876–880. doi:10.1161/01.cir.49.5.876

Doltra, A., Bijnens, B., Tolosana, J. M., Borràs, R., Khatib, M., Penela, D., et al. (2014). Mechanical Abnormalities Detected with Conventional Echocardiography Are Associated with Response and Midterm Survival in CRT. *JACC Cardiovasc Imaging* 7–10. doi:10.1016/j.jcmg.2014.03.022

Gabrielli, L., Marincheva, G., Bijnens, B., Doltra, A., Tolosana, J. M., Borras, R., et al. (2014). Septal Flash Predicts Cardiac Resynchronization Therapy Response in Patients with Permanent Atrial Fibrillation. *Europace* 16, 1342–1349. doi:10.1093/europace/euu023

Gjesdal, O., Remme, E. W., Opdahl, A., Skulstad, H., Russell, K., Kongsgaard, E., et al. (2011). Mechanisms of Abnormal Systolic Motion of the Interventricular Septum during Left Bundle-Branch Block. *Circ. Cardiovasc. Imaging* 4, 264–273. doi:10.1161/circimaging.110.961417

Grace, A., Willems, S., Meyer, C., Verma, A., Heck, P., Zhu, M., et al. (2019). High-resolution Noncontact Charge-Density Mapping of Endocardial Activation. *JCI insight* 4 (6). doi:10.1172/jci.insight.126422

Grines, C. L., Bashore, T. M., Boudoulas, H., Olson, S., Shafer, P., and Wooley, C. F. (1989). Functional Abnormalities in Isolated Left Bundle Branch Block. The Effect of Interventricular Asynchrony. *Circulation* 79, 845–853. doi:10.1161/01.cir.79.4.845

Gyöngyösi, M., and Dib, N. (2011). Diagnostic and Prognostic Value of 3D NOGA Mapping in Ischemic Heart Disease. *Nat. Rev. Cardiol.* 8 (7), 393–404. doi:10.1038/nrcardio.2011.64

Jansen, A. H. M., van Dantzig, J. M., Bracke, F., Meijer, A., Peels, K. H., van den Brink, R. B., et al. (2007). Qualitative Observation of Left Ventricular Multiphasic Septal Motion and Septal-To-Lateral Apical Shuffle Predicts Left Ventricular Reverse Remodeling after Cardiac Resynchronization Therapy. *Am. J. Cardiol.* 99 (7), 966–969. doi:10.1016/j.amjcard.2006.11.044

Menet, A., Bernard, A., Tribouilloy, C., Leclercq, C., Gevaert, C., Guyomar, Y., et al. (2017). Clinical Significance of Septal Deformation Patterns in Heart Failure Patients Receiving Cardiac Resynchronization Therapy. *Eur. Heart J.* 18, 1388–1397. doi:10.1093/ehjci/jew289

Mercier, J. C., DiSessa, T. G., Jarmakani, J. M., Nakanishi, T., Hiraishi, S., Isabel-Jones, J., et al. (1982). Two-dimensional Echocardiographic Assessment of Left Ventricular Volumes and Ejection Fraction in Children. *Circulation* 65 (5), 962–969. doi:10.1161/01.cir.65.5.962

Nafis, C., and Jensen, V. (2008). ""Method for Evaluating Compatibility of Commercial Electromagnetic (EM) Micro Sensor Tracking Systems with Surgical and Imaging Tables," Vol. 6918," in Proceedings of SPIE - The International Society for Optical Engineering, 1–15.

Odland, H. H., Villegas-Martinez, M., Ross, S., Holm, T., Cornelussen, R., Remme, E. W., et al. (2021). Shortening of Time-To-Peak Left Ventricular Pressure Rise (Td) in Cardiac Resynchronization Therapy. *Esc. Hear. Fail.* 8 (6), 5222–5236. doi:10.1002/ehf2.13601

Parsai, C., Bijnens, B., Sutherland, G. R., Baltabaeva, A., Claus, P., Marciniak, M., et al. (2009). Toward Understanding Response to Cardiac Resynchronization Therapy: Left Ventricular Dyssynchrony Is Only One of Multiple Mechanisms. *Eur. Heart J.* 30, 940–949. doi:10.1093/eurheartj/ehn481

Remme, E. W., Niederer, S., Gjesdal, O., Russell, K., Hyde, E. R., Smith, N., et al. (2016). Factors Determining the Magnitude of the Pre-ejection Leftward Septal Motion in Left Bundle Branch Block. *Europace* 18 (12), 1905–1913.

Risum, N., Tayal, B., Hansen, T. F., Bruun, N. E., Jensen, M. T., Lauridsen, T. K., et al. (2015). Identification of Typical Left Bundle Branch Block Contraction by Strain Echocardiography Is Additive to Electrocardiography in Prediction of Long-Term Outcome after Cardiac Resynchronization Therapy. *J. Am. Coll. Cardiol.* 66 (6), 631–641. doi:10.1016/j.jacc.2015.06.020

Ross, S., Nestaas, E., Kongsgaard, E., Odland, H. H., Haland, T. F., Hopp, E., et al. (2020). Septal Contraction Predicts Acute Haemodynamic Improvement and Paced QRS Width Reduction in Cardiac Resynchronization Therapy. *Eur. Heart J. Cardiovasc Imaging* 21, 845–852. doi:10.1093/ehjci/jez315

Sohal, M., Amraoui, S., Chen, Z., Sammut, E., Jackson, T., Wright, M., et al. (2014). Combined Identification of Septal Flash and Absence of Myocardial Scar by Cardiac Magnetic Resonance Imaging Improves Prediction of Response to Cardiac Resynchronization Therapy. *J. Interv. Card. Electrophysiol.* 40 (2), 179–190. doi:10.1007/s10840-014-9907-x

Stankovic, I., Prinz, C., Ciarka, A., Daraban, A. M., Kotrc, M., Aarones, M., et al. (2016). Relationship of Visually Assessed Apical Rocking and Septal Flash to Response and Long-Term Survival Following Cardiac Resynchronization Therapy (PREDICT-CRT). *Eur. Heart J. Cardiovasc Imaging* 17, 262–269. doi:10.1093/ehjci/jev288

Suzuki, H., Shimano, M., Yoshida, Y., and Inden, Y. (2010). Clinical Investigations Maximum Derivative of Left Ventricular Pressure Predicts Cardiac Mortality after Cardiac Resynchronization Therapy. *Clin. Cardiol.* 23, 18–23.

Van Bommel, R. J., Bax, J. J., Abraham, W. T., Chung, E. S., Pires, L. A., Tavazzi, L., et al. (2009). Characteristics of Heart Failure Patients Associated with Good and Poor Response to Cardiac Resynchronization Therapy: a PROSPECT (Predictors of Response to CRT) Sub-analysis. *Eur. Heart J.* 30, 2470–2477. doi:10.1093/eurheartj/ehp368

Van Rossum, G. (1995). *Python Tutorial, Technical Report CS-R9526," Cent*. voor Wiskd. en Inform..

Vernooy, K., Verbeek, X. A. A. M., Peschar, M., Crijns, H. J. G. M., Arts, T., Cornelussen, R. N. M., et al. (2005). Left Bundle Branch Block Induces Ventricular Remodelling and Functional Septal Hypoperfusion. *Eur. Heart J.* . 26 (1), 91–98. doi:10.1093/eurheartj/ehi008

Walmsley, J., Huntjens, P. R., Prinzen, F. W., Delhaas, T., and Lumens, J. (2015). Septal Flash and Septal Rebound Stretch Have Different Underlying Mechanisms. *Am. J. Physiol. Hear. Circ. Physiol.* 3, 394–403.

Conflict of Interest: The authors declare that the research was conducted in the absence of any commercial or financial relationships that could be construed as a potential conflict of interest.

frontiers | Frontiers in Physiology

TYPE Original Research
PUBLISHED 15 September 2022
DOI 10.3389/fphys.2022.996640

OPEN ACCESS

EDITED BY
David Christini,
Downstate Health Sciences University,
United States

REVIEWED BY
Liliana Tavares,
Tufts School of medicine MW,
United States
Shijie Zhou,
Miami University, United States

*CORRESPONDENCE
Keping Chen,
chenkepingfw@126.com

†These authors have contributed equally to this work and share first authorship

SPECIALTY SECTION
This article was submitted to Cardiac Electrophysiology,
a section of the journal
Frontiers in Physiology

RECEIVED 18 July 2022
ACCEPTED 31 August 2022
PUBLISHED 15 September 2022

CITATION
Hu Q, Lu W, Chen K, Dai Y, Lin J, Xu N, Lin J, Chen R, Li Y, Cheng C, Zhou Y and Zhang S (2022), Long-term follow-up results of patients with left bundle branch pacing and exploration for potential factors affecting cardiac function.
Front. Physiol. 13:996640.
doi: 10.3389/fphys.2022.996640

Long-term follow-up results of patients with left bundle branch pacing and exploration for potential factors affecting cardiac function

Qingyun Hu[1†], Wenzhao Lu[1†], Keping Chen[1*], Yan Dai[1], Jinxuan Lin[1], Nan Xu[2], Jingru Lin[2], Ruohan Chen[1], Yao Li[1], Chendi Cheng[1], Yu'an Zhou[1] and Shu Zhang[1]

[1]Department of Cardiology, Fuwai Hospital, National Center for Cardiovascular Diseases, Chinese Academy of Medical Sciences and Peking Union Medical College, Beijing, China, [2]Department of Echocardiography, Fuwai Hospital, National Center for Cardiovascular Diseases, Chinese Academy of Medical Sciences and Peking Union Medical College, Beijing, China

Background: Left bundle branch pacing (LBBP) is an alternative strategy for His bundle pacing (HBP). This study aimed to analyze the long-term performance of LBBP and the potential factors affecting long-term cardiac function.

Methods: Patients with LBBP were continuously enrolled from January 2018 to August 2020. Pacing parameters, electrocardiogram (ECG), and echocardiography were collected. The anatomic position of LBBP leads was described by echocardiographic and fluoroscopic parameters.

Results: A total of 91 patients with a median follow-up of 18 months were enrolled. Most patients maintained stable pacing parameters during follow-up. The intra-septal position of the 3830 lead also remained stable as the distance from the lead tip to the left surface of the ventricular septum was 0.4 (0, 1.4) mm. The overall level of left ventricular ejection fraction (LVEF) slightly increased. 59 patients had improved LVEF (ΔLVEF > 0), while 28 patients had unchanged or reduced LVEF (ΔLVEF $\leq$ 0). The declines of baseline LVEF, Δ Paced QRSd, and corrected longitudinal distance (longit-dist) of lead-implanted site correlated with LVEF improvement, and these three factors had negative linear correlations with ΔLVEF. Patients with tricuspid valve regurgitation (TVR) deterioration had longer follow-up duration (20.5 vs. 15.0 months, p = 0.01) and shorter Lead-TVA-dist (18.6 vs. 21.6 mm, p = 0.04) than those without TVR deterioration.

Conclusion: Patients with LBBP generally remained stable in pacing performance, anatomic lead positions, and cardiac function in long-term follow-up. Baseline LVEF, Δ Paced QRSd, and corrected longit-dist might be associated with potential LVEF decrease, which required further confirmation.

KEYWORDS

left bundle branch pacing, long-term follow-up, pacing performance, echocardiographic evaluation, cardiac function

1 Introduction

His bundle pacing (HBP) is considered the most physiological form of pacing, as it captures the intrinsic conduction system and delivers physiological ventricular activation (Lustgarten et al., 2015; Abdelrahman et al., 2018; Arnold et al., 2018; Sharma et al., 2018; Vijayaraman et al., 2018). However, HBP still has limitations, such as a steep learning curve, elevations of pacing threshold, a low R wave amplitude, and complicated pacemaker programming (Keene et al., 2019). Left bundle branch pacing (LBBP) is an alternative near-physiological pacing method that is considered to conquer the above shortcomings of HBP (Zhang et al., 2019). It has been shown to achieve favorable left ventricular (LV) electrical and mechanical synchrony similar to HBP (Hou et al., 2019). Although short-term and relatively long-term safety and feasibility have been demonstrated in several studies (Chen et al., 2019; Vijayaraman et al., 2019; Padala et al., 2020; Sharma et al., 2021; Su et al., 2021), these studies lacked detailed descriptions of the anatomical position of the LBBP lead in the ventricular septum and potential factors affecting patients' cardiac function after LBBP.

This study aimed to provide the long-term follow-up data of patients who received LBBP in Fuwai Hospital and explore the factors associated with potential changes in cardiac function while describing the anatomical position stability of LBBP lead.

2 Materials and methods

2.1 Study population and follow-up

This study is a prospective study. Patients who indicated permanent pacing according to current AHA/ACC/HRS guidelines and underwent successful LBBP implantation from January 2018 to August 2020 were prospectively followed up. Finally, those who had a pre-operative left ventricular ejection fraction (LVEF) ≥ 40% and a follow-up time ≥ 9 months with integral echocardiographic evaluation were included for analysis.

Patients with the following conditions were excluded: 1) receiving triple-chamber pacemaker implantation; 2) upgrading to conventional or LBBP-optimized cardiac resynchronization therapy (CRT) within 9 months.

Successful LBBP was defined as follow: the paced QRS morphology manifests as a right bundle branch block (RBBB) pattern; recording an LBB potential; transition from non-selective LBBP (ns-LBBP) to selective LBBP (s-LBBP) during threshold testing; or transition from left ventricular septal pacing (LVSP) to ns-LBBP or the stimulus to R wave peak time in V6 ECG lead (V6RWPT) was abruptly shortened (≥10 ms) at a higher output (5 V/0.4 ms) and (or) remained short (≤80 ms) and constant at different outputs (Li et al., 2019).

Patients were recommended for outpatient follow-up at 1, 3, and subsequently every 6 months. If there were any problems or discomforts about pacing or arrhythmia, additional clinic visits would be required.

The study was approved by the Ethics Committee of Fuwai Hospital (Approval No. 2019-1149) and obeyed the Declaration of Helsinki. Patients had signed written informed consents for pacemaker implantation and clinical data use before the operations.

2.2 Implantation procedure of left bundle branch pacing

We used the trans-ventricular-septal approach to achieve LBBP as previously described (Chen and Li, 2019). Briefly, the 3830 pacing lead (SelectSecure™, Model 3830, Medtronic, Minneapolis, MN, United States) was located on the right side of the interventricular septum (IVS) *via* the C315HIS sheath (Medtronic, Minneapolis, MN, United States) in the right anterior oblique (RAO) 30° fluoroscopic view; unipolar (tip) pacing with 2.0 V/0.5 ms was applied to select a targeted site and confirm the excellent contact between the lead and the septum. Then the lead was screwed perpendicularly into the IVS and towards the left side of IVS (left bundle branch area, LBB area). Advancing the lead while monitoring the paced QRS morphology until the criteria for successful LBBP (for details, see Section 2.1) were achieved.

During the procedure, 12-lead ECG and intracardiac electrogram (EGM) were displayed and recorded in real-time by the Bard system (Bard LabSystem Pro EP Recording System 2.4a.65.0, MA, United States). The procedure was terminated if the paced QRS morphology failed to meet the criteria for successful LBBP (for details, see Section 2.1) within five attempts.

2.3 Pacing and electrocardiogram parameters

Pacemaker programming and ECG inspection were performed on the day after operations and the clinic follow-up (Figure 1). The last follow-up date was included in the analysis. Pacing parameters included R wave amplitude, pacing threshold, and impedance. ECG data included intrinsic QRS duration (QRSd), paced QRSd, V6RWPT, the stimulus to R

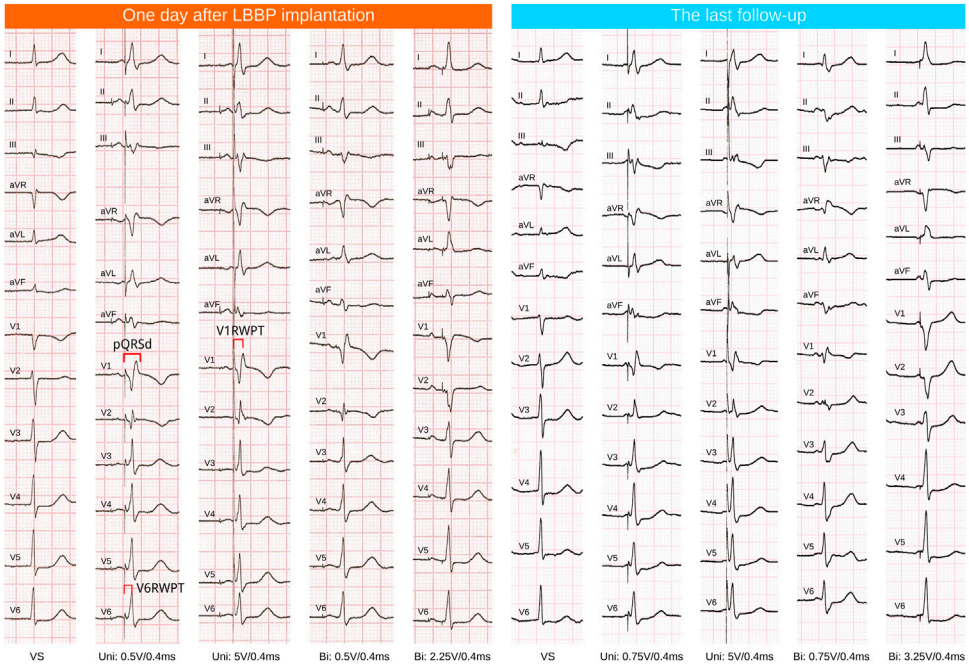

FIGURE 1
ECG follow-up of one case. LBBP, left bundle branch pacing; VS, ventricular sensing or intrinsic rhythm; Uni, unipolar tip pacing; Bi, bipolar pacing, anodal ring capture was observed at relatively high outputs (the QRS morphology showed the absence of a R' wave in ECG lead V1).

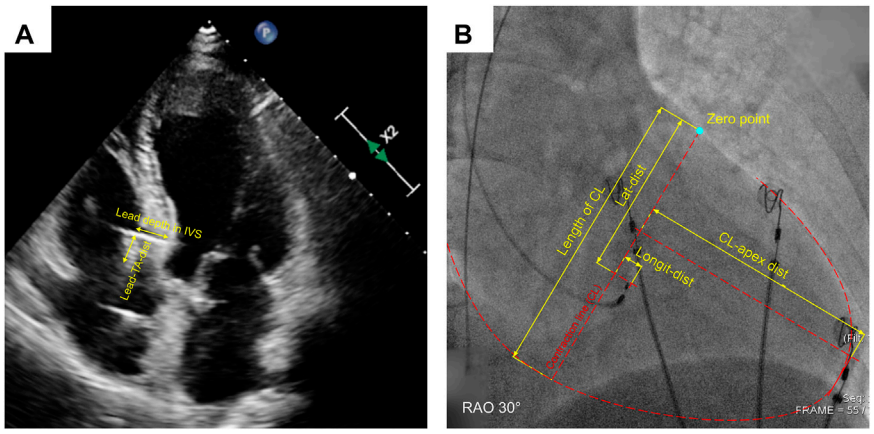

FIGURE 2
Measurement of echocardiographic **(A)** and fluoroscopic distance parameters **(B)**. IVS, interventricular septum; Lead-TA-dist, distance from the lead-implanted site on the right surface of IVS to the septal leaflet of tricuspid annulus; CL, contraction line; CL-apex-dist, distance from CL to apex; Longit-dist, longitudinal distance; Lat-dist, lateral distance.

wave peak time in V1 ECG lead (V1RWPT), and V6-V1 interpeak interval (V1RWPT-V6RWPT). All the above ECG parameters were measured during unipolar pacing at the LBB capture threshold in VVI mode at 10 bpm above the intrinsic rate (VVI at 60 bpm was used for those without intrinsic ventricular rhythm or complete atrioventricular block). At least three paced QRS complexes were measured, and the average was taken (Lin et al., 2021).

2.4 Echocardiographic parameters

Parameters of the anatomic position of 3830 lead for all enrolled patients were verified by echocardiography at the last follow-up, including lead depth in IVS (from the lead-implanted site on the right surface of IVS to the lead tip), IVS thickness at the lead-implanted site, distance from lead tip to the left surface of IVS (tip-to-LVS), and the distance from the lead-implanted site on the right surface of IVS to the septal leaflet of tricuspid annulus (Lead-TA-dist) (Figure 2A). These parameters were measured during the ventricular end-diastolic phase in the apical three/four-chamber and parasternal short-axis views. Other functional parameters were also measured at baseline and follow-up, including LVEF (evaluated with 2D biplane modified Simpson method), left ventricular end-diastolic dimension (LVEDD), and degrees of tricuspid valve regurgitation (TVR), TVR flow speed, and TVR pressure gradient. The degree of TVR was evaluated with the proximal isovelocity surface area (PISA) method and semi-quantitatively assessed in four classes (none, PISA radius ≤ 5 mm mild, 6~9 mm moderate, >9 mm severe). TVR deterioration was defined as the TVR degree elevated by at least one class. The ultrasonic machine (EPIQ 7C, Philips Inc.) was used in all patients.

2.5 Fluoroscopic distance parameters of lead-implanted sites

We have invented a coordinate system to describe the distribution of the lead-implanted sites quantitatively (Lu et al., 2021). The definitions of contraction line (CL), distance from CL to apex (CL-apex-dist), longitudinal distance (longit-dist), lateral distance (lat-dist), corrected longit-dist, and corrected lat-dist were described in the Supplementary Materials along with the measuring and conversion methods (Supplementary Table S1) and illustrated in Figure 2B. Image measurement was performed with at least three-time repeats on the LibreCAD 2.1.3 software, and the average was taken.

2.6 Statistical analysis

Continuous variables were presented as mean ± SD (normal distribution) or median (IQR) (non-normal distribution), while categorical variables were presented as numbers and percentages. Data between baseline and follow-up were compared using the paired-sample *t*-test (normal distribution) or the Wilcoxon signed-rank test; Inter-group comparisons were made by the independent-sample *t*-test or the Wilcoxon rank-sum test. Categorical variables were compared by the Chi-square test or Fisher's exact test. Linear correlations between variables were assessed by linear regression. Changes in variables from baseline to the last follow-up were presented as "Δvariable".

TABLE 1 Baseline clinical and demographic characteristics.

Characteristics	Enrolled patients (n = 91)
Age (years)	67 (58.5, 73.0)
Male sex	39 (42.9)
Pacing indications	
Sick sinus syndrome	36 (39.6)
Atrioventricular block	50 (54.9)
AF with bradycardia	5 (5.5)
Comorbidity	
Coronary heart disease	26 (28.6)
Hypertension	51 (56.0)
Diabetes mellitus	19 (20.9)
Hyperlipidemia	38 (41.8)
Stroke history	12 (13.2)
Intrinsic QRS duration (ms)	89.4 (84.4, 96.9)
Intrinsic QRS duration > 120 ms	13 (14.3)
Intrinsic QRS morphology	
Narrow	77 (84.6)
Right bundle branch block	10 (11.0)
Left bundle branch block	4 (4.4)

Data was presented as n (%) or median (IQR).

After univariate comparison, variables with $p < 0.15$ were considered as potential confounding factors and further screened by the logistic least absolute shrinkage and selection operator (Lasso) regression model, which is a shrinkage method to select the more relevant and explainable predictors from numerous variables with potential multicollinearity while avoiding overfitting (Falconer, 2011). The higher the lambda (λ) value was, the more strict the penalty was, while fewer variables remained. The largest λ value within one standard error (1SE) of the minimum binomial deviance was used for variable selection to generate the more simplified but still representative model. The SEs of variable coefficients in the Lasso model were estimated by the bootstrapping re-sampling algorithm (500 replicates). All tests were two-sided. $p < 0.05$ was considered statistically significant.

3 Results

3.1 Study population

A total of 176 patients underwent successful LBBP within the time window of patient enrollment, among whom 26 had the baseline LVEF < 40% (24 received CRT device and 2 upgraded to CRT) and 59 had a follow-up time of fewer than 9 months (Supplementary Figure S1). Eventually, 91 patients were included for analysis.

TABLE 2 Distance parameters of the 3830 lead under echocardiography and fluoroscopy.

Distance parameters	All patients (n = 91)
Echocardiography	
Lead depth in IVS (mm)	10.8 ± 2.1
IVS thickness (mm)	11.7 ± 2.2
Lead tip to LVS (mm)	0.4 (0, 1.4)
Lead-TA-dist (mm)	20.8 ± 6.7
Fluoroscopy	
Length of CL (mm)	147.5 (140.1, 155.7)
CL-apex-dist (mm)	118.5 ± 12.7
Longit-dist (mm)	25.6 ± 11.6
Lat-dist (mm)	79.2 ± 13.4
Corrected longit-dist (mm)	25.6 ± 11.1
Corrected lat-dist (mm)	79.4 ± 13.3

Data was presented as mean ± SD or median (IQR). IVS, interventricular septum; LVS, left surface of ventricular septum; Lead-TA-dist, distance from the lead-implanted site on the right surface of interventricular septum to the septal leaflet of tricuspid annulus; CL, contraction line; CL-apex-dist, distance from CL to apex; Longit-dist, longitudinal distance; Lat-dist, lateral distance.

The median follow-up time was 18 (13, 23) months. The baseline characteristics are summarized in Table 1. Distance parameters of the 3830 lead under echocardiography and fluoroscopy are summarized in Table 2. Echocardiography revealed that the lead depth in IVS was 10.8 ± 2.1 mm, the IVS thickness at lead-implanted sites was 11.7 ± 2.2 mm, and the median tip-to-LVS was 0.4 (0, 1.4) mm. Despite the resolution limitation of the ultrasound imaging, it was reasonable to consider that the tip of the leads kept stable at the sub-endocardial area of LVS during the follow-up period.

3.2 Comparisons of baseline and follow-up characteristics

Comparisons between baseline and follow-up characteristics are given in Table 3. During follow-up, the threshold and the R wave amplitude mildly increased but the pacing impedance decreased more prominently [750 (643, 880) vs. 399 (361, 427) ohm, $p < 0.001$]. However, the changes of pacing parameters were still within the clinically acceptable range, and the pacing performance could be considered stable. Regarding the ECG parameters, although V6RWPT (68.1 ± 9.7 to 71.1 ± 9.9 ms, $p < 0.001$) and V1RWPT (100.9 ± 11.1 to 103.6 ± 10.7 ms, $p = 0.004$) during follow-up were significantly prolonged compared with baseline, the magnitude of these changes were negligible; the paced QRSd and V6-V1 interpeak interval remained stable throughout follow-up. Echocardiographic parameters also remained stable during follow-up. Despite the increment was small, LVEF did increase significantly [63.0 (60, 65) % to 65.0 (61.0, 68.5) %, ΔLVEF = 2.5% ± 6.2%].

Compared with baseline, at the last follow-up, seven patients' V6RWPT (7.8%) and nine patients' paced QRSd (9.9%) were

TABLE 3 Comparison of pacing/ECG and echocardiographic parameters between baseline and follow-up.

Variables	Baseline (n = 91)	Follow-up (n = 91)	p value
Pacing/ECG parameters			
R wave amplitude (mV)	12.0 (7.8, 16.4)	15.7 (12.0, 20.0)	<0.001
Pacing impedance (ohm)	750 (643, 880)	399 (361, 427)	<0.001
Threshold (V/0.4 ms)	0.6 ± 0.4	1.03 ± 0.6	<0.001
Paced QRS duration (ms)	104.7 ± 11.9	105.7 ± 12.5	0.29
V6RWPT (ms)	68.1 ± 9.7	71.1 ± 9.9	<0.001
V1RWPT (ms)	100.9 ± 11.1	103.6 ± 10.7	0.004
V6-V1 interpeak interval (ms)	32.8 ± 10.0	32.6 ± 10.7	0.59
Echocardiography			
LVEF (%)	63.0 (60, 65)	65.0 (61.0, 68.5)	<0.001
LVEDD (mm)	47.0 (45, 50)	46.4 (44, 50)	0.06
TVR severity grades			
None	31 (34.0)	23 (25.3)	0.26
Mild	29 (31.9)	36 (39.6)	0.35
Moderate	23 (25.3)	16 (17.6)	0.28
Severe	8 (8.8)	16 (17.6)	0.13
TVR flow speed (m/s)	2.3 (0, 2.6)	2.2 (0, 2.5)	0.72
TVR pressure gradient (mmHg)	21.2 (0, 27)	20.0 (0, 24.5)	0.58

Data was presented as n (%), mean ± SD, or median (IQR). ECG, electrocardiogram; V6RWPT, stimulus to R wave peak time in V6 ECG lead; V1RWPT, stimulus to R wave peak time in V1 ECG lead; LVEF, left ventricular ejection fraction; LVEDD, left ventricular end-diastolic dimension; TVR, tricuspid valvular regurgitation.

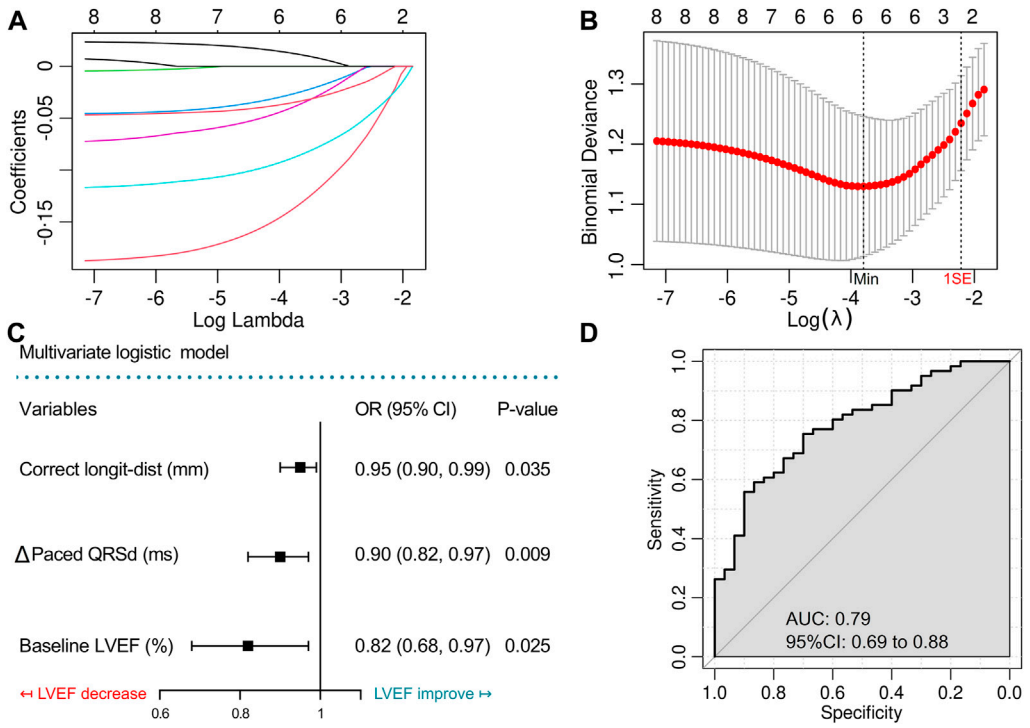

FIGURE 3
Variable screening by Lasso regression model and construction of the multivariate logistic model with ROC evaluation. **(A)** Lasso regularization of the binomial logistic model, the higher the lambda value was, the heavier was the penalty, while the remaining variables were less. **(B)** Cross-validation of the Lasso model to determine the optimal lambda value. **(C)** Forest plot shows the results of the final multivariate logistic model. **(D)** Receiver operating characteristic (ROC) curve to evaluate the final multivariate logistic model. Longit-dist, longitudinal distance; QRSd, QRS duration; LVEF, left ventricular ejection fraction; AUC, area under curve.

prolonged more than 10 ms at the LBB capture thresholds, while four patients (4.4%) lost the typical RBBB pattern in V1 ECG lead.

3.3 Comparison between patients with improved and unchanged/reduced left ventricular ejection fraction

During the follow-up, 59 (67.8%) patients had improved LVEF (ΔLVEF > 0), while 28 (32.2%) patients had unchanged or reduced LVEF (ΔLVEF ≤ 0). Using ΔLVEF = ±5% as the cut-offs, the number of patients was 29 (33%), 48 (55.2%), 10 (11.5%) in the ranges of ΔLVEF ≥ 5%, ΔLVEF from −5% to 5%, and ΔLVEF < −5%, respectively. The result indicated that the cardiac function of most patients with successful LBBP remained stable, while a small proportion had a significant reduction in LVEF (ΔLVEF < −5%).

Differences between patients with ΔLVEF > 0 and ΔLVEF ≤ 0 were shown in Supplementary Table S2. Baseline LVEF [62 (60, 65) % vs. 65 (62, 65.3) %, $p = 0.003$], ΔPaced QRSd [−0.4 (−5.1, 4.7) vs. 2.5 (−0.7, 9.3) ms, $p = 0.006$], ΔV6RWPT [2.0 (−0.6, 5.6) vs. 5.1 (0.4, 6.9) ms, $p = 0.04$], ΔV1RWPT (1.2 ± 7.3 vs. 4.6 ± 6.0 ms, $p = 0.03$) were significantly lower and the corrected longit-dist (23.4 ± 11.0 vs. 29.1 ± 10.5 mm, $p = 0.02$) was shorter in patients with ΔLVEF > 0. The results indicated that patients with improved LVEF might have worse baseline cardiac function (although the difference is small), higher stability of ECG depolarization parameters, and closer lead-implanted sites towards the CL. These were the potential correlated factors for LVEF changes in patients with long-term LBBP.

3.4 Correlative factors for the change of left ventricular ejection fraction

To investigate the independent ΔLVEF related factors, we recruited variables with $p < 0.15$ in the univariate comparison between ΔLVEF > 0 and ΔLVEF ≤ 0 groups (including age, baseline paced QRSd, baseline LVEF, ΔPaced QRSd, ΔV6RWPT, ΔV1RWPT, lead-TA-dist, corrected longit-dist) in multivariate analysis. Variables were screened by the Logistic-Lasso regression model. As shown in Figure 3A, with the increase of λ value, coefficients of more and more variables shrunk to zero, and the

TABLE 4 Screen variables by the Lasso regression model.

Variables	Coefficients (bootstrap SE)
	λ = 0.097, log (λ) = −2.33
Age (years)	0
Baseline LVEF (%)	−0.031 (0.062)
Baseline paced QRSd (ms)	0
ΔPaced QRSd (ms)	−0.029 (0.031)
ΔV6RWPT (ms)	0
ΔV1RWPT (ms)	0
Lead-TA-dist (mm)	0
Corrected longit-dist (mm)	−0.003 (0.017)

The Lasso regression model enrolled variables with the p values < 0.15 in the comparison between patients with improved and decreased LVEF. The optimal lambda value of 0.097 was chosen which was one-fold standard error (1 SE) away from the lambda of the minimum binomial deviance (λ = 0.020). Variables with beta equaling to 0 was excluded. LVEF, left ventricular ejection fraction; QRSd, QRS duration; ΔPaced QRSd/V6RWPT/V1RWPT, changes of QRSd/V6RWPT/V1RWPT from baseline to follow-up; V6RWPT, stimulus to R wave peak time in V6 lead; V1RWPT, stimulus to R wave peak time in V1 lead; Lead-TA-dist, distance from the lead-implanted site on the right surface of interventricular septum to the septal leaflet of tricuspid annulus; Longit-dist, longitudinal distance.

remaining variables became fewer. When the binomial deviance was minimized [λ = 0.02, log (λ) = −3.91], the model still contained six variables without enough simplification. Finally, the largest λ value [λ = 0.097, log (λ) = −2.33] within 1SE of the minimum binomial deviance (Figure 3B) was applied to generate the less complicated model containing three variables, including baseline LVEF, Δ Paced QRSd and corrected longit-dist (Table 4).

The three variables were then incorporated into a simplified logistic regression model, revealing that the declines in these variables correlated to LVEF improvement (Figure 3C). The receiver operating characteristic (ROC) curve (AUC = 0.79, 95%CI 0.69–0.88) indicated the favorable efficacy of this triple-variate model (Figure 3D). These three variables' data were conformed to normal distribution (Supplementary Figure S2), and negative linear correlations were demonstrated between the three variables and ΔLVEF (Figures 4A–C).

3.5 Correlative factors for tricuspid valve regurgitation deterioration

In the present study, the comparison between patients with and without TVR deterioration was described in Supplementary Table S3. Patients with TVR deterioration had significantly longer follow-up duration [20.5 (17.0, 24.0) vs. 15.0 (12.5, 21.5) month, p = 0.01] and shorter Lead-TVA-dist [18.6 (14.0, 23.0) vs. 21.6 (18.9, 25.8) mm, p = 0.04] than those without TVR deterioration (Supplementary Figures S3A, B). Among them, only 6 (6.6%) patients with TVR levels deteriorated ≥ 2 classes and the absolute level higher than moderate. These six patients had shorter average lead-TVA-dist (18.5 ± 9.6 vs. 20.9 ± 6.6 mm, p = 0.61) and significant longer follow-up time (23.3 ± 2.7 vs. 18.6 ± 6.6 months, p = 0.005) than the other patients, corresponding to the results above.

4 Discussion

There were several primary findings in our study: 1) in patients indicated for pacemaker implantation with LVEF > 40%, LBBP maintained stable and acceptable pacing and ECG parameters; 2) echocardiographic measurements revealed that the tip of the leads kept stable at the sub-endocardial area of LVS, and functional parameters remained stable or even slightly improved in the long-term follow-up period; 3) baseline LVEF, Δ Paced QRSd and corrected longit-dist negatively and independently correlated with the change of LVEF, which might be the indicator for long-term potential LVEF decrease in these population.

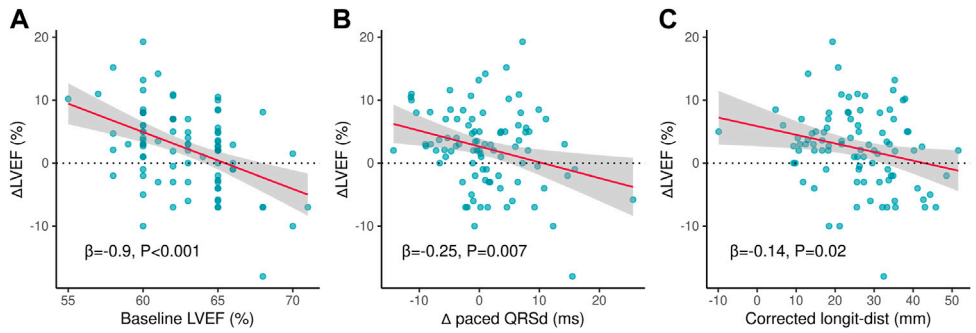

FIGURE 4
Linear correlated variables of ΔLVEF. **(A)** Negative linear correlation between ΔLVEF and baseline LVEF. **(B)** Negative linear correlation between ΔLVEF and Δpaced QRSd. **(C)** Negative linear correlation between ΔLVEF and corrected longit-dist. ΔLVEF, changes of left ventricular ejection fraction from baseline to follow-up; Δpaced QRSd, changes of paced QRS duration from baseline to follow-up; Longit-dist, longitudinal distance.

In recent years, LBBP has been considered a novel and feasible pacing maneuver to achieve near-physiological pacing. The short-term feasibility and effectiveness of this technique have been demonstrated, with the advantages compared to HBP such as the shorter learning curve, the higher success rate, and rare perioperative complications (Chen et al., 2019; Li et al., 2020; Liu et al., 2021). Subsequently, several mid/long-term studies investigated the performance of LBBP, revealing that LBBP could maintain stable pacing and ECG parameters during the follow up (Padala et al., 2020; Sharma et al., 2021; Su et al., 2021). Our study provided further evidence to support these results. Through a detailed comparison of baseline and follow-up ECG, we observed a constant pacing performance with acceptable pacing parameters in most patients. Although the pacing impedance was within the clinically acceptable range and maintained around 400 Ω, the reduction in the pacing impedance was still prominent, which was also found in other studies (Chen et al., 2020; Su et al., 2021). For the traditional RVP, the decrease in impedance was usually accompanied by increased pacing threshold and/or decreased R wave amplitude and was considered to be suggestive of the abrasion of lead or the ventricular septal perforation. However, we thought the decreased impedance in LBBP might be related to the 3830 lead characteristics and the myocardial properties of the left bundle branch area, rather than as a sign of the lead wear or ventricular septal perforation. Still, the exact reason remains unclear and requires further confirmation. Only a few patients had signs suggesting degeneration of pacing performance, such as significant prolonged (>10 ms) paced QRSd (9.9%) and V6RWPT (7.8%), or disappearance of RBBB pattern in V1 ECG lead (4.4%). As patients' data were collected during clinic visits, it was difficult to confirm LBB capture and judge the LBB capture threshold *via* normal speed (25 mm/s) ECG; Besides, there is no direct and established method or standard to determine LBB capture except electrophysiologic study, the transition of QRS morphology from s-LBBP or LVSP to ns-LBBP is not sensitive enough as it depends on the obvious discrepancy of capture threshold between myocardium and LBB.

In addition to the pacing and ECG parameters, the anatomic position stability of 3830 lead was also evaluated. In the study by Vijayaraman et al. (2019), echocardiography was performed in Left bundle branch area pacing (LBBAP) patients to assess the average intra-septal depth of the lead along the course of the lead, which was 1.4 ± 0.23 cm (range 1.1–1.8 cm). However, the distance from the tip to LVS was not assessed and whether the tip was located at the sub-endocardial area of LVS was not elucidated. In the study with the largest sample size of LBBP, the long-term stability of anatomic lead positions was not evaluated as well (Su et al., 2021). In the present study, echocardiographic measurement was performed at follow-up and revealed the median distance from the lead tip to LVS was 0.4 mm (0.8 ± 1.1 mm). This result demonstrated that most of the leads' tip was stable at the sub-endocardial area of LVS.

LBBP could achieve favorable LV electrical and mechanical synchrony similar to HBP(8). Previous studies pointed out that LBBP could maintain or even improve cardiac function in the acute postoperative phase, and improve long-term clinical outcomes compared to traditional RVP, especially in patients with a high burden of ventricular pacing (Li et al., 2020; Li et al., 2021; Liu et al., 2021). In this series, the results demonstrated 29 (33%) patients had the ΔLVEF ≥ 5%, 48 (55.2%) had the ΔLVEF ranging from −5% to 5%, and only 10 (11.5%) had the ΔLVEF < −5%. These results indicated that the adverse effect of LBBP on long-term LVEF was small in patients without reduced cardiac function. The overall improvement of LVEF we reported was lower than prior studies. The population in our study had a better baseline cardiac function than patients enrolled in previous study, which limited the potential rise in LVEF.

Although a stable trend has been observed for long-term LVEF after LBBP, which group of patients is more likely to show an improvement or decline in LVEF remained unknown. As a result, comparison between patients with ΔLVEF > 0 and ΔLVEF ≤ 0 was performed to explored the potential correlated factors for LVEF changes in this population. The Logistic-Lasso regression model was applied to rule out the possible confounding effects of these factors, as it was considered as a more solid and scientific method of variable screen. Finally, the three-variable model was obtained with favorable fitness (AUC = 0.79), including baseline LVEF, ΔPaced QRSd, and corrected longit-dist, which were associated with LVEF decrease. Further, we demonstrated the negative linear correlation of these variables to ΔLVEF.

We believe that these results are clinically reasonable, as the greater baseline LVEF was, the smaller space remained for the long-term rise of LVEF, even a decrease of LVEF due to the progress of comorbidity or cardiac risk factors. Lower ΔPaced QRSd meant the paced QRSd was less prolonged, which correlated to a more stable and synchronized ventricular depolarization during follow-up, which might contribute to the maintenance or the improvement of cardiac function. Corrected longit-dist was proposed as a novel distance parameter for describing the position of LBBP lead (Lu et al., 2021). By eliminating the influence of inter-individual variations of cardiac dimension, corrected longit-dist could more accurately reflect the LBBP lead implanted at the upper or lower region of the IVS. Lower corrected longit-dist meant that the LBBP lead was implanted at the upper region of the IVS. Considering the LBB trunk is commonly located in the upper portion of the IVS, the lead with lower corrected longit-dist (upper IVS) was more likely to capture the LBB trunk; besides, pacing from the upper part of IVS might generate an electrical axis more similar to intrinsic rhythm. Therefore, we considered that the lead with a lower corrected longit-dist could make the paced ventricular depolarization more physiological by capturing

the LBB trunk and generating a near-normal electrical axis, which was theoretically beneficial to the long-term cardiac function.

Moderate or greater TVR is associated with adverse RV function, increased risk of new-onset heart failure, and poor long-term survival (Topilsky et al., 2014; Papageorgiou et al., 2020). About 5%–21.7% of patients developed TVR deterioration after RV lead implantation (Van De Heyning et al., 2019; Papageorgiou et al., 2020), but the data after LBBP was rare. The patients with TVR deterioration had longer follow-up time and shorter Lead-TA-dist. However, the effects of LBBP on the tricuspid valve remained to be further validated.

5 Study limitations

As a single-center and relatively small-sample observational study in patients undergone LBBP for symptomatic bradycardia, there were inevitable observational bias and lower statistical power. The follow-up intervals of echocardiography were not consistent for all patients, which might also influence the results. However, the results supported that the pacing parameters, cardiac function, and lead's anatomic position were stable after a relatively long-term period of LBBP. The absolute value of average LVEF improvement was small since patients included in the study had a relatively normal cardiac function. Although we found the potential factors correlated to ΔLVEF which were insufficient to construct a clinical prediction model for cardiac function improvement or deterioration, these results still possessed referential value in clinical practice. Studies with larger sample size and prolonged follow-up period are required to confirmed the results.

6 Conclusion

The results from this single-center prospective observational study supported the long-term stability of LBBP regarding pacing performance, the anatomic position of the leads, and patients' cardiac function, indicating the long-term safety and feasibility of LBBP in bradyarrhythmia patients. Besides, the baseline LVEF, Δ Paced QRSd and corrected longit-dist were potential factors correlated to long-term changes of LVEF, while patients with TVR deterioration had longer follow-up time and shorter Lead-TA-dist, which required further confirmation.

Data availability statement

The raw data supporting the conclusion of this article will be made available by the authors, without undue reservation.

Ethics statement

The studies involving human participants were reviewed and approved by The Institutional Review Board of Fuwai Hospital. The patients/participants provided their written informed consent to participate in this study.

Author contributions

QH, WL, and KC conceptualized and designed the study. QH, WL, KC, YD, JxL, NX, JgL, RC, YL, CC, YZ, and SZ were responsible for the acquisition of data. WL was responsible for the analysis, and interpretation of data. QH drafted the manuscript. KC and YD critically revised the manuscript. All authors contributed to the article and approved the submitted version.

Funding

This work was supported by the National Natural Science Foundation of China (Grant No. 81870260).

Acknowledgments

We thank Hongzhao You from Fuwai Hospital for his excellent revising opinions to this manuscript.

Conflict of interest

The authors declare that the research was conducted in the absence of any commercial or financial relationships that could be construed as a potential conflict of interest.

Publisher's note

Supplementary material

The Supplementary Material for this article can be found online at: https://www.frontiersin.org/articles/10.3389/fphys.2022.996640/full#supplementary-material

References

Abdelrahman, M., Subzposh, F. A., Beer, D., Durr, B., Naperkowski, A., and Sun, H. (2018). Clinical outcomes of his bundle pacing compared to right ventricular pacing. *J. Am. Coll. Cardiol.* 71 (20), 2319–2330. doi:10.1016/j.jacc.2018.02.048

Arnold, A. D., Shun-Shin, M. J., Keene, D., Howard, J. P., Sohaib, S. M. A., and Wright, I. J. (2018). His resynchronization versus biventricular pacing in patients with heart failure and left bundle branch block. *J. Am. Coll. Cardiol.* 72 (24), 3112–3122. doi:10.1016/j.jacc.2018.09.073

Chen, K., Li, Y., Dai, Y., Sun, Q., Luo, B., and Li, C. (2019). Comparison of electrocardiogram characteristics and pacing parameters between left bundle branch pacing and right ventricular pacing in patients receiving pacemaker therapy. *Europace* 21 (4), 673–680. doi:10.1093/europace/euy252

Chen, K., and Li, Y. (2019). How to implant left bundle branch pacing lead in routine clinical practice. *J. Cardiovasc. Electrophysiol.* 30 (11), 2569–2577. doi:10.1111/jce.14190

Chen, X., Jin, Q., Bai, J., Wang, W., Qin, S., and Wang, J. (2020). The feasibility and safety of left bundle branch pacing vs. Right ventricular pacing after mid-long-term follow-up: A single-centre experience. *Europace.* 22, ii36–ii44. doi:10.1093/europace/euaa294

Hou, X., Qian, Z., Wang, Y., Qiu, Y., Chen, X., and Jiang, H. (2019). Feasibility and cardiac synchrony of permanent left bundle branch pacing through the interventricular septum. *Europace* 21 (11), 1694–1702. doi:10.1093/europace/euz188

Keene, D., Arnold, A. D., Jastrzebski, M., Burri, H., Zweibel, S., and Crespo, E. (2019). His bundle pacing, learning curve, procedure characteristics, safety, and feasibility: Insights from a large international observational study. *J. Cardiovasc. Electrophysiol.* 30 (10), 1984–1993. doi:10.1111/jce.14064

Li, X., Zhang, J., Qiu, C., Wang, Z., Li, H., and Pang, K. (2021). Clinical outcomes in patients with left bundle branch area pacing vs. Right ventricular pacing for atrioventricular block. *Front. Cardiovasc. Med.* 8, 685253. doi:10.3389/fcvm.2021.685253

Li, Y., Chen, K., Dai, Y., Li, C., Sun, Q., and Chen, R. (2019). Left bundle branch pacing for symptomatic bradycardia: Implant success rate, safety, and pacing characteristics. *Heart rhythm.* 16 (12), 1758–1765. doi:10.1016/j.hrthm.2019.05.014

Li, Y., Yan, L., Dai, Y., Zhou, Y., Sun, Q., and Chen, R. (2020). Feasibility and efficacy of left bundle branch area pacing in patients indicated for cardiac resynchronization therapy. *Europace.* 22, ii54–ii60. doi:10.1093/europace/euaa271

Lin, J., Hu, Q., Chen, K., Dai, Y., Chen, R., and Sun, Q. (2021). Relationship of paced left bundle branch pacing morphology with anatomic location and physiological outcomes. *Heart rhythm.* 18 (6), 946–953. doi:10.1016/j.hrthm.2021.03.034

Liu, Q., Yang, J., Bolun, Z., Pei, M., Ma, B., and Tong, Q. (2021). Comparison of cardiac function between left bundle branch pacing and right ventricular outflow tract septal pacing in the short-term: A registered controlled clinical trial. *Int. J. Cardiol.* 322, 70–76. doi:10.1016/j.ijcard.2020.08.048

Lu, W., Lin, J., Chen, K., Dai, Y., Chen, R., and Hu, Q. (2021). Quantitative distance and electrocardiographic parameters for lead-implanted site selection to enhance the success likelihood of left bundle branch pacing. *Clin. Res. Cardiol.* doi:10.1007/s00392-021-01965-1

Lustgarten, D. L., Crespo, E. M., Arkhipova-Jenkins, I., Lobel, R., Winget, J., and Koehler, J. (2015). His-bundle pacing versus biventricular pacing in cardiac resynchronization therapy patients: A crossover design comparison. *Heart rhythm.* 12 (7), 1548–1557. doi:10.1016/j.hrthm.2015.03.048

Padala, S. K., Master, V. M., Terricabras, M., Chiocchini, A., Garg, A., and Kron, J. (2020). Initial experience, safety, and feasibility of left bundle branch area pacing: A multicenter prospective study. *JACC. Clin. Electrophysiol.* 6 (14), 1773–1782. doi:10.1016/j.jacep.2020.07.004

Papageorgiou, N., Falconer, D., Wyeth, N., Lloyd, G., Pellerin, D., and Speechly-Dick, E. (2020). Effect of tricuspid regurgitation and right ventricular dysfunction on long-term mortality in patients undergoing cardiac devices implantation: >10-Year follow-up study. *Int. J. Cardiol.* 319, 52–56. doi:10.1016/j.ijcard.2020.05.062

Falconer, D. (2011). Regression shrinkage and selection via the Lasso: A retrospective. *J. R. Stat. Soc. Ser. B Stat. Methodol.* 73, 273–282. doi:10.1111/j.1467-9868.2011.00771.x

Sharma, P. S., Naperkowski, A., Bauch, T. D., Chan, J. Y. S., Arnold, A. D., and Whinnett, Z. I., Permanent his bundle pacing for cardiac resynchronization therapy in patients with heart failure and right bundle branch block. *Circ. Arrhythm. Electrophysiol.* (2018) 11(9):e006613doi:10.1161/CIRCEP.118.006613

Sharma, P. S., Patel, N. R., Ravi, V., Zalavadia, D. V., Dommaraju, S., and Garg, V. (2021). Clinical outcomes of left bundle branch area pacing compared to right ventricular pacing: Results from the geisinger-rush conduction system pacing registry. *Heart rhythm.* doi:10.1016/j.hrthm.2021.08.033

Su, L., Wang, S., Wu, S., Xu, L., Huang, Z., and Chen, X. (2021). Long-term safety and feasibility of left bundle branch pacing in a large single-center study. *Circ. Arrhythm. Electrophysiol.* 14 (2), e009261. doi:10.1161/CIRCEP.120.009261

Topilsky, Y., Nkomo, V. T., Vatury, O., Michelena, H. I., Letourneau, T., and Suri, R. M. (2014). Clinical outcome of isolated tricuspid regurgitation. *JACC. Cardiovasc. Imaging* 7 (12), 1185–1194. doi:10.1016/j.jcmg.2014.07.018

Van De Heyning, C. M., Elbarasi, E., Masiero, S., Brambatti, M., Ghazal, S., and Al-Maashani, S. (2019). Prospective study of tricuspid regurgitation associated with permanent leads after cardiac rhythm device implantation. *Can. J. Cardiol.* 35 (4), 389–395. doi:10.1016/j.cjca.2018.11.014

Vijayaraman, P., Chung, M. K., Dandamudi, G., Upadhyay, G. A., Krishnan, K., and Crossley, G. (2018). His bundle pacing. *J. Am. Coll. Cardiol.* 72 (8), 927–947. doi:10.1016/j.jacc.2018.06.017

Vijayaraman, P., Subzposh, F. A., Naperkowski, A., Panikkath, R., John, K., and Mascarenhas, V. (2019). Prospective evaluation of feasibility and electrophysiologic and echocardiographic characteristics of left bundle branch area pacing. *Heart rhythm.* 16 (12), 1774–1782. doi:10.1016/j.hrthm.2019.05.011

Zhang, S., Zhou, X., and Gold, M. R. (2019). Left bundle branch pacing: Jacc Review topic of the week. *J. Am. Coll. Cardiol.* 74 (24), 3039–3049. doi:10.1016/j.jacc.2019.10.039

frontiers | Frontiers in Cardiovascular Medicine

TYPE Original Research
PUBLISHED 15 September 2022
DOI 10.3389/fcvm.2022.979581

OPEN ACCESS

EDITED BY
Marta Focardi,
University of Siena, Italy

REVIEWED BY
Federico Landra,
Ospedale Santa Maria alle Scotte, Italy
Maria Concetta Pastore,
Università del Piemonte Orientale, Italy

*CORRESPONDENCE
Hans Henrik Odland
hanshenrikodland@gmail.com

SPECIALTY SECTION
This article was submitted to Heart Failure and Transplantation, a section of the journal Frontiers in Cardiovascular Medicine

RECEIVED 27 June 2022
ACCEPTED 23 August 2022
PUBLISHED 15 September 2022

CITATION
Odland HH, Holm T, Cornelussen R and Kongsgård E (2022) Determinants of the time-to-peak left ventricular dP/dt (Td) and QRS duration with different fusion strategies in cardiac resynchronization therapy. *Front. Cardiovasc. Med.* 9:979581. doi: 10.3389/fcvm.2022.979581

Determinants of the time-to-peak left ventricular dP/dt (Td) and QRS duration with different fusion strategies in cardiac resynchronization therapy

Hans Henrik Odland[1]*, Torbjørn Holm[2], Richard Cornelussen[3] and Erik Kongsgård[2]

[1]Department of Cardiology and Pediatric Cardiology, Section for Arrhythmias, Oslo University Hospital, Oslo, Norway, [2]Department of Cardiology, Section for Arrhythmias, Oslo University Hospital, Oslo, Norway, [3]Bakken Research Center, Medtronic, Maastricht, Netherlands

Background: Cardiac resynchronization therapy (CRT) is helpful in selected patients; however, responder rates rarely exceed 70%. Optimization of CRT may therefore benefit a large number of patients. Time-to-peak dP/dt (Td) is a novel marker of myocardial synergy that reflects the degree of myocardial dyssynchrony with the potential to guide and optimize treatment with CRT. Optimal electrical activation is a prerequisite for CRT to be effective. Electrical activation can be altered by changing the electrical wave-front fusion resulting from pacing to optimize resynchronization. We designed this study to understand the acute effects of different electrical wave-front fusion strategies and LV pre-/postexcitation on Td and QRS duration (QRSd). A better understanding of measuring and optimizing resynchronization can help improve the benefits of CRT.

Methods: Td and QRSd were measured in 19 patients undergoing a CRT implantation. Two biventricular pacing groups were compared: pacing the left ventricle (LV) with fusion with intrinsic right ventricular activation (FUSION group) and pacing the LV and right ventricle (RV) at short atrioventricular delay (STANDARD group) to avoid fusion with intrinsic RV activation. A quadripolar LV lead enabled pacing from widely separated electrodes; distal (DIST), proximal (PROX) and both electrodes combined (multipoint pacing, MPP). The LV was stimulated relative in time to RV activation (either RV pace-onset or QRS-onset), with the LV stimulated prior to (PRE), simultaneous with (SIM) or after (POST) RV activation. In addition, we analyzed the interactions of the two groups (FUSION/STANDARD) with three different electrode configurations (DIST, PROX, MPP), each paced with three different degrees of LV pre-/postexcitation (PRE, SIM, POST) in a statistical model.

Results: We found that FUSION provided shorter Td and QRSd than STANDARD, MPP provided shorter Td and QRSd than DIST and PROX, and SIM provided both the shortest QRSd and Td compared to PRE and POST. The interaction analysis revealed that pacing MPP with fusion with

10.3389/fcvm.2022.979581

intrinsic RV activation simultaneous with the onset of the QRS complex (MPP*FUSION*SIM) shortened QRSd and Td the most compared to all other modes and configurations. The difference in QRSd and Td from their respective references were significantly correlated ($\beta = 1$, $R = 0.9$, $p < 0.01$).

Conclusion: Pacing modes and electrode configurations designed to optimize electrical wave-front fusion (intrinsic RV activation, LV multipoint pacing and simultaneous RV and LV activation) shorten QRSd and Td the most. As demonstrated in this study, electrical and mechanical measures of resynchronization are highly correlated. Therefore, Td can potentially serve as a marker for CRT optimization.

KEYWORDS

heart failure, cardiac resynchronization therapy, fusion with native conduction, acute hemodynamic response, QRS duration, LV dP/dt$_{max}$

Introduction

Cardiac resynchronization therapy (CRT) is helpful in selected patients; however, responder rates rarely exceed 70% (1). Furthermore, CRT may have adverse effects if implemented in the wrong patients (2). Therefore, optimized strategies for implementation of CRT are sought (3). Optimal resynchronization is linked to optimal electrical activation (4). Nevertheless, measures of improved electrical activation do not reflect improvements in cardiac function with CRT in the long term (5), and measures of improved cardiac function do not align with responder rates (6). The left ventricular maximal pressure rise is one marker of cardiac contractility, measured as LV dP/dt$_{max}$. LV dP/dt$_{max}$ is highly dependent on preload and heart rate and could be significantly altered with CRT. We have previously shown how LV dP/dt$_{max}$ is predominantly determined by LV preexcitation and not by resynchronization in patients (7). Therefore, LV dP/dt$_{max}$ is invalid as a biomarker to determine the resynchronization treatment effect. Mechanical recoordination is likely better aligned with long-term response (8–10). Recoordination combines electrical timing and mechanical contraction.

We have recently shown how the time-to-peak left ventricle pressure derivative (Td), a marker of myocardial recoordination, accurately predicts long-term volumetric remodeling in patients in an observational clinical study (11). Td is a measure of the time-delay from the earliest electrical activation until the left ventricular peak pressure rise (dP/dt) or the timing of when the dP/dt$_{max}$ occurs (without considering its amplitude), and therefore combines both electrical activation and resulting mechanical contraction. The peak pressure rise is directly linked to the onset of exponential pressure rise, and this onset marks the time at which the regions of the left ventricle contracts in synergy. Synergistic contractions results in exponential pressure increase. In a typical dyssynchronous heart with left bundle branch block the earliest electromechanical event is the septal beaking (12). The septal beaking is, however, not resulting in exponential pressure rise, but rather in a passive uncoordinated stretch of the adjacent myocardium since the remainder of the left ventricle is resting at this time. Early septal shortening contraction is not coordinated with later lateral wall contraction. The early septal contraction occurs at low loads so that the myofibrils are shortening, mimicking isotonic contraction. Hence, the septal potential energy is wasted at this point.

The exponential increase in pressure occurs later, as electrical wave-front propagation results in more active contraction and subsequent active and passive stiffening of the remaining cardiac walls. Synergistic contraction at this point enables active force generation that results in exponential pressure increase ("isometric state"). The lateral wall performs super-normal work against the maximal load with the delayed pressure increase (13). This mechanism is probably the reason for the delay in peak dP/dt (Td) with dyssynchrony (11). Td shortens once effective biventricular pacing is applied to reflect the reversal of the dyssynchronous mechanisms and to reflect better myocardial coordination. Td has therefore the potential to both diagnose dyssynchrony, but even more so to diagnose effective resynchronization. Effective biventricular pacing should include optimal electrical activation that translate into shortening of Td. In this study, we wanted to investigate how Td and QRS duration responds to single point and multipoint pacing (MPP) with various degrees of optimal and suboptimal electrical fusion in an acute experimental study of patients undergoing CRT implantation.

Materials and methods

Ethics statement

This study was an acute-single center observational, experimental hemodynamic study approved by the Regional Committees for Medical and Health Research Ethics in Norway

and conducted following the Declaration of Helsinki principles. We obtained written, informed consent from all patients.

Study population

Heart failure patients admitted for CRT implantation according to current ESC/AHA guidelines were asked to participate in the study. Inclusion criteria were sinus rhythm, New York Heart Association functional class II and III heart failure on optimal medical therapy, QRSd larger than 130 ms and a left ventricular ejection fraction of <35%. In addition, exclusion criteria were age <18 years and above 80 years, ongoing atrial fibrillation and complete atrioventricular block. We successfully positioned the quadripolar LV lead in what we determined was the optimal lateral branch of the coronary sinus in each patient. We considered the optimal coronary sinus branch to be a lateral/ posterolateral branch that allowed positioning of both the distal and the proximal electrodes within the mid to basal portion of the LV wall with adequate pacing capture. An apical and strict anterior position was avoided in all patients. LV pacing (LVP) was set up in an extended bipolar configuration with the cathode on the LV electrode and the anode on the RV defibrillation coil. Therefore, MPP was limited to simultaneous pacing from distal LV electrode to RV coil and proximal LV electrode to RV coil, a configuration superior to other MPP configurations (14). Data from the same patients have been used in a similar study (7).

Pacing interventions: Pacing mode, electrode configurations and VV-interval (LV pre-/postexcitation)

The atrial pacing (AP) rate was set 10% higher than baseline sinus rhythm, and the AP-QRS interval was measured. First, we paced the right ventricle (RV) at baseline in DDD mode with AV-delay at 80% of the measured AP-QRS interval. Next, we used the AP-QRS interval to calculate the AP-left ventricular paced (LVP) interval to pace the left ventricle (LV) relative to QRS-onset in the fusion with the intrinsic RV activation group (FUSION). Following this, the FUSION group was the only one to allow intrinsic RV activation. In the STANDARD pacing group, the AV-delay to RV pace (RVP) was set to 80% of the AP-QRS interval to avoid intrinsic RV activation and enable standard biventricular pacing (BIVP). We then applied LVP from three different electrode configurations within each intervention group (FUSION/STANDARD). LVP was paced first from the distal electrode (DIST), then from the proximal electrode (PROX), and finally, we combined electrodes DIST+PROX (multipoint pacing, MPP). Also, as in the previously described setup (7), an off-set between LV and RV activation was achieved (VV-interval) as the LV was paced from each electrode configuration with a different extent of LV pre-/postexcitation in three different groups:

LV preexcitation (PRE): LVP between 75 and 25 ms before QRS (FUSION) or RV pace onset (STANDARD).

Simultaneous (SIM): LVP within 25 ms before or after QRS (FUSION) or RV pace onset (STANDARD).

LV postexcitation (POST): LVP between 25 and 75 ms after QRS (FUSION) or RV pace onset (STANDARD).

With this, we created two main groups (FUSION/STANDARD) with three different electrode configurations (DIST, PROX, MPP), each paced repeatedly with three different degrees of LV pre-/postexcitation (PRE, SIM, POST) within each main group in each patient. AV-delay consequently differed between the groups, with AV-delay being shorter in the STANDARD group to avoid intrinsic RV activation compared to the FUSION group. The AV-delay was even shorter when we paced the LV before RV or QRS-onset, as in PRE and SIM. The actual AV-delay within each beat was measured and included in the analyses (the interval from AP to the first ventricular activation; LVP, RVP or QRS-onset). All biventricular pacing interventions were performed similarly in every patient. QRS morphology was visually inspected, compared to successive paced beats and fully paced beats to confirm stable fusion and LV pre-/postexcitation during interventions. We averaged all measurements from 8 to 10 consecutive beats during each pacing intervention.

Data collection, pacing setup and measurements

We collected electrophysiology signals and ECGs with the BARD Pro EP recording system with Clearsign Amplifier (Boston Scientific Inc.). Pressures were measured *via* femoral artery access from the left ventricle with the Millar Micro-Cath^{TM} pressure sensor catheter (Millar Inc., USA) and collected with the PCU-2000 Pressure Control Unit (Millar Inc., USA). We allowed pressures to stabilize with pacing before measuring the resulting LV dP/dt_{max}. Signals were collected in real-time from the recording system to a data acquisition unit (PowerLab, ADInstruments LTD, UK) and analyzed using the LabChart Pro 8.0 software. We performed pacing with the EPS 320 cardiac stimulator (Micropace EP Inc., USA). We determined QRS-onset as the first fluctuation above the isoelectric line, resulting in a complete QRS complex and QRS duration (QRSd) from onset Q to global end of S wave from all ECG leads. Time-to-peak dP/dt (Td) was measured from the earliest of (i) onset of QRS or (ii) onset of the pacing spike until

10.3389/fcvm.2022.979581

the peak positive first-order derivative of the low-pas (15 Hz) filtered left ventricular pressure curve.

Statistical analysis

We used linear mixed models (SPSS 26.0) that consider individual baseline values for the repeated measurements. We chose compound symmetry as covariance type for both fixed and random effects, with each subject as random effects, with Bonferroni correction for comparison of main effects. The model with covariates that provided the lowest Akaike's information criteria was selected. The statistical output provides the estimated marginal means ± SEM for each fixed effects group, considering random effects and covariates. It allowed us to analyze the effects of and the interactions between the modes of pacing (FUSION and STANDARD), electrodes used (DIST, PROX, MPP) and pre-/postexcitation (PRE, SIM, POST). We used general linear models to compare groups with no repeated measures. Numbers from descriptive statistics are mean ± SD. A p-value of <0.05 was considered statistically significant.

Results

Baseline patient characteristics

We included 19 patients with sinus rhythm and a standard indication for a CRT device in the study with characteristics as previously published (7). 84% of the patients had strict LBBB while 16% had intraventricular conduction disease. Demographics are described in Table 1. Table 2 shows the average pre-/postexcitation intervals and AV-delays in the pacing mode groups (FUSION/ STANDARD). In addition, we calculated the onset of QRS to sensed EGM in the LV electrode (Q-LV). Q-LV to distal electrode was 127 ± 19 ms, and Q-LV to proximal electrode was 133 ± 20 ms (mean ± SD), with a linear relationship between the two ($\beta = 0.82$, $R = 0.86$, $P < 0.01$) (7). Table 3 shows the paced intervals within SIM relative to QRS-onset in FUSION/ STANDARD.

TABLE 1 Demographics.

	All patients ($n = 19$)
Age (years)	64 ± 10 years
Gender (%)	
Male	68 (13)
Weight (kg)	89 ± 18
Height (cm)	176 ± 8
Heart failure etiology (%)	
Non-ischemic	53 (10)
Ischemic	42 (8)
Radiation	5 (1)
Medication (%)	
ACE inhibitors/ ARB	89 (17)
Beta-blocker	74 (14)
Aldosterone antagonists	53 (10)
Diuretics	47 (9)
QRS configuration (%)	
LBBB	84 (16)
IVCD	16 (3)
QRS duration (ms)	168 ± 11
NYHA class	2.4 ± 0.5
NYHA class II (%)	58 (11)
NYHA class III (%)	42 (8)

LBBB, left bundle branch block; IVCD, intraventricular conduction disease; NYHA class, New York Heart Association class. Numbers are mean ± SD.

TABLE 2 Pacing intervals used for left ventricular pre-/postexcitation and mode of pacing (FUSION/STANDARD).

	Overall	Fusion	Standard
LV preexcitation (PRE)	−47 ± 14 ms	−49 ± 14 ms	−42 ± 13 ms
Simultaneous (SIM)	−2 ± 10 ms	−3 ± 15 ms	−1 ± 7 ms
LV postexcitation (POST)	39 ± 11 ms	40 ± 12 ms	37 ± 10 ms
AV-delay (ms)		199 ± 29 ms	169 ± 36 ms
QRS (ms)	172 ± 12 ms		

LV, left ventricle; AV-delay, atrioventricular paced delay. Numbers are mean ± SD.

TABLE 3 The simultaneous (SIM) pacing group subdivided into within 25 ms before or after RV activation.

	Fusion	Standard
LV pace 25 ms before	−14 ± 8 ms	−3 ± 6 ms
LV pace 25 ms after	11 ± 7 ms	13 ± 5 ms

Numbers are mean ± SD.

The effect of mode of pacing (STANDARD vs. FUSION) on QRSd and Td

We analyzed the overall effect of different LV electrodes (DIST, PROX or MPP) used for biventricular stimulation (STANDARD) on QRSd and Td and compared this to LV pacing with fusion with intrinsic RV activation (FUSION). We found a significant difference in QRSd between STANDARD and FUSION (155 ± 2 ms vs. 153 ± 2, $p < 0.01$) and in Td (148 ± 4 ms vs. 145 ± 4 ms, $p < 0.01$). When we included measurements with a VV-interval between −25 and 25 ms only, the difference in QRSd between STANDARD and FUSION was 154 ± 2 ms vs. 144 ± 2 ms ($p < 0.01$), while the difference in Td was 147 ± 4 vs. 136 ± 4 ms ($p < 0.01$). We also analyzed the differences in Td with LV pacing within 25 ms before QRS-onset

(FUSION, 141 ± 4 ms) or before RV-pace onset (STANDARD, 146 ± 4 ms, $p < 0.01$) and compared this to LV pacing within 25 ms after QRS-onset (FUSION, 135 ± 4 ms) or before RV-pace onset (STANDARD, 149 ± 4 ms, $p < 0.01$). Similarly, QRSd changed accordingly with LV pacing within 25 ms before QRS with FUSION (151 ± 2 ms) and STANDARD (154 ± 2 ms, $p < 0.01$) pacing and compared this to LV pacing within 25 ms after QRS onset with FUSION (142 ± 2 ms) and STANDARD (155 ± 2 ms, $p < 0.01$) pacing.

The effect of electrode configuration (DIST vs. PROX vs. MPP) on QRSd and Td

QRSd shortened with MPP compared to both distal and proximal electrodes [152 ± 2 ms (MPP) vs. 157 ± 2 ms (DIST) vs. 155±2 ms (PROX), $p < 0.01$]. Similarly, Td shortened with MPP (144 ± 4 ms, $p < 0.01$) compared to DIST (148 ± 4 ms) and PROX (151 ± 5 ms).

Interaction between mode of pacing and electrode configuration

MPP with fusion with intrinsic conduction (MPP*FUSION) provided the shortest QRS and the shortest Td compared to all other measurements (Figure 1). When STANDARD pacing was analyzed separately, we found that MPP shortened Td the most (146 ± 4 ms, $p < 0.01$), followed by DIST (147 ± 4 ms) and PROX (152 ± 4 ms), we also found that MPP shortened QRSd the most (153 ± 2 ms, $p < 0.01$) followed by PROX (155 ± 2 ms) and DIST (157 ± 2 ms). We found a similar pattern for Td and QRSd with FUSION (Td: MPP 141 ± 4 ms vs. DIST 149 ± 4 ms vs. PROX 149 ± 4 ms, $p < 0.01$; QRSd: MPP 150 ± 2 ms vs. PROX 155 ± 2 ms and DIST 156 ± 2 ms and) with significantly lower values for MPP ($p < 0.01$).

The effect of LV pre-/postexcitation on QRSd and Td

We found that simultaneous pacing (SIM) provided the shortest QRSd (152 ± 2 ms, $p < 0.01$) compared to preexcitation (PRE) at 158 ± 2 ms and postexcitation (POST) at 155 ± 2 ms, with a significant difference also between the latter ($p < 0.01$). We also found a similar pattern for Td; simultaneous pacing (SIM) provided the shortest Td (144 ± 4 ms, $p < 0.01$) compared to preexcitation (PRE) at 153 ± 4 ms and postexcitation (POST) at 148 ± 4 ms, with a significant difference also between the latter ($p < 0.01$).

The interaction between LV pre-/postexcitation with the mode of pacing

Pacing the LV almost simultaneous with QRS onset (SIM) from intrinsic RV activation (FUSION) provided both the shortest QRSd and the shortest Td compared to PRE and POST (Figure 2). We found a weak linear relationship between QRSd and Td ($\beta = 0.24$, $R = 0.3$, $p < 0.01$), QRSd and degree of preexcitation ($\beta = -0.07$, $R = 0.14$, $p < 0.01$) as well as Td and degree of preexcitation ($\beta = -0.07$, $R = 0.12$, $p < 0.01$). When analyzing the effect of pre-/postexcitation on QRSd in the STANDARD group, we found that SIM (154 ± 2 ms, $p < 0.01$) was lower compared to PRE (160 ± 2 ms) and POST (157 ± 2 ms). Similarly, the FUSION group SIM (147 ± 3 ms, $p < 0.01$) was lower compared to PRE (159 ± 3 ms) and POST (153 ± 3 ms). We found similar effects on Td in the STANDARD group, with SIM (146 ± 4 ms, $p < 0.01$) being lower compared to PRE (153 ± 4 ms) and POST (152 ± 4 ms). Td was also lower with SIM (137 ± 4 ms, $p < 0.01$) compared to PRE (153 ± 4 ms) and POST (145 ± 4 ms) in the FUSION group.

The interaction between mode of pacing, electrode configuration and LV pre-/postexcitation

Finally, we analyzed the overall effects of the interaction between pacing mode, electrode position and VV-interval. Figure 3A shows the estimated marginal means. Td shortened with fusion with intrinsic conduction regardless of pre-/postexcitation group and to the most considerable extent with MPP (−19 ± 1 ms, $p < 0.01$) compared to all other interventions. QRSd (Figure 3B) shortened the most with simultaneous pacing (SIM) with FUSION, PROX and MPP ($p < 0.01$), with no difference between the two. We also excluded the measurements with FUSION and pacing within 25 ms after QRS-onset because of a possible bias caused by measuring from QRS onset instead of RV-pace onset and found that simultaneous (SIM) MPP provided the lowest Td and QRSd compared to all other measurements ($p < 0.01$). Figure 3C shows the corresponding change in dP/dt_{max}.

Agreement between electrical and mechanical measures of resynchronization

We used the results from the linear mixed models to display the linear relationship between Td, QRSd and dP/dt_{max} and the corresponding Bland-Altman Plot for the significant linear relationships between the mechanical and electrical

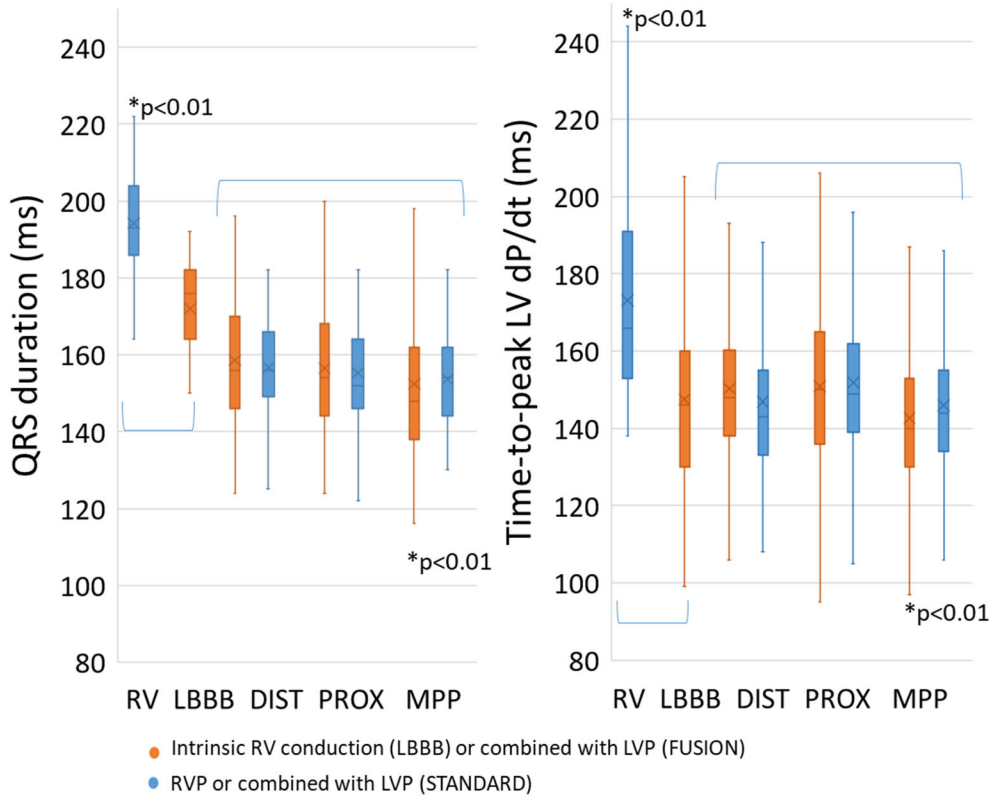

FIGURE 1
Mode of pacing and fusion with intrinsic RV conduction. A significant increase was found for both QRS duration and time-to-peak dP/dt with RV pacing compared to baseline LBBB. Multipoint pacing with intrinsic RV conduction significantly shortened QRS duration and time-to-peak dP/dt compared to the others ($p < 0.01$). RV, right ventricle; LBBB, left bundle-branch block; DIST, distal electrode; PROX, proximal electrode; MPP, multipoint pacing. * $p < 0.01$ compared to all others.

measures of resynchronization (Figure 4). The results show that the difference in Td due to different pacing modes, pre-/postexcitation and electrode configuration is similar and linearly related to the difference in QRSd (Figure 4A) with a good agreement and a fixed bias of the mean of −4.6 ms with no further proportional bias (Figure 4B). On the other hand, the difference in dP/dt_{max} was not reflected in either Td or QRSd.

Discussion

We have previously shown how deformation during the preejection period and synchronicity of the left ventricle are associated with Td. We have also introduced the term synergy to describe mechanical effects from pacing measured as a decrease in Td (11). Shortening Td is associated with more synergy from pacing and a better long-term prognosis (11). In this study, we wanted to demonstrate how stimulation of the LV from two sites at a quadripolar lead (MPP) could be captured by concordant shortening in Td and QRSd, reflecting more synergy and synchrony at the same time. This study is the first to show how MPP improves myocardial synergy on top of electrical synchrony.

RV pacing leads to longer RV activation times compared to intrinsic RV activation and partly explains prolongation in QRSd with RV pacing compared to intrinsic activation, as seen in Figure 1 (15). RV pacing does also affect left ventricular conduction time and contraction patterns (16). The effect of RV pacing on time duration is greater in the LV than in RV (15, 16). Figure 1 shows that Td is lower with intrinsic activation compared to RV pacing showing that a change in electrical activation patterns also translates into changes in contraction patterns. The changes in LV electrical wave-front patterns with RV pacing may increase the LV area of late activation but depends on individual variations and are not necessarily reflected in the QRSd (17). Our study found that MPP shortened QRSd regardless of RV activation patterns (RV pacing or intrinsic RV activation). The effect of MPP on QRSd, therefore, comes on top of the effects seen from RV pacing and indicates that MPP shortens QRSd solely by shortening LVAT (4). We found the same pattern of shortening with

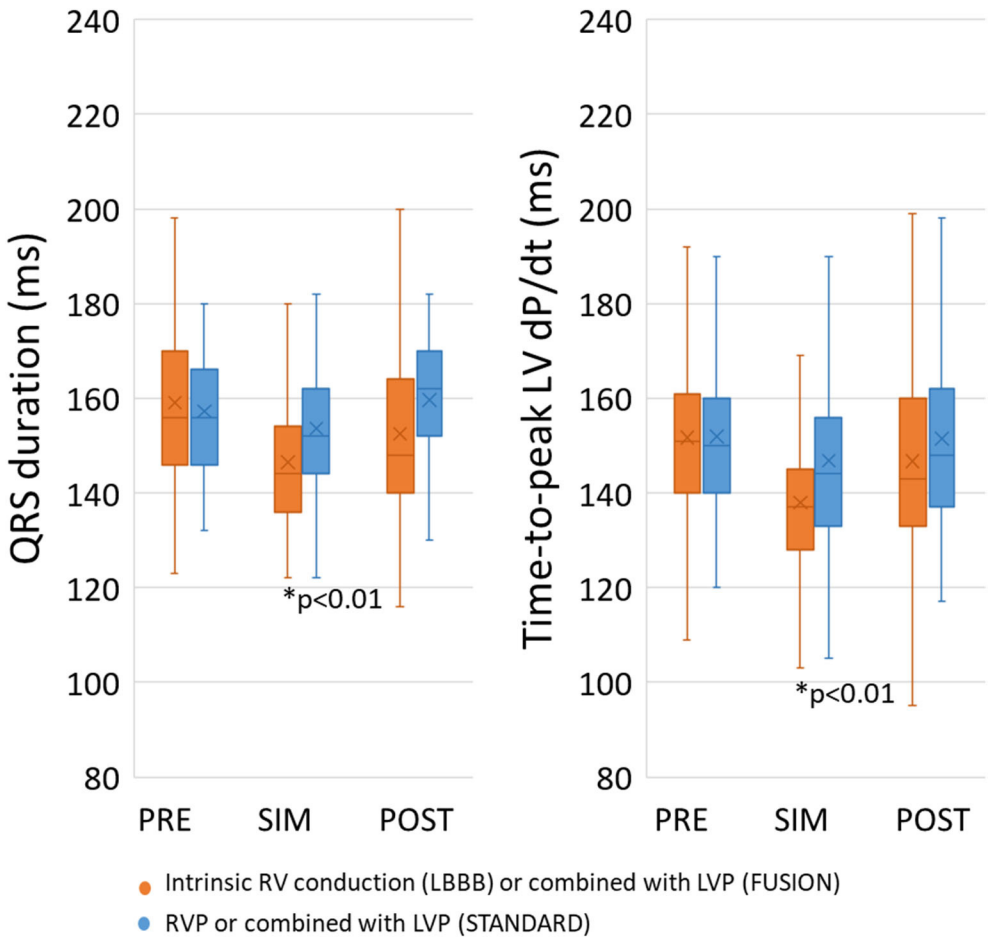

FIGURE 2
Effect on LV pre-/postexcitation on QRS duration and Td. Simultaneous pacing (SIM) with intrinsic RV conduction shortened both QRS duration and Time-to-peak dP/dt compared to pre-excitation and postexcitation. PRE, pre-excitation of the LV between 75 and 25 ms prior to QRS onset of RV pace onset; SIM, pacing the LV between 25 ms before and 25 ms after QRS onset or RV pace onset; POST, postexcitation of the LV 25–75 ms after QRS onset or RV pace onset. * $p < 0.01$ compared to all others.

MPP. The shortening effect on QRSd and Td is more evident with simultaneous pacing (SIM) than pre- and postexcitation (PRE, POST). The diagrammatic (Figure 5) shows how LV pre-/postexcitation and MPP may affect LVAT, RVAT and QRSd differently. The diagram is an ideal representation of electrode positions in 2D, following the principle of electrical cancellation caused by refractoriness of the myocardial tissue after excitation when two or electrical wave-fronts meet (18). Shortening the LVAT with the recruitment of excitable tissue from two areas is also an effect of multipoint pacing (4, 19).

It is also clear from the illustrative diagram (Figure 5) that changing electrode positions and RV activation times may change the resulting QRSd (20). We do not expect every individual patient have ideal electrode positions, and activation times may vary depending on the underlying myocardial disease. On top of this comes that electrical activation patterns resulting from each electrode may have significant individual variations, and the reaction of the electrical substrate to LV pacing is inconsistent (21). Heart size is another factor that may impact the interpretation of QRSd (22, 23). Although it is clear that QRSd and shortening with CRT are among factors critical for response to CRT (1, 24, 25), QRSd is still an inconsistent and unreliable marker for response (25–28), thus highlighting the need for a measure of resulting mechanical effect (9, 10, 29). The shortening of Td with a shorter QRSd seen in this study is in keeping with animal data showing concordance between synchrony and Td (11).

Another exciting aspect is myocardial discoordination, with some areas shortening while others stretch (10, 12, 13, 30, 31). We have described this as dyssynergistic contraction patterns during the preejection period reflected in time-dependent measures of cardiac contraction, measured as Td (11). The dyssynergistic contraction patterns are contributed to by dyssynchronous electrical activation, typically evident in

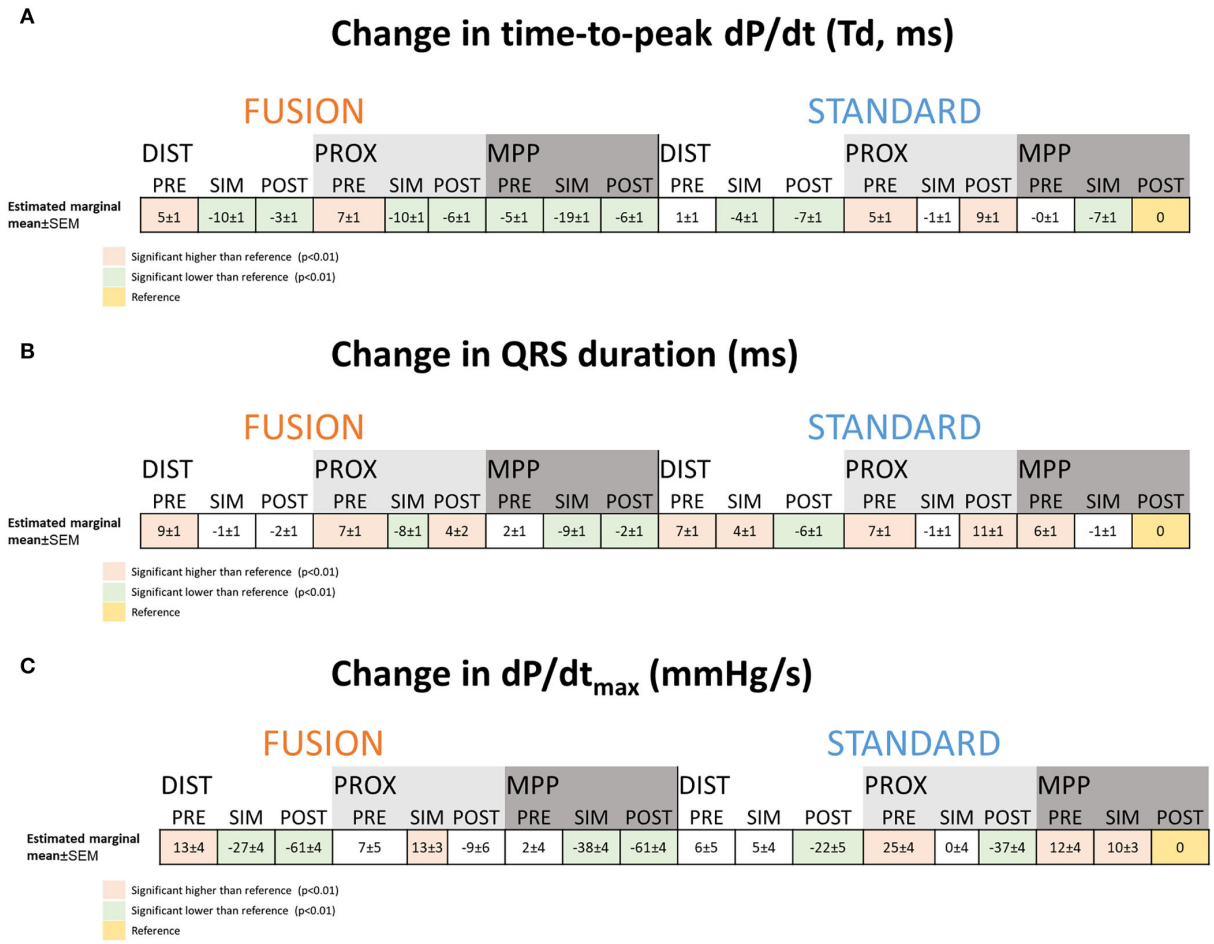

FIGURE 3
Analysis of the interaction effect between mode of pacing, electrode configuration and LV pre-/postexcitation on the change in Td and QRS duration. The tables show the estimated marginal means and standard error of the linear mixed models analysis for each interaction for time-to-peak dP/dt **(A)**, QRS duration **(B)**, and dP/dt_{max} **(C)**. The numbers are the estimated change from the reference selected as STANDARD*MPP*POST (marked in yellow). Colors that mark the estimates indicate a significant change compared to the reference ($p < 0.01$). Numbers are estimated marginal means ± SEM. DIST, distal electrode; PROX, proximal electrode; MPP, multipoint pacing; PRE—pre-excitation of the LV between 75 and 25 ms prior to QRS onset of RV pace onset; SIM— pacing the LV between 25 ms before and 25 ms after QRS onset or RV pace onset; POST, postexcitation of the LV 25–75 ms after QRS onset or RV pace onset, Td—time-to-peak dP/dt; dP/dt, first order derivative of pressure.

LBBB or LV pre- and postexcitation. In Figure 5, electrical dyssynchrony of the left ventricle is visualized by areas of LV preactivation resulting from either RV or LV electrodes. Dyssynchrony of the LV is ideally at its minimum with near-simultaneous activation of the electrode pair. Pacing from more electrodes recruits more tissue simultaneously, allowing more synergy from muscular contraction to occur (4).

We found a linear relationship between the change in Td and QRSd, indicating that the two markers reflect a similar underlying substrate. The change was measured relative to the reference being STANDARD*MMP*POST and is therefore sensitive to any errors in the reference. The correlation plot accounts for this. However, the dependency of the reference may explain the fixed bias in the Bland-Altman plot (Figure 3C). Other factors could also explain the fixed bias between the two measurements, such as the QRSd being dependent on both RV and LV activation while Td only depends on LV activation. Td shortens by a mean of almost 5 ms more than the QRSd. Shortening of LVAT could be partly concealed in the QRSd. Shortening in LVAT resulting from MPP will only translate into a corresponding change in the part of the QRSd solely resulting from LV activation (Figure 5). The portion of the QRSd that results from RV activation only will remain unchanged unless MPP directly affects RV activation (4). Changes in QRSd and Td seen in this study are small, and it is not clear from this study if the effect of MPP on QRSd and Td will translate into

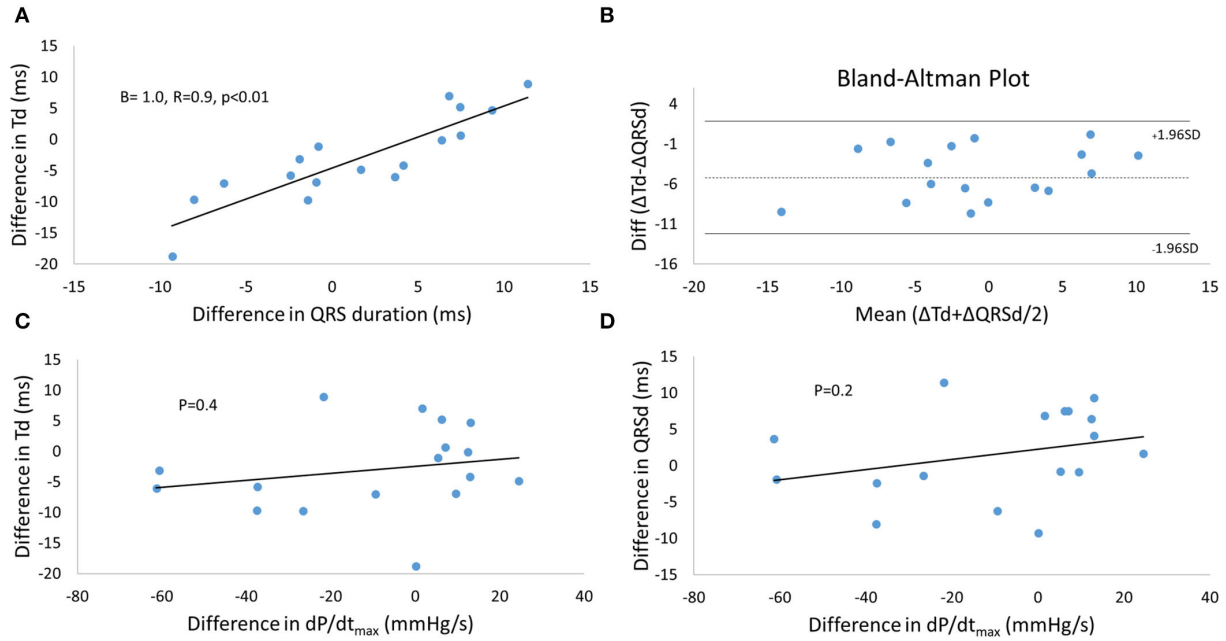

FIGURE 4
Agreement between mechanical and electrical measures during resynchronization with different modes of pacing and electrode configurations. **(A)** The relationship between the difference in Td and QRSd from the reference (STANDARD*MPP*POST, see Figure 3) as a result of resynchronization, and the Bland-Altman Plot **(B)** to demonstrate the agreement between the measurements. Linear relationships between the difference in Td **(C)** or the difference in QRSd **(D)** and the difference in dP/dt_{max} were not found. Td, time-to-peak dP/dt; dP/dt, first order derivative of pressure.

better long-term outcomes compared to standard pacing from a single LV electrode. The main point made in the study is that Td is a very sensitive marker of myocardial resynchronization that responds to small changes in electrical activation and wave-front fusion, not necessarily captured by the QRS complex. Td could be valuable for the optimization of resynchronization therapy.

We have previously published data on dP/dt_{max} from the current investigation and shown that dP/dt_{max} is mainly determined by LV preexcitation rather than effective resynchronization (7). As can be seen from Figure 3C, dP/dt_{max} trended to be higher with LV preexcitation and lower with LV postexcitation.

Clinical implications

QRS morphology and shortening of QRSd with CRT are predictive of response to CRT, however not perfect. Td seems to reflect the mechanical effects of electrical resynchronization directly and could therefore be helpful for optimization of the application of CRT. An increasing amount of evidence points toward restoring LV mechanics as the most critical mechanism for initiating the reverse remodeling processes. Measures of LV mechanical resynchronization are likely more accurate than QRSd for response prediction, as Td directly reflects left ventricular contraction patterns resulting from CRT. In addition, Td shortens with the restoration of LV synergistic contraction patterns following electrical resynchronization. The synergy effect from biventricular pacing measured by Td is predictive of long-term volumetric response. More data is, however, needed to confirm that the shortening of Td following optimization strategies will translate into better patient outcomes.

Limitations

A small number of patients limits the conclusions drawn from this study. The lack of direct insight into LV activation time intervals and exact electrical propagation in the tissue also limits this study. LV activation time, propagation and activated area over time would be better measures of the effect of fusion and resynchronization than QRSd. MPP may promote better resynchronization in the presence of a scar (19, 32). We used electrodes with limited spacing, and MPP with a longer electrode separation could have provided an even more apparent LV preexcitation effect (33). We did not structure the patients into long-term responders since the numbers of patients were small.

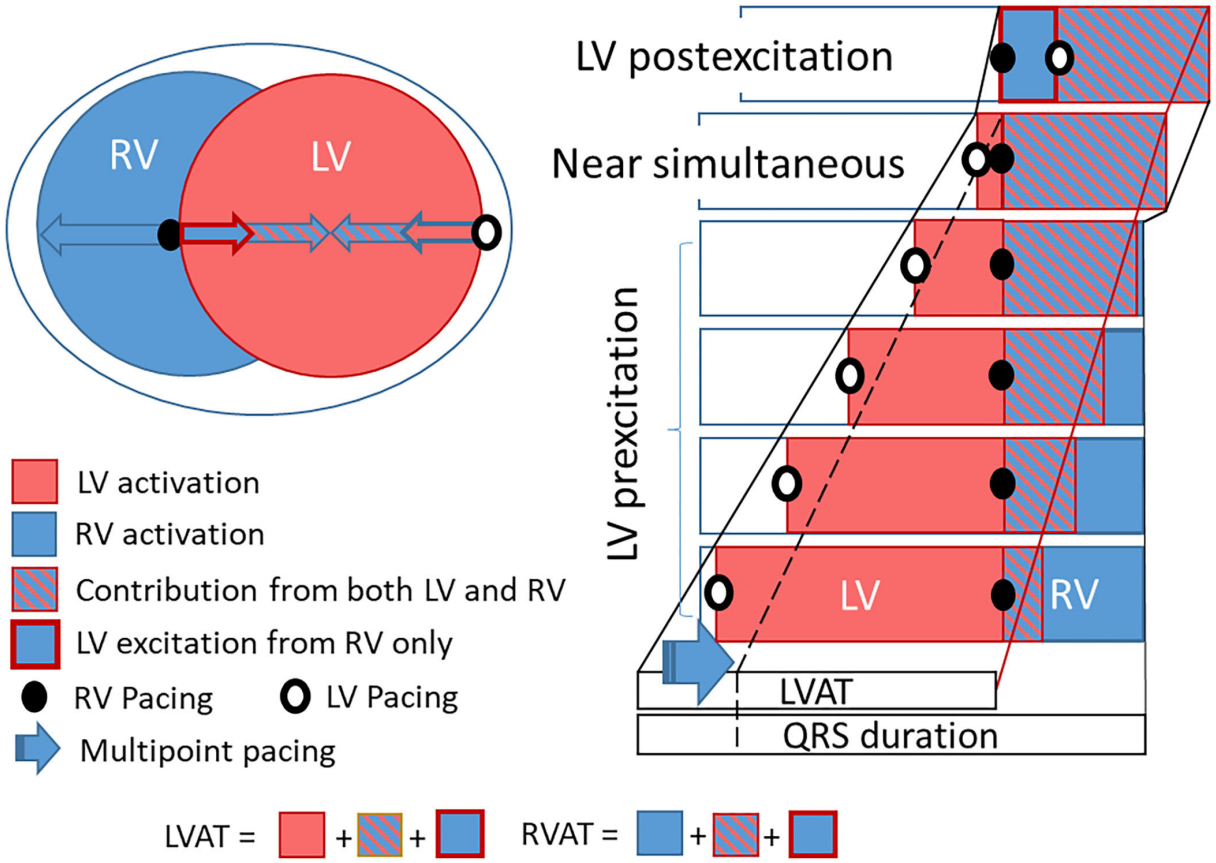

FIGURE 5
Diagramatic figure showing an ideal electrical activation diagram with the effect of LV pre-/postexcitation and electrodes on LVAT, RVAT and QRS duration. The diagram shows the theoretical change in LVAT and QRS duration relative to LV pre-/postexcitation based on pacing from the LV electrode, with ideally placed RV and LV electrodes. With near maximal LV pre-excitation, the LV is almost fully activated once RV is paced. The residual area, the area not yet activated from the LV as RV is paced, will be recruited from both the RV paced electrode and the LV paced electrode. Hence recruitment in the area will occur in a shorter time. This effect is more pronounced with less LV pre-excitation up to simultaneous pacing when the effect of combined activation of residual areas reaches its maximum, as the residual area recruited from both LV and RV electrodes is at its largest. LVAT and QRS duration shorten with less LV pre-excitation in this diagram down to simultaneous stimulation. Once the LV is postexcitated, the residual area shrinks and LVAT and QRS duration increase (as long as LVAT > RVAT). Shortening LVAT and QRS duration may also occur from multipoint pacing (MPP) with LV pre-excitation (blue arrow and stippled black line). It is clear from this diagram that the LV electrode position may largely affect LVAT and subsequently QRS duration and that intrinsic RV activation (that may shorten both RVAT and LVAT) will impact how this diagram reads. LV, left ventricle; RV, right ventricle; LVAT, left ventricular activation time; RVAT, right ventricular activation time.

Similarly, we could not stratify patients based on QRS morphology. IVCD patients may have a different Td response to CRT than LBBB patients. We have previously shown that non-responders may increase Td as a response to CRT, and such effects may have impacted our results (11). Another limitation of this paper is the comparison of Td measurements resulting from different references, referenced either from pacing or the onset of QRS. When paced, the measurement of Td and QRSd may be shorter than when measured from the onset of QRS (11). However, when measurements from QRS-onset were excluded, we still found that MPP*Sim provided the shortest Td indicating that the effect may not have affected the results. The effects would also be similar for QRSd and Td, and the linear relationship between the changes within the two also supports that the measurement reference may not have significantly impacted the conclusions in this study.

Conclusion

Multipoint pacing and fusion with right ventricular intrinsic activation improved the electrical resynchronization and the resulting myocardial synergy measured by Td. Pacing the left ventricular electrode(s) simultaneously with the onset of intrinsic right ventricular activation (QRS onset) shortens Td the most in patients with an indication for CRT. The shortening of QRSd was concordant with the shortening in Td. Td has the potential to serve as a marker for CRT optimization.

Data availability statement

The raw data supporting the conclusions of this article will be made available by the authors, without undue reservation.

Ethics statement

The studies involving human participants were reviewed and approved by Regional Ethics Committee South-East 2015/1624. The patients/participants provided their written informed consent to participate in this study.

Author contributions

HO conceived study protocol, organized the study, performed analyses, and wrote the manuscript. TH participated in the study and revised the manuscript. RC conceived study protocol, organized the study, and revised the manuscript. EK conceived study protocol, participated in the study, and revised manuscript. All authors contributed to the article and approved the submitted version.

Funding

The study was supported by a grant from Helse Sør-Øst RHF.

Conflict of interest

Author RC was employed by Medtronic.

The remaining authors declare that the research was conducted in the absence of any commercial or financial relationships that could be construed as a potential conflict of interest.

Publisher's note

References

1. Okafor O, Zegard A, van Dam P, Stegemann B, Qiu T, Marshall H, et al. Changes in QRS area and QRS duration after cardiac resynchronization therapy predict cardiac mortality, heart failure hospitalizations, and ventricular arrhythmias. *J Am Heart Assoc.* (2019) 8:e013539. doi: 10.1161/jaha.119.013539

2. Stankovic I, Stefanovic M, Prinz C, Ciarka A, Daraban AM, Kotrc M, et al. The association of mechanical dyssynchrony and resynchronization therapy with survival in heart failure with a wide QRS complex: a two-world study. *Int J Cardiovasc Imaging.* (2020) 36:1507–14. doi: 10.1007/s10554-020-01865-x

3. Mullens W, Auricchio A, Martens P, Witte K, Cowie MR, Delgado V, et al. Optimized Implementation of cardiac resynchronization therapy—a call for action for referral and optimization of care. *Eur J Heart Fail.* (2020) 22:2349–69. doi: 10.1002/ejhf.2046

4. Albatat M, Arevalo H, Bergsland J, Strom V, Balasingham I, Odland HH. Optimal pacing sites in cardiac resynchronization by left ventricular activation front analysis. *Comput Biol Med.* (2021) 128:104159. doi: 10.1016/j.compbiomed.2020.104159

5. Stephansen C, Sommer A, Kronborg MB, Jensen JM, Nørgaard BL, Gerdes C, et al. Electrically vs. imaging-guided left ventricular lead placement in cardiac resynchronization therapy: a randomized controlled trial. *EP Europace.* (2019) 21:1369–77. doi: 10.1093/europace/euz184

6. Manav Sohal M, Shoaib Hamid M, Giovanni Perego M, Paolo Della Bella M, Shaumik Adhya M, John Paisey M, et al. A multicenter prospective randomized controlled trial of cardiac resynchronization therapy guided by invasive dP/dt. *Heart Rhythm O2.* (2021) 2:19–27. doi: 10.1016/j.hroo.2021.01.005

7. Odland HH, Holm T, Gammelsrud LO, Cornelussen R, Kongsgaard E. Determinants of LV dP/dt. *Open Heart.* (2021) 8:1615. doi: 10.1136/openhrt-2021-001615

8. Aalen JM, Remme EW, Larsen CK, Andersen OS, Krogh M, Duchenne J, et al. Mechanism of abnormal septal motion in left bundle branch block: role of left ventricular wall interactions and myocardial scar. *JACC Cardiovasc Imaging.* (2019) 12:2402–13. doi: 10.1016/j.jcmg.2018.11.030

9. Duchenne J, Aalen JM, Cvijic M, Larsen CK, Galli E, Bezy S, et al. Acute redistribution of regional left ventricular work by cardiac resynchronization therapy determines long-term remodelling. *Eur Heart J Cardiovasc Imaging.* (2020) 21:619–28. doi: 10.1093/ehjci/jeaa003

10. Aalen JM, Donal E, Larsen CK, Duchenne J, Lederlin M, Cvijic M, et al. Imaging predictors of response to cardiac resynchronization therapy: left ventricular work asymmetry by echocardiography and septal viability by cardiac magnetic resonance. *Eur Heart J.* (2020) 41:3813–23. doi: 10.1093/eurheartj/ehaa603

11. Odland HH, Villegas-Martinez M, Ross S, Holm T, Cornelussen R, Remme EW, et al. Shortening of time-to-peak left ventricular pressure rise (Td) in cardiac resynchronization therapy. *ESC Heart Fail.* (2021) 8:5222–36. doi: 10.1002/ehf2.13601

12. Remme EW, Niederer S, Gjesdal O, Russell K, Hyde ER, Smith N, et al. Factors determining the magnitude of the pre-ejection leftward septal motion in left bundle branch block. *Europace.* (2016) 18:1905–13. doi: 10.1093/europace/euv381

13. Russell K, Eriksen M, Aaberge L, Wilhelmsen N, Skulstad H, Remme EW, et al. A novel clinical method for quantification of regional left ventricular pressure-strain loop area: a non-invasive index of myocardial work. *Eur Heart J.* (2012) 33:724–33. doi: 10.1093/eurheartj/ehs016

14. Thibault B, Dubuc M, Khairy P, Guerra PG, Macle L, Rivard L, et al. Acute haemodynamic comparison of multisite and biventricular pacing with a quadripolar left ventricular lead. *Europace.* (2013) 15:984–91. doi: 10.1093/europace/eus435

15. Varma N, Jia P, Ramanathan C, Rudy Y. RV electrical activation in heart failure during right, left, and biventricular pacing. *JACC Cardiovasc Imaging.* (2010) 3:567–75. doi: 10.1016/j.jcmg.2009.12.017

16. O'Donnell D, Manyam H, Pappone C, Park SJ, Leclercq C, Lunati M, et al. Ventricular activation patterns during intrinsic conduction and right ventricular pacing in cardiac resynchronization therapy patients. *Pacing Clin Electrophysiol.* (2021) 44:1663–70. doi: 10.1111/pace.14329

17. Varma N. Left ventricular electrical activation during right ventricular pacing in heart failure patients with LBBB: visualization by electrocardiographic imaging and implications for cardiac resynchronization therapy. *J Electrocardiol.* (2015) 48:53–61. doi: 10.1016/j.jelectrocard.2014.09.002

18. Bank AJ, Gage RM, Schaefer AE, Burns KV, Brown CD. Electrical wavefront fusion in heart failure patients with left bundle branch block and cardiac

resynchronization therapy: implications for optimization. *J Electrocardiol.* (2020) 61:47–56. doi: 10.1016/j.jelectrocard.2020.05.015

19. Albatat M, Bergsland J, Arevalo H, Odland HH, Wall S, Sundnes J, et al. Multisite pacing and myocardial scars: a computational study. *Comput Methods Biomech Biomed Eng.* (2020) 23:248–60. doi: 10.1080/10255842.2020.1711885

20. Derval N, Bordachar P, Lim HS, Sacher F, Ploux S, Laborderie J, et al. Impact of pacing site on QRS duration and its relationship to hemodynamic response in cardiac resynchronization therapy for congestive heart failure. *J Cardiovasc Electrophysiol.* (2014) 25:1012–20. doi: 10.1111/jce.12464

21. Varma N. Variegated left ventricular electrical activation in response to a novel quadripolar electrode: visualization by non-invasive electrocardiographic imaging. *J Electrocardiol.* (2014) 47:66–74. doi: 10.1016/j.jelectrocard.2013.09.001

22. Rickard J, Baranowski B, Grimm RA, Niebauer M, Varma N, Tang WHW, et al. Left ventricular size does not modify the effect of QRS duration in predicting response to cardiac resynchronization therapy. *Pacing Clin Electrophysiol.* (2017) 40:482–7. doi: 10.1111/pace.13043

23. Varma N, Lappe J, He J, Niebauer M, Manne M, Tchou P. Sex-specific response to cardiac resynchronization therapy: effect of left ventricular size and QRS duration in left bundle branch block. *JACC Clin Electrophysiol.* (2017) 3:844–53. doi: 10.1016/j.jacep.2017.02.021

24. Korantzopoulos P, Zhang Z, Li G, Fragakis N, Liu T. Meta-analysis of the usefulness of change in qrs width to predict response to cardiac resynchronization therapy. *Am J Cardiol.* (2016) 118:1368–73. doi: 10.1016/j.amjcard.2016.07.070

25. Molhoek SG, Vane L, Bootsma M, Steendijk P, Van Der Wall EE, Schalij MJ. QRS duration and shortening to predict clinical response to cardiac resynchronization therapy in patients with end-stage heart failure. *Pacing Clin Electrophysiol PACE.* (2004) 27:308–13. doi: 10.1111/j.1540-8159.2004.00433.x

26. Biton Y, Kutyifa V, Cygankiewicz I, Goldenberg I, Klein H, McNitt S, et al. Relation of QRS duration to clinical benefit of cardiac resynchronization therapy in mild heart failure patients without left bundle branch block: the multicenter automatic defibrillator implantation trial with cardiac resynchronization therapy substudy. *Circ Heart Fail.* (2016) 9:e002667. doi: 10.1161/circheartfailure.115.002667

27. Engels EB, Mafi-Rad M, van Stipdonk AM, Vernooy K, Prinzen FW. Why QRS duration should be replaced by better measures of electrical activation to improve patient selection for cardiac resynchronization therapy. *J Cardiovasc Transl Res.* (2016) 9:257–65. doi: 10.1007/s12265-016-9693-1

28. Gijsberts CM, Benson L, Dahlström U, Sim D, Yeo DP, Ong HY, et al. Ethnic differences in the association of QRS duration with ejection fraction and outcome in heart failure. *Heart.* (2016) 102:1464–71. doi: 10.1136/heartjnl-2015-309212

29. Ross S, Nestaas E, Kongsgaard E, Odland HH, Haland TF, Hopp E, et al. Septal contraction predicts acute haemodynamic improvement and paced QRS width reduction in cardiac resynchronization therapy. *Eur Heart J Cardiovasc Imaging.* (2020) 21:845–52. doi: 10.1093/ehjci/jez315

30. Wouters PC, Leenders GE, Cramer MJ, Meine M, Prinzen FW, Doevendans PA, et al. Acute recoordination rather than functional hemodynamic improvement determines reverse remodelling by cardiac resynchronisation therapy. *Int J Cardiovasc Imaging.* (2021) 37:1903–11. doi: 10.1007/s10554-021-02174-7

31. Gjesdal O, Remme EW, Opdahl A, Skulstad H, Russell K, Kongsgaard E, et al. Mechanisms of abnormal systolic motion of the interventricular septum during left bundle-branch block. *Circ Cardiovasc Imaging.* (2011) 4:264–73. doi: 10.1161/circimaging.110.961417

32. Ginks MR, Duckett SG, Kapetanakis S, Bostock J, Hamid S, Shetty A, et al. Multi-site left ventricular pacing as a potential treatment for patients with postero-lateral scar: insights from cardiac magnetic resonance imaging and invasive haemodynamic assessment. *Europace.* (2012) 14:373–9. doi: 10.1093/europace/eur336

33. Heckman LIB, Kuiper M, Anselme F, Ziglio F, Shan N, Jung M, et al. Evaluating multisite pacing strategies in cardiac resynchronization therapy in the preclinical setting. *Heart Rhythm O2.* (2020) 1:111–9. doi: 10.1016/j.hroo.2020.03.003

frontiers | Frontiers in Cardiovascular Medicine

TYPE Case Report
PUBLISHED 14 November 2022
DOI 10.3389/fcvm.2022.992675

OPEN ACCESS

EDITED BY
Hans Henrik Odland,
Oslo University Hospital, Norway

REVIEWED BY
Binni Cai,
Xiamen University, China
Vedran Velagic,
University Hospital Centre
Zagreb, Croatia
Sandro Brusich,
Clinical Hospital Centre Rijeka, Croatia

*CORRESPONDENCE
David Žižek
david.zizek@kclj.si

†These authors share senior authorship

SPECIALTY SECTION
This article was submitted to
Heart Failure and Transplantation,
a section of the journal
Frontiers in Cardiovascular Medicine

RECEIVED 12 July 2022
ACCEPTED 21 October 2022
PUBLISHED 14 November 2022

CITATION
Žlahtič T, Fister M, Radšel P, Noč M, Šinkovec M and Žižek D (2022) Case report: Treatment of tachycardia-induced cardiogenic shock with permanent His bundle pacing and atrioventricular node ablation.
Front. Cardiovasc. Med. 9:992675.
doi: 10.3389/fcvm.2022.992675

Case report: Treatment of tachycardia-induced cardiogenic shock with permanent His bundle pacing and atrioventricular node ablation

Tadej Žlahtič[1], Miša Fister[2], Peter Radšel[2], Marko Noč[2†], Matjaž Šinkovec[1†] and David Žižek[1*]

[1]Department of Cardiology, University Medical Centre Ljubljana, Ljubljana, Slovenia, [2]Department of Intensive Internal Medicine, University Medical Centre Ljubljana, Ljubljana, Slovenia

Tachycardia-induced cardiomyopathy (T-CMP) related to supraventricular arrhythmia is a rare and often unrecognized cause of refractory cardiogenic shock. When rhythm control interventions are ineffective or no longer pursued, atrioventricular node ablation (AVNA) with pacemaker implantation is indicated. Conduction system pacing provides normal synchronous activation of the ventricles after AVNA. However, there is a lack of data on pace and ablate strategy in hemodynamically unstable patients. We report on 2 patients with T-CMP presenting with refractory cardiogenic shock who were successfully treated with His bundle pacing in conjunction with AVNA.

KEYWORDS

His bundle pacing, cardiogenic shock, mechanical circulatory support, cardiac resynchronization therapy, tachycardia-induced cardiomyopathy, AV node ablation

Introduction

Tachycardia-induced cardiomyopathy (T-CMP) is defined as the presence of reversible left ventricular (LV) dysfunction due to persistent rapid ventricular rate, regardless of tachycardia etiology (1). The common causes of T-CMP are supraventricular arrhythmias, namely atrial fibrillation (AF), atrial flutter, and atrial tachycardia (1, 2). Most of the patients present with heart failure (HF) symptoms and palpitations, while cardiogenic shock and cardiac arrest remain relatively rare (1). Treatment of T-CMP consists of suppression of ventricular rate with antiarrhythmic drugs (AADs), arrhythmia elimination with radiofrequency ablation (RFA) or electrical cardioversion (EC), and atrioventricular node ablation (AVNA) with pacemaker implantation when rhythm control interventions are ineffective or no longer pursued (2). Recently, conduction system pacing was introduced into clinical practice which, in contrast to standard right ventricular (RV), provides normal synchronous activation and

10.3389/fcvm.2022.992675

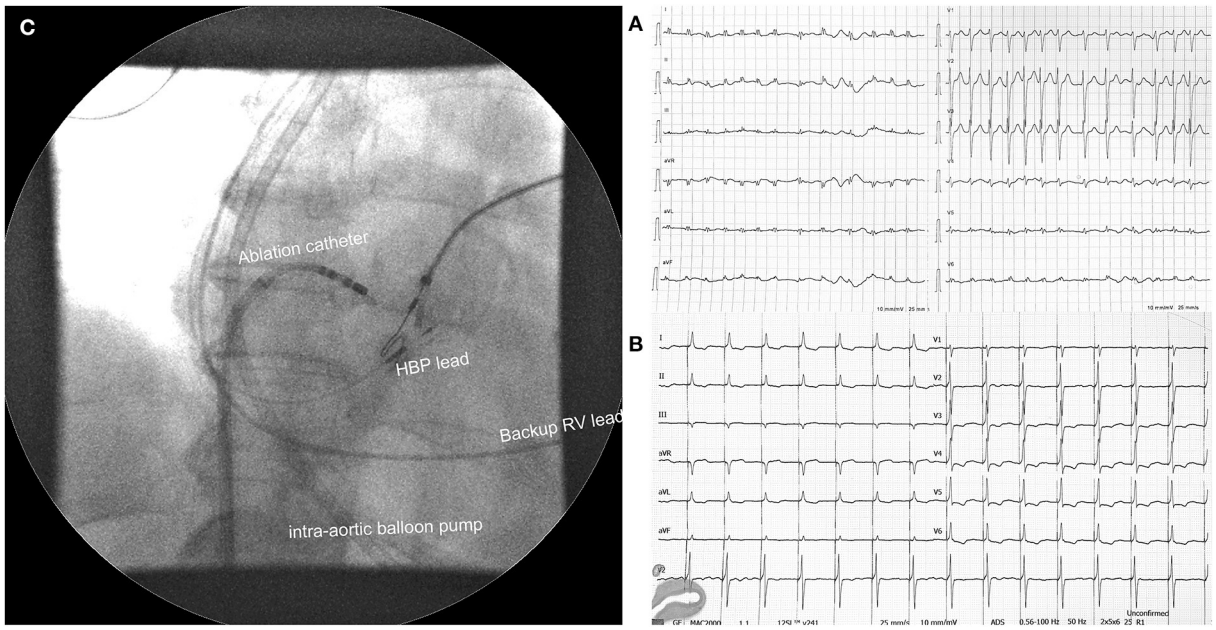

FIGURE 1
(A) Electrocardiogram at admission with visible atrial fibrillation with a ventricular rate of 150 bpm. **(B)** Electrocardiogram after atrioventricular node ablation and His bundle pacing. **(C)** Position of pacing leads and ablation catheter during fluoroscopy with visible intra-aortic balloon pump in the background. HBP, His bundle pacing; RV, right ventricle.

preserves LV function in HF patients (3). However, evidence for the use of "ablate and pace" strategy with HBP in the T-CMP presenting with cardiogenic shock are scarce.

We report two patients with T-CMP who were admitted to the intensive care unit (ICU) due to cardiogenic shock and were successfully treated with HBP and AVNA.

Case report

Case 1

A 65-year-old woman with a history of AF, diabetes type II, and ischemic CMP was admitted due to progressive dyspnea and peripheral oedema. As she was not attending regular outpatient clinic follow-ups, the level of heart rate control or the duration of AF was not well-established. On examination at the emergency department, she was hypotensive (93/56 mmHg) with signs of cardiogenic shock. A 12-lead ECG revealed AF with a ventricular rate of around 150 bpm (Figure 1). Bedsides, echocardiography showed severely dilated LV with severely reduced EF and dilated right ventricle (RV) with reduced systolic function. The left atrium was severely dilated (Table 1). Laboratory findings showed metabolic acidosis (pH 7.32), increased lactate levels (11,4 mmol/L), acute kidney injury [creatinine levels of 164 μmol/l, glomerular filtration rate (GFR) 28 mL/min/1,73m^2], severely elevated transaminases with international normalized ratio (INR) of 7, negative troponin, elevated NT-proBNP (7,024 pg/mL), and normal inflammatory markers. Initial supportive intravenous therapy did not result in clinical improvement. Invasive mechanical ventilation (MV) was initiated together with inhaled nitric oxide due to concomitant RV failure. Landiolol infusion resulted in a moderate heart rate decline from 170 to 140 bpm but shock persisted. Coronary angiography did not reveal obstructive coronary lesions. Intra-aortic balloon pump (IABP) was inserted but resulted in low augmented pressure due to tachycardia. Laboratory tests showed normal thyroid function. Bilateral stellate ganglion blockade did not result in a significant heart rate decrease. After 1 week of hospitalization and several unsuccessful synchronized EC, the "ablate and pace" strategy was attempted. Non-selective HBP was achieved with a stable pacing threshold of 2.25 V at 1 ms (Figure 1). There were no procedure-related complications. Hours after the procedure there was a significant improvement in LV function. Twenty-four h after the procedure her condition improved and IABP could be removed. We started with low dose HF therapy. Her condition further improved, and she was weaned from MV on day 17. Her blood pressure normalized, and LV function further improved. She was discharged from the hospital on day 43. At 1-year follow-up, her condition was stable (Table 1).

TABLE 1 Summary of clinical presentations, cardiac function, and pacing parameters.

	Case 1	Case 2
Clinical presentation	Cardiogenic shock with multiorgan failure needing mechanical circulatory support, on intra-aortic balloon pump, pulmonary oedema needing mechanical ventilation.	Cardiogenic shock with multiorgan failure on VA-ECMO, pulmonary oedema needing mechanical ventilation, thyrotoxicosis.
History	Ischemic cardiomyopathy (LVEF 55%), permanent atrial fibrillation	None
Medications	Warfarin, bisoprolol 7.5 mg q.d., furosemide 60 mg q.d., rosuvastatin 40 mg q.d.. Perindopril, spironolactone, and metildigoxin were canceled 1 week before admission due to worsening kidney function, hypotension, and high digoxin levels	No regular medication
Admission	EDV 140 ml LVEF 10% LVOT VTI 6 cm TAPSE 0.9 cm LAVI 57 ml/m2	EDV 170 ml LVEF 10% LVOT VTI 4 cm TAPSE 0.8 cm LAVI 52 ml/m2
After the procedure	EDV 140 ml LVEF 25% LVOT VTI 13 cm TAPSE 1.1 cm HBP threshold 2.25V@1 ms, impedance 418 Ohm Fluoroscopic time: 20 min Procedure duration: 90 min	EDV 170 ml LVEF 30% LVOT VTI 13 cm TAPSE 1.4 cm HBP threshold 0.75V@1 ms, impedance 510 Ohm Fluoroscopic time: 4.5 min Procedure duration: 50 min
At discharge	EDV 120 ml LVEF 39% LVOT VTI 15 cm TAPSE 1.3 cm HBP threshold 2.75V@1 ms	EDV 150 ml LVEF 45% LVOT VTI 20 cm TAPSE 2.4 cm HBP threshold 1.25V@1 ms
1 year follow up	EDV 116 ml LVEF 46% LVOT VTI 15 cm TAPSE 1.4 cm HBP threshold 3V@1 ms	EDV 140 ml LVEF 51% LVOT VTI 15 cm TAPSE 2.3 cm HBP threshold 1.5V@1 ms

VA-ECMO, veno-arterial extracorporeal membrane oxygenation; LVEF, left ventricular ejection fraction; EDV, end diastolic volume; LAVI, left atrial volume index; LVOT VTI, left ventricular outflow tract velocity time integral; TAPSE, tricuspid annular plane systolic excursion; HBP, His bundle pacing.

Case 2

A 51-year-old, previously healthy male, visited the emergency department due to progressive weakness and palpitations. On examination, he was hypotensive (94/73 mmHg) with signs of cardiogenic shock. The electrocardiogram showed AF with a rapid ventricular rate of 175 bpm (Figure 2). Laboratory results showed elevated lactate levels (3.6 mmol/L) with metabolic acidosis (pH 7.29), severely elevated transaminases, acute kidney injury (creatinine 226 μmol/l, GFR 28 mL/min/1,73m^2) with moderate hyperkaliemia (6 mmol/l). Within hours, the patient's status further deteriorated. Invasive MV was initiated, and a high dose of norepinephrine was needed. Transesophageal echo revealed dilated LV, enlarged atria, and severely decreased ventricular contractility (Table 1). No thrombi were found in the left atrium appendage. A coronary angiogram revealed non-obstructive coronary artery disease. Several synchronized EC attempts and intravenous AADs were unsuccessful in eliminating arrhythmia or markedly decreasing the ventricular rate. Due to refractory cardiogenic shock, peripheral percutaneous veno-arterial extracorporeal membrane oxygenation (VA-ECMO) was inserted. Further laboratory analysis confirmed elevated levels of thyroxin. Intravenous steroids and thiamazole were initiated. However,

multi-organ failure worsened rapidly and 4,5 L/min of ECMO flow was insufficient. Thus, we proceeded with an urgent "ablate and pace" strategy. His bundle pacing lead was inserted and selective HBP was achieved with a stable threshold of 0.75V at 1 ms. A return to sinus rhythm and significant improvement of cardiac function was expected, atrial and RV backup leads were also inserted and connected to the atrio-biventricular device (Figure 2). Within an hour after the procedure, the pulsatile flow was noted. The norepinephrine dose was lowered, and cardiac function improved significantly after 24 h. On day 5, VA-ECMO could be removed, and low dose HF therapy was initiated. Further ICU stay was prolonged due to bacterial ventilator associated pneumonia, gastric perforation, fungal infection, and critical illness myopathy with long ventilation weaning. The patient was discharged from hospital on day 47 with significantly improved cardiac function and sinus rhythm. At the 1-year follow-up, his condition was stable (Table 1).

His bundle pacing and atrioventricular node ablation procedure

In both presented cases device implantation was performed first followed by AVNA during the same procedure as previously described (4). We used SelectSecure 3,830 (Medtronic, Minneapolis, USA) active fixation leads and dedicated delivery sheaths. His bundle area mapping was performed in a unipolar setting with LAB system Pro (BARD/Boston Scientific, Lowell, USA) electrophysiological system. Atrioventricular node ablation was done with irrigated Flexability™ (Abbott, USA) or Celsius® Thermocool® (Biosense Webster, USA) tip ablation catheter in a temperature-controlled mode (40 W, up to 60 s). The lower rate of the pacing device was initially set to 80 bpm and programmed to 70 bpm at follow-up.

Discussion

With our case series, we were able to show that HBP in conjunction with AVNA could present a feasible and safe treatment option even in the T-CMP presenting with cardiogenic shock.

In a recent retrospective analysis, Hékimian et al. showed the feasibility of the "ablate and pace" strategy with temporary septal RV and later conversion to BiV pacing in patients with T-CMP requiring mechanical circulatory support (5). Nonetheless, the "ablate and pace" strategy is generally utilized in hemodynamically stable symptomatic patients with supraventricular tachycardia refractory to pharmacological therapy and RFA (2). However, several studies reported neutral findings regarding HF progression and survival, implying that the beneficial effects of rate control after AVNA could be

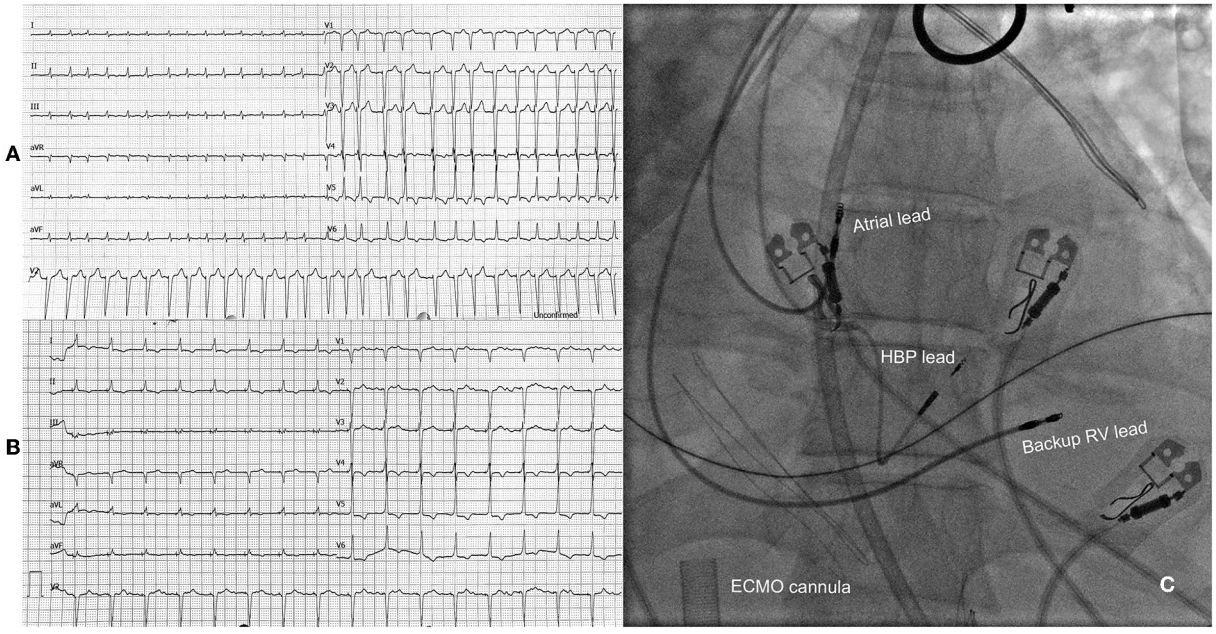

FIGURE 2
(A) Electrocardiogram at admission with visible atrial fibrillation with a ventricular rate of 175 bpm. **(B)** Electrocardiogram after atrioventricular node ablation and His bundle pacing. **(C)** Position of pacing leads during fluoroscopy with visible ECMO cannula in the background. HBP, His bundle pacing; RV, right ventricle; ECMO, extracorporeal membrane oxygenation.

hampered by non-physiologic dyssynchronous RV pacing (6). While biventricular pacing in conjunction with AVNA has shown better results compared to RV pacing, the benefit was much less distinct in patients with narrow QRS or normal left ventricular function (3, 6). By stimulating the native conduction system through a bundle of His, normal synchronous activation of the ventricles can be obtained. Therefore, it could represent an alternative to BiV pacing in patients with an expected high percentage of pacing with concomitant severe left ventricular dysfunction and narrow QRS (3, 7). Recent randomized trials further confirmed that HBP could deliver better improvement of EF compared to BiV in patients undergoing AVNA (8). However, there are some limitations associated with HBP, e.g.: higher capture thresholds, need for RV back-up lead, lower success rates, etc (4). Thus, left bundle branch area pacing could present an even better physiological pacing option to overcome these limitations, especially in the setting of AVNA (9).

An alternative approach could have adopted rhythm control with pulmonary vein isolation (PVI). Catheter ablation of AF has become a well-established procedure in HF patients as sinus rhythm restoration significantly lowers the rate of death or hospitalization for worsening heart failure compared with medical therapy alone (10, 11). However, there is still insufficient data on ablation in case of hemodynamic instability due to AF. Mantini et al. (11) reported successful ablation of atrial arrhythmias in five patients with cardiogenic shock on mechanical circulatory support. Although there were no complications reported, there were concerns about the safety of the procedure in critically ill patients with rapidly progressing cardiogenic shock (11). Ablation procedures in persistent AF are no more than 20–60% successful in maintaining the sinus rhythm. Furthermore, several patient characteristics play an important role in AF ablation success rates, for example, the need for high direct current energies for the restoration of sinus rhythm in cardioversion prior to ablation, left atrial size, AF duration, patient age, renal dysfunction, and substrate visualized on magnetic resonance imaging (10, 11). Therefore, it is conceivable to assume that the AF ablation strategy with PVI in our presented cases would not yield a significant probability of acute sinus rhythm restoration, especially in the setting of cardiogenic shock. Similar observations were noted by Hékimian et al., where only 1 ablation procedure was performed in 35 patients presenting with T-CMP and cardiogenic shock (5).

In conclusion, in the T-CMP presenting with cardiogenic shock "ablate and pace" strategy with HBP could present a feasible and safe treatment option for arrhythmia reduction. Further clinical studies are warranted to address the best strategy for addressing the severest forms of T-CMP.

Data availability statement

The original contributions presented in the study are included in the article/supplementary material, further inquiries can be directed to the corresponding author/s.

Ethics statement

Written informed consent was obtained from the individual(s) for the publication of any potentially identifiable images or data included in this article.

Author contributions

TŽ and DŽ have written majority of the manuscript. MF and PR contributed to conception and wrote sections of the manuscript. MN and MŠ have equally contributed to the manuscript revision. All authors contributed to manuscript revision, read, and approved the submitted version.

Conflict of interest

The authors declare that the research was conducted in the absence of any commercial or financial relationships that could be construed as a potential conflict of interest.

Publisher's note

References

1. Huizar JF, Ellenbogen KA, Tan AY, Kaszala K. Arrhythmia-induced cardiomyopathy. *J Am Coll Cardiol.* (2019) 73:2328–44. doi: 10.1016/j.jacc.2019.02.045

2. Brugada J, Katritsis DG, Arbelo E, Arribas F, Bax JJ, Blomström-Lundqvist C, et al. 2019 esc guidelines for the management of patients with supraventricular tachycardiathe task force for the management of patients

with supraventricular tachycardia of the European society of cardiology (Esc): developed in collaboration with the association for European paediatric and congenital cardiology (Aepc). *Eur Heart J.* (2019) 41:655–720. doi: 10.1093/eurheartj/ehz467

3. Huang W, Su L, Wu S, Xu L, Xiao F, Zhou X, et al. Benefits of permanent his bundle pacing combined with atrioventricular node ablation in atrial fibrillation patients with heart failure with both preserved and reduced left ventricular ejection fraction. *J Am Heart Assoc.* (2017) 6:e005309. doi: 10.1161/JAHA.116.005309

4. Vijayaraman P, Chung MK, Dandamudi G, Upadhyay GA, Krishnan K, Crossley G, et al. His bundle pacing. *J Am Coll Cardiol.* (2018) 72:927–47. doi: 10.1016/j.jacc.2018.06.017

5. Hékimian G, Paulo N, Waintraub X, Bréchot N, Schmidt M, Lebreton G, et al. Arrhythmia-induced cardiomyopathy: a potentially reversible cause of refractory cardiogenic shock requiring venoarterial extracorporeal membrane oxygenation. *Heart Rhythm.* (2021) 18:1106–12. doi: 10.1016/j.hrthm.2021.03.014

6. Stavrakis S, Garabelli P, Reynolds DW. Cardiac resynchronization therapy after atrioventricular junction ablation for symptomatic atrial fibrillation: a meta-analysis. *EP Europace.* (2012) 14:1490–7. doi: 10.1093/europace/eus193

7. Žižek D, Antolič B, Mežnar AZ, Zavrl-Džananović D, Jan M, Štublar J, et al. Biventricular versus his bundle pacing after atrioventricular node ablation in heart failure patients with narrow qrs. *Acta Cardiol.* (2021) 2021:1–9. doi: 10.1080/00015385.2021.1903196

8. Huang W, Wang S, Su L, Fu G, Su Y, Chen K, et al. His-bundle pacing vs biventricular pacing following atrioventricular nodal ablation in patients with atrial fibrillation and reduced ejection fraction: a multicenter, randomized, crossover study—the alternative-af trial. *Heart Rhythm.* (2022) 14:S1547-5271(22)02172-5. doi: 10.1016/j.hrthm.2022.07.009

9. Zhang S, Zhou X, Gold MR. Left bundle branch pacing. *J Am Coll Cardiol.* (2019) 74:3039–49. doi: 10.1016/j.jacc.2019.10.039

10. Hindricks G, Potpara T, Dagres N, Arbelo E, Bax JJ, Blomström-Lundqvist C, et al. 2020 esc guidelines for the diagnosis and management of atrial fibrillation developed in collaboration with the European association of cardio-thoracic surgery (Eacts): the task force for the diagnosis and management of atrial fibrillation of the European society of cardiology (Esc) developed with the special contribution of the European heart rhythm association (Ehra) of the esc. *Eur Heart J.* (2020) 42:373–498. doi: 10.1093/eurheartj/ehaa612

11. Mantini N, Zipse M, Tompkins C, Varosy PD, Sauer WH, Nguyen DT. Ablation of atrial arrhythmias in patients with cardiogenic shock on mechanical circulatory support. *HeartRhythm Case Rep.* (2018) 5:115–9. doi: 10.1016/j.hrcr.2018.11.008

frontiers | Frontiers in Physiology

TYPE Original Research
PUBLISHED 14 December 2022
DOI 10.3389/fphys.2022.1049214

OPEN ACCESS

EDITED BY
Maciej M. Sterlinski,
National Institute of Cardiology, Poland

REVIEWED BY
Joakim Sundnes,
Simula Research Laboratory, Norway
Yawer Saeed,
Aga Khan University, Pakistan

*CORRESPONDENCE
Marina Strocchi,
marina.strocchi@kcl.ac.uk

SPECIALTY SECTION
This article was submitted to Cardiac Electrophysiology, a section of the journal Frontiers in Physiology

RECEIVED 20 September 2022
ACCEPTED 28 November 2022
PUBLISHED 14 December 2022

CITATION
Strocchi M, Wijesuriya N, Elliott MK, Gillette K, Neic A, Mehta V, Vigmond EJ, Plank G, Rinaldi CA and Niederer SA (2022), Leadless biventricular left bundle and endocardial lateral wall pacing versus left bundle only pacing in left bundle branch block patients. *Front. Physiol.* 13:1049214. doi: 10.3389/fphys.2022.1049214

Leadless biventricular left bundle and endocardial lateral wall pacing versus left bundle only pacing in left bundle branch block patients

Marina Strocchi[1]*, Nadeev Wijesuriya[1,2], Mark K. Elliott[1,2], Karli Gillette[3,4], Aurel Neic[5], Vishal Mehta[1,2], Edward J. Vigmond[6,7], Gernot Plank[3,4], Christopher A. Rinaldi[1,2] and Steven A. Niederer[1]

[1]School of Biomedical Engineering and Imaging Sciences, King's College London, London, United Kingdom, [2]Guy's and St Thomas' NHS Foundation Trust, London, United Kingdom, [3]BioTechMed-Graz, Graz, Austria, [4]Gottfried Schatz Research Center, Medical University of Graz, Graz, Austria, [5]NumeriCor GmbH, Graz, Austria, [6]University of Bordeaux, CNRS, Bordeaux, France, [7]IHU Liryc, Bordeaux, France

Biventricular endocardial (BIV-endo) pacing and left bundle pacing (LBP) are novel delivery methods for cardiac resynchronization therapy (CRT). Both pacing methods can be delivered through leadless pacing, to avoid risks associated with endocardial or transvenous leads. We used computational modelling to quantify synchrony induced by BIV-endo pacing and LBP through a leadless pacing system, and to investigate how the right-left ventricle (RV-LV) delay, RV lead location and type of left bundle capture affect response. We simulated ventricular activation on twenty-four four-chamber heart meshes inclusive of His-Purkinje networks with left bundle branch block (LBBB). Leadless biventricular (BIV) pacing was simulated by adding an RV apical stimulus and an LV lateral wall stimulus (BIV-endo lateral) or targeting the left bundle (BIV-LBP), with an RV-LV delay set to 5 ms. To test effect of prolonged RV-LV delays and RV pacing location, the RV-LV delay was increased to 35 ms and/or the RV stimulus was moved to the RV septum. BIV-endo lateral pacing was less sensitive to increased RV-LV delays, while RV septal pacing worsened response compared to RV apical pacing, especially for long RV-LV delays. To investigate how left bundle capture affects response, we computed 90% BIV activation times (BIVAT-90) during BIV-LBP with selective and non-selective capture, and left bundle branch area pacing (LBBAP), simulated by pacing 1 cm below the left bundle. Non-selective LBP was comparable to selective LBP. LBBAP was worse than selective LBP (BIVAT-90: 54.2 $\pm$ 5.7 ms vs. 62.7 $\pm$ 6.5, $p < 0.01$), but it still significantly reduced activation times from baseline. Finally, we compared leadless LBP with RV pacing against optimal LBP delivery through a standard lead system by simulating BIV-LBP and selective LBP alone with and without optimized atrioventricular delay (AVD). Although LBP alone with optimized AVD was better than BIV-LBP, when AVD optimization was not possible BIV-LBP

outperformed LBP alone, because the RV pacing stimulus shortened RV activation (BIVAT-90: 54.2 ± 5.7 ms vs. 66.9 ± 5.1 ms, $p < 0.01$). BIV-endo lateral pacing or LBP delivered through a leadless system could potentially become an alternative to standard CRT. RV-LV delay, RV lead location and type of left bundle capture affect leadless pacing efficacy and should be considered in future trial designs.

KEYWORDS

cardiac resynchronization therapy, left bundle branch block, leadless pacing, dyssynchrony, conduction system pacing, left bundle pacing, endocardial pacing

Introduction

Cardiac resynchronization therapy (CRT) is an effective treatment for heart failure patients with left bundle branch block (LBBB). Conventional CRT is delivered through a right ventricular (RV) lead, normally implanted in the RV apex, and a transvenous left ventricular (LV) lead implanted in the coronary sinus targeting the latest activated region, to achieve biventricular (BIV) pacing. Despite a large amount of evidence of CRT benefits on patients with LV dyssynchrony, between 30% and 50% of patients receiving CRT do not experience target clinical improvements (Sieniewicz et al., 2019). CRT inefficacy has been attributed to many factors, including challenging coronary sinus anatomy, presence of scar and phrenic nerve stimulation (Butter et al., 2021). Furthermore, transvenous leads are associated with risk of lead infection or rupture, sometimes requiring risky extraction procedures (Bernard, 2016).

Endocardial pacing and conduction system pacing (CSP) have emerged as potential alternatives to standard CRT, to reduce the rate of non-responders. Biventricular endocardial (BIV-endo) pacing delivered through an RV apical lead and an LV endocardial lead was shown to be more beneficial than standard CRT (Behar et al., 2016). BIV-endo pacing is not restricted by the coronary sinus anatomy, provides faster access to the ventricular fast conducting system and preserves physiological transmural activation from endocardium to epicardium (Prinzen et al., 2009; Hyde et al., 2015). However, the implantation of an LV endocardial lead requires lifelong anticoagulation to reduce the risk of stroke (Morgan et al., 2016). Furthermore, ventricular resynchronization relies on the fusion of two unphysiological wavefronts spreading from the RV apex and the LV free wall. CSP has the potential to restore the native synchronous activation of the patient prior to the block. CSP delivered through His bundle pacing (HBP) was shown to be more beneficial than standard CRT (Arnold et al., 2018), but it requires high pacing thresholds and is challenging to perform, restricting this method to centers with experienced operators. Compared to HBP, left bundle pacing (LBP) offers lower and more stable thresholds with a larger area to target, making it easier to perform. Response to LBP might however depend on atrioventricular (AV) delay optimization (Strocchi et al., 2020b; Lin et al., 2020) and type of left bundle capture (selective vs. non-selective vs. septal myocardium pacing). Often, LBP is delivered through a lead screwed deep in the septum from the RV side, although pacing is not always achievable through this method. Pacing through the LV septum may be more reliable, but this would increase the risk of stroke with a conventional lead pacing system.

As mentioned above, BIV-endo pacing and LV LBP applicability is hindered by the risk of stoke following lead implantation. These risks can be attenuated by delivering pacing through a leadless pacing system. The WiSE-CRT system (EBR Systems Inc., Sunnyvale, CA) is the only commercially available leadless LV pacing system (Auricchio et al., 2014). The system consists of a battery connected to an ultrasound transducer implanted subcutaneously between the ribs and an LV leadless endocardial receiver electrode. It also requires a device capable of performing continuous RV pacing, such as a transvenous pacemaker, implantable cardioverter defibrillator (ICD), or a leadless RV pacemaker such as MICRA™ (Medtronic, Minneapolis, NN). The transmitter and the battery then detect the RV pacing spike and, within 10 ms, the ultrasound transmitter emits several ultrasound pulses to locate the receiving LV electrode, normally located in the lateral wall (Auricchio et al., 2014; Reddy et al., 2017; Sieniewicz et al., 2020). Once the electrode is located, a longer pulse is emitted and converted by the electrode to a pacing stimulus, resulting in BIV-endo lateral wall pacing. LBP delivery could also be improved by delivering LV septal pacing through an LV leadless system. The feasibility, safety and short-term response of LBP through the WiSE-CRT system was assessed by Elliott et al. in patients and pigs (Elliott et al., 2021; Elliott et al., 2022). In (Elliott et al., 2022), LBP alone was performed first with a temporary mapping catheter to ensure correct targeting of the left bundle. Once left bundle capture was achieved, the leadless electrode was implanted and anchored to perform leadless LBP. Short-term safety and response were assessed, although there remain questions about long-term effects of this implantation technique. Despite the development of BIV-endo pacing, LBP and leadless pacing (Behar et al., 2016; Reddy et al., 2017; Sieniewicz et al., 2020; Elliott et al., 2021), there are still questions about how the RV lead location (apex vs. septum), LV lead location (lateral wall vs. septum), RV-LV delay and LBP type of capture affect response.

This study aims to use computational electrophysiology to address unanswered clinical questions about BIV-endo pacing and LBP delivered through leadless pacing in LBBB patients. We run simulations to mimic the protocol used in (Elliott et al., 2022) to quantify the efficacy of leadless LBP (e.g., LBP in conjunction with RV pacing) vs. LBP alone in resynchronizing ventricular activation. The effect of RV pacing location and RV-LV delay on response is quantified by repeating the pacing protocol with an RV apical lead and an RV septal lead, and by increasing the RV-LV delay from 5 ms to 35 ms. The effect of the type of left bundle capture is assessed by simulating selective LBP, non-selective LBP and left bundle branch area pacing (LBBAP) by pacing 1 cm below the left bundle. In addition, we compare leadless LBP to BIV-endo lateral wall pacing to assess the effect of the LV electrode location on simulated electrical response.

Methods

Electrophysiology simulations

We performed electrophysiology simulations on twenty-four chamber heart geometries generated from heart failure patients and published as part of a previous study (Strocchi et al., 2020a). The meshes were made of linear tetrahedral elements, with an average resolution of 1 mm. Local ventricular activation times were computed using the Eikonal equation (Neic et al., 2017). The Eikonal model computes the local time $t_a(\mathbf{x})$ at each node with location $\mathbf{x}$ within a domain Ω, provided an initial activation time t_0 at an initial stimulus location Γ and the conduction velocity (CV) tensor $\mathbf{V}$, containing the squared CV along the fiber, sheet and normal to sheet directions.

$$\sqrt{\nabla t_a(x)^T V \nabla t_a(x)} = 1, x \in \Omega$$
$$t_a(x) = t_0, x \in \Gamma$$

In this study, the domain Ω consisted of the ventricular myocardium and the His-Purkinje network. The stimulus locations Γ were set to the first node of the His and to the CRT stimuli locations (as detailed below) during baseline and pacing simulations, respectively. Ventricular myocardium was simulated as a transversely isotropic conduction medium with fibers and cross-fibers CV set to 0.6 m/s and 0.24 m/s (Taggart et al., 2000), respectively, while the His-Purkinje CV was set to 3.0 m/s (Ono et al., 2009). The Eikonal equation was solved with the Fast Iterative Algorithm, as described in (Neic et al., 2017).

For each geometry, we generated a His-Purkinje network with proximal LBBB. The Purkinje tree was grown on the endocardial surfaces of the ventricles and accounted for five fascicles: LV anterior, LV posterior, LV septal, RV septal and RV moderator band. The location for the fascicle root points was provided according to early activation sites in the Durrer maps, using the universal ventricular coordinates (UVCs) (Bayer et al., 2018) to ensure consistency across the meshes. The ventricular myocardium and the His-Purkinje system were coupled by connecting each terminal point of the Purkinje network with the points of the myocardium within 1 mm distance to allow for stimulus propagation from the Purkinje system to the myocardium and *vice versa*. The anterograde and retrograde delay were set to 10 ms and 3 ms, respectively, based on (Behradfar et al., 2014) Further details about the His-Purkinje network generation can be found in the Supplement and in (Gillette et al., 2021; Gillette et al., 2022). In the supplement, we also provide a validation of our model during LBBB baseline by comparing the simulated activation pattern and metrics against electrocardiographic imaging data.

Figure 1 summarizes the CRT simulations performed in this study. The pacing locations listed below provide stimuli regions Γ (see Eikonal equation above) where we prescribe an activation time. The earliest stimulus location was assigned with an activation time of 0 ms, while other pacing locations (if any) were stimulated according to a specified delay. Leadless BIV pacing was simulated by stimulating the RV at the apex and the LV at the lateral wall (BIV-endo lateral) or at the septum, selectively targeting the left bundle (BIV-LBP). Unless otherwise specified, the RV-LV delay was set to 5 ms, simulating a nearly simultaneous LV stimulus after RV pacing spike detection through the transducer, in keeping with real-world techniques. LBP through a standard lead was simulated by pacing the LBP selectively without RV pacing. LBP alone was simulated both with and without AV delay optimization. In LBP simulations with AV delay optimization, we paced the left bundle and the first node of the His to simulate two activation waves, one starting at the LBP site and one travelling from the atria down to the ventricles. We stimulated these sites with delays of 0 ms, e.g. left bundle paced when the activation wave enters the His, 10 ms, 20 ms or 30 ms, e.g. the left bundle is stimulated 30 ms after the activation wave enters the His. We also simulated LBP-ahead pacing, where the left bundle is stimulated 10 ms, 20 ms or 30 ms before the activation wave enters the His. We then selected the simulation that provided the shortest activation times, defined according to the activation metrics described below. All simulations apart from LBP with optimized AV delay were carried out under the assumption that pacing completely overwrites the patient's native activation. All pacing stimuli were prescribed with a radius of 1.5 mm.

Patients with septal scar might have different response to pacing compared to patients with proximal LBBB alone. To investigate the effect of the presence of septal scar on our analysis, we ran simulations in the presence of septal scar, and we presented our results in the supplement. We mapped a patient-specific scar and border zone geometry from a publicly available LV mesh (Mendonca Costa et al., 2019) using the UVCs (Bayer et al., 2018). The UVCs were computed on the LV of our twenty-four meshes and on the LV of the mesh the scar was mapped from. Then, the scar and

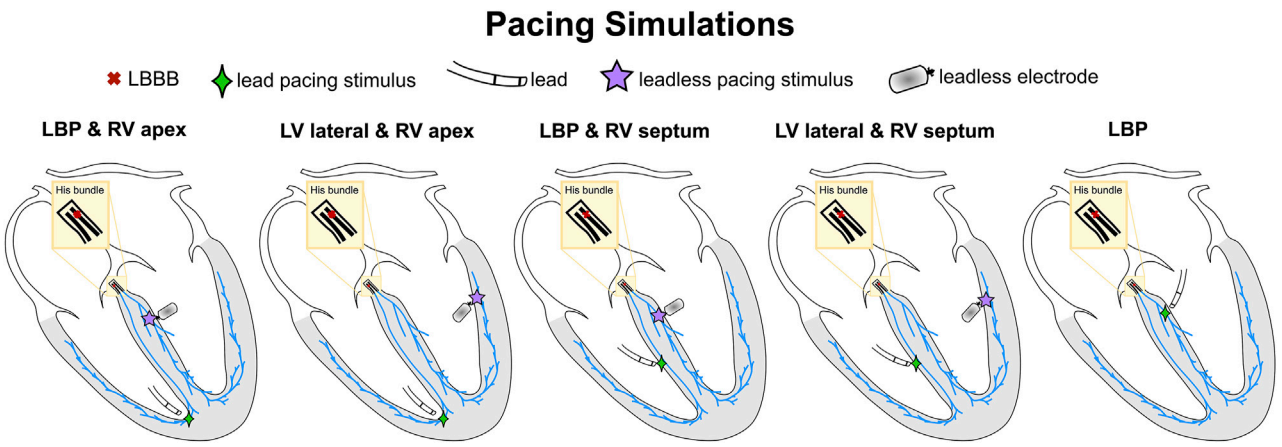

FIGURE 1
Schematic representation of pacing simulations. The red cross shows the proximal LBBB introduced along the His. The green diamonds and the purple stars represent the pacing locations through a standard lead and a leadless electrode, respectively.

border zone were mapped by finding the closest element in UVC distance on the target mesh. Scar tissue was simulated as non-conducting, while the border zone was assigned with an isotropic CV of 0.24 m/s (Mendonca Costa et al., 2019). The Purkinje overlapping the scar was also simulated as non-conducting.

Electrical response

We studied the effect of RV lead location and RV-LV delay on response to BIV-endo lateral pacing and BIV-LBP, and how the type of LBP capture affects BIV-LBP efficacy. To this end, BIV-endo lateral pacing and BIV-LBP simulations were repeated with an increased RV-LV delay of 10, 20, 30 and 35 ms. The RV pacing stimulus was then moved from the apex to the septum to quantify changes in response caused by the RV lead location. Finally, to investigate the effect of left bundle capture, BIV-LBP simulations were repeated with three different types of left bundle capture: selective, non-selective and septal myocardium capture (e.g., left bundle branch area pacing, LBBAP). Selective LBP was simulated by selectively pacing the left bundle. Non-selective pacing and LBBAP were simulated by extending the LBP stimulus to the surrounding myocardium and by pacing the LV septum1 cm below the left bundle, respectively.

To quantify LV and BIV synchrony, we computed LVAT-95 and BIVAT-90 as the shortest interval to activate 95% of the LV and 90% of the ventricles, respectively. Additionally, we quantified the LV and BIV dyssynchronous index (LVDI and BIVDI) as the standard deviation of the LV and BIV activation times, respectively. The area around the four cardiac valves were excluded when computing activation times.

Simulation results were compared using one-way analysis of variance (ANOVA). Post-hoc comparison analysis was performed to see which pairwise comparisons were statistically different using the Tukey's honestly significant difference test.

Results

Comparison between leadless BIV pacing and selective LBP

We used computational electrophysiology to mimic the pacing protocol in (Elliott et al., 2022), with LBP alone followed by leadless LBP (e.g., BIV-LBP). BIV-LBP was simulated with an RV apical stimulus and selective LBP with an RV-LV delay of 5 ms, while selective LBP alone was simulated by pacing the left bundle, both with and without optimized AV delay. Figure 2 shows the simulated activation times (A) and the response metrics (B) during baseline and pacing. Selective LBP with optimized AV delay led to optimal synchrony, with shorter LV activation compared to baseline, where the LV was activated later than the RV. In the presence of complete AV block (e.g. when AV delay optimization is not possible), the LV was still activated quickly, but the RV activation was delayed because the patient's intrinsic activation was unable to travel down from the atria along the right bundle to activate the RV. The RV stimulus introduced during BIV-LBP improved RV activation compared to selective LBP with AV block. In terms of activation metrics (Figure 2B), selective LBP with and without AV delay optimization and BIV-LBP significantly shortened LV and BIV activation times compared to baseline. Selective LBP with optimized AV delay was better than BIV-LBP, although the difference was not statistically significant for BIVAT-90 (BIVAT-90: 54.2 ± 5.7 ms P = 0.09, LVAT-95: 64.0 ± 6.3 ms,

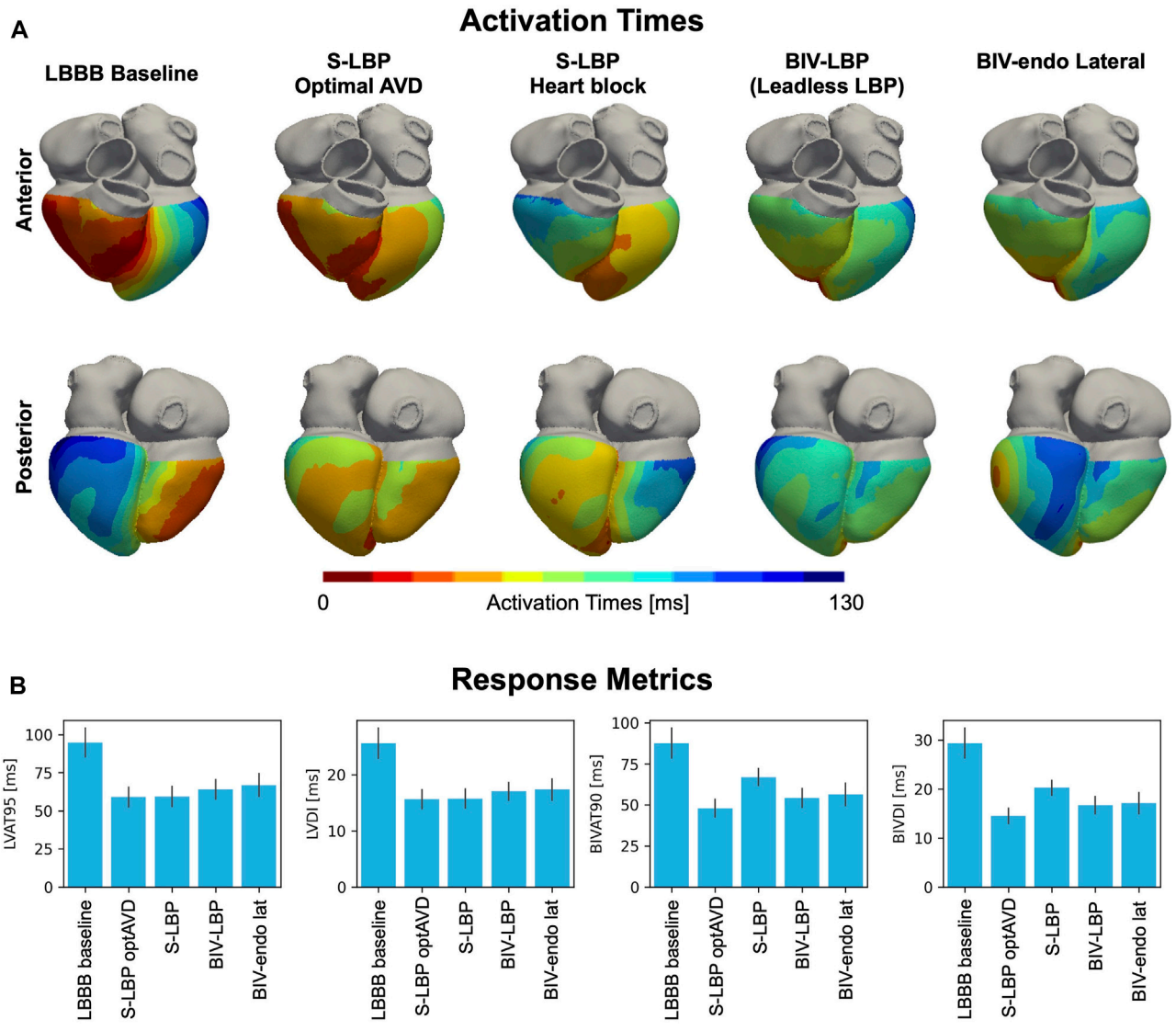

FIGURE 2
(A) Simulated activation times: Red and blue areas represent early and late activated regions, respectively. We show simulations during LBBB baseline, selective LBP (S-LBP) with and without AV delay optimization, leadless S-LBP (BIV-LBP, e.g., with an additional RV apical stimulus) and BIV-endo pacing with the LV lead in the lateral wall (BIV-endo lat). **(B)** Response metrics: BLVAT-95, LVDI, BIVAT-90 and BIVDI are shown for baseline and pacing. The bar plot represents the mean while the black segments represent ±standard deviation.

$p < 0.01$). However, when AV delay optimization was not possible, BIV-LBP achieved better synchrony compared to LBP without RV pacing (BIVAT-90: 54.2 ± 5.7 ms vs. 66.9 ± 5.1 ms, $p < 0.01$). Although selective LBP with optimized AV delay delivered through a standard pacing lead remains the best LBP delivery method for patients without AV block or atrial fibrillation, when AV delay optimization is not possible a leadless system offers better synchrony than LBP alone.

We compared BIV-LBP and selective LBP alone with BIV-endo lateral wall pacing, as the LV lateral wall is the standard location for the LV leadless electrode implantation. The last column of Figure 2A shows activation times simulated during BIV-endo lateral pacing. Pacing from the LV endocardial lateral wall improved activation compared to baseline, as the LV lateral wall stimulus shortened LV activation while the RV apical stimulus kept RV activation short. Similarly, to BIV-LBP and selective LBP alone, BIV-endo lateral wall pacing significantly shortened LV and BIV activation times compared to baseline. However, BIV-endo lateral wall pacing was significantly worse than selective LBP alone with optimized AV delay in terms of both ventricular (BIVAT-90: 48.0 ± 5.3 ms vs. 56.4 ± 6.8 ms, $p < 0.01$) and LV activation times (LVAT-95: 59.0 ± 6.5 ms vs. 66.9 ±

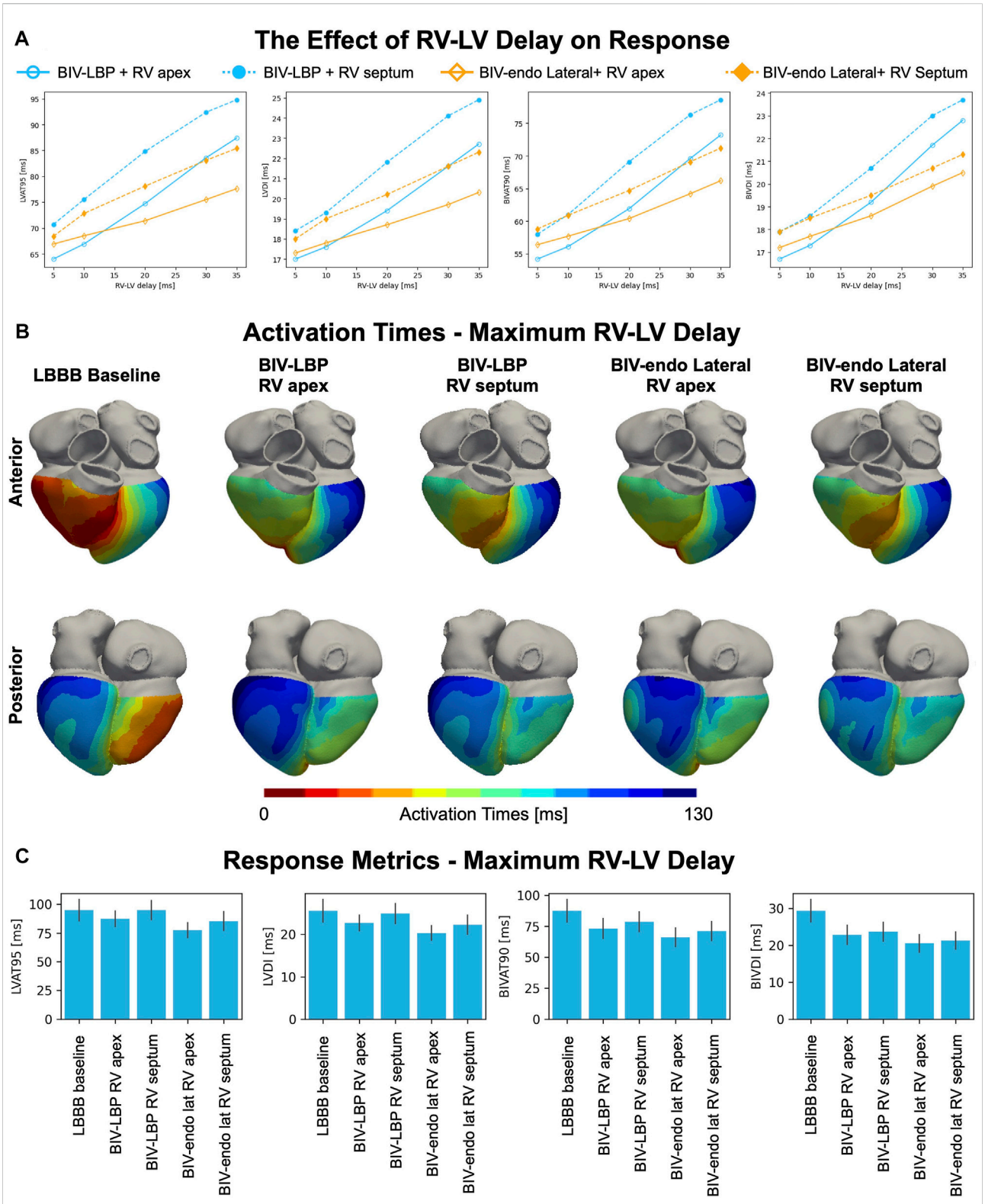

FIGURE 3
The effect of RV-LV delay and RV pacing location on response. **(A)** Mean LVAT-95, LVDI, BIVAT-90 and BIVDI achieved with BIV-endo lateral pacing or BIV-LBP with RV apical or septal pacing for different RV-LV delays. **(B)** Simulated activation times during baseline and pacing for maximum RV-LV delay (35 ms). **(C)** Response metrics (mean ± standard deviation) simulated during baseline and pacing.

7.4 ms, $p < 0.01$). BIV-endo lateral wall pacing was however comparable to BIV-LBP (BIVAT-90: 54.2 ± 5.7 ms vs. 56.4 ± 6.8 ms, $p = 0.9$), indicating that placing the LV leadless electrode in the LV lateral wall does not result in a significantly different response compared to selectively targeting the left bundle.

In the supplement, we analyzed the effect of septal scar on our results by repeating the comparisons above in the presence of non-conductive tissue in the septum. Our results show that septal scar makes BIV-LBP and LBP completely ineffective because the LBP stimulus does not capture the healthy myocardium or Purkinje. On the other hand, BIV-endo lateral pacing remains effective.

The effect of prolonged RV-LV delay

Although BIV-LBP and BIV-endo lateral wall pacing were comparable with an RV-LV delay of 5 ms, response to pacing might be affected by the RV-LV delay or by the RV lead location. To test this, we repeated BIV-LBP and BIV-endo lateral wall pacing simulations for increasingly long RV-LV delays and with the RV stimulus moved from the RV apex to the RV septum (Figure 3). BIV-endo lateral wall pacing was less sensitive to prolonged RV-LV delays compared to BIV-LBP (Figure 3A, solid lines), and moving the electrode from the RV apex to the RV septum worsened response (Figure 3A, dashed lines). LV lateral wall pacing however remained less sensitive to prolonged RV-LV delay compared to selective LBP. The distribution of simulated activation times in Figure 3B shows that when the RV-LV delay was long (35 ms), BIV-LBP led to similar activation to baseline. In particular, when the RV lead is placed in the septum, LV activation remains unchanged from baseline because when the LV stimulus is fired, the LV septum has already been activated by the RV stimulus, preventing LV septum capture. On the other hand, BIV-endo lateral wall pacing allowed for shorter LV activation. The response metrics in Figure 3C computed for long RV-LV delays (35 ms) show that LVAT-95 during selective LBP and RV septal pacing were similar to baseline (94.8 ± 9.3 ms vs. 94.8 ± 8.3 ms, $p = 0.9$). LVAT-95 and BIVAT-90 were shortened by all other pacing modalities, despite prolonged RV-LV delay. BIV-endo lateral wall pacing attenuated the effect of delayed LV stimulus compared to BIV-LBP (RV apex: BIV-endo lateral: 66.2 ± 7.5 ms vs. LBP: 73.2 ± 8.0 ms, $p = 0.03$; RV septum: BIV-endo lateral: 71.2 ± 7.5 ms vs. LBP: 78.6 ± 7.9 ms, $p = 0.01$). When the RV-LV delay was short, RV septal or apical pacing combined with either selective LBP or LV lateral wall pacing led to similar response. LV lateral wall pacing was however less sensitive to prolonged RV-LV delays compared to LBP.

The effect of suboptimal left bundle capture

The simulations presented above assumed perfect selective capture of the left bundle. However, in reality, purely selective LBP is hard to achieve. To test the effect of suboptimal BIV-LBP with a leadless system on response to pacing, we repeated simulations with non-selective LBP and LBBAP, simulated by pacing 1 cm below the left bundle, all combined with an RV apical lead and an RV-LV delay of 5 ms. Figure 4 shows the response metrics simulated during baseline and pacing. Non-selective left bundle capture was comparable to selective capture in terms of LVAT-95 (64.0 ± 6.3 ms vs. 67.0 ± 6.0 ms, $p = 0.9$) and BIVAT-90 (54.2 ± 5.7 ms vs. 55.9 ± 5.6 ms, $p = 0.9$). Although LBBAP significantly worsened response compared to selective LBP (BIVAT-90: 62.7 ± 6.5, $p < 0.01$), ventricular activation was still improved from baseline ($p < 0.01$ for all metrics). Targeting the left bundle selectively or non-selectively does not alter response to BIV-LBP. However, when the left bundle is not targeted correctly, response can worsen significantly.

Discussion

We carried out an *in silico* clinical trial to investigate response to BIV-endo lateral wall pacing and BIV-LBP delivered through a leadless system in LBBB patients. When AV delay optimization was possible, selective LBP alone through a standard LV lead was more effective than BIV-LBP. However, in the presence of complete AV block, BIV-LBP achieved better synchrony over LBP alone, as the RV pacing stimulus shortened RV activation. We studied the effect of RV-LV delay and RV pacing location on response by increasing the RV-LV delay from 5 ms to 35 ms, and by changing the location of the RV stimulus from apex to septum. BIV-endo lateral wall pacing was less sensitive to prolonged RV-LV delays compared to BIV-LBP, while RV septal pacing worsened response. RV septal pacing combined with LBP with a 35 ms RV-LV delay led to unchanged LV activation from baseline because the LV septum became refractory following RV septal pacing, preventing left bundle capture. To test the effect of the type of left bundle capture on synchrony induced by BIV-LBP, we simulated selective LBP, non-selective LBP and LBBAP. While non-selective LBP was comparable to selective LBP, LBBAP worsened response, although all activation metrics were still significantly improved from baseline.

BIV-endo pacing has emerged as an alternative to conventional CRT for patients who could not receive or did not respond to conventional CRT (Derval et al., 2010; Ginks et al., 2012; Behar et al., 2016; Morgan et al., 2016; Padeletti et al., 2016). However, there are concerns about increased stroke risks, that could be mitigated by performing pacing through a leadless pacing system. The first feasibility study of the WiSE-CRT system reported successful implant in 92% of patients, did not report any thrombo-embolic events. Consistent with our simulation study, these patients achieved a significant enhanced electrical synchrony compared to baseline (Auricchio et al., 2014). Similarly, in the SELECT-LV study 97.1% of patients were successfully delivered with WiSE-CRT system pacing, with

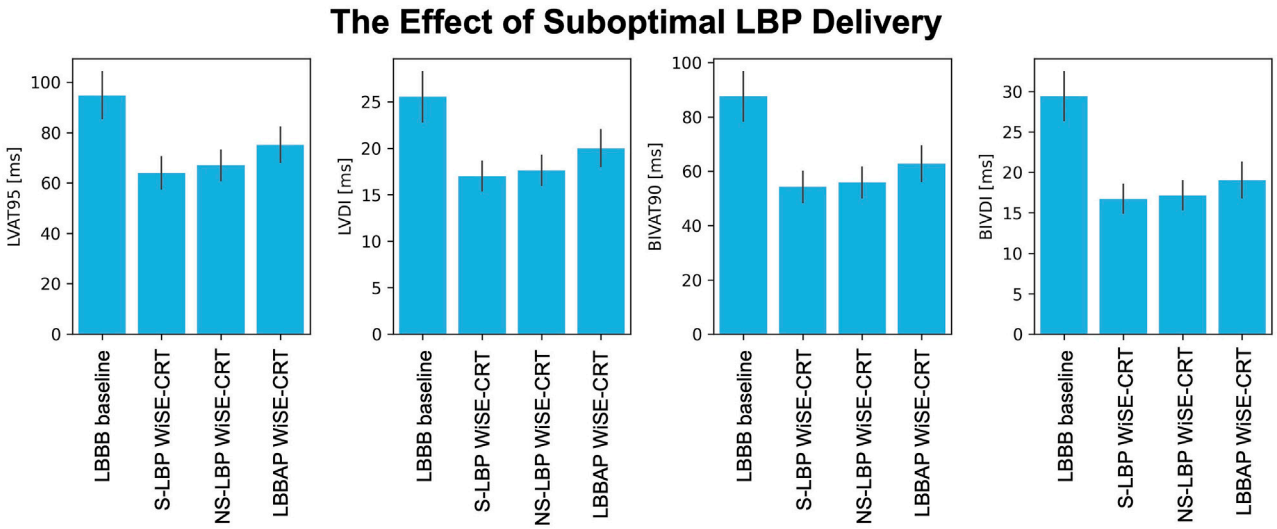

FIGURE 4
The effect of suboptimal LBP delivery. Response metrics (mean ± standard deviation) simulated during baseline and LBP pacing simulated through the WiSE-CRT system with selective capture, non-selective capture and LBBAP (pacing 1 cm below the left bundle). All pacing simulations were performed with RV apical pacing and 5 ms RV-LV delay.

significant QRS duration reduction compared to baseline. However, device- or procedure-related complications occurred in 8.6% of patients within the first 24 h, and in 22.9% of patients between 1 day and 1 month, respectively (Reddy et al., 2017). Sieniewicz et al. reported similar complication rates following WiSE-CRT system implantation, improved LV haemodynamics and shortened QRS duration following pacing in the optimal LV endocardial pacing location (Sieniewicz et al., 2020). Despite these promising results, safety of BIV-endo pacing through the WiSE-CRT system needs to be assessed in larger clinical trials, before this technique is widely used (Wijesuriya et al., 2022).

Most studies reporting on the WiSE-CRT system implanted the LV leadless electrode at the LV free wall. However, targeting the left bundle with the LV electrode could potentially provide added benefits thanks to CSP. Elliott et al. reported the first case of leadless LBP (Elliott et al., 2021). The authors tested different locations of the LV lead during BIV-endo pacing, achieving the best acute haemodynamic response by pacing in the LV mid-lateral wall. Consistent with our study, both BIV-endo lateral pacing and BIV-LBP through the WiSE-CRT system significantly improved electrical synchrony compared to baseline. LBP allowed for superior QRS narrowing compared to BIV-endo lateral wall (106 ms vs. 132 ms). BIV-LBP using the WiSE-CRT system was subsequently performed in a series of eight patients (Elliott et al., 2022). These studies showed the technical feasibility of LBP through a leadless system, however the safety and efficacy of this technique, and the importance of targeting of the left bundle, remains unclear. Our results mimic the pacing study that was performed in (Elliott et al., 2022), and showed that, although selective LBP alone is better when AV delay optimization, BIV-LBP is more effective when AV delay optimization is not possible. Although typically the WiSE-CRT system delivers BIV pacing, LV only pacing could be achieved with sub-capture RV pacing output or with further device modification as shown by (Elliott et al., 2022). This could be particularly relevant not only in patients with complete AV block, but also for patients with atrial fibrillation, who represent a significant proportion (about 26%) of CRT patients (Dickstein et al., 2018). On the other hand, patients with RBBB or septal scar are unlikely to respond to leadless LBP due to preserved delayed RV activation during pacing, as we have shown in a previous modelling study (Strocchi et al., 2022) and in the supplement, respectively. In these patient groups, leadless BIV-endo lateral wall pacing might be a better treatment option. Finally, we have shown that longer RV-LV delays worsen response. Studies have reported superiority of optimized RV-LV delay compared to simultaneous BIV pacing, with LV or RV pre-pacing being beneficial for different patients (Sogaard et al., 2002). Other clinical studies instead have reported that RV-LV delay optimization brings no additional benefits to CRT (Boriani et al., 2006; Rao et al., 2007; Bogaard et al., 2013). Therefore, the RV-LV delay is likely to be patient specific and highly dependent on the electrical substrate causing dyssynchrony. While RV-LV delay optimization could be achieved in future with WiSE-CRT through device modifications, it is currently not possible to set a specific RV-LV delay. The conclusions of our study provide insight into response to leadless pacing, and which device parameters are important for response to pacing. This will help in the design of larger clinical trials investigating the efficacy and safety of leadless pacing.

Limitations

The main limitation of our study is that we assume acute electrical response correlates with long-term functional response. However, although other factors affect response to CRT, there is strong evidence showing that patients who respond acutely to pacing in terms of QRS narrowing are more likely to experience long-term benefits (Bryant et al., 2013; Bazoukis et al., 2020).

The study presented in this paper accounts for a limited number of patients. Even if the twenty-four geometries we used are representative of the heart failure population with CRT indication, a much larger number of meshes should have been considered to model the large heterogeneity observed in patients with dyssynchrony. Over the next decade, the progress in image analysis, segmentation and simulation software will hopefully allow for larger virtual clinical trial including >1000 patients, consistent with large multi-centre trials (Bristow et al., 2004).

Our models make use of synthetic His-Purkinje systems that do not represent the conduction system of a specific patient. However, at present, patient-specific His-Purkinje networks cannot be generated due to the lack of imaging techniques able to resolve these intricate structures. The electrophysiology model we employed was simplified as it discarded cellular ionic dynamics, tissue heterogeneities within the myocardium and electrical signal propagation across the torso. More detailed and personalized simulations would have required more extensive computational resources and were outside the scope of this study. We showed in the supplement that our models replicate baseline metrics and activation pattern of LBBB. However, due to the rule-based His-Purkinje network and the simplified electrophysiology model we employed, the results presented in this study should be interpreted with care.

Despite its limitation, our *in silico* trial succeeds in providing insight into response to pacing delivered through a leadless system, and how RV lead location, LV lead location, RV-LV delay and type of LBP capture alter synchrony. The results we presented lay the foundation for clinical trial design investigating leadless pacing safety and efficacy.

Conclusion

When AV delay optimization is possible, selective LBP delivered through a standard LV lead (e.g., no RV pacing) offers better synchrony compared to BIV-LBP, while delayed RV activation makes LBP less effective when AV delay optimization is not possible. BIV-endo lateral wall pacing is less sensitive to prolonged RV-LV delays, and RV septal pacing worsens response compared to RV apical pacing, especially for longer RV-LV delays. Non-selective capture of the left bundle is comparable to selective LBP, while LBBAP worsens response compared to selective LBP.

Data availability statement

The raw data supporting the conclusions of this article will be made available by the authors, without undue reservation.

Author contributions

MS, SN, CR, ME, VM, and NW contributed to conception and design of the study. KG, GP, EV, and AN implemented the software used to run simulations. MS wrote the first draft of the manuscript, ran simulations and analyzed the results. All authors contributed to manuscript revision and approved the final submitted version.

Funding

This work was supported by the Wellcome/EPSRC Centre for Medical Engineering (WT 203148/Z/16/Z). SN is supported by NIH R01-HL152256, ERC PREDICT-HF 453 (864055), BHF (RG/20/4/34803), EPSRC (EP/P01268X/1). This study received financial support from the French Government as part of the "Investments of the Future" program managed by the National Research Agency (ANR) (ANR-10-IAHU-04). AN is employed by NumeriCor GmbH, Graz, Austria.

Conflict of interest

AN is employed by NumeriCor GmbH, Graz, Austria.

The remaining authors declare that the research was conducted in the absence of any commercial of financial relationships that could be construed as a potential conflict of interest.

Publisher's note

Supplementary material

The Supplementary Material for this article can be found online at: https://www.frontiersin.org/articles/10.3389/fphys.2022.1049214/full#supplementary-material

References

Arnold, A. D., Shun-Shin, M. J., Keene, D., Howard, J. P., Afzal Sohaib, S. M., Wright, I. J., et al. (2018). His resynchronization therapy vs. biventricular pacing for heart failure with LBBB: A within-patient comparison of effects on acute haemodynamic function and ventricular activation. *Europace* 20 (Suppl. 4), iv25. doi:10.1093/europace/euy201.001

Auricchio, A., Delnoy, P. P., Butter, C., Brachmann, J., van Erven, L., Spitzer, S., et al. (2014). Feasibility, safety, and short-term outcome of leadless ultrasound-based endocardial left ventricular resynchronization in heart failure patients: Results of the Wireless Stimulation Endocardially for CRT (WiSE-CRT) study. *Europace* 16, 681–688. doi:10.1093/europace/eut435

Bayer, J., Prassl, A. J., Pashaei, A., Gomez, J. F., Frontera, A., Neic, A., et al. (2018). Universal ventricular coordinates: A generic framework for describing position within the heart and transferring data. *Med. Image Anal.* 45, 83–93. doi:10.1016/j.media.2018.01.005

Bazoukis, G., Naka, K. K., Alsheikh-Ali, A., Tse, G., Letsas, K. P., Korantzopoulos, P., et al. (2020). Association of QRS narrowing with response to cardiac resynchronization therapy—A systematic review and meta-analysis of observational studies. *Heart fail. Rev.* 25, 745–756. doi:10.1007/s10741-019-09839-5

Behar, J. M., Jackson, T., Hyde, E., Claridge, S., Gill, J., Bostock, J., et al. (2016). Optimized left ventricular endocardial stimulation is superior to optimized epicardial stimulation in ischemic patients with poor response to cardiac resynchronization therapy: A combined magnetic resonance imaging, electroanatomic contact mapping, and hemodynamic study to target endocardial lead placement. *JACC. Clin. Electrophysiol.* 2, 799–809. doi:10.1016/j.jacep.2016.04.006

Behradfar, E., Nygren, A., and Vigmond, E. J. (2014). The role of purkinje-myocardial coupling during ventricular arrhythmia: A modeling study. *PLoS One* 9, e88000. doi:10.1371/journal.pone.0088000

Bernard, M. L. (2016). Pacing without wires: Leadless cardiac pacing. *Ochsner J.* 16, 238–242.

Bogaard, M. D., Meine, M., and Doevendans, P. A. (2013). Programmed versus effective VV delay during CRT optimization: When what you see is not what you get. *Pacing Clin. Electrophysiol.* 36, 403–409. doi:10.1111/pace.12065

Boriani, G., Müller, C. P., Seidl, K. H., Grove, R., Vogt, J., Danschel, W., et al. (2006). Randomized comparison of simultaneous biventricular stimulation versus optimized interventricular delay in cardiac resynchronization therapy. The Resynchronization for the HemodYnamic Treatment for Heart Failure Management II implantable cardioverter defibrillator (RHYTHM II ICD) study. *Am. Heart J.* 151, 1050–1058. doi:10.1016/j.ahj.2005.08.019

Bristow, M. R., Saxon, L. A., Boehmer, J., Krueger, S., Kass, D. A., de Marco, T., et al. (2004). Cardiac-resynchronization therapy with or without an implantable defibrillator in advanced chronic heart failure. *N. Engl. J. Med.* 350, 2140–2150. doi:10.1056/nejmoa032423

Bryant, A. R., Wilton, S. B., Lai, M. P., and Exner, D. v. (2013). Association between QRS duration and outcome with cardiac resynchronization therapy: A systematic review and meta-analysis. *J. Electrocardiol.* 46, 147–155. doi:10.1016/j.jelectrocard.2012.12.003

Butter, C., Georgi, C., and Stockburger, M. (2021). Optimal CRT implantation—where and how to place the left-ventricular lead? *Curr. Heart Fail. Rep.* 18, 329–344. doi:10.1007/s11897-021-00528-9

Derval, N., Steendijk, P., Gula, L. J., Deplagne, A., Laborderie, J., Sacher, F., et al. (2010). Optimizing hemodynamics in heart failure patients by systematic screening of left ventricular pacing sites. The lateral left ventricular wall and the coronary sinus are rarely the best sites. *J. Am. Coll. Cardiol.* 55, 566–575. doi:10.1016/j.jacc.2009.08.045

Dickstein, K., Normand, C., Auricchio, A., Bogale, N., Cleland, J. G., Gitt, A. K., et al. (2018). CRT survey II: A European society of Cardiology survey of cardiac resynchronisation therapy in 11 088 patients—who is doing what to whom and how? *Eur. J. Heart Fail.* 20, 1039–1051. doi:10.1002/ejhf.1142

Elliott, M. K., Jacon, P., Sidhu, B. S., Smith, L. J., Mehta, V. S., Gould, J., et al. (2021). Technical feasibility of leadless left bundle branch area pacing for cardiac resynchronization: A case series. *Eur. Heart J. Case Rep.* 5, ytab379. doi:10.1093/ehjcr/ytab379

Elliott, M. K., Vergara, P., Wijesuriya, N., Mehta, V. S., Bosco, P., Jacon, P., et al. (2022). Feasibility of leadless left ventricular septal pacing with the WiSE-CRT system to target the left bundle branch area: A porcine model and multicenter patient experience. *Heart rhythm.* 19, 1974–1983. doi:10.1016/j.hrthm.2022.07.017

Gillette, K., Gsell, M. A. F., Bouyssier, J., Prassl, A. J., Neic, A., Vigmond, E. J., et al. (2021). Automated framework for the inclusion of a his–purkinje system in cardiac digital twins of ventricular electrophysiology. *Ann. Biomed. Eng.* 49, 3143–3153. doi:10.1007/s10439-021-02825-9

Gillette, K. K., Gsell, M. A. F., Neic, A., Manninger, M., Scherr, D., Roney, C. H., et al. (2022). A personalized real-time virtual model of whole heart electrophysiology. *Front. Physiology*, 1860. doi:10.3389/fphys.2022.907190

Ginks, M. R., Shetty, A. K., Lambiase, P. D., Duckett, S. G., Bostock, J., Peacock, J. L., et al. (2012). Benefits of endocardial and multisite pacing are dependent on the type of left ventricular electric activation pattern and presence of ischemic heart disease: Insights from electroanatomic mapping. *Circ. Arrhythm. Electrophysiol.* 5, 889–897. doi:10.1161/CIRCEP.111.967505

Hyde, E. R., Behar, J. M., Claridge, S., Jackson, T., Lee, A. W. C., Remme, E. W., et al. (2015). Beneficial effect on cardiac resynchronization from left ventricular endocardial pacing is mediated by early access to high conduction velocity tissue: Electrophysiological simulation study. *Circ. Arrhythm. Electrophysiol.* 8, 1164–1172. doi:10.1161/CIRCEP.115.002677

Lin, J., Dai, Y., Wang, H., Li, Y., Chen, K., and Zhang, S. (2020). A comparison of left bundle branch pacing with His bundle pacing in a patient with heart failure and left bundle branch block. *Hear. Case Rep.* 6, 293–296. doi:10.1016/j.hrcr.2019.10.007

Mendonca Costa, C., Neic, A., Kerfoot, E., Porter, B., Sieniewicz, B., Gould, J., et al. (2019). Pacing in proximity to scar during cardiac resynchronization therapy increases local dispersion of repolarization and susceptibility to ventricular arrhythmogenesis. *Heart rhythm.* 16, 1475–1483. doi:10.1016/j.hrthm.2019.03.027

Morgan, J. M., Biffi, M., Gellér, L., Leclercq, C., Ruffa, F., Tung, S., et al. (2016). ALternate site cardiac ResYNChronization (alsync): A prospective and multicentre study of left ventricular endocardial pacing for cardiac resynchronization therapy. *Eur. Heart J.* 37, 2118–2127. doi:10.1093/eurheartj/ehv723

Neic, A., Campos, F. O., Prassl, A. J., Niederer, S. A., Bishop, M. J., Vigmond, E. J., et al. (2017). Efficient computation of electrograms and ECGs in human whole heart simulations using a reaction-eikonal model. *J. Comput. Phys.* 346, 191–211. doi:10.1016/j.jcp.2017.06.020

Ono, N., Yamaguchi, T., Ishikawa, H., Arakawa, M., Takahashi, N., Saikawa, T., et al. (2009). Morphological varieties of the purkinje fiber network in mammalian hearts, as revealed by light and electron microscopy. *Arch. Histol. Cytol.* 72, 139–149. doi:10.1679/aohc.72.139

Padeletti, L., Pieragnoli, P., Ricciardi, G., Innocenti, L., Checchi, L., Padeletti, M., et al. (2016). Simultaneous His bundle and left ventricular pacing for optimal cardiac resynchronization therapy delivery: Acute hemodynamic assessment by pressure-volume loops. *Circ. Arrhythm. Electrophysiol.* 9, e003793. doi:10.1161/circep.115.003793

Prinzen, F. W., van Deursen, C., van Geldorp, I. E., Rademakers, L. M., van Hunnik, A., Kuiper, M., et al. (2009). Left ventricular endocardial pacing improves resynchronization therapy in canine left bundle-branch hearts. *Circ. Arrhythm. Electrophysiol.* 2, 580–587. doi:10.1161/CIRCEP.108.846022

Rao, R. K., Kumar, U. N., Schafer, J., Viloria, E., de Lurgio, D., and Foster, E. (2007). Reduced ventricular volumes and improved systolic function with cardiac resynchronization therapy: A randomized trial comparing simultaneous biventricular pacing, sequential biventricular pacing, and left ventricular pacing. *Circulation* 115, 2136–2144. doi:10.1161/CIRCULATIONAHA.106.634444

Reddy, V. Y., Miller, M. A., Neuzil, P., Søgaard, P., Butter, C., Seifert, M., et al. (2017). Cardiac resynchronization therapy with wireless left ventricular endocardial pacing: The SELECT-LV study. *J. Am. Coll. Cardiol.* 69, 2119–2129. doi:10.1016/j.jacc.2017.02.059

Sieniewicz, B. J., Betts, T. R., James, S., Turley, A., Butter, C., Seifert, M., et al. (2020). Real-world experience of leadless left ventricular endocardial cardiac resynchronization therapy: A multicenter international registry of the WiSE-CRT pacing system. *Heart rhythm.* 17, 1291–1297. doi:10.1016/j.hrthm.2020.03.002

Sieniewicz, B. J., Gould, J., Porter, B., Sidhu, B. S., Teall, T., Webb, J., et al. (2019). Understanding non-response to cardiac resynchronisation therapy: Common problems and potential solutions. *Heart fail. Rev.* 24, 41–54. doi:10.1007/s10741-018-9734-8

Sogaard, P., Egeblad, H., Pedersen, A. K., Kim, W. Y., Kristensen, B., Hansen, P. S., et al. (2002). Sequential versus simultaneous biventricular resynchronization for severe heart failure: Evaluation by tissue Doppler imaging. *Circulation* 106,

2078–2084. doi:10.1161/01.CIR.0000034512.90874.8E

Strocchi, M., Augustin, C. M., Gsell, M. A. F., Karabelas, E., Neic, A., Gillette, K., et al. (2020a). A publicly available virtual cohort of fourchamber heart meshes for cardiac electromechanics simulations. *PLoS One* 15, e0235145. doi:10.1371/journal.pone.0235145

Strocchi, M., Gillette, K., Neic, A., Elliott, M. K., Wijesuriya, N., Mehta, V., et al. (2022). Comparison between conduction system pacing and cardiac resynchronization therapy in right bundle branch block patients. *Front. Physiol.* 13, 1011566. doi:10.3389/fphys.2022.1011566

Strocchi, M., Lee, A. W. C., Neic, A., Bouyssier, J., Gillette, K., Plank, G., et al. (2020b). His-bundle and left bundle pacing with optimized atrioventricular delay achieve superior electrical synchrony over endocardial and epicardial pacing in left bundle branch block patients. *Heart rhythm.* 17, 1922–1929. doi:10.1016/j.hrthm.2020.06.028

Taggart, P., Sutton, P. M., Opthof, T., Coronel, R., Trimlett, R., Pugsley, W., et al. (2000). Inhomogeneous transmural conduction during early ischaemia in patients with coronary artery disease. *J. Mol. Cell. Cardiol.* 32, 621–630. doi:10.1006/jmcc.2000.1105

Wijesuriya, N., Elliott, M. K., Mehta, V., Sidhu, B. S., Behar, J. M., Niederer, S., et al. (2022). Leadless left ventricular endocardial pacing for cardiac resynchronization therapy: A systematic review and meta-analysis. *Heart rhythm.* 19, 1176–1183. doi:10.1016/j.hrthm.2022.02.018

frontiers | Frontiers in Physiology

TYPE Review
PUBLISHED 15 December 2022
DOI 10.3389/fphys.2022.1045740

OPEN ACCESS

EDITED BY
Maciej M Sterlinski,
National Institute of Cardiology, Poland

REVIEWED BY
Josef Halamek,
Institute of Scientific Instruments (ASCR), Czechia
Junmeng Zhang,
First Hospital of Tsinghua University, China

*CORRESPONDENCE
Keping Chen,
chenkeping@263.net

SPECIALTY SECTION
This article was submitted to Cardiac Electrophysiology, a section of the journal Frontiers in Physiology

RECEIVED 16 September 2022
ACCEPTED 02 December 2022
PUBLISHED 15 December 2022

CITATION
Chen Z, Zhou X, Ma X and Chen K (2022), Recruitment of the cardiac conduction system for optimal resynchronization therapy in failing heart.
Front. Physiol. 13:1045740.
doi: 10.3389/fphys.2022.1045740

Recruitment of the cardiac conduction system for optimal resynchronization therapy in failing heart

Zhongli Chen[1], Xiaohong Zhou[2], Xuan Ma[3] and Keping Chen[1]*

[1]State Key Laboratory of Cardiovascular Disease, Arrhythmia Center, Fuwai Hospital, National Center for Cardiovascular Diseases, Chinese Academy of Medical Sciences and Peking Union Medical College, Beijing, China, [2]Medtronic, Inc, Dublin, Ireland, [3]Department of Magnetic Resonance Imaging, Fuwai Hospital, National Center for Cardiovascular Diseases, Chinese Academy of Medical Sciences and Peking Union Medical College, Beijing, China

Heart failure (HF) is a leading health burden around the world. Although pharmacological development has dramatically advanced medication therapy in the field, hemodynamic disorders or mechanical desynchrony deteriorated by intra or interventricular conduction abnormalities remains a critical target beyond the scope of pharmacotherapy. In the past 2 decades, nonpharmacologic treatment for heart failure, such as cardiac resynchronization therapy (CRT) *via* biventricular pacing (BVP), has been playing an important role in improving the prognosis of heart failure. However, the response rate of BVP-CRT is variable, leaving one-third of patients not benefiting from the therapy as expected. Considering the non-physiological activation pattern of BVP-CRT, more efforts have been made to optimize resynchronization. The most extensively investigated approach is by stimulating the native conduction system, e.g., His-Purkinje conduction system pacing (CSP), including His bundle pacing (HBP) and left bundle branch area pacing (LBBAP). These emerging CRT approaches provide an alternative to traditional BVP-CRT, with multiple proof-of-concept studies indicating the safety and efficacy of its utilization in dyssynchronous heart failure. In this review, we summarize the mechanisms of dyssynchronous HF mediated by conduction disturbance, the rationale and acute effect of CSP for CRT, the recent advancement in clinical research, and possible future directions of CSP.

KEYWORDS

heart failure, cardiac resynchronization therapy, biventricular pacing, His bundle pacing, left bundle branch area pacing

Introduction

Heart failure (HF) is a global health burden with increasing morbidity and mortality with a 1-year mortality rate of 10–35%. (Ambrosy et al., 2014). Even with guideline-directed medical treatment (GDMT) (Huang H. T. et al., 2022), a significant proportion of patients remain symptomatic with irreversible reduced left

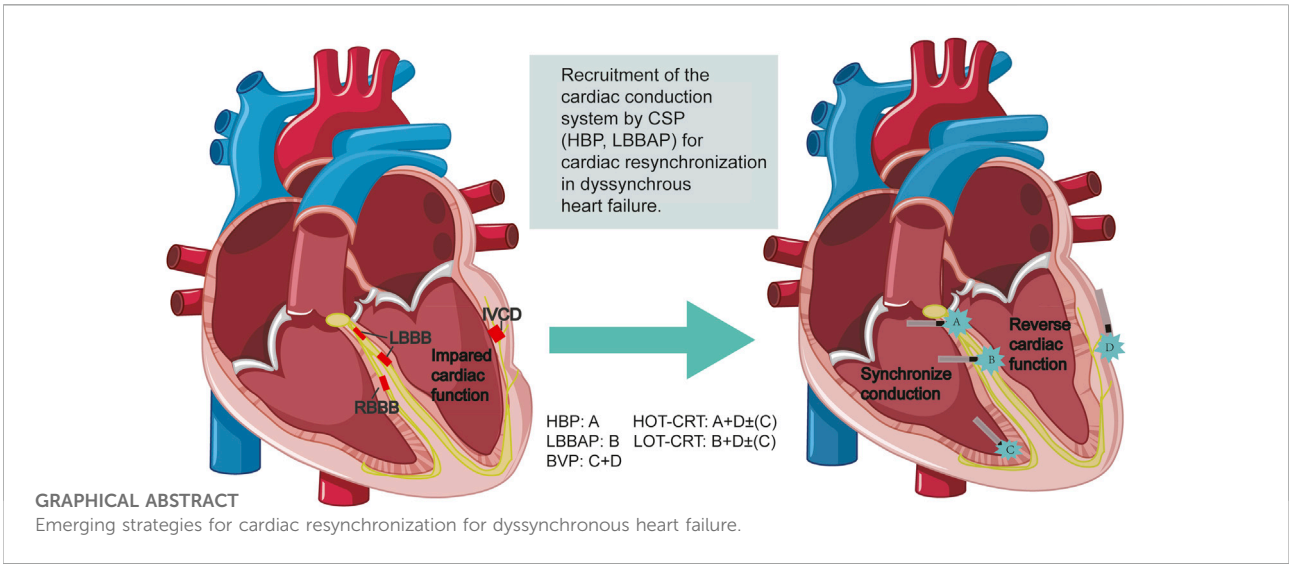

GRAPHICAL ABSTRACT
Emerging strategies for cardiac resynchronization for dyssynchronous heart failure.

ventricular ejection fraction (LVEF). While multiple underlying causes (volume overload, inflammation, ischemia, neuroendocrine disorders) contribute to chronic heart failure, ventricular dyssynchrony, caused by impaired cardiac conduction system, is another underlying mechanism occuring in 24%–47% of the heart failure patients with reduced ejection fraction (HFrEF) patients and is often refractory to pharmacological therapies. (Lund et al., 2013; Prinzen et al., 2022). The so-called ventricular dyssynchrony refers to the discoordination of the electrical activation and mechanical contraction within or between the ventricles. Impaired cardiac conduction system disturbance, including left bundle branch block (LBBB), right bundle branch block (RBBB), and intraventricular conduction delay (IVCD), presents with wide QRS complex and is associated with the development of heart failure.

To correct electrical dyssynchrony in heart failure patients with wide QRS complex and reduced LVEF, cardiac resynchronization therapy (CRT) *via* biventricular pacing (BVP) was introduced in early 2000 and has brought remarkable benefits to HF prognosis, including a reduction of the all-cause mortality by 29% (Rivero-Ayerza et al., 2006) and heart failure hospitalization (HFH) rate from 0.338 to 0.204 events per patient-year (Varma et al., 2021). However, despite tremendous efforts, the traditional BVP approach of CRT is also facing challenges including difficulties in left ventricular (LV) lead positioning and a non-responding rate of approximately 30% (Kaza et al., 2022). Therefore, efforts have been made to pursue optimal electrical and mechanical synchrony through the conduction system pacing (CSP) *via* direct activation of the His bundle or left bundle branch, which can restore the functionality of impaired cardiac conduction system so as to produce physiological ventricular activation propagation and better mechanical synchrony. More recently, evidence for clinical utility of CSP for CRT accumulates, providing prospect of CSP in positive modulation of the failing heart. Herein, we discuss the ventricular conduction disturbance-mediated dyssynchrony in the deterioration of HF, the rationale of CSP for CRT, the recent clinical evidence for potential indications for patient selection and future directions of CSP.

Progress in assessment of ventricular dyssynchrony

Ventricular dyssynchrony can be recognized through different assessments. Both electrical and mechanical synchrony can be measured directly through ventricular endocardial mapping and catheterization. But these measurements are invasive, risky, operator-dependent, and time-consuming, which limits their use in routine clinical practice. Therefore, non-invasive methods have been the mainstream for synchrony evaluation. The most commonly used non-invasive tool to quantify electrical synchrony is the 12-lead electrocardiogram (ECG.) The QRS duration (QRSd), left ventricular activation time in lead V5 or V6 and the QRS morphology have been adopted for a long time to assess the electrical dyssynchrony prior to or after the CRT. Another simple parameter is the ECG-derived QRS area, which provided a strong association with CRT response (Emerek et al., 2019). Recently, ECG imaging (ECGi), ECG belt, and ultra-high-frequency ECG (UHF-ECG) have been used as non-invasive tools that provide more detailed information about ventricular activation. Not only the right ventricle (RV) and LV dyssynchrony parameters can be assessed separately (for example, the standard deviation of

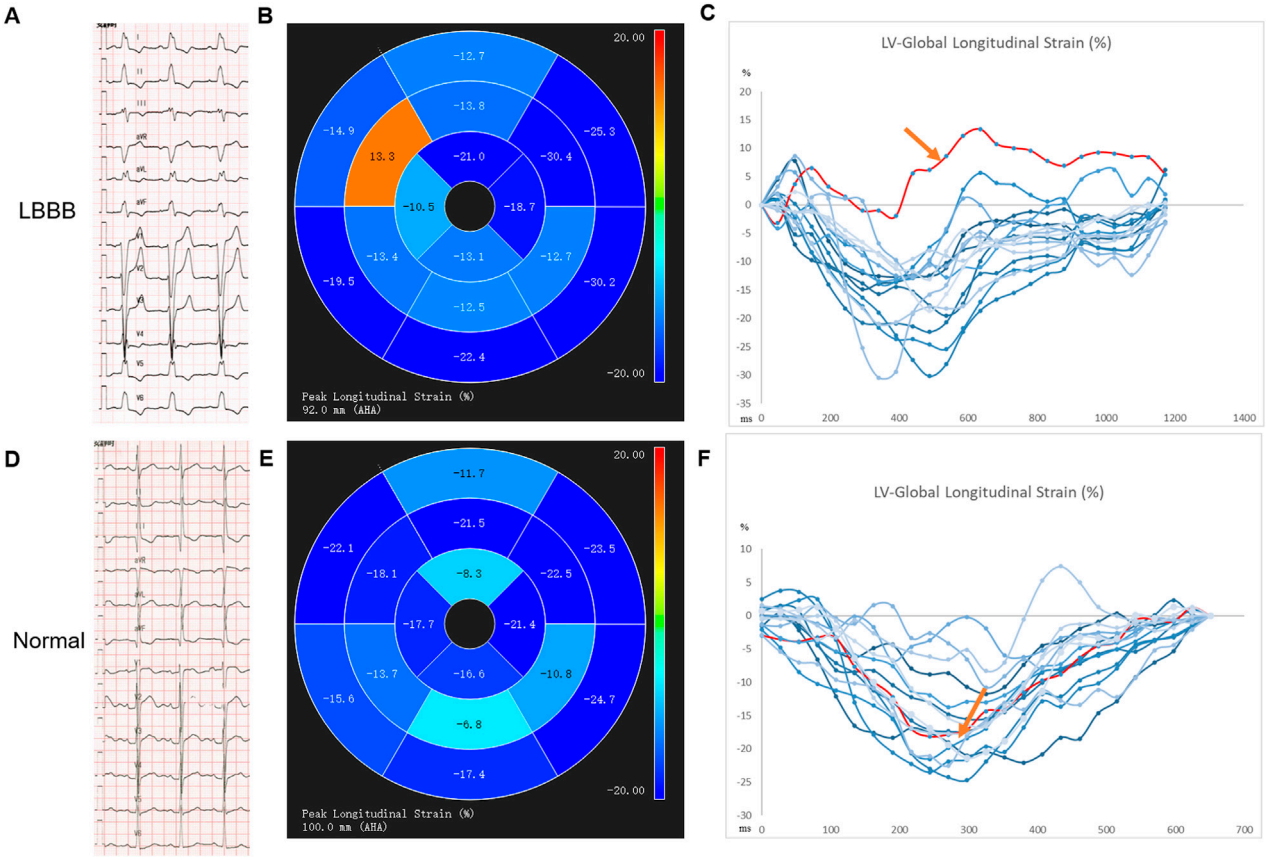

FIGURE 1
The impaired global longitudinal strain of the septal segment of a LBBB patient with preserved LVEF by CMR-feature tracking technique. **(A–C)** an example from an LBBB patient: A electrocardiogram of the LBBB; B-C AHA segment diagram of 2D long axis GLS, segment eight in septum shows abnormal GLS with a positive value, represented the contradictory motion of septum, red spline; an example from a healthy control patient by **(D–F)**: D electrocardiogram of normal intrinsic rhythm, **(E–F)**: AHA segment diagram of 2D long axis GLS, the same segment in septum shows normal GLS with a negative value, represented as red spline.

activation times, left ventricular dyssynchrony index (LVDI), LV/RV total activation/depolarization time), but also the interventricular dyssynchrony can be evaluated (eg: e-DYS) (Mizner, 2022).

Additionally, mechanical dyssynchrony can be measured using Doppler echocardiography, 2-dimensional (D) specking-tracking echocardiography, 3D echocardiography, or the cardiac magnetic resonance (CMR) strain analysis. Several qualitative markers such as septal flash and pre-systole rebound stretch, and quantitative indices like the peaking time, excursion amount, or myocardial wasted work can be calculated (Fang et al., 2010; Zweerink et al., 2018). The commonly used LVEF, LVESV, beat-to-beat blood pressure, (Arnold et al., 2018), and rate of LV pressure rise (expressed as dp/dt max) (Kato et al., 2022)do not directly reveal the mechanical dyssynchrony, but represent the structural or functional status associated with the electrical and mechanical dysynchrony, thus they are usually applied in the clinical evaluation of CRT benefits.

The pathophysiological mechanism of dyssynchronous heart failure

LBBB morphology and cardiac dyssynchrony

Asynchronous ventricular activation and contraction are associated with cardiac dysfunction. Clinically, the most prominent form of the underlying conduction disturbance is LBBB, followed by non-specific IVCD and RBBB. Previous studies have demonstrated the causal relationship between conduction disturbance and cardiac remodeling, especially LBBB in regulating electromechanical dysynchrony and impairing cardiac function (Vernooy et al., 2005; Byrne et al., 2007; Vernooy et al., 2007). Specifically, in LBBB, the rapid intrinsic conduction in LV is impaired, and ventricular activation starts from the right ventricle, then to the LV endocardium, in which electrical activation propagates *via* the

working myocardium. It has been reported that in true or complete LBBB, trans-septal conduction time takes 30–40 m and the LV free wall is activated even later, resulting in the marked prolongation of LV activation time (LVAT) and a wide-notched QRS complex (Auricchio et al., 2004), followed by mechanical dyssynchrony (Kroon et al., 2015).

For example, echocardiographic studies indicate that in LBBB, early activation of the right ventricle free wall (RVFW) and later contraction of LVFW causes the septal flash and pre-systole septal systolic rebound stretch, leading to supranormal contraction of the latest activated LVFW (Walmsley et al., 2016). Similar motion abnormalities of the septum were also evaluated by CMR (Figure 1). The myocardial work redistributes, so does the blood flow, and more wasted work is done by the ventricular myocardium, making energy metabolism more inefficient (Russell et al., 2012). As a consequence, LV structure and function are impaired as displayed by the rightward shift of the pressure-volume (PV) loop, larger LV end-diastolic volume (LVEDV), lower strains, and reduced LVEF. (Vernooy et al., 2005; Smiseth and Aalen, 2019).

Non-LBBB morphology and dyssynchrony

The non-LBBB conduction disturbances such as RBBB and IVCD, which together account for about one-third of patients with QRS complex widening, represent the severity of the myocardial disease, inducing cardiac asynchrony and deteriorating cardiac function. RBBB, featuring evident delayed activation of RVFW segment (Dou et al., 2009), is related to a predominant reduction of RVEF and all-cause mortality in patients with and without heart failure (Gaba et al., 2020; Lai et al., 2020). Human studies in patients with RBBB and HF found that total/regional LV endocardial activation time of RBBB patients did not differ significantly from that in LBBB patients (Fantoni et al., 2005), and a higher prevalence (50%) of mechanical dyssynchrony was detected compared with the non-RBBB control group (Sillanmäki et al., 2020). But the specific mechanism of the RBBB-induced dyssynchrony remains to be elucidated.

IVCD, which always accompanies LBBB, holds heterogeneous delayed activation in various ventricular myocardial segments (Viswanathan et al., 2006). Different from LBBB, IVCD is characterized by multiple LV breakthroughs along the septum with the presence of heterogeneous localized areas of late activation along the LV free wall (Derval et al., 2017). Therefore, though a less remarkable degree of RV/LV dyssynchrony has been observed in IVCD compared with BBB, significant intraventricular dyssynchrony exists (Kerwin et al., 2000). IVCD reflects the diseased structural substrate of the myocardium and serves as a predictor of a higher risk of both cardiovascular death or HF hospitalization and all-cause mortality in HFrEF patients (Nguyên et al., 2018; Kristensen et al., 2020).

Pacing mediated dyssynchrony in patients with synchronous heart failure

RV pacing mimics the LBBB-type activation pattern even in patients with narrower intrinsic QRS complex. However, the LV mechanical dyssynchrony pattern in RV pacing is not identical to intrinsic LBBB. Specifically, in patients with RV-pacing-induced LBBB, the mid- and apical septal regions are activated earliest while in patients with intrinsic LBBB, the basal septum is activated earlier. Furthermore, an even higher degree of mechanical delay was reported in the lateral segments among the RV-pacing-induced LBBB pattern compared to the intrinsic LBBB (Ghani et al., 2011). Therefore, long-term RV pacing can decrease effective myocardial work and depress pump function (Tanaka et al., 2010; Ghani et al., 2011; Naqvi and Chao, 2021).

The rationale, electrical and hemodynamic effects for conduction system pacing in CRT

The traditional BVP significantly normalizes the total activation time, inter-ventricular electrical coupling, and mechanical synchrony in patients with LBBB (Kerwin et al., 2000; Ploux et al., 2015) and hence provides clear clinical benefits in many clinical trials. However, BVP still brings non-physiological ventricular activation patterns due to pacing at two separate non-physiological sites, e.g., one in the LV epicardial site and the other in RV endocardial site. The study by Nguyên UC, et al. found that on the LV surface, there were curvilinear activation delays near the LV pacing site, forming the island of early activation. (Nguyên et al., 2018). Despite the reduction of LV activation delay in the LBBB group, the RV total activation time also increased (Nguyên et al., 2018). The randomized clinical trial also demonstrated that BVP could have detrimental effects in heart failure patients with narrow QRSd (Moss et al., 2009). In patients with narrow QRS complex or IVCD, a significant increase of total LVAT was reported, further proving the dyssynchronous electrical ventricular activation brought by BVP, as compared with the normal intrinsic conduction, which at least partly explains the detrimental effect of BVP-CRT on the hemodynamic response in patients with little or no electrical dyssynchrony (Ploux et al., 2015).

Effect of HBP on electrical and mechanical synchrony

In comparison to BVP, CSP directly stimulates the native specialized conduction system, allowing for complete restoration of electrical depolarization and repolarization

and leading to true physiological resynchronization. The rationale of His bundle pacing (HBP) for correcting LBBB mainly originates from the longitudinal dissociation hypothesis described by Narula in 1977, who revealed that before the separation of bundle branches, individual bundle branches also existed in a single cable within the His bundle (Narula, 1977). Therefore, LBBB with lesions within the His bundle can be corrected by pacing the distal region of the block area of the His bundle (HB). In 2005, the first case report of HBP in a 62-year-old female patient with reduced left ventricular ejection fraction (LVEF: 35%), LBBB [QRS duration (QRSd):160 ms], and left ventricle asynchrony was initiated by Dr. Vázquez (Morina-Vazquez et al., 2005). They got a constant capture of HB at an output of 1.6 V at 0.5 ms with an accompanying significant reduction in QRSd (30 m shorter than intrinsic QRSd). After a 6-month follow-up, the HBP threshold was stable at 2 V at 0.5 m and echocardiographic findings demonstrated a minimal delay of the left lateral wall, indicating that HBP could correct the electrical and mechanical dyssynchrony in HF. Later, studies detailing the electrical activation and the acute hemodynamic patterns of CSP and comparative analyses of CSP and BVP were performed. HBP, as described by electrophysiological studies in both animals and humans, provides a short total activation time (TAT), narrow QRS complex, and activation sequence most similar to normal physiological sinus activation. A more physiological ventricular activation pattern of HBP over BVP was also reported in LBBB patients using non-invasive epicardial mapping *via* 252-electrode ECGi vest and computer simulations (Arnold et al., 2018; Strocchi et al., 2020) The study reveals that HBP delivers a greater reduction of QRS duration, shorter LVAT, and better LV synchrony (evaluated by significantly reduced LVDI). The shortening of ventricular activation in HBP is also associated with incremental acute hemodynamic response, as supported by increased systolic blood pressure in HBP compared with the LBBB and the BVP groups (Arnold et al., 2018).

Additionally, HBP contains two subtypes of capture, one is by exclusive stimulation of the intrinsic His bundle, which is called selective HBP (S-HBP); the other is through activation of both the His bundle and the local myocardium, known as the non-selective HBP (NS-HBP)]. Whether one is superior to the other in terms of electrical and mechanical synchrony raises discussion. In a non-invasive epicardial electrical mapping study of 20 patients (60% LBBB, 10%RBBB), it is found that S-HBP and NS-HBP displayed similar LV activation patterns, whereas NS-HBP displays early activation in the basal to the mid-region of RV due to the capture of local para-Hisian myocardium. However, LVAT is preserved and RVAT is not significantly prolonged in NS-HBP compared with S-HBP, implying that a minor difference in electrical depolarization may not pose a great impact on the overall activation of ventricles in either S-HBP or NS-HBP (Arnold et al., 2021). Hemodynamic improvements are also found similar in both S-HBP and NS-HBP in patients with the narrow QRS complex. The echocardiographic measurements reveal that compared with RV pacing, both S-HBP and NS-HBP result in better inter and intra-ventricular synchrony without differences between the two groups (Catanzariti et al., 2006). But the non-inferior effect of NS-HBP to S-HBP can be explained by the capture of the conduction system because even pacing in the same para-Hisian area, pure myocardial pacing without the capture of intrinsic His-Purkinje system still leads to substantial QRSd prolongation and interventricular dssynchrony (Zhang et al., 2018; Curila et al., 2020). Therefore, it is reasonable to consider that although there are some differences in early activation sites, NS-HBP may not result in great electrical dyssynchrony or clinically different hemodynamic improvements when the conduction system is stably captured.

Effect of LBBAP in electrical and mechanical synchrony

LBBAP, compromising the left ventricular septal myocardial pacing (LVSP) and direct capture of the left bundle branch (LBBP), offers another choice of CSP with a relatively lower and stable capture threshold and capacity of bypassing the pathological lesion and capturing the nearby conduction branch to overcome Infra-Hisian “distal” LBBB that cannot be corrected by HBP with a low capture threshold. (Upadhyay et al., 2019a).

Recent preclinical and clinical investigations have delineated the effects of each subtype of LBBAP on electrical and mechanical synchrony and further compared these characteristics with both HBP and BVP. One computer simulation study indicates that LBBP and HBP are superior to BVP-CRT with a greater reduction of LVAT. However, interventricular synchrony of LBBAP is not as ideal as HBP due to a longer RVAT, but this can be mitigated by optimizing AV delay or bilateral bundle area pacing (Lin et al., 2020; Strocchi et al., 2020). The same electrical effect is also observed in our initial experience with an HF patient with LBBB who underwent successful implantation of both HBP and LBBP leads (Figure 2). With optimization of the sensed AV delay, LBBP produced equally narrow QRSd as HBP, with a stable lower LBBB correction threshold at implantation and after a 3-month follow-up. An echocardiographic analysis also suggested that either LBBP or HBP significantly alleviated the delayed activation and increased the average LV excursion.

Subsequent clinical studies further confirm the beneficial hemodynamic effect of LBBAP compared with HBP or BVP in both AVB and LBBB patients. Hu and others reported similar improvement of mechanical dispersion in both LBBP and HBP groups after 3-month follow-up while LBBP had

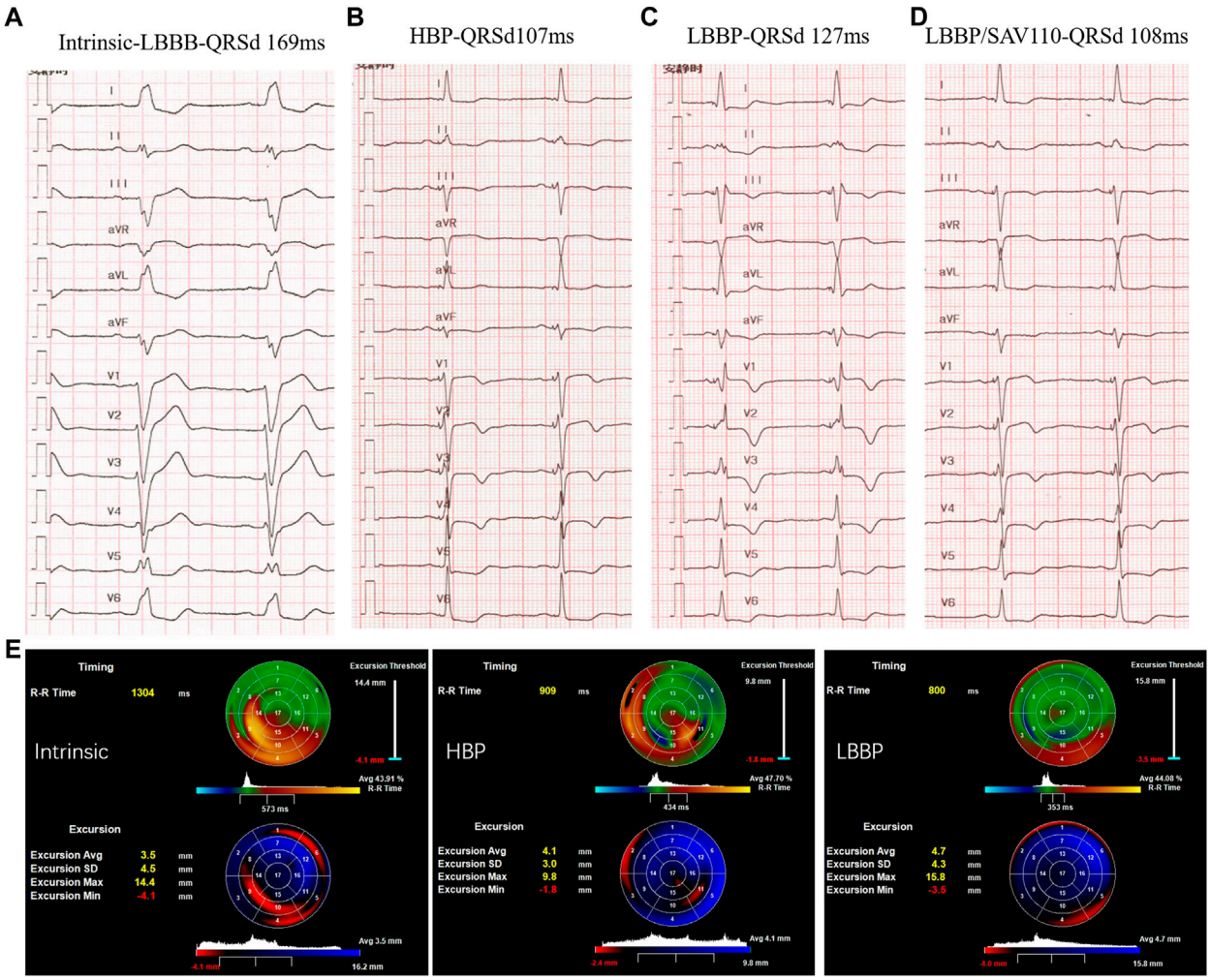

FIGURE 2
Comparison of LBBP and HBP in electrical and mechanical synchrony in a HF patient with LBBB: **(A)** Intrinsic rhythm with QRS duration (QRSd) of 169 ms; **(B)** Selective HBP at left bundle branch block (LBBB) correction threshold of 3 Vat 0.5 ms with QRSd equal to 107 ms. **(C)** LBBP at 0.5 V at 0.4 ms with QRSd of 127 ms and RV conduction delay pattern. **(D)** LBBP in DDD mode with SAV delay 110 ms with QRSd reduced to 108 ms. **(E)** 3-dimensional echocardiogram between selective His bundle pacing (HBP) and left bundle branch pacing (LBBP). Right: intrinsic rhythm; Middle: HBP in VVI mode; Left: LBBP in VVI mode. The upper "bull's eye" depicts the timing of contraction green areas represent synchronous areas, blue areas contract early and red/yellow areas show late contraction. The lower "bull's eye" shows the wall excursion with dark/red areas referring to reduced excursion and bright blue areas indicating the largest systolic radial excursion.

better pacing parameters and shorter procedure time (Hu et al., 2021). By used two-dimensional speckle tracking echocardiographic imaging, they found LBBAP delivered a greater reduction of QRSd, reduced global wasted work, improved cardiac work efficiency, and led to better mechanical synchronization and efficiency than the traditional BVP-CRT (Liu et al., 2021).

Notably, the electrical and mechanical superiority among LVSP, S-LBBP and NS-LBBP have also been heatedly discussed. In a study comparing ventricular depolarization of LBBAP and HBP using UHF-ECG in bradycardia patients, both the NS-LBBP and LVSP led to longer septal and RV depolarization duration compared with HBP. Compared with NS-LBBP that preserves physiological LV depolarization but increases interventricular electrical dyssynchrony, the LVSP tended to preserve the interventricular synchrony while prolonged the depolarization time of the LV lateral wall (Curila et al., 2021a). Another study delineated that LBBP offered more significant ventricular synchrony with significantly decreased QRS area which was almost equal to normal ventricular activation when compared to LVSP and RV pacing, whereas the LVAT and QRS vector did not differ between the LVSP and LBBP and normal ventricular

activation. Non-etheless, a recent study used UHF-ECG to analyze the superiority of LVSP over LBBP reported that LVSP from the proximity to the LBB region preserved interventricular dyssynchrony (described by e-DYS, the difference between the first and last activation in UHF-ECG), which was better than both S-LBBP and NS-LBBP (e-DYS: LVSP vs. NS-LBBP, vs. NS-LBBP: 16 m vs. -24 m vs-31 m), but did not prolong LV lateral wall activation (described by width of the UHF-QRS complex at 50% of its amplitude, Vd) among bradycardia patients. The study also compared S-LBBP and NS-LBBP in electrical activation and synchrony and found that S-LBBP produced shorter QRSd but led to greater interventricular dyssynchrony than NS-LBBP (Curila et al., 2021b).

Taken together, HBP and LBBAP are compelling alternatives for CRT with more physiological electrical and better hemodynamical effects than BVP. Though LBBAP does not capture the right side of the conduction system, it guarantees almost equal physiological LV activation as compared with HBP and can produce a similar narrow QRS complex and mechanical synchrony by optimizing the AV delay. In both types of CSP, recruitment of at least part of the conduction system enables shorter LV activation duration and narrower QRS duration. LVSP seems to induce better interventricular electrical synchrony compared with LBBP, but whether such minor differences in electrical synchrony can translate into clinical differences remains to be evaluated.

Conduction system pacing: The evidence for clinical efficacy

Application of HBP for patients with intrinsic conduction disturbance and indication for traditional CRT

Early in 2013, Barba-Pichardo pioneered a prospective study for HBP in 16 patients with LBBB and successfully achieved permanent HBP in nine patients, with mean QRSd shortening from 166 ms to 97 ms. After a mean follow-up time of 31.3 months, they reported a significant improvement in clinical and remodeling parameters of LV function (Barba-Pichardo et al., 2013). The first large sample size multi-center study was reported by Sharma et al. They assessed the feasibility and efficacy of HBP as a rescue strategy or a primary alternative to BVP in a group of systolic heart failure patients with LVEF lower than 50%, among whom 45% held BBB and 39% had RV pacing. After a mean follow-up of 14 months, both the rescue and the primary HBP groups showed a significantly narrowed QRSd and increased LVEF in both the LBBB (26%–41%) and non-LBBB morphology (32%–49%) groups (Sharma et al., 2018a). This research group further proved the efficacy of HBP for improving electrical synchrony and LV function in 39 patients with RBBB and reduced LVEF. They reported a significant reduction of QRSd from 158 to 127 m and observed an increase of LVEF from 31% to 39% after a mean follow-up of 15 months (Sharma et al., 2018b). These results provide a cornerstone for future randomized controlled trials in evaluating HBP as an alternative to BVP in patients who failed LV pacing and as a primary option for CRT. Regarding the long-term effect, Huang and others published 3-year results of a single-center prospective study of HBP for CRT in heart failure patients with typical LBBB and demonstrated the stable LBBB correction threshold along with the improvement in reverse remodeling echocardiographic metrics and clinical response (Huang et al., 2019). Subsequently, numerous observational studies of HBP for CRT were published, most of which corroborated these findings of the effective electrical synchrony, and functional and clinical improvement especially in patients with LBBB.

HBP for patients with pacing-induced dyssynchrony CRT upgradation

For those with chronic RV pacing or intranodal block, early observational studies also proved HBP as an applicable approach for normalizing QRS complex and T waves. Furthermore, in those with pacing-induced cardiomyopathy (PICM) and decreasing LVEF, HBP was also feasible with a highly successful implantation rate of nearly 90% and induced a significant improvement of LVEF, NYHA class, while alleviating mitral valve regurgitation and brain natriuretic peptide levels (Shan et al., 2018; Vijayaraman et al., 2019a). The latest report compared the efficacy of HBP and BVP in patients with PICM and found HBP brought more considerable improvement in LVEF and more significant reverse remodeling than BVP, indicating the potential of HBP as an alternative to BVP for CRT upgrading among PICM patients. (Gardas et al., 2022).

Clinical comparison of HBP and BVP

Compared with BVP, HBP appears to display more benefits in terms of acute hemodynamic improvements and echocardiographic response according to early results of small observational studies. The first randomization cross-over investigation comparing HBP and BVP for CRT was reported by Lustgartenl in 2015 (Lustgarten et al., 2015), in which in 12 patients who completed the entire protocol, the LVEF, NYHA, and quality of life scores all improved from baseline but did not differ between the HBP and BVP groups. The subsequent His-Sync study is the first multi-center randomized controlled trial (RCT) comparing HBP *in lieu* of BVP (Upadhyay et al., 2019b; Upadhyay et al., 2019c). The study randomized

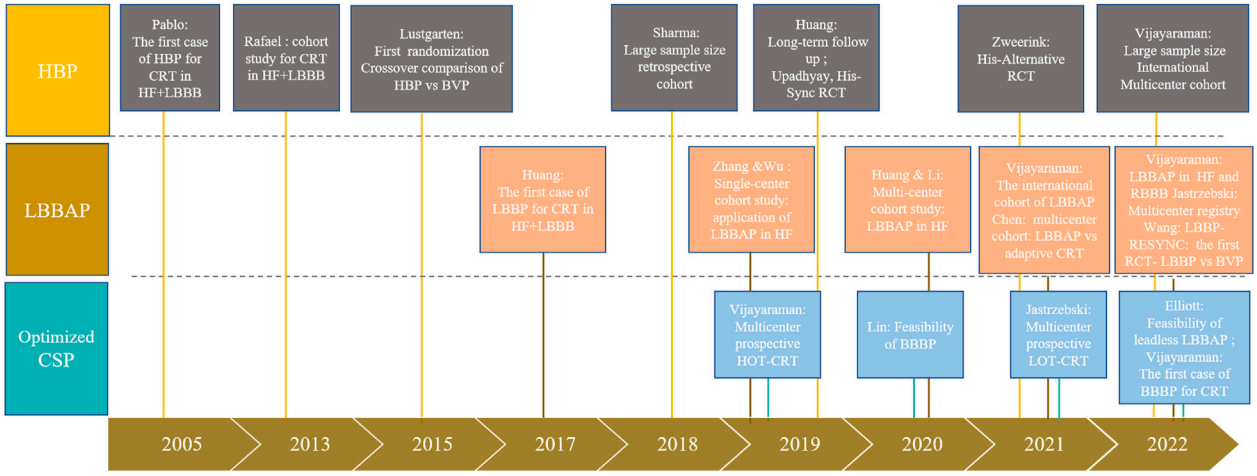

FIGURE 3
Landmark studies of CSP for CRT.

41 patients with CRT indication to HBP-CRT or BVP CRT group. In the intention-to-treat (ITT, sample size in HBP vs. BVP: 21 vs. 20), treatment received (TR, sample size in HBP vs. BVP: 16 vs. 24), and per-protocol (PP, sample size in HBP vs. BVP: 11 vs. 14) analyses, HBP resulted in narrower QRSd compared with the BVP group but the LVEF improvement and echocardiographic response rate did not show a significant difference despite the numerically higher improvement of LVEF and a trend towards higher response rate in HBP group in PP analysis. However, numerous shortcomings of the study were identified including a small sample size, high bi-directional crossover rate, and broad criteria for patient selection (especially IVCD), limiting the power and evidence sufficiency of the results. The His-alternative CRT is another randomized study comparing HBP and BVP for symptomatic HF patients with Strauss LBBB. 50 patients were randomized to the HBP and BVP group with a cross-over rate of 28% from HBP to BVP. ITT analysis demonstrated non-superior effect of HBP to BVP in QRSd narrowing or echocardiographic response, while PP analysis showed higher LVEF and lower LVESV after 6 months of follow-up in the HBP group than in the BVP group. Although the evidence generated to date is insufficient to claim that HBP is superior over BVP for CRT, these results provide the potential for better electrical synchrony of HBP and laid a foundation for HBP as an alternative to BVP (Supplementary Table S1, Figure 3).

Application of LBBAP for patients with intrinsic conduction disturbance and indication for traditional CRT

Given the drawbacks of a higher pacing capture threshold and a relatively long learning curve in HBP, LBBAP, with a lower capture threshold and higher success rate, sheds light on CSP for CRT. The landmark study of LBBAP for CRT was conducted by Dr. Huang in 2017 in a heart failure (LVEF of 32%) patient with typical LBBB (QRSd 180 ms). After the failure of left ventricular lead placement, HBP also failed to correct the LBBB at an output of 10 V. LBB was captured at 0.5 V at 0.5 ms, after optimization of atrioventricular (AV) delay, QRSd was reduced to 94 ms and the threshold was stable after a 1-year follow-up, with significant improvement of LVEF (32%–62%) and NYHA class (IV to I) (Huang et al., 2017). Since the anatomic merits of LBB fan-shape distribution (Ponnusamy et al., 2020), LBBAP has been widely applied in different centers rapidly while clinical evidence has been accumulated since 2017 (Supplementary Table S2, Figure 3). In 2019, two single-center observational studies carried out respectively by Zhang and Wu documented a significant reduction in QRSd and improvement in cardiac function after a mean follow-up of 6.7 and 32.5 months (Wu et al., 2019; Zhang et al., 2019), providing promising evidence for LBBAP feasibility and efficacy as a CRT approach in HF patients with LBBB. Afterward, a multi-center prospective cohort study by Huang and Li further confirmed the effectiveness of LBBAP in improving electrical synchrony and functional improvement of heart failure with LBBB (Huang et al., 2020; Li et al., 2020). A larger international multicenter cohort study initiated by Vijayaraman and coworkers analyzed the LBBAP in a board population with LVEF <50% and indication for CRT (including both LBBB and non-LBBB patients). They found in both the LBBB and non-LBBB group, the LBBAP provided significant QRS narrowing (LBBB 162 ms–133 ms; non-LBBB 160 ms to 143 ms, $p < 0.01$) and improved clinical and echocardiographic outcomes (NYHA class: LBBB 2.8 to 1.7, non-LBBB 2.7 to 1.8; LVEF: LBBB 30%–44%; non-LBBB 33%–43%, all $p < 0.01$).

The latest clinical evidence also suggested LBBAP in the population of HF patients with RBBB. Though the QRSd only showed a modest reduction, LBBAP was still associated with improvement in LVEF and NYHA class, indicating that LBBAP might be a choice of alternative CRT for patients with cardiac dysfunction and RBBB (Vijayaraman et al., 2022).

LBBAP for patients with pacing-induced dyssynchrony and CRT upgradation

Similar to HBP, LBBAP was also proved feasible for patients with pacing-induced cardiomyopathy (PICM) and RV pacing upgrading in small sample studies (Li et al., 2021; Qian et al., 2021; Chen et al., 2022). Permanent LBBAP was successfully achieved in 93%–100% of patients with PICM and could also be performed safely in those with intranodal blocks. After the follow-up time ranging from 6 to 12 months (Qian et al., 2021; Rademakers et al., 2022), LBBAP could result in significant narrowing of QRSd, and improvement of LVEF and NYHA function with no observations of upgrade-related complications. But clinical observations comparing the efficacy of BVP and LBBAP for CRT upgradation are still lacking.

Clinical comparison among LBBAP, HBP, and BVP

The first multi-center comparison of LBBAP and optimized BVP was reported recently by Chen et al. (Chen et al., 2022) to compare LBBAP with BVP with the adaptive algorithm in HF patients with LVEF ≤35% and LBBB. The results revealed a better electrical and mechanical resynchronization and higher super-response rate of LBBAP compared to BVP (Chen et al., 2022).

In a non-randomized treatment investigation comparing treatment outcomes of LBBAP, HBP, and BVP among patients with HFrEF and typical LBBB (Wu et al., 2021), similar improvements in symptoms and LV function were observed between LBBAP and HBP groups that were better than BVP. A recently published large multicenter cohort study in a large sample size of HF patients with LVEF lower than 35%, and CRT indications (in which 87 underwent HBP, 171 underwent LBBAP, 258 underwent BVP) found significantly narrower QRS complex, greater improvement of LVEF and lower rates of death or HFH during a mean follow-up of 27 months in patients receiving CSP as compared with BVP. But no significant differences in death or HFH were observed between the HBP vs. LBBAP group. In the latest study including patients with AF after atrioventricular junction ablation, LBBP held higher successful implantation rates, better pacing parameters, and fewer lead-related complications compared with HBP, though both achieved similar improvement in clinical outcomes (Cai et al., 2022). More recently, the first RCT (LBBP-RESYNC trail) to compare CRT efficacy between LBBP and BVP among heart failure patients with non-ischemic cardiomyopathy and LBBB found more improvement in LVEF by LBBP-CRT than BVP-CRT after 6-month follow-up (Wang et al., 2022).

As for the different clinical effects between LBBP and LVSP, there is still no head-to-head comparison. The study by Jiang et al. found that both the LBBP and LVSP groups significantly lowered the incidence of heart failure hospitalizations and all-cause mortality in LBBB patients with baseline LVEF higher than 35% compared with patients with LVEF lower than 35% during 12 months-follow-up (Jiang et al., 2022). Another study including patients with LBBB also reported improvement of cardiac functional parameters in LBBAP (LBBP and LVSP) groups in patients with LVEF lower than 50% after a 6-month follow-up (Shan et al., 2021). But these studies did not specify the improvement in each group for comparison. Only in the sub-group analysis of one published study, those who underwent LBB optimized CRT (LOT-CRT) with LBB capture showed better echocardiographic (11.1% vs. 4.7% of LVEF improvement, p = 0.0196) and clinical response (82% vs. 61%, p = 0.035) than the LVSP group, indicating that capture of LBB might provide a clinical benefit over LVSP (Jastrzębski et al., 2021). Recently, Jimenez et al. reported a significant improvement in LVEF and a decrease in LVESV following LBBP but diminished LVEF and increased LVESV in those without LBB capture in a small group of patients with a comparable baseline LVEF and wide QRSd (Ramos Jimenez et al., 2022). So far, the evidence is still lacking, and comparable studies or randomized trials are warranted for comparing the long-term clinical effects between LBBP and LVSP.

Optimal lead position

The quest for the optimal lead position is based on clinical evaluations of CSP as a novel approach to CRT. The optimal lead position should preserve or restore the functionality (ventricular electrical synchrony) of the cardiac conduction system with consideration of technical efficiency and pacing parameters. CSP introduces better LV electrical synchrony with a narrow QRS complex compared with traditional BVP, with HBP displaying more physiological activation similar to the normal intrinsic activation in the absence of relative RV delay observed in LBBAP. Regarding the implantation process and pacing parameters, LBBAP can be a technically more promising way due to the shorter learning curve, higher successful implantation rate and stable pacing parameters when compared to HBP. But recently reported distal HBP may overcome these drawbacks through deep septal His-bundle capture (Supplementary Table S3) (Vijayaraman, 2020).

Besides, the evaluation of the optimal lead position may be individualized and tailored for a different population. Current clinical evidence from small RCTs and observational studies suggest that LBBAP may bring a higher improvement of LVEF, and a similar survival rate compared with BVP in

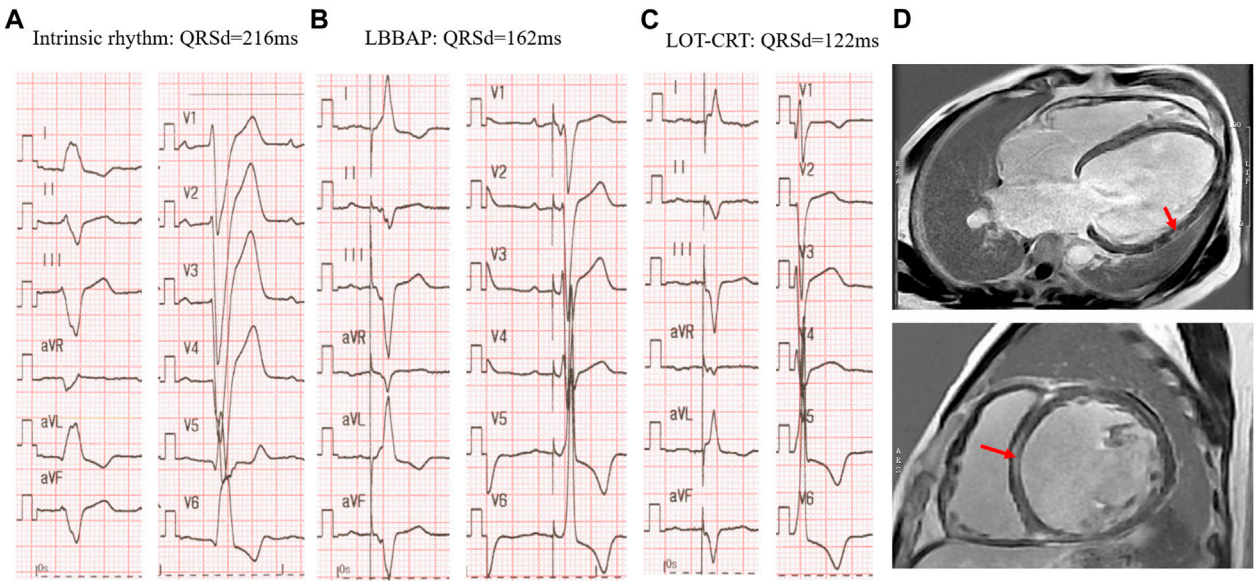

FIGURE 4
LOT-CRT for further correction of LBBB in a patient with myocardium scars. **(A)** Intrinsic rhythm with LBBB morphology and very wide QRS complex of 216 ms; **(B)** LBBAP alone at 3v at 0.4 ms in DDD mode with SAV of 120 ms; **(C)** LOT-CRT at 3.5 Vat 0.4 ms in DDD mode with SAV of 120 m and LBBAP prior to LV pacing of 60 ms. **(D)** Myocardial scars detected by CMR-late gadolinium enhancement prior to operation: upper LV four-chamber view, the arrow represents the scar in LV lateral wall; lower, short axis view, arrow indicates the septal scar.

patients with NICM and LBBB as compared with patients with non-LBBB and/or ICM. However, clinical evidence of the efficacy of CSP compared with BVP among patients with non-LBBB morphology is limited. Therefore, CSP may be best suited for LBBB patients while the BVP might be more appropriate for those with non-LBBB pattern, but more clinical evidence in patients with non-LBBB morphology is required (Wouters et al., 2021; Strocchi et al., 2022).

Previous studies and guidelines suggest that in patients with reduced LVEF and narrow QRS complex, BVP provides limited benefit (Moss et al., 2009; Tracy et al., 2012). Compelling results of applying CSP in patients with PICM, RV pacing upgrading as well as AV node ablation in atrial fibrillation patients are accumulating (Vijayaraman et al., 2017; Cai et al., 2022; Huang W. et al., 2022; Ivanovski et al., 2022). Hence, we expect that CSP may be a better option for primary and upgrading therapy in HF patients who have intact intraventricular conduction but need high RV pacing burden due to bradycardia or AV node ablation.

Optimization of CSP

His-optimized CRT

The prerequisite of CSP is to place the pacing lead tip at the appropriate site of the conduction system. However, the coexisting IVCD can delay the activation of the myocardium segments, hampering the full correction of electrical disturbance. Hence, the His and LBB-optimized CRT have been introduced to further narrow the QRS complex by stimulating both the native conduction system and the later activated myocardial areas. Vijayaraman performed the His-optimized CRT (HOT-CRT) in 27 patients with LVEF≤35% and LBBB/IVCD that could not be fully corrected by HBP alone and observed a remarkable reduction in QRSd from baseline 183 m–120 m by HOT-CRT (HBP plus LV pacing) than the BVP (mean QRSd 162 m) or HBP alone (mean QRSd 151 m). They also found that HOT-CRT brought significant clinical and echocardiographic response rates of 84% and 92% respectively (Vijayaraman et al., 2019b). By using ECGi, Alwin Zweerink further found that the HOT-CRT appeared to bring more synchronous activation, as compared with BVP-CRT (including multipoint pacing, MMP) and HBP-CRT, and not only remarkably increased the ventricular electrical synchrony by reducing LVAT (LVAT reduction: HOT vs. HBP: 17 m, HOT vs. BVP: 22 m, HOT vs. MMP: 11 m) but also improved RV synchrony in RBBB patients (Zweerink et al., 2021).

LBB-optimized CRT

The feasibility of LBB-optimized CRT (LOT-CRT) was conducted by a multicenter observational study in

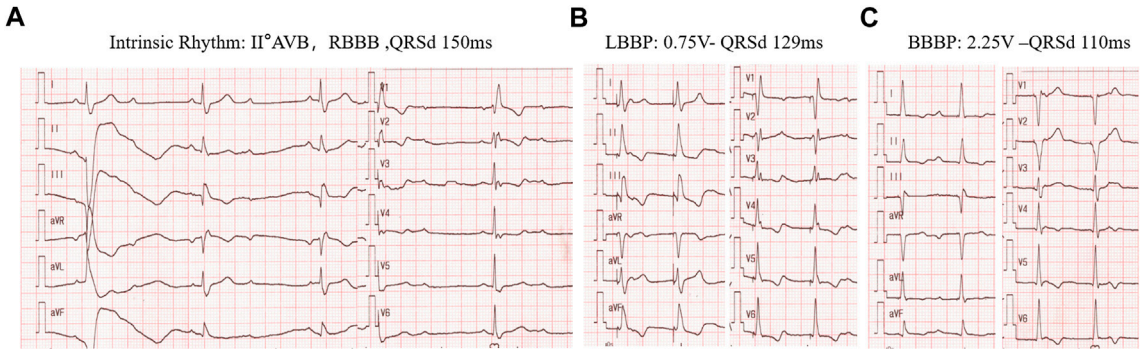

FIGURE 5
BBBP for correction of RBBD induced by LBBAP in a patient with intrinsic RBBB rhythm. **(A)** intrinsic rhythm of RBBB pattern with II° AV block and QRSd of 150 ms. **(B)** left bundle branch pacing by pacing the cathodal tip electrode alone at 0.75v at 0.4 ms with the RV delay pattern. **(C)**, Bilateral bundle branch area pacing (BBBP) with the cathodal tip electrode and the anodal ring electrode at 2.25 v at0.4 ms with QRSd further reduced to 110 ms.

112 patients with CRT indication, including 42% LBBB, 22% IVCD, 23% RV pacing, and 12% RBBB. LOT-CRT resulted in acutely improved electrical resynchronization, with the reduction of QRSd three times greater than BVP pacing and superior LVAT compared with LBBAP alone (mean QRSd: baseline 182 m, BVP 170 m, LBBAP 162 m, LOT-CRT 144 m) as well as improvement of LVEF (from 28.5% to 37.2%) and NYHA class (from 2.9 to 1.9) (Jastrzębski et al., 2021).

These findings suggest that in patients with more advanced dysfunction of the conduction system/heart muscle as evidenced by wider baseline QRSd (eg.>180 m) or myocardial scars (Figure 4), despite proximal HB or LBB capture, additional LV pacing may be required to further correct the ventricular delay and achieve better cardiac synchrony as well as functional improvement.

Bilateral bundle branch area pacing

As described above, although LBBAP normalizes LVAT, it also creates significant right ventricular conduction delays compared with normal intrinsic rhythm or HBP. Therefore, effects have been made to diminish the RBBB during LBBP to obtain better interventricular synchrony. Despite the previously discussed optimization of AV delay for fusing intrinsic RV conduction with LBBP, in 2020, a new concept of bilateral bundle branch area pacing (BBBP) was initiated by Lin et al., which involves simultaneous stimulation of both the left branch bundle area and the right branch bundle area. With BBBP, the RBBB pattern brought by LBBP was resolved and delayed right ventricular activation was diminished with significantly shorter QRSd as compared with LBBP. (Lin et al., 2020). Such a strategy may be particularly important for optimizing the electrical synchrony in those with intrinsic RBBB (Figure 5), among whom the existing RV delay may not be diminished by programming AV delay alone.

More recently, Vijayaraman delineated another way of BBBP by the direct right bundle pacing and left bundle pacing *via* two leads with a lower capture threshold (1-2v) in a 78-year-old HF patient with LBBB, and achieved complete right and left ventricular electrical resynchronization with a QRS complex similar to that of HBP at high threshold (8 V) (Vijayaraman, 2022).

Nevertheless, bilateral bundle branch area pacing still needs further investigation. The anatomical characteristics of the RBB, which, unlike the left bundle branch, is a cord-like thin structure with a shorter intramuscular course within the septum and then distributes in sub-endocardium region of the RV (Padala et al., 2022). Therefore, compared with the fan-shaped LBB, the pacing of the RBB is more difficult. It has been reported that the transition of QRSd during distal RBBP can be more pronounced in the frontal QRS axis, thus being more likely to be missed during threshold testing (Burri and Zimmermann, 2021). However, whether pacing the RBB area can bring more benefit to the electrical and mechanical synchrony, especially in those who have intrinsic RV electrical or mechanical delay still needs to be evaluated.

Leadless LBBAP

Another compelling innovation, leadless LBBAP, which combines the attractive concepts of CSP and leadless pacing was initiated by Elliott, et al., in 2021. They provided the technical feasibility of leadless LBBAP to achieve better electrical synchrony from the LV septal pacing with the WISE-CRT delivery system (Elliott et al., 2021). A multi-center study

further provided the feasibility and efficacy of leadless LBBAP *via* the WISE-CRT delivery system in two swine models and eight HF patients with wide QRSd. Preclinical data suggest the possibility of electrode tines in pacing the LV septal close to Purkinje tissue. All patients had the LV septal electrode and WISE-CRT implanted successfully, and temporary LV pacing significantly reduced the QRSd from 187.1 m to 139.8 m. At an early follow-up of 82.5 days, the median LV pacing percentage was 98.5%, and 62.5% of patients had symptom improvement (Elliott et al., 2022). The board distribution of the LBB conduction network provides histological merits for leadless LBBAP. It may be a promising option for patients with venous approach issues. Future studies are required regarding the long-term safety and efficacy of the technique, stable capture of the conduction system, and resynchronization effect compared with BVP-CRT or lead-based CSP.

The above studies or cases in optimization and innovation of CSP are conceptually attractive, but long-term clinical consequences or accumulative experiences for safety and efficacy remain to be validated in the future.

Consideration of device programming

Since there are no CRT devices particularly designed for CSP, the programming of CSP remains confusing and challenging. Experience derived from previous clinical practice may be considered when programming biventricular devices.

Specifically, in patients with sinus rhythm and an atrial lead, the HBP or LBBAP lead is often connected to the LV port with RV backup pacing lead or defibrillation lead connected to the RV port, which can be used for ventricular sensing. Sequential pacing can be programmed with the CSP as a priority. Considering that anodal capture can attenuate the delay of RV activation in some patients, the bipolar configuration can be programmed for LBBAP (Lin et al., 2020). Moreover, adequate AV delay programming after the procedure allows the fusion of LBBAP with native right bundle conduction to provide another option to minimize the delay of RV activation (Raymond-Paquin et al., 2021).

For patients with atrial fibrillation, the CSP lead can be connected to the atrial port, with the RV and LV leads being connected to the corresponding RV and LV ports for HOT-CRT or LOT-CRT (Vijayaraman et al., 2019b; Zweerink et al., 2021). For HOT-CRT, the empiric value of HBP-VP delay of 60 m was reported to generate better HBP and ventricular pacing (LV, RV, BVP) fusion with shorter LVAT (Zweerink et al., 2021). More recently, the combination of adaptive CRT algorithm with LOT-CRT was proved feasible in patients with reduced LVEF and LBBB, which was associated with shorter paced QRSd, LVAT, and significant improvements in clinical NYHA and LVEF compared with BVP-CRT (Feng et al., 2022).

Nevertheless, there is still no clinical evidence to verify which pattern of device programming is optimal for CSP. Besides the successful implantation, clinical pitfalls should be evaluated and automatic device settings designed for CSP are urgently needed to ensure efficient CSP for CRT.

Current recommendation and future directions

Providing the attractive concept of physiological pacing and initial encouraging results from multiple clinical observations, CSP has updated the conception of CRT for the treatment of electrical dyssynchrony-caused HF. Currently, guidelines from the American Heart Association (AHA) and the European Society of Cardiology (ESC) had also emphasized its role as a promising approach for CRT. In the 2018 AHA guidelines, HBP is recommended as a Class II indication for patients with AV block and LVEF between 36% and 50%, with an expected RV pacing rate over 40% (Kusumoto et al., 2019). In the 2021 ESC guidelines, HBP is recommended as a Class II recommendation as a bail-out for CRT candidates with unsuccessful coronary sinus lead placement (Authors/Task Force Members et al., 2022). By contrast, the newly released Chinese expert consensus on His-Purkinje conduction system pacing takes more proactive attitude towards the usage of both forms of CSP, revealing that CSP may be considered as a rescue approach for traditional CRT-non responders or a primary approach for CRT among HF patients with LBBB, QRSd over 130 m, LVEF lower than 35% and NYHA class II-IV after GDMT (Chinese Society of Pacing and Electrophysiology and Chinese Society of Arrhythmias, 2021).

However, whether CSP can serve as a primary CRT as BVP-CRT in routine clinical practice for patients with CRT indications needs more clinical evidence. Furthermore, for CRT response whether the previously established metrics of BVP can be used with HBP or LBBAP is unknown. The similarity and differences in characteristics of the target population appropriate for BVP and CSP remain to be addressed. Finally, novel approaches for CSP such as leadless LBBAP or bilateral bundle pacing are promising, but the safety, efficacy, and technology-specific advantages remain to be explored.

Conclusion

CSP allows for a more physiological approach to CRT by recruitment of the native conduction system and studies in

CSP demonstrate cumulative clinical evidence for its safety and efficacy in HF treatment. Although the clinical evidence from small RCT and observational studies is still insufficient to pose the CSP as a superior approach to BVP, the previous encouraging results underpin the prospect of the novel pacing modality as a primary CRT approach. The tailored candidates of CSP in CRT should be further defined by well-designed, prospective, randomized controlled studies with long-term follow-up and hard clinical outcomes including the mortality rate and HF hospitalization.

Author contributions

ZC drafted the manuscript, XM provide imaging evaluation and interpretation, and XZ and KC contribute to the conception, design and editing of the work. All authors approved the work for publication.

Funding

This work was supported by the National Natural Science Foundation of China (Grant/Award Number: 81870260).

Conflict of interest

XZ was employeed by the company Medtronic, Inc.

The remaining authors declare that the research was conducted in the absence of any commercial or financial relationships that could be construed as a potential conflict of interest.

Publisher's note

All claims expressed in this article are solely those of the authors and do not necessarily represent those of their affiliated organizations, or those of the publisher, the editors and the reviewers. Any product that may be evaluated in this article, or claim that may be made by its manufacturer, is not guaranteed or endorsed by the publisher.

Supplementary material

The Supplementary Material for this article can be found online at: https://www.frontiersin.org/articles/10.3389/fphys.2022.1045740/full#supplementary-material

References

Ambrosy, A. P., Fonarow, G. C., Butler, J., Chioncel, O., Greene, S. J., Vaduganathan, M., et al. (2014). The global health and economic burden of hospitalizations for heart failure: Lessons learned from hospitalized heart failure registries. *J. Am. Coll. Cardiol.* 63 (12), 1123–1133. doi:10.1016/j.jacc.2013.11.053

Arnold, A. D., Shun -Shin Matthew, J., Keene, D., Howard, J. P., Sohaib, S. M. A., Wright, I. J., et al. (2018). His resynchronization versus biventricular pacing in patients with heart failure and left bundle branch block. *J. Am. Coll. Cardiol.* 72 (24), 3112–3122. doi:10.1016/j.jacc.2018.09.073

Arnold, A. D., Shun-Shin, M. J., Ali, N., Keene, D., Howard, J. P., Chow, J. J., et al. (2021). Left ventricular activation time and pattern are preserved with both selective and nonselective His bundle pacing. *Heart Rhythm O2* 2 (5), 439–445. doi:10.1016/j.hroo.2021.08.001

Auricchio, A., Fantoni, C., Regoli, F., Carbucicchio, C., Goette, A., Geller, C., et al. (2004). Characterization of left ventricular activation in patients with heart failure and left bundle-branch block. *Circulation* 109 (9), 1133–1139. doi:10.1161/01.CIR.0000118502.91105.F6

Authors/Task Force MembersMcDonagh, T. A., Metra, M., Adamo, M., Gardner, R. S., Baumbach, A., et al. (2022). 2021 ESC Guidelines for the diagnosis and treatment of acute and chronic heart failure: Developed by the Task Force for the diagnosis and treatment of acute and chronic heart failure of the European Society of Cardiology (ESC). With the special contribution of the Heart Failure Association (HFA) of the ESC. *Eur. J. Heart Fail.* 24 (1), 4–131. doi:10.1002/ejhf.2333

Barba-Pichardo, R., Sanchez, A. M., Fernandez-Gomez, J. M., Morina-Vazquez, P., Venegas-Gamero, J., and Herrera-Carranza, M. (2013). Ventricular resynchronization therapy by direct His-bundle pacing using an internal cardioverter defibrillator. *Europace* 15 (1), 83–88. doi:10.1093/europace/eus228

Burri, H., and Zimmermann, M. (2021). Infranodal Wenckebach conduction block and illustration of the gap phenomenon. *Hear. Case Rep.* 7, 63–64. doi:10.1016/j.hrcr.2020.11.005

Byrne, M. J., Helm, R. H., Daya, S., Osman, N. F., Halperin, H. R., Berger, R. D., et al. (2007). Diminished left ventricular dyssynchrony and impact of resynchronization in failing hearts with right versus left bundle branch block. *J. Am. Coll. Cardiol.* 50 (15), 1484–1490. doi:10.1016/j.jacc.2007.07.011

Cai, M., Wu, S., Wang, S., Zheng, R., Jiang, L., Lian, L., et al. (2022). Left bundle branch pacing postatrioventricular junction ablation for atrial fibrillation: Propensity score matching with his bundle pacing. *Circ. Arrhythm. Electrophysiol.* 15 (10), e010926. doi:10.1161/CIRCEP.122.010926

Catanzariti, D., Maines, M., Cemin, C., Broso, G., Marotta, T., and Vergara, G. (2006). Permanent direct his bundle pacing does not induce ventricular dyssynchrony unlike conventional right ventricular apical pacing. *J. Interv. Card. Electrophysiol.* 16 (2), 81–92. doi:10.1007/s10840-006-9033-5

Chen, X., Ye, Y., Wang, Z., Jin, Q., Qiu, Z., Wang, J., et al. (2022). Cardiac resynchronization therapy via left bundle branch pacing vs. optimized biventricular pacing with adaptive algorithm in heart failure with left bundle branch block: a prospective, multi-centre, observational study. *Europace.* 24, 807–816. doi:10.1093/europace/euab249

Chinese Society of Pacing and Electrophysiology, and ; Chinese Society of Arrhythmias (2021). Chinese expert consensus on His-Purkinje conduction system pacing. *Chin. J. Card. Arrhyth* 25 (1), 10–36. doi:10.3760/cma.j.cn.113859-20201110-00290

Curila, K., Prochazkova, R., Jurak, P., Jastrzebski, M., Halamek, J., Moskal, P., et al. (2020). Both selective and nonselective His bundle, but not myocardial, pacing preserve ventricular electrical synchrony assessed by ultra-high-frequency ECG. *Heart Rhythm.* 17 (4), 607–614. doi:10.1016/j.hrthm.2019.11.016

Curila, K., Jurak, P., Jastrzebski, M., Prinzen, F., Waldauf, P., Halamek, J., et al. (2021). Left bundle branch pacing compared to left ventricular septal myocardial pacing increases interventricular dyssynchrony but accelerates left ventricular lateral wall depolarization. *Heart Rhythm.* 18 (8), 1281–1289. doi:10.1016/j.hrthm.2021.04.025

Curila, K., Jurak, P., Vernooy, K., Jastrzebski, M., Waldauf, P., Prinzen, F., et al. (2021). Left ventricular myocardial septal pacing in close proximity to LBB does not prolong the duration of the left ventricular lateral wall depolarization compared to LBB pacing. *Front. Cardiovasc. Med.* 8, 787414. doi:10.3389/fcvm.2021.787414

Derval, N., Duchateau, J., Mahida, S., Eschalier, R., Sacher, F., Lumens, J., et al. (2017). Distinctive left ventricular activations associated with ECG pattern in heart failure patients. *Circ. Arrhythm. Electrophysiol.* 10 (6), e005073. doi:10.1161/CIRCEP.117.005073

Dou, J., Xia, L., Zhang, Y., Shou, G., Wei, Q., Liu, F., et al. (2009). Mechanical analysis of congestive heart failure caused by bundle branch block based on an electromechanical canine heart model. *Phys. Med. Biol.* 54 (2), 353–371. doi:10.1088/0031-9155/54/2/012

Elliott, M. K., Jacon, P., Sidhu, B. S., Smith, L. J., Mehta, V. S., Gould, J., et al. (2021). Technical feasibility of leadless left bundle branch area pacing for cardiac resynchronization: a case series. *Eur. Heart J. Case Rep.* 5 (11), ytab379. doi:10.1093/ehjcr/ytab379

Elliott, M. K., Vergara, P., Wijesuriya, N., Mehta, V. S., Bosco, P., Jacon, P., et al. (2022). Feasibility of leadless left ventricular septal pacing with the WiSE-CRT system to target the left bundle branch area: A porcine model and multicenter patient experience. *Heart Rhythm.* 19, 1974–1983. doi:10.1016/j.hrthm.2022.07.017

Emerek, K., Friedman, D. J., Sørensen, P. L., Hansen, S. M., Larsen, J. M., Risum, N., et al. (2019). Vectorcardiographic QRS area is associated with long-term outcome after cardiac resynchronization therapy. *Heart Rhythm.* 16 (2), 213–219. doi:10.1016/j.hrthm.2018.08.028

Fang, F., Chan, J. Y. S., Yip, G. W. K., Xie, J. M., Zhang, Q., Fung, J. W. H., et al. (2010). Prevalence and determinants of left ventricular systolic dyssynchrony in patients with normal ejection fraction received right ventricular apical pacing: a real-time three-dimensional echocardiographic study. *Eur. J. Echocardiogr.* 11 (2), 109–118. doi:10.1093/ejechocard/jep171

Fantoni, C., Kawabata, M., Massaro, R., Regoli, F., Raffa, S., Arora, V., et al. (2005). Right and left ventricular activation sequence in patients with heart failure and right bundle branch block: a detailed analysis using three-dimensional non-fluoroscopic electroanatomic mapping system. *J. Cardiovasc. Electrophysiol.* 16 (2), 112–119. doi:10.1046/j.1540-8167.2005.40777.x

Feng, X. F., Yang, L. C., Zhao, Y., Yu, Y. C., Liu, B., and Li, Y. G. (2022). Effects of adaptive left bundle branch–optimized cardiac resynchronization therapy: a single centre experience. *BMC Cardiovasc. Disord.* 22 (1), 360. doi:10.1186/s12872-022-02742-2

Gaba, P., Pedrotty, D., DeSimone, C. V., Bonikowske, A. R., Allison, T. G., and Kapa, S. (2020). Mortality in patients with right bundle-branch block in the absence of cardiovascular disease. *J. Am. Heart Assoc.* 9 (19), e017430. doi:10.1161/JAHA.120.017430

Gardas, R., Golba, K. S., Soral, T., Biernat, J., Kulesza, P., Sajdok, M., et al. (2022). The effects of his bundle pacing compared to classic resynchronization therapy in patients with pacing-induced cardiomyopathy. *J. Clin. Med.* 11 (19), 5723. doi:10.3390/jcm11195723

Ghani, A., Delnoy, P. P. H. M., Ottervanger, J. P., Ramdat Misier, A. R., Smit, J. J. J., and Elvan, A. (2011). Assessment of left ventricular dyssynchrony in pacing-induced left bundle branch block compared with intrinsic left bundle branch block. *Europace* 13 (10), 1504–1507. doi:10.1093/europace/eur117

Hu, Y., Li, H., Gu, M., Hua, W., Niu, H., Zhang, N., et al. (2021). Comparison between his-bundle pacing and left bundle branch pacing in patients with atrioventricular block. *J. Interv. Card. Electrophysiol.* 62 (1), 63–73. doi:10.1007/s10840-020-00869-w

Huang, W., Su, L., Wu, S., Xu, L., Xiao, F., Zhou, X., et al. (2017). A novel pacing strategy with low and stable output: Pacing the left bundle branch immediately beyond the conduction block. *Can. J. Cardiol.* 33 (12), 1736.e1–1736. doi:10.1016/j.cjca.2017.09.013

Huang, W., Su, L., Wu, S., Xu, L., Xiao, F., Zhou, X., et al. (2019). Long-term outcomes of His bundle pacing in patients with heart failure with left bundle branch block. *HEART* 105 (2), 137–143. doi:10.1136/heartjnl-2018-313415

Huang, W., Wu, S., Vijayaraman, P., Su, L., Chen, X., Cai, B., et al. (2020). Cardiac resynchronization therapy in patients with nonischemic cardiomyopathy using left bundle branch pacing. *JACC. Clin. Electrophysiol.* 6 (7), 849–858. doi:10.1016/j.jacep.2020.04.011

Huang, H. T., Huang, J. L., Lin, P. L., Lee, Y. H., Hsu, C. Y., Chung, F. P., et al. (2022). Clinical impacts of sacubitril/valsartan on patients eligible for cardiac resynchronization therapy. *Esc. Heart Fail.* Epub ahead of print. doi:10.1002/ehf2.14107

Huang, W., Wang, S., Su, L., Fu, G., Su, Y., Chen, K., et al. (2022). His-bundle pacing vs biventricular pacing following atrioventricular nodal ablation in patients with atrial fibrillation and reduced ejection fraction: A multicenter, randomized, crossover study—the ALTERNATIVE-AF trial. *Heart Rhythm.* 19 (12), 1948–1955. doi:10.1016/j.hrthm.2022.07.009

Ivanovski, M., Mrak, M., Mežnar, A. Z., and Žižek, D. (2022). Biventricular versus conduction system pacing after atrioventricular node ablation in heart failure patients with atrial fibrillation. *J. Cardiovasc. Dev. Dis.* 9 (7), 209. doi:10.3390/jcdd9070209

Jastrzębski, M., Moskal, P., Huybrechts, W., Curila, K., Sreekumar, P., Rademakers, L. M., et al. (2021). Left bundle branch–optimized cardiac resynchronization therapy (LOT-CRT): Results from an international LBBAP collaborative study group. *Heart Rhythm.* 19 (1), 13–21. doi:10.1016/j.hrthm.2021.07.057

Jiang, Z., Wu, T., Wu, Y., Chen, Z., Yang, W., Chen, C., et al. (2022). Clinical outcomes of permanent left bundle branch area pacing in patients with left bundle branch block and left ventricular ejection fraction >35 vs. ≤35. *Front. Cardiovasc. Med.* 9, 838708. doi:10.3389/fcvm.2022.838708

Kato, H., Yanagisawa, S., Sakurai, T., Mizuno, C., Ota, R., Watanabe, R., et al. (2022). Efficacy of his bundle pacing on LV relaxation and clinical improvement in HF and LBBB. *JACC. Clin. Electrophysiol.* 8 (1), 59–69. doi:10.1016/j.jacep.2021.06.011

Kaza, N., Keene, D., and Whinnett, Z. I. (2022). Generating evidence to support the physiologic promise of conduction system pacing: Status and update on conduction system pacing trials. *Card. Electrophysiol. Clin.* 14 (2), 345–355. doi:10.1016/j.ccep.2022.01.002

Kerwin, W. F., Botvinick, E. H., O'Connell, J. W., Merrick, S. H., DeMarco, T., Chatterjee, K., et al. (2000). Ventricular contraction abnormalities in dilated cardiomyopathy: effect of biventricular pacing to correct interventricular dyssynchrony. *J. Am. Coll. Cardiol.* 35 (5), 1221–1227. doi:10.1016/S0735-1097(00)00555-6

Kristensen, S. L., Castagno, D., Shen, L., Jhund, P. S., Docherty, K. F., Rorth, R., et al. (2020). Prevalence and incidence of intra-ventricular conduction delays and outcomes in patients with heart failure and reduced ejection fraction: insights from PARADIGM-HF and ATMOSPHERE. *Eur. J. Heart Fail.* 22 (12), 2370–2379. doi:10.1002/ejhf.1972

Kroon, W., Lumens, J., Potse, M., Suerder, D., Klersy, C., Regoli, F., et al. (2015). *In vivo* electromechanical assessment of heart failure patients with prolonged QRS duration. *Heart Rhythm.* 12 (6), 1259–1267. doi:10.1016/j.hrthm.2015.03.006

Kusumoto, F. M., Schoenfeld, M. H., Barrett, C., Edgerton, J. R., Ellenbogen, K. A., Gold, M. R., et al. (2019). 2018 ACC/AHA/HRS guideline on the evaluation and management of patients with bradycardia and cardiac conduction delay: A report of the American college of Cardiology/American heart association task Force on clinical practice guidelines and the heart rhythm society. *Circulation* 140 (8), e382–e482. doi:10.1161/CIR.0000000000000628

Lai, L., Jiang, R., Fang, W., Yan, C., Tang, Y., Hua, W., et al. (2020). Prognostic impact of right bundle branch block in hospitalized patients with idiopathic dilated cardiomyopathy: a single-center cohort study. *J. Int. Med. Res.* 48 (1), 300060518801478. doi:10.1177/0300060518801478

Li, X., Qiu, C., Xie, R., Ma, W., Wang, Z., Li, H., et al. (2020). Left bundle branch area pacing delivery of cardiac resynchronization therapy and comparison with biventricular pacing. *Esc. Heart Fail.* 7 (4), 1711–1722. doi:10.1002/ehf2.12731

Li, H., Wang, L., Peng, X., and Wu, J. (2021). The quality of life of patients with pacemaker-induced cardiomyopathy after they upgrade to left bundle branch pacing. *Am. J. Transl. Res.* 13 (4), 3044–3053.

Lin, J., Chen, K., Dai, Y., Sun, Q., Li, Y., Jiang, Y., et al. (2020). Bilateral bundle branch area pacing to achieve physiological conduction system activation. *Circ. Arrhythm. Electrophysiol.* 13 (8), e008267. doi:10.1161/CIRCEP.119.008267

Liu, W., Hu, C., Wang, Y., Cheng, Y., Zhao, Y., Liu, Y., et al. (2021). Mechanical synchrony and myocardial work in heart failure patients with left bundle branch area pacing and comparison with biventricular pacing. *Front. Cardiovasc. Med.* 8, 727611. doi:10.3389/fcvm.2021.727611

Lund, L. H., Jurga, J., Edner, M., Benson, L., Dahlstrom, U., Linde, C., et al. (2013). Prevalence, correlates, and prognostic significance of QRS prolongation in heart failure with reduced and preserved ejection fraction. *Eur. Heart J.* 34 (7), 529–539. doi:10.1093/eurheartj/ehs305

Lustgarten, D. L., Crespo, E. M., Arkhipova-Jenkins, I., Lobel, R., Winget, J., Koehler, J., et al. (2015). His-bundle pacing versus biventricular pacing in cardiac resynchronization therapy patients: A crossover design comparison. *HEART Rhythm.* 12 (7), 1548–1557. doi:10.1016/j.hrthm.2015.03.048

Mizner, J. (2022). Ventricular dyssynchrony and pacing-induced cardiomyopathy in patients with pacemakers, the utility of ultra-high-frequency ECG and other dyssynchrony assessment tools. Published online April 9, 2022. Available at: https://www.aerjournal.com/articles/ventricular-dyssynchrony-and-pacing-induced-cardiomyopathy-patients-pacemakers-utility (Accessed November 3, 2022).

Morina-Vazquez, P., Barba-Pichardo, R., Venegas-Gamero, J., and Herrera-Carranza, M. (2005). Cardiac resynchronization through selective his bundle pacing in a patient with the so-called InfraHis atrioventricular block. *Pacing Clin. Electrophysiol.* 28 (7), 726–729. doi:10.1111/j.1540-8159.2005.00150.x

Moss, A. J., Hall, W. J., Cannom, D. S., Klein, H., Brown, M. W., Daubert, J. P., et al. (2009). Cardiac-resynchronization therapy for the prevention of heart-failure events. *N. Engl. J. Med.* 361 (14), 1329–1338. doi:10.1056/NEJMoa0906431

Naqvi, T. Z., and Chao, C. J. (2021). Adverse effects of right ventricular pacing on cardiac function: prevalence, prevention and treatment with physiologic pacing.

Trends Cardiovasc. Med. 4 (21), S105000128–S105017386. doi:10.1016/j.tcm.2021.10.013

Narula, O. S. (1977). Longitudinal dissociation in the His bundle. Bundle branch block due to asynchronous conduction within the His bundle in man. *Circulation* 56 (6), 996–1006. doi:10.1161/01.CIR.56.6.996

Nguyên, U. C., Verzaal, N. J., van Nieuwenhoven, F. A., Vernooy, K., and Prinzen, F. W. (2018). Pathobiology of cardiac dyssynchrony and resynchronization therapy. *Europace* 20 (12), 1898–1909. doi:10.1093/europace/euy035

Padala, S. K., Cabrera, J. A., and Ellenbogen, K. A. (2022). Anatomy of the cardiac conduction system. Wiley Online Library. Available at: https://onlinelibrary.wiley.com/doi/abs/10.1111/pace.14107 (Accessed November 3, 2022).

Ploux, S., Eschalier, R., Whinnett, Z. I., Lumens, J., Derval, N., Sacher, F., et al. (2015). Electrical dyssynchrony induced by biventricular pacing: Implications for patient selection and therapy improvement. *Heart Rhythm.* 12 (4), 782–791. doi:10.1016/j.hrthm.2014.12.031

Ponnusamy, S., Arora, V., Namboodiri, N., Kumar, V., Kapoor, A., and Vijayaraman, P. (2020). Left bundle branch pacing: A comprehensive review. *J. Cardiovasc. Electrophysiol.* 31 (9), 2462–2473. doi:10.1111/jce.14681

Prinzen, F. W., Auricchio, A., Mullens, W., Linde, C., and Huizar, J. F. (2022). Electrical management of heart failure: From pathophysiology to treatment. *Eur. Heart J.* 43 (20), 1917–1927. doi:10.1093/eurheartj/ehac088

Qian, Z., Wang, Y., Hou, X., Qiu, Y., Wu, H., Zhou, W., et al. (2021). Efficacy of upgrading to left bundle branch pacing in patients with heart failure after right ventricular pacing. *Pacing Clin. Electrophysiol.* 44 (3), 472–480. doi:10.1111/pace.14147

Rademakers, L. M., Bouwmeester, S., Mast, T. P., Dekker, L., Houthuizen, P., and Bracke, F. A. (2022). Feasibility, safety and outcomes of upgrading to left bundle branch pacing in patients with right ventricular pacing induced cardiomyopathy. *Pacing Clin. Electrophysiol.* 45 (6), 726–732. doi:10.1111/pace.14515

Ramos Jimenez, J., Marco Del Castillo, A., Paredes Hurtado, N., Borrego Bernabe, L., Fontenla, A., Rodriguez Munoz, D., et al. (2022). Echocardiographic outcomes of left bundle branch versus deep septal pacing. *Europace* 24. doi:10.1093/europace/euac053.417

Raymond-Paquin, A., Padala, S. K., and Ellenbogen, K. A. (2021). Left bundle branch pacing: A perfect compromise? *Arrhythm. Electrophysiol. Rev.* 10 (4), 241–243. doi:10.15420/aer.2021.60

Rivero-Ayerza, M., Theuns, D. A. M. J., Garcia-Garcia, H. M., Boersma, E., Simoons, M., and Jordaens, L. J. (2006). Effects of cardiac resynchronization therapy on overall mortality and mode of death: a meta-analysis of randomized controlled trials. *Eur. Heart J.* 27 (22), 2682–2688. doi:10.1093/eurheartj/ehl203

Russell, K., Eriksen, M., Aaberge, L., Wilhelmsen, N., Skulstad, H., Remme, E. W., et al. (2012). A novel clinical method for quantification of regional left ventricular pressure-strain loop area: a non-invasive index of myocardial work. *Eur. Heart J.* 33 (6), 724–733. doi:10.1093/eurheartj/ehs016

Shan, P., Su, L., Zhou, X., Wu, S., Xu, L., Xiao, F., et al. (2018). Beneficial effects of upgrading to His bundle pacing in chronically paced patients with left ventricular ejection fraction < 50. *Heart Rhythm.* 15 (3), 405–412. doi:10.1016/j.hrthm.2017.10.031

Shan, Q. J., Xu, H., Zhou, X. J., Chang, Q., Ji, L., Chen, C., et al. (2021). Effects of permanent left bundle branch area pacing on QRS duration and short-term cardiac function in pacing-indicated patients with left bundle branch block. *Chin. Med. J.* 134 (9), 1101–1103. doi:10.1097/CM9.0000000000001380

Sharma, P. S., Dandamudi, G., Herweg, B., Wilson, D., Singh, R., Naperkowski, A., et al. (2018). Permanent his-bundle pacing as an alternative to biventricular pacing for cardiac resynchronization therapy: A multicenter experience. *Heart Rhythm.* 15 (3), 413–420. doi:10.1016/j.hrthm.2017.10.014

Sharma, P. S., Naperkowski, A., Bauch, T. D., Chan, J. Y. S., Arnold, A. D., Whinnett, Z. I., et al. (2018). Permanent his bundle pacing for cardiac resynchronization therapy in patients with heart failure and right bundle branch block. *Circ. Arrhythm. Electrophysiol.* 11 (9), e006613. doi:10.1161/CIRCEP.118.006613

Sillanmäki, S., Aapro, S., Lipponen, J. A., Tarvainen, M. P., Laitinen, T., Hedman, M., et al. (2020). Electrical and mechanical dyssynchrony in patients with right bundle branch block. *J. Nucl. Cardiol.* 27 (2), 621–630. doi:10.1007/s12350-018-1418-1

Smiseth, O. A., and Aalen, J. M. (2019). Mechanism of harm from left bundle branch block. *Trends Cardiovasc. Med.* 29 (6), 335–342. doi:10.1016/j.tcm.2018.10.012

Strocchi, M., Lee, A. W. C., Neic, A., Bouyssier, J., Gillette, K., Plank, G., et al. (2020). His-bundle and left bundle pacing with optimized atrioventricular delay achieve superior electrical synchrony over endocardial and epicardial pacing in left bundle branch block patients. *Heart Rhythm.* 17 (11), 1922–1929. doi:10.1016/j.hrthm.2020.06.028

Strocchi, M., Gillette, K., Neic, A., Elliott, M. K., Wijesuriya, N., Mehta, V., et al. (2022). Comparison between conduction system pacing and cardiac resynchronization therapy in right bundle branch block patients. *Front. Physiol.* 13, 1011566. doi:10.3389/fphys.2022.1011566

Tanaka, H., Hara, H., Adelstein, E. C., Schwartzman, D., Saba, S., and Gorcsan, J. (2010). Comparative mechanical activation mapping of RV pacing to LBBB by 2D and 3D speckle tracking and association with response to resynchronization therapy. *JACC. Cardiovasc. Imaging* 3 (5), 461–471. doi:10.1016/j.jcmg.2009.12.014

Tracy, C. M., Epstein, A. E., Darbar, D., DiMarco, J. P., Dunbar, S. B., Estes, N. A. M., et al. (2012). 2012 ACCF/AHA/HRS focused update of the 2008 guidelines for device-based therapy of cardiac rhythm abnormalities: a report of the American college of Cardiology foundation/American heart association task Force on practice guidelines and the heart rhythm society. [corrected]. *Circulation* 126 (14), 1784–1800. doi:10.1161/CIR.0b013e3182618569

Upadhyay, G. A., Cherian, T., Shatz, D. Y., Beaser, A. D., Aziz, Z., Ozcan, C., et al. (2019). Intracardiac delineation of septal conduction in left bundle-branch block patterns: Mechanistic evidence of left intrahisian block circumvented by his bundle pacing. *Circulation* 139 (16), 1876–1888. doi:10.1161/CIRCULATIONAHA.118.038648

Upadhyay, G. A., Vijayaraman, P., Nayak, H. M., Verma, N., Dandamudi, G., Sharma, P. S., et al. (2019). His corrective pacing or biventricular pacing for cardiac resynchronization in heart failure. *J. Am. Coll. Cardiol.* 74 (1), 157–159. doi:10.1016/j.jacc.2019.04.026

Upadhyay, G. A., Vijayaraman, P., Nayak, H. M., Verma, N., Dandamudi, G., Sharma, P. S., et al. (2019). On-treatment comparison between corrective his bundle pacing and biventricular pacing for cardiac resynchronization: A secondary analysis of the his-SYNC pilot trial. *Heart Rhythm.* 16 (12), 1797–1807. doi:10.1016/j.hrthm.2019.05.009

Varma, N., Hu, Y., Connolly, A. T., Thibault, B., Singh, B., Mont, L., et al. (2021). Gain in real-world cardiac resynchronization therapy efficacy with SyncAV dynamic optimization: Heart failure hospitalizations and costs. *Heart Rhythm.* 18 (9), 1577–1585. doi:10.1016/j.hrthm.2021.05.006

Vernooy, K., Verbeek, X. A. A. M., Peschar, M., Crijns, H. J. G. M., Arts, T., Cornelussen, R. N. M., et al. (2005). Left bundle branch block induces ventricular remodelling and functional septal hypoperfusion. *Eur. Heart J.* 26 (1), 91–98. doi:10.1093/eurheartj/ehi008

Vernooy, K., Cornelussen, R. N. M., Verbeek, X. A. A. M., Vanagt, W. Y. R., van Hunnik, A., Kuiper, M., et al. (2007). Cardiac resynchronization therapy cures dyssynchronopathy in canine left bundle-branch block hearts. *Eur. Heart J.* 28 (17), 2148–2155. doi:10.1093/eurheartj/ehm207

Vijayaraman, P., Subzposh, F. A., and Naperkowski, A. (2017). Atrioventricular node ablation and His bundle pacing. *Europace* 19, iv10–iv16. doi:10.1093/europace/eux263

Vijayaraman, P., Herweg, B., Dandamudi, G., Mittal, S., Bhatt, A. G., Marcantoni, L., et al. (2019). Outcomes of His-bundle pacing upgrade after long-term right ventricular pacing and/or pacing-induced cardiomyopathy: Insights into disease progression. *Heart Rhythm.* 16 (10), 1554–1561. doi:10.1016/j.hrthm.2019.03.026

Vijayaraman, P., Herweg, B., Ellenbogen, K. A., and Gajek, J. (2019). His-optimized cardiac resynchronization therapy to maximize electrical resynchronization: A feasibility study. *Circ. Arrhythm. Electrophysiol.* 12 (2), e006934. doi:10.1161/CIRCEP.118.006934

Vijayaraman, P., Cano, O., Ponnusamy, S. S., Molina-Lerma, M., Chan, J. Y. S., Padala, S. K., et al. (2022). Left bundle branch area pacing in patients with heart failure and right bundle branch block: Results from International LBBAP Collaborative-Study Group. *Heart Rhythm O2* 3, 358–367. doi:10.1016/j.hroo.2022.05.004

Vijayaraman, P. (2020). Deep septal, distal His bundle pacing for cardiac resynchronization therapy. *Hear. Case Rep.* 6 (10), 791–793. doi:10.1016/j.hrcr.2020.07.024

Vijayaraman, P. (2022). Simultaneous right and left bundle pacing for cardiac resynchronization therapy. Available at: https://pubmed.ncbi.nlm.nih.gov/35057978/(Accessed August 22, 2022).

Viswanathan, K., Ghosh, J., Kaye, G. C., and Cleland, J. G. (2006). Cardiac resynchronization therapy: redefining the role of device therapy in heart failure. *Expert Rev. Pharmacoecon. Outcomes Res.* 6 (4), 455–469. doi:10.1586/14737167.6.4.455

Walmsley, J., Huntjens, P. R., Prinzen, F. W., Delhaas, T., and Lumens, J. (2016). Septal flash and septal rebound stretch have different underlying mechanisms. *Am. J. Physiol. Heart Circ. Physiol.* 310 (3), H394–H403. doi:10.1152/ajpheart.00639.2015

Wang, Y., Zhu, H., Hou, X., Wang, Z., Zou, F., Qian, Z., et al. (2022). Randomized trial of left bundle branch vs biventricular pacing for cardiac resynchronization therapy. *J. Am. Coll. Cardiol.* 80 (13), 1205–1216. doi:10.1016/j.jacc.2022.07.019

Wouters, P. C., Vernooy, K., Cramer, M. J., Prinzen, F. W., and Meine, M. (2021). Optimizing lead placement for pacing in dyssynchronous heart failure: The patient in the lead. *Heart Rhythm.* 18 (6), 1024–1032. doi:10.1016/j.hrthm.2021.02.011

Wu, S., Su, L., and Xiang, W. (2019). Long-term benefits and feasibility of permanent left bundle branch pacing in patients with left bundle branch block. *Chin. J. Cardiac Arrhythm.* 23 (5), 399–404. doi:10.3760/cma.j.issn.1007-6638.2019.05.004

Wu, S., Su, L., Vijayaraman, P., Zheng, R., Cai, M., Xu, L., et al. (2021). Left bundle branch pacing for cardiac resynchronization therapy: Nonrandomized on-treatment comparison with his bundle pacing and biventricular pacing. *Can. J. Cardiol.* 37 (2), 319–328. doi:10.1016/j.cjca.2020.04.037

Zhang, J., Guo, J., Hou, X., Wang, Y., Qian, Z., Li, K., et al. (2018). Comparison of the effects of selective and non-selective His bundle pacing on cardiac electrical and mechanical synchrony. *Europace* 20 (6), 1010–1017. doi:10.1093/europace/eux120

Zhang, W., Huang, J., Qi, Y., Wang, F., Guo, L., Shi, X., et al. (2019). Cardiac resynchronization therapy by left bundle branch area pacing in patients with heart failure and left bundle branch block. *HEART Rhythm.* 16 (12), 1783–1790. doi:10.1016/j.hrthm.2019.09.006

Zweerink, A., van Everdingen, W. M., Nijveldt, R., Salden, O. A. E., Meine, M., Maass, A. H., et al. (2018). Strain imaging to predict response to cardiac resynchronization therapy: a systematic comparison of strain parameters using multiple imaging techniques. *Esc. Heart Fail.* 5 (6), 1130–1140. doi:10.1002/ehf2.12335

Zweerink, A., Zubarev, S., Bakelants, E., Potyagaylo, D., Stettler, C., Chmelevsky, M., et al. (2021). His-optimized cardiac resynchronization therapy with ventricular fusion pacing for electrical resynchronization in heart failure. *JACC. Clin. Electrophysiol.* 7 (7), 881–892. doi:10.1016/j.jacep.2020.11.029

frontiers | Frontiers in Cardiovascular Medicine

TYPE Review
PUBLISHED 17 January 2023
DOI 10.3389/fcvm.2022.1048673

OPEN ACCESS

EDITED BY
Maciej M. Sterlinski,
National Institute of Cardiology, Poland

REVIEWED BY
Ludmila Danilowicz-Szymanowicz,
Medical University of Gdańsk, Poland
Rajiv Sankaranarayanan,
Liverpool University Hospitals NHS Foundation Trust, United Kingdom

*CORRESPONDENCE
Gábor Széplaki
✉ szeplaki.gabor@gmail.com

SPECIALTY SECTION
This article was submitted to Heart Failure and Transplantation, a section of the journal Frontiers in Cardiovascular Medicine

RECEIVED 19 September 2022
ACCEPTED 28 December 2022
PUBLISHED 17 January 2023

CITATION
Boros AM, Perge P, Merkely B and Széplaki G (2023) Risk scores in cardiac resynchronization therapy–A review of the literature. *Front. Cardiovasc. Med.* 9:1048673. doi: 10.3389/fcvm.2022.1048673

Risk scores in cardiac resynchronization therapy–A review of the literature

András Mihály Boros[1], Péter Perge[1], Béla Merkely[1] and Gábor Széplaki[1,2,3]*

[1]Heart and Vascular Center, Semmelweis University, Budapest, Hungary, [2]Heart and Vascular Centre, Mater Private Hospital, Dublin, Ireland, [3]Royal College of Surgeons in Ireland, Dublin, Ireland

Cardiac resynchronization therapy (CRT) for selected heart failure (HF) patients improves symptoms and reduces morbidity and mortality; however, the prognosis of HF is still poor. There is an emerging need for tools that might help in optimal patient selection and provide prognostic information for patients and their families. Several risk scores have been created in recent years; although, no literature review is available that would list the possible scores for the clinicians. We identified forty-eight risk scores in CRT and provided the calculation methods and formulas in a ready-to-use format. The reviewed score systems can predict the prognosis of CRT patients; some of them have even provided an online calculation tool. Significant heterogeneity is present between the various risk scores in terms of the variables incorporated and some variables are not yet used in daily clinical practice. The lack of cross-validation of the risk scores limits their routine use and objective selection. As the number of prognostic markers of CRT is overwhelming, further studies might be required to analyze and cross-validate the data.

KEYWORDS

CRT, cardiac resynchronization therapy, prediction model, risk scores, mortality, response

Introduction

According to the most recent guidelines, cardiac resynchronization therapy (CRT) is recommended for symptomatic heart failure patients in sinus rhythm with a QRS duration ≥150 ms and left bundle branch block (LBBB) QRS morphology and with left ventricular ejection fraction (LVEF) ≤35% despite optimal medical therapy to improve symptoms and reduce morbidity and mortality (1, 2). However, mortality is still high; and approximately one-third of the patients do not respond to CRT as adequately as expected, in whom no quality of live improvement or reverse remodeling of the left ventricle is seen (3).

Consequently, there is a great need for tools that might help in optimal patient selection and provide prognostic information for the patients and their families. Ever since the first implementation of CRT, several clinical factors and biomarkers have been tested in prediction models to identify those patients who might benefit the most from the therapy (4, 5). Prediction models are useful to reveal which parameters are statistically significant in the outcome prediction by giving the hazard and odds ratios, but they are not interpretable at the level of the individual patient in the clinical practice. Therefore, risk scores have been developed that constitute predominantly categorized variables with attributed points. The sum of the points reveals the exact risk of the individual; so that, patients can be easily and quickly grouped into risk categories with meaningful information.

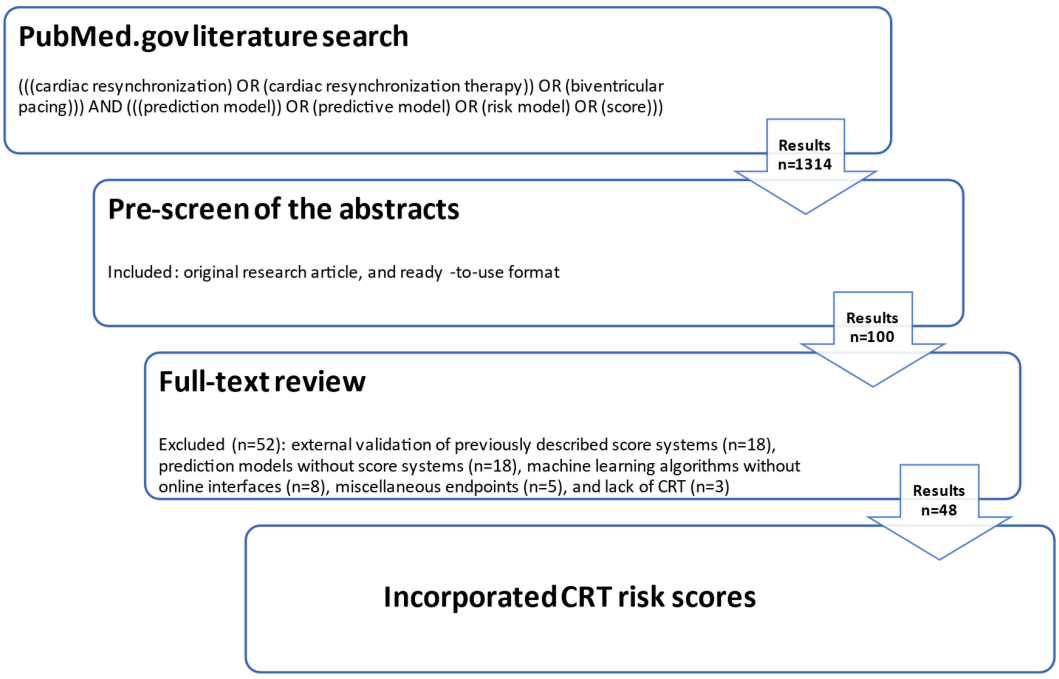

FIGURE 1
Flowchart of the review process.

Several risk scores have been created in CRT in recent years; however, no literature review is available that would list the possible scores for the clinicians.

Therefore, we aimed to systematically review the risk scores in CRT and provide the calculation methods and formulas in a ready-to-use format.

Materials and methods

The literature search was performed in November 2021 and then updated in September 2022 by using the search engine PubMed.gov[1] with the input of the following equation: (((cardiac resynchronization) OR (cardiac resynchronization therapy)) OR (biventricular pacing))) AND (((prediction model)) OR (predictive model) OR (risk model) OR (score))). The flowchart of the review process is presented by **Figure 1**.

Since we applied no language or publication date restrictions, the result was 1,314 possible papers. Two investigators (AB and PP) independently pre-screened the abstracts of these manuscripts by considering further inclusion criteria: original research article, and ready-to-use format. This resulted in a sum of 100 records that were further assessed by full-text review. A total of 52 papers were excluded based on the following reasons: external validation of previously described score systems (n = 18), prediction models without score systems (n = 18), machine learning algorithms without online interfaces (n = 8), miscellaneous endpoints (n = 5), and lack of CRT (n = 3). Consequently, forty-eight CRT risk scores were incorporated into the present review.

1 https://www.ncbi.nlm.nih.gov/

Results

To date, we identified 48 ready-to-use risk scores in heart failure patients with CRT **Table 1**. Summarizes the details of the models with the interpretation of the results and presents the formulas or the calculation methods of the scores **Figure 2**. Overviews the risk scores and helps in the selection of the appropriate risk score by considering the available data about the patient.

The primary endpoint of the models was all-cause death or a composite of death in the majority of the cases (n = 33, 69%), otherwise, it was echocardiographic or clinical response to CRT (n = 15, 32%). The most commonly used variables in the models were ischemic etiology (n = 21, 44%), renal function (n = 21, 44%), age (n = 20, 42%), New York Heart Association classification (n = 18, 38%), LVEF (n = 15, 33%), QRS morphology (n = 15, 31%), QRS width (n = 14, 30%), atrial fibrillation (n = 13, 27%), gender (n = 13, 27%), and left ventricular dimensions (n = 12, 25%).

Discussion

The very first risk score in CRT was developed by Heist et al. (6). It investigated the immediate hemodynamic response (improved contractility as assessed by the dP/dt of the mitral regurgitation jet) to CRT by using echocardiographic and electrophysiologic parameters (6). Following that, the Charlson comorbidity index (CCI) from Charlson et al. (7), was tested in 463 heart failure patients with CRT; a CCI score ≥5, meaning several comorbidities and worse overall state, reflected a more than 3 times mortality risk (8). In parallel, the MADIT-CRT score was created by Goldenberg et al. (9) by using the data of the 1,761 patients enrolled in the Multicenter Automatic Defibrillator Implantation Trial With Cardiac Resynchronization

TABLE 1 Risk scores in cardiac resynchronization therapy.

References	Study pop.	Num. of pat.	Primary endpoint	Duration (months)	Score	Score details	Results
Heist et al. (6)	CRT	39	$\Delta dp/dt > 25\%$ of mitral regurgitation jet	acute	Response score	4 parameters, 0–4 points	There was a significant association between response score (0 to 4 points) and acute hemodynamic response to CRT ($p < 0.0001$).
Response score's calculation: LV/right ventricular distance $\geq$ 10 cm, LV lead electrical delay $\geq$ 50%, baseline maximum $\Delta dP/dt \leq$ 600 mm Hg/s, maximum time difference $\geq$ 100 ms. One point was attributed to each predictor.							
Vidal et al. (37)	CRT	147	Alive, no HTX + Δ6-min $\geq$ 10%	12		3 variables, score: 0–3	Patients with higher scores showed a significantly higher likelihood of non-response to CRT ($x^2 = 12\ 891$, $p = 0.005$). Rates of response ranged from 80% for patients who scored 0 to 25% in patients with a score of 3.
Calculation: LVEDV $\geq$ 200 mL, mitral regurgitant orifice area $\geq$ 16 mm^2, and score in the Minnesota questionnaire $\geq$ 41. One point was attributed to each predictor.							
Goldenberg et al. (9)	CRT-D, ICD	1,761	All-cause death $\pm$ HF hospitalization	12	MADIT-CRT score	7 parameters, risk score 0–14 points	Multivariate analysis showed a 13% ($p < 0.001$) increase in the clinical benefit of CRT-D per 1-point increment in the response score.
MADIT-CRT score's calculation: female sex (2 points), non-ischemic origin (2 points), LBBB (2 points), QRS $\geq$ 150 ms (2 points), prior hospitalization for HF (1 point), LVEDV $\geq$ 125 mL/m^2 (2 points), and LA volume $\geq$ 40 mL/m^2 (3 points).							
Shen et al. (38)	CRT	100	ΔLVESV $\geq$ 15% reduction after 6-month	24		3 parameters, risk score 0–4 points	Cardiac resynchronization therapy responders in patients with response score $>$ 2 and $\leq$ 2 were 36/38 (95%) and 7/62 (11%, $p < 0.001$), respectively.
Calculation: 1 point for RV pacing-induced LBBB, 1 point for wall motion score index $\leq$ 1.59, and 2 points for time difference between LV ejection measured by tissue Doppler and pulsed wave Doppler $>$ 50 ms.							
Theuns et al. (8)	CRT-D	463	All-cause death	36	Charlson comorbidity index (CCI)	17 comorbid conditions, online calculator https://www.mdcalc.com/charlson-comorbidity-index-cci	CCI score $\geq$ 5 was a predictor of mortality (hazard ratio 3.69, 95% CI 2.06–6.60; $p < 0.001$) independent of indication for ICD therapy, and from ICD interventions during the clinical course.
CCI's calculation: myocardial infarction, cerebrovascular disease, chronic obstructive pulmonary disease, diabetes, peripheral vascular disease, renal failure, and any malignancy excluding metastatic tumors. The comorbidity index was calculated by assigning a weight of 2 to renal failure and any malignancy, and a weight of 1 to the other comorbid conditions. The comorbidity score for each patient is the arithmetic sum of the value assigned to each identified comorbid condition. To account for the effects of increasing age, the comorbidity score was adjusted by adding one point to the score for each decade of life over the age of 50 at the time of implantation.							
Perrotta et al. (14)	CRT	342	All-cause death $\pm$ HTX $\pm$	24	Seattle Heart Failure Model (SHFM)	25 parameters, online calculator https://depts.washington.edu/shfm/?width=1360&height=768	The SHFM was a good fit of death from any cause/cardiac transplantation, without significant differences between observed and SHFM-predicted survival.
SHFM's calculation: age (years); weight (kg); gender (male/female); ischemic etiology (yes/no); NYHA (1–4); LVEF (%); systolic blood pressure (mm Hg); aldosterone blocker use (yes/no); statin use (yes/no); allopurinol use (yes/no); ACEI use (yes/no); ARB use (yes/no); diuretic dose/kg: furosemide, bumetanide, torsemide, metolazone, hydrochlorothiazide, chlorothiazide; hemoglobin (g/dL); lymphocyte count (%); uric acid (mg/dL); sodium (meq/L); total cholesterol (mg/dL); intravenous diuretics (yes/no); pressors (number); intra-aortic balloon pump, ventilator, ultrafiltration (yes/no); ICD, CRT-P, CRT-D (yes/no); wide QRS (yes/no), LBBB (yes/no).							
Park et al. (17)	CRT	334	ΔLVESV $\geq$ 15% reduction after 12-month	12	EchoCG score	6 parameters, including strain analysis, risk score of 0–37 points	Total score of $>$ 17 (95% CI: 13–17) showed optimal sensitivity (84%) and specificity (79%) for response.
EchoCG score's calculation: LA area $<$ 26 cm^2 = 1 point, intermediate for RV end-diastolic area index $<$ 10.0 cm^2/m^2 = 2 points, RA area $<$ 20 cm^2 = 2 points, LV end-diastolic dimension index $<$ 3.1 cm/m^2 = 6 points, LVGLS $<$ –7.0% = 6 points, RVFAC $\geq$ 35% = 20 points.							
Kydd et al. (18)	CRT	294	ΔLVESV $\geq$ 15% reduction after 6-month	24		3 parameters, including strain analysis. The *p*-score ranged from -1.1 to 9.4	A *p*-score $>$ 3.28 offered high specificity (specificity 86%, sensitivity 70%) to predict response.
Calculation: [0.022 $\times$ IVMD (ms)] + [0.034 $\times$ RSD (%)] – [0.13 $\times$ LVGLS (%)] – [2.3 if suboptimal LV lead, 0 if optimal LV lead].							

(Continued)

10.3389/fcvm.2022.1048673

TABLE 1 (Continued)

References	Study pop.	Num. of pat.	Primary endpoint	Duration (months)	Score	Score details	Results
Khatib et al. (26)	CRT	608	All-cause mortality	36	EAARN score	5 parameters, risk score of 0–5 points	One predictor, HR 3.28 (95% CI 1.37–7.8, p = 0.008); two, HR 5.23 (95% CI 2.24–12.10, $p < 0.001$); three, HR 9.63 (95% CI 4.1–22.60, $p < 0.001$); and four or more, HR 14.38 (95% CI 5.8–35.65, $p < 0.001$).
EAARN score's calculation: LVEF < 22%, AF, Age ≥ 70 years, GFR < 60 mL/min/1.73 m^2, NYHA IV. One point was attributed to each predictor.							
Brunet-Bernard et al. (39)	CRT	162	ΔLVESV ≥ 15% reduction after 6-month	6	L2ANDS2 score	5 parameters, risk score of 0–7 points	A score > 5 had a high positive likelihood ratio [+ LR (5.64), whereas a score < 2 had a high negative likelihood ratio (–LR (0.19)].
L2ANDS2 score's calculation: LBBB (2 points), age > 70 years (1 point), non-ischemic origin (1 point), LVEDD < 40 mm/m^2 (1 point), and septal flash (2 points).							
Rickard et al. (40)	CRT	879	All-cause death ± HTX ± LVAD	6	Early demise score	4 parameters, risk score of 0–4 points	The specificity for ≥ 2 and ≥ 3 risk factors was 72.6 and 94.6%, respectively.
Early demise score's calculation: non-LBBB, pre-CRT LVEDD ≥ 6.5 cm, serum creatinine ≥ 1.5 mg/dL, and lack of β-blocker. One point was attributed to each predictor.							
Paoletti Perini et al. (41)	CRT-D	559	All-cause death ± HF hospitalization	72	$CHADS_2$ and CHA_2DS_2-VASc score	7 parameters, risk score 0–9 points	CHA_2DS_2-VASc score (for HF hospitalization $p < 0.013$; for the combined event, $p < 0.007$), while the $CHADS_2$ score was not independently associated with either the endpoints.
Calculation: $CHADS_2$ score: congestive heart failure (1 point), hypertension blood pressure ≥ 140/90 mm Hg (1 point), age ≥ 75 years (1 point), diabetes mellitus (1 point), prior stroke, TIA or thromboembolism (2 points); and CHA_2DS_2-VASc score: congestive heart failure (1 point), hypertension blood pressure ≥ 140/90 mm Hg (1 point), age ≥ 75 years (2 points), diabetes mellitus (1 point), prior stroke, TIA or thromboembolism (2 points), vascular disease (1 point), age 65–74 years (1 point), female sex (1 point).							
Nauffal et al. (28)	CRT-D	305	All-cause death ± HTX ± LVAD	60	HF-CRT score	5 parameters, a score-system was created and divided into: category 1 (score 0–1), category 2 (score 2–3), and category 3 (score 4–5)	Patients with scores 0–1, 2–3, and 4–5 had a 3-year cumulative event-free survival of 96.8, 79.7, and 35.2%, respectively (log-rank, $p < 0.001$).
HF-CRT score's calculation: hsCRP ≥ 9.42 ng/L, NYHA III/IV, creatinine ≥ 1.2 mg/dL, red blood cell count ≤ 4.3 × 106/μL, and cardiac troponin T ≥ 28 ng/L. One point was attributed to each predictor.							
Gasparini et al. (27)	CRT	5,153	All-cause mortality	60	VALID-CRT score	9 parameters, five quintiles. I: -1.841 - 0.061, II: 0.062 - 0.558, III: 0.559 - 0.937, IV: 0.938 - 1.364, V: 1.365 - 3.157	At 5 years, total mortality was 10.3, 18.6, 27.6, 36.1, and 58.8%, from the first to the fifth quintile.
VALID-CRT score's calculation: 0.028 × age 66 - 0.044 × LVEF25 + 0.646 × AF1 - 0.154 × AF2 - 0.656 × ICD + 0.405 × GENDER + 0.317 × CAD + 0.844 × NYHA34 + 0.167 × diabetes. Where: age66 = age-66 years; LVEF25 = LVEF-25; AF1 = 1 if AF without AVJA is present, 0 otherwise (meaning both sinus rhythm or AF + AVJA); AF2 = 1 if AF with AVJA is present, 0 otherwise (meaning both sinus rhythm or AF without AVJA); ICD, CAD, NYHA III–IV, diabetes = 1 if present, 0 otherwise; gender = 1 if male, 0 if female.							
Bani et al. (21)	CRT	172	ΔLVEF ≥ 10% increase ± ΔLVESV ≥ 15% reduction after 6-month	24	Simplified Selvester Score (SSc)	The Simplified-SSc is created utilizing an ECG analysis. Patients are divided into 4 groups according to the presence of 0, 1, 2 or ≥ 3 points	The response rate was 85, 60, 60, and 50% within the 4 groups. Simplified-SSc was inversely correlated with response to CRT (p = 0.048).
SSc's calculation: Lead I: R/S ≤ 1.5 = 1 point; Lead aVL: Q ≥ 50 ms = 2 points, R/S ≤ 1.0 = 1 point; Lead II: Q ≥ 30 ms = 1 point; Lead aVF: R/S ≤ 0.5 = 1 point; Lead V1: R ≥ 20 ms = 1 point, Lead V2: notch in the initial 40 ms of the QRS = 1 point; Lead V2: S/S' ≥ 1.5 = 1 point; Lead V5: any Q = 1 point; Lead V6: R/S ≤ 2.0 = 1 point.							
Kang et al. (19)	CRT	93	ΔLVESV ≥ 15% reduction after 6-month	24		3 parameters, including strain analysis, risk score of 0–4 points	The sensitivity and specificity for prediction of a positive response to CRT at a score > 2 were 0.823 and 0.850, respectively (AUC: 0.92295% CI 0.691–0.916, $p < 0.001$).
Calculation: tricuspid annular plane systolic excursion ≥ 14.8 mm (2 points), longitudinal strain (LS) ≤ –7.22% (1 point), and complete LBBB with wide QRS duration (1 point).							

(Continued)

10.3389/fcvm.2022.1048673

TABLE 1 (Continued)

References	Study pop.	Num. of pat.	Primary endpoint	Duration (months)	Score	Score details	Results
Seo et al. (11)	CRT	171	ΔLVESV ≥ 15% reduction after 6-month.	36	START score	6 parameters, including strain analysis, risk score (0–17 points)	A probability > 0.5 corresponded to a START score ≥ 10, and a probability > 0.9 corresponded to a score of ≥ 14.
START score's calculation: 1 point for LBBB or RV pacing; mitral regurgitation index ≤ 40% was 2 points; use of beta-blocker, BUN ≤ 30 mg/dL, and LV dimension at end-systole ≤ 50 mm were 3 points, and CS-SD (standard deviation of time from QRS onset to the first peak on the circumferential strain curves) ≥ 116 ms was 4 points.							
Barra et al. (42)	CRT	638	All-cause mortality	60	Goldenberg risk score	5 parameters, two groups: risk score of 0–2 and score of ≥ 3	No significant differences in mortality rates were seen in patients with scores ≥ 3 (57.9% with CRT-D vs. 56.9% with CRT-P, $p = 0.8$).
Goldenberg risk score's calculation: NYHA > 2, atrial fibrillation, QRS duration > 120 ms, age > 70 years, and BUN > 26 mg/dL. One point was attributed to each predictor.							
Höke et al. (29)	CRT	1,053	All-cause mortality	60	CRT-SCORE	15 parameters, risk groups: L5 [-4.42 – –1.60], L10 [-1.60 – -1.31], L20 [-1.31 – -0.82], L40 [-0.82 – -0.16], M [-0.16 – 0.28], H40 [0.28 – 0.79], H20 [0.79 – 1.18], H10 [1.18 – 1.44], H5 [1.44 – 2.89]	Estimated mean survival rates of 98% at 1 year and 92% at 5 years were observed in the lowest 5% risk group; whereas the highest 5% risk group showed poor survival rates: 78% at 1 year and 22% at 5 years.
CRT SCORE's calculation: (−0.169 x AVJA) + (0.037 x Age) + (0.367 x Male gender) + (0.221 x Ischemic etiology) + (0.048 x AF) + (0.516 x diabetes mellitus) – (0.173 x LBBB) + (0.394 x NYHA class III) + (0.826 x NYHA class IV) – (0.156 x QRS duration ≥ 150 ms) – (0.013 x GFR) – (0.084 x Hemoglobin level) – (0.026 x LVEF) + (0.259 x Mitral regurgitation ≥ 3) + (0.325 x Restrictive LV function).							
Nauffal et al. (43)	CRT-D	305	HF hospitalization and appropriate ICD therapy	60	PROSE-ICD score	5 parameters, two score-systems were created and divided into: category 1 (score 0–1), category 2 (score 2), and category 3 (score ≥ 3)	Five-year cumulative risk of appropriate therapy was 4, 14.6, and 47.2% for score categories 1, 2 and 3, respectively ($p < 0.001$). Five-year cumulative risk of HF hospitalization was 21.1, 40.3 and 69.8% for score categories 1, 2, and 3, respectively ($p < 0.001$).
PROSE-ICD score's calculation: predictors of appropriate ICD therapy: BUN > 20 mg/dL, hsCRP > 9.42 mg/L, no beta blocker therapy, and hematocrit ≥ 38%; predictors of HF hospitalization: atrial fibrillation, NYHA class III/IV, LVEF ≤ 20%, HS-IL6 > 4.03 pg/ml, hemoglobin < 12 g/dL. One point was attributed to each predictor.							
Wilkoff et al. (25)	ICD, CRT-D	57893 ICD and 67929 CRT-D.	All-cause mortality	36	Heart Rate (Hr) Score	Hr Score is determined from the atrial paced and sensed histogram	Hr Score 30–70% compared to Hr Score > 70% was associated with increased survival (CRT-D HR = 0.85; $p < 0.001$ and ICD HR = 0.88; $p < 0.001$).
Hr Score's calculation: the height in the percentage of all beats in the tallest 10 beats/min rate histogram bin was defined as the Hr Score. Thus, if all beats were in one bin the Hr Score would be 100%.							
Nevzorov et al. (44)	ICD, CRT-D	2,617	All-cause mortality	12	AAACC score	4 parameters, risk score (0–10 points)	Mortality risk increased (from 1% with 0 point to 12.5% with > 4 points).
AAACC score's calculation: age greater than 75 years (3 points), anemia (2 points), AF (1 point), chronic renal disease GFR < 30 min/mL/1.73 m^2 (3 points) and chronic lung disease (1 point).							
Biton et al. (45)	ICD, CRT-D	756	All-cause mortality	12	MADIT-CRT score in mild HF	4 parameters, risk score (0–4 points)	1 point increase in the score was associated with two-fold increased mortality within the CRT-D arm ($p < 0.001$).
MADIT-CRT score in mild HF's calculation: age ≥ 65, creatinine ≥ 1.4 mg/dL, history of CABG, LVEF < 26%. One point was attributed to each predictor.							
Providencia et al. (31)	CRT	1,301	ΔNYHA ≥ 1 improvement ± ΔLVEF ≥ 5% increase after 12-month	12	ScREEN score	5 parameters, risk score (0–5 points)	46.7% of patients with a score of 0 met the criteria for response, while 93.9% of individuals with a score of 5 were responders, $p < 0.001$.

(Continued)

10.3389/fcvm.2022.1048673

TABLE 1 (Continued)

References	Study pop.	Num. of pat.	Primary endpoint	Duration (months)	Score	Score details	Results
ScREEN score's calculation: female gender, GFR ≥ 60 mL/min/1.73 m^2, QRS width ≥ 150 ms, LVEF ≥ 25%, NYHA ≤ 3. Each was assigned 1 point.							
Bakos et al. (46)	CRT	202	All-cause death ± HTX ± LVAD ± HF hospitalization.	36	CRT response score	Three 6-month response criteria formed a risk score	1 point increase was associated with a 31% decreased risk for the primary endpoint [HR 0.69 (95% CI: 0.50–0.96), $p = 0.03$].
CRT response score's calculation: one point each for positive clinical (≥ 1 NYHA class improvement), echocardiographic (≥ 15% LVESV reduction) and biomarker (≥ 25% reduction in NT-proBNP) response 6 months after implantation.							
Végh et al. (22)	CRT	491	All-cause death ± HTX ± LVAD ± HF hospitalization	36	ECG score	Three post-implant ECG parameters were measured and compared to pre-implantation measurements, score (0–3)	The total score was an independent predictor for event-free survival [HR 0.65 (0.54–0.77) $p < 0.001$].
The predetermined ECG score was based on the standard 12-lead ECG, and included three parameters: (1) One point was assigned for a reduction of QRS width of at least 20 ms compared from baseline ECG to post-implant ECG. (2) One point was assigned for a reduction of at least 50% in the summed amplitude of R + S in lead V1 from baseline ECG to postimplant ECG. (3) One point was assigned if the intrinsicoid deflection point was identified within the first 40 ms from QRS onset at the follow-up ECG in the V1 lead.							
Maass et al. (24)	CRT	240	LVESVi reduction after 6-month	12	CAVIAR score	4 parameters (including vectorcardiography), risk score (0–9 points)	The predicted change of LVESVi: - 2 point = −1.3%, −1 point = −7.1%, 0 point = −12.5%, 1 point = −17.6%, 2 points = −22.4%, 3 points = −26.9%, 4 points = −31.2%, 5 points = −35.2%, 6 points = −38.9%, 7 points = −42.5%, 8 points = −45.8%, 9 points = −49.0%.
The CAVIAR score is the sum of the applicable values with minimum −2 and maximum 9 points. Age: year < 60 = 1 point, 60–74 years = 0 point, ≥ 75 years = −1 point; Vectorcardiographic QRS AREA: < 80 μVs = −2 points, 80–99 μVs = −1 point, 100–119 μVs = 0 point, 120–139 μVs = 1 point, 140–159 μVs = 2 points, 160–179 μVs = 2 points, 180–199 μVs = 3 points, 200–219 μVs = 4 points, ≥ 220 μVs = 5 points; Inter-ventricular mechanical delay < 15 ms = −1 point, 15–44 ms = 0 point, 45–74 ms = 1 point, ≥ 75 ms = 2 points; Apical Rocking: Absent = 0 point, Present = 2 points.							
Kisiel et al. (30)	CRT	552	All-cause mortality	108	AL-FINE score	6 parameters, risk score (0–6 points)	Overall mortality (C-statistics of 0.701) at seven years was in the range of 28% (0–1 points) to 74% (3–6 points).
AL-FINE score's calculation: Age > 75 years, non-LBBB, Furosemide dose > 80 mg, Ischemic etiology, NYHA > III, LVEF < 20%. One point was attributed to each predictor							
Theuns et al. (47)	CRT-D	1,282	All-cause mortality	36	Risk Score	7 parameters, five quintiles: I: ≤ 0.3230, II: 0.3231–0.9044, III: 0.9045–1.4384, IV: 1.4385–2.0510, V: > 2.0510	Mortality ranged from 2.8% (lowest quintile) to 31.9% (highest quintile).
Risk Score's calculation:0.656 × (MI) + 0.323 × (LVEF) + 0.641 × (COPD) + 0.992 × (CKD) + 0.941 × (hyponatremia) + 0.427 × (anemia) – 0.660 × (QRS150), where: LVEF = per 5% decrease of LVEF in patients with LVEF ≤ 35%. In patients with LVEF > 35%, the score associated with LVEF is 0; CKD = estimated GFR < 60 mL/min/1.73 m^2, 1 if present, otherwise 0; Hyponatremia = serum level of sodium < 136 mmol/L, 1 if present, otherwise 0; Anemia = serum level of hemoglobin < 12 g/dL, 1 if present, otherwise 0; QRS150 = QRS duration ≥ 150 ms, 1 if present, otherwise 0; MI, COPD = 1 if present, otherwise 0.							
Feeny et al. (34)	CRT	925	ΔLVEF ≥ abs. 10% increase at 24-month	24		9 parameters, machine learning http://riskcalc.org:3838/CRTResponseScore/	Machine learning vs. guideline prediction AUC (0.70 versus 0.65; $p = 0.012$) and greater discrimination of event-free survival (concordance index, 0.61 versus 0.56; $p < 0.001$).
Calculation: QRS morphology (LBBB/RBBB/IVCD/RV-paced, QRS duration (ms), NYHA (1–4), LVEF (%) and end-diastolic diameter (mm), sex (male/female), ischemic cardiomyopathy (yes/no), atrial fibrillation (yes/no), and epicardial left ventricular lead (yes/no).							
Weber et al. (48)	CRT-D	720	Appropriate ICD therapy or death without prior appropriate ICD therapy (so-called prior death).	120		11 parameters, two risk scores. Risk cut-off values for prior death: low < 7, intermediate 7–10, high > 10; for appropriate ICD therapy: low < 0, intermediate 0–6, high > 6	Stratification according to predicted benefit translated into significantly different overall survival ($p < 0.001$) and correspondingly ranked survival curves.

(Continued)

10.3389/fcvm.2022.1048673

TABLE 1 (Continued)

References	Study pop.	Num. of pat.	Primary endpoint	Duration (months)	Score	Score details	Results
Calculation: appropriate ICD therapy: NYHA functional class III/IV = 5 points, age at implantation = (−0.1 x Age) points, ischemic cardiomyopathy = 2 points, diuretic use = 5 points; Prior death: age at implantation = (0.1 x Age) points, male gender = 2 points, BMI ≥ 30 = 2 points, systolic blood pressure ≤ 100 mmHg = 2 points, impaired renal function (GFR ≤ 60 mL/min/1.73 m^2) = 2 points, history of cancer = 3 points, peripheral artery disease = 3 points.							
Spinale et al. (10)	CRT	758	ΔLVESV ≥ 15 mL reduction after 6-month	12	Biomarker CRT Score	4 biomarkers, risk score (0–4 points)	Absolute change in LVESV ($P < 0.001$). 0 point: −30 ± 39, 1 point: −25 ± 50, 2 points: + 14 ± 43, 3 points: −13 ± 41, 4 points: −5 ± 36 mL.
Biomarker CRT Score's calculation: sTNFr-II ≥ 7,090 pg/mL, sST-2 ≥ 23,721 pg/mL, hsCRP ≥ 7,381 ng/mL, and MMP-2 ≥ 982,000 pg/mL. One point value was assigned for each biomarker that exceeded the specific threshold.							
Manlucu et al. (33)	CRT-D, ICD	1,798	All-cause mortality	6	MAGGIC score	13 parameters, three risk categories: low:0–16 points, intermediate: 17–24 points, high: > 24 points. http://www.heartfailurerisk.org/	When patients were divided into 3 cohorts based on low, intermediate, and high MAGGIC scores, patients with high MAGGIC scores had lower 3-year survival rates than those with intermediate or low scores (73.0% versus 88.1% versus 96.8%; $P < 0.001$).
MAGGIC score's calculation: input the following parameters to the online calculator: age (years), gender, diabetes, COPD, heart failure diagnosed within the last 18 months, current smoker, NYHA class, receives beta blockers, receives ACEi/ARB, BMI (kg/m2), systolic blood pressure (mmHg), creatine (umol/L), LVEF (%).							
Liu et al. (23)	CRT	387	ΔLVEF ≥ abs. 15% increase at 6-month	12	QQ-LAE Score	5 parameters, three risk categories	The proportion of super-response after 6-month CRT implantation in patients with scores 0–3, 4, and 5 was 14.6, 40.3, and 64.1%, respectively ($p < 0.001$).
QQ-LAE Score's calculation: prior no fragmented QRS, QRS duration ≥ 170 ms, LBBB, left atrial diameter < 45 mm, and left ventricular end-diastolic dimension < 75 mm. One point was attributed to each predictor, and three score categories were identified.							
Cai et al. (49)	CRT and Afib	152	All-cause mortality and HF readmissions	60	Prognostic nomogram	5 parameters, nomogram https://pubmed.ncbi.nlm.nih.gov/32404049/#&gid=article-figures&pid=fig-3-uid-2	The C-index was 0.70 with a 95% CI of 0.61–0.78.
Prognostic nomogram's calculation: NT-proBNP > 1,745 pg/mL, history of syncope, previous pulmonary hypertension, moderate or severe tricuspid regurgitation, thyroid-stimulating hormone > 4 mIU/L. Cross the line on the nomogram.							
Tokodi et al. (35)	CRT	1,510	All-cause mortality	60	SEMMELWEIS-CRT score	33 parameters, machine learning, online calculator https://arguscognitive.com/crt	AUC of the 5-year mortality was 0.803 (95% CI: 0.733–0.872, $p < 0.001$).
SEMMELWEIS-CRT score's calculation: age at CRT implantation, gender, height, weight, medical history of hypertension, diabetes mellitus, type of atrial fibrillation (paroxysmal, persistent, permanent), NYHA, systolic blood pressure, LVEF assessed with two-dimensional echocardiography, etiology of heart failure (ischemic or non-ischemic), QRS morphology and width, type of the implanted device (CRT-P or CRT-D), current medical treatment with furosemide, other loop diuretics, thiazide diuretics, mineralocorticoid receptor antagonists, angiotensin-converting enzyme inhibitors and angiotensin II receptor blockers, beta-blockers, statins, amiodarone, allopurinol, digitalis, percentage of lymphocytes, glomerular filtration rate, hemoglobin concentration, serum levels of sodium, cholesterol, creatinine, urea and NT-proBNP.							
Patel et al. (50)	CRT	877	All-cause mortality	120		8 parameters, three risk categories (number of predictors > 1, > 3, > 5)	The sensitivity of factors > 5 was 0.65 with a specificity of 0.77 and a positive likelihood for survival of longer than 10 years of 2.83.
Calculation: Age < 65.53 years, LVEDD < 6.75 cm, QRS > 149 ms, BNP < 255 pg/mL, creatinine < 1.05 mg/dL, female sex, non-ischemic cardiomyopathy, no presence of atrial fibrillation. One point was attributed to each predictor.							
Yang et al. (51)	CRT in NICM	422	All-cause mortality or HTX	24	Alpha-score	5 parameters, three risk categories: (0–1 point = low, 2–3 points = intermediate, 4–5 points = high)	The cumulative survival free of the primary endpoint were 80%, 60%, 20% in the low, high, and intermediate-risk groups.
Alpha-score's calculation: left atrial diameter > 44.5 cm, non-LBBB, NT-proBNP > 13.53 per 100 pg/ml, hsCRP > 2.87 umol/L, NYHA class IV. One point was attributed to each predictor.							
Milner et al. (52)	CRT or CRT upgrade	283	All-cause mortality	12	Modified Frailty Index (mFI)	11 parameters, frail if mFI ≥ 3	Frailty was associated with an increased risk of 1-year mortality (hazard ratio 5.87, $p = 0.033$).

(Continued)

10.3389/fcvm.2022.1048673

TABLE 1 (Continued)

References	Study pop.	Num. of pat.	Primary endpoint	Duration (months)	Score	Score details	Results
Modified Frailty Index included non-activities of daily living independent, diabetes, COPD or congestive heart failure in the last 30 days, myocardial infarction within 6 months, previous percutaneous coronary intervention/CABG)/angina, hypertension, peripheral vascular disease, impaired sensorium, and TIA/cerebrovascular accident with or without deficits. The total number of components satisfied by each patient was added together to yield an integer score of 0 to 11.							
Liang et al. (36)	CRT	725	ΔLVEF ≥ abs. 10% increase at 1-year	12		19 parameters, machine learning, online calculator http://www.crt-response.com/	Ridge regression AUC = 0.77 (0.69–0.84); Support vector machine AUC = 0.76 (0.68–0.83); Logistic regression AUC = 0.77 (0.69–0.84).
Calculation: weight (kg), GFR (ml/min/1.73 m^2), creatine kinase-MB (U/L), QRS duration (ms), left atrial diameter (mm), history of percutaneous coronary intervention (yes/no), amiodarone (yes/no), albumin (g/L), serum uric acid (mmol/L), free triiodothyronine (pmol/L), RR interval (ms), LVESD (mm), history of CABG (yes/no), aspartate transaminase (U/L), total cholesterol (mmol/L), free thyroxine (pmol/L), corrected QT interval (ms), LVEF (%), QRS morphology (LBBB/RBBB/IVCD/paced).							
Theuns et al. (53)	CRT-D	648	All-cause mortality	60	Heart Failure Meta-score	15 parameters, five quintiles. I: 0.64–1.75, II: 1.75–2.16, III: 2.16–2.59, IV: 2.59–3.05, V: 3.05–6.17, online calculator http://www.hfmetascore.org/HeartScore.aspx	Mortality ranged from 12% (95% CI, 7–20%) to 53% (95% CI, 44–62%), for quintiles 1 to 5, (overall log-rank $p < 0.001$).
Heart Failure Meta-score's calculation: age (years), LVEF (%), creatinine (mg/dL), NYHA (1–4); male gender, African-American race, diabetes, COPD, peripheral vascular disease, ischemic cardiomyopathy, HF admission within 1 year before CRT, atrial fibrillation, wide QRS (≥ 120 ms), secondary prevention indication, history of ICD shocks.							
Younis et al. (12)	ICD, CRT-D	4,503	VT/VF and non-arrhythmic mortality	36	MADIT-ICD benefit score	12 parameters, three benefit groups. highest (score 76–100), intermediate (score 26–75), lowest (score < 25), online calculator https://redcap.urmc.rochester.edu/redcap/surveys/index.php?s=3H888TJ8N7	In the highest benefit group, the 3-year predicted risk of VT/VF was three-fold higher than the risk of non-arrhythmic mortality (20% vs. 7%, $p < 0.001$).
MADIT-ICD benefit score's calculation: VT/VF (male, age < 75 years, prior non-sustained VT, HR > 75 bpm, systolic blood pressure < 140 mmHg, LVEF ≤ 25%, myocardial infarction, and atrial arrhythmia) and non-arrhythmic mortality (age > 75 years, diabetes mellitus, BMI < 23 kg/m^2, LVEF < 25%, NYHA > II, ICD vs. CRT-D, and atrial arrhythmia).							
Zoni-Berisso et al. (54)	ICD, CRT-D	983	All-cause mortality	24	DECODE survival score index (SUSCI)	7 parameters, five risk groups according to the SUSCI (< 1, 1–4, 4–7, 7–10, and > 10)	The risk of death increased according to the severity of the risk profile ranging from 0% (low risk) to 47% (high risk).
DECODE SUSCI's calculation: [(1.9359*ICM) + (2.2583* AGE ≥ 75) + (2.0295*INS) + (2.2369*NYHA) + (2.293*HOSP) + (1.7199*AF) + (2.1744*BMI)]. ICM [ischemic cardiomyopathy (0 = No; 1 = Yes)]; AGE [age at the time of device replacement/upgrade ≥ 75 years (0 = No; 1 = Yes)]; INS [insulin-dependent diabetes (0 = No; 1 = Yes)]; NYHA [0 = ≤ 2; 1 ≥ 3]; HOSP [hospitalization in the 30 days before the procedure (0 = No; 1 = Yes)]; AF [history of atrial fibrillation (0 = No; 1 = Yes)], and BMI < 26 kg/m2 [0 = No; 1 = Yes].							
Orszulak et al. (20)	CRT	49	ΔLVESV ≥ 15% reduction after follow-up	15	Regional Strain Pattern Index (RSPI)	Strain analysis, RSPI was calculated as the sum of dyssynchronous components	RSPI ≥ 7 points was a predictor of favorable CRT effect (OR: 12; 95% CI = 1.33–108.17; $p = 0.004$).
RSPI was calculated from all three apical views across 12 segments as the sum of dyssynchronous components. From every apical view, the presence of four components was assessed: (1) contraction of the early-activated wall; (2) prestretching of the late activated wall; (3) contraction of the early-activated wall in the first 70% of the systolic ejection phase; (4) peak contraction of the late-activated wall after aortic valve closure. Each component scored 1 point, thus the maximum was 12 points.							

(Continued)

10.3389/fcvm.2022.1048673

TABLE 1 (Continued)

References	Study pop.	Num. of pat.	Primary endpoint	Duration (months)	Score	Score details	Results
Yamada et al. (55)	CRT	180	HF death amd lethal arrhythmic event	50	ALBI	2 parameters, ALBI score before CRT was High (> -2.60) or Low (≤ -2.60). The patients were then reclassified based on the ALBI score before and 6 months after CRT; High/High, High/Low, Low/High, and Low/Low ALBI groups.	High/High ALBI scores were an independent predictor of HF deaths compared with Low/Low ALBI scores (hazard ratio, 3.449, $p = 0.008$).
The ALBI score was calculated as follows: [log10 total bilirubin (mmol/L) × 0.66) + [albumin (g/L) × -0.085].							
Ikeya et al. (56)	CRT	263	All-cause mortality	31	CONUT	3 parameters, three groups according to the CONUT (0–1, 2–4, 5–12)	CONUT score ≥ 5 was significantly associated with all-cause mortality after adjusting for previously reported clinically relevant factors and the conventional risk score (VALID-CRT risk score) (all $p < 0.05$).
The CONUT score is the sum of the followings: serum albumin g/dL: 3.5–4.5 = 0 point, 3.0–3.49 = 2 points, 2.5–2.9 = 4 points, < 2.5 = 6 points; total lymphocytes/mL: > 1,600 = 0 point, 1,200–1,599 = 1 point, 800–1,199 = 2 points, < 800 = 3 points; cholesterol mg/dL: > 180 = 0 point, 140–180 = 1 point, 100–139 = 2 points, < 100 = 3 points.							
Saito et al. (57)	CRT	283	All-cause mortality	30	MELD-XI	2 parameters, three risk groups first tertile (MELD-XI = 9.44), second tertile (9.44 < MELD-XI < 13.4), and third tertile (MELD-XI ≥ 13.4)	The MELD-XI score was independently associated with mortality (adjusted hazard ratio: 1.04, 95% confidence interval: 1.00–1.07, $P = 0.014$).
MELD-XI score can be calculated as follows: 11.76 × ln (creatinine [mg/dL]) + 5.11 × ln (total bilirubin [mg/dL]) + 9.44.11. If a patient had a creatinine or total bilirubin level lower than 1.0 mg/dL, a value of 1.0 mg/dL was used to prevent negative logarithmic values in the formula.							
Maille et al. (32)	CRT-D	23 029	All-cause mortality	12	CRT-D Futility score	14 parameters, four risk groups: low (0–3), medium low (4–7), medium high (8–11), high (> 12).	The one-year mortality risk in the four groups were 1.7, 3.9, 8.1, and 16.6%.
The CRT-D Futility score can be calculated as: age (> 61 = 1 point, > 69 = 2 point > 75 = 3 point), undernutrition = 2 points, CKD = 2 points, liver disease = 2 points, anemia = 2 points, diabetes mellitus = 2 points, AF = 2 points, LBBB = minus 1 point, mitral regurgitation = 2 points, aortic stenosis = 2 points, history of hospital stay with heart failure = 2 points, history of pulmonary edema = 2 points.							

Δ6-min, changes in the 6-min walking test; Δdp/dt, measure of contractility; ΔLVEF, changes in the left ventricular ejection fraction; LVESV, changes in the left ventricular end-systolic volume; ΔNYHA, changes in the New York Heart Association functional class; ACEI, angiotensin-converting-enzyme inhibitor; AF, atrial fibrillation; ARB, angiotensin receptor blocker; AUC, area under the curve; AVJA, atrio-ventricular junctional ablation; BMI, body mass index; BNP, brain natriuretic peptide; BUN, blood urea nitrogen; CABG, coronary artery bypass graft surgery; CAD, coronary artery disease; CI, confidence interval; CKD, chronic kidney disease; COPD, chronic obstructive pulmonary disease; CRT, cardiac resynchronization therapy; CRT-D, cardiac resynchronization therapy with defibrillator; CRT-P, cardiac resynchronization therapy with pacing only; ECG, electrocardiography; GFR, glomelural filtration rate; HF, heart failure; HR, hazard ratio; hsCRP, high-sensitivity C-reactive protein; HS-IL6, high-sensitivity interleukin 6; HTX, heart transplantation; ICD, implantable cardioverter defibrillator; IVCD, intraventricular conduction delay; IVMD, interventricular mechanical dyssynchrony; LA, left atrium; LBBB, left bundle branch block; LV, left ventricle; LVAD, left ventricular assist device; LVEDD, left ventricular end-diastolic diameter; LVEDV, left ventricular end-diastolic volume; LVEF, left ventricular ejection fraction; LVESV, left ventricular end-systolic volume; LVESVi, indexed left ventricular end-systolic volume; LVGLS, left ventricular global longitudinal strain; MI, myocardial infarction; MMP-2, matrix metalloproteinase-2; NT-proBNP, N-terminal prohormone of brain natriuretic peptide; Num. of pat., number of patients; NYHA, New York Heart Association functional classification; OR, odds ratio; Publ. year, publication year; QRS, width of the QRS complex; RBBB, right bundle branch block; Ref, reference; RSD, radial strain delay; RV, right ventricular; RVFAC, right ventricular fractional area change; sST-2, soluble ST2 interleukin; sTNFr-II, soluble tumor necrosis factor receptor type II; TIA, transient ischaemic attack; VT/VF, ventricular tachycardia; ventricular fibrillation; x^2, chi square.

10.3389/fcvm.2022.1048673

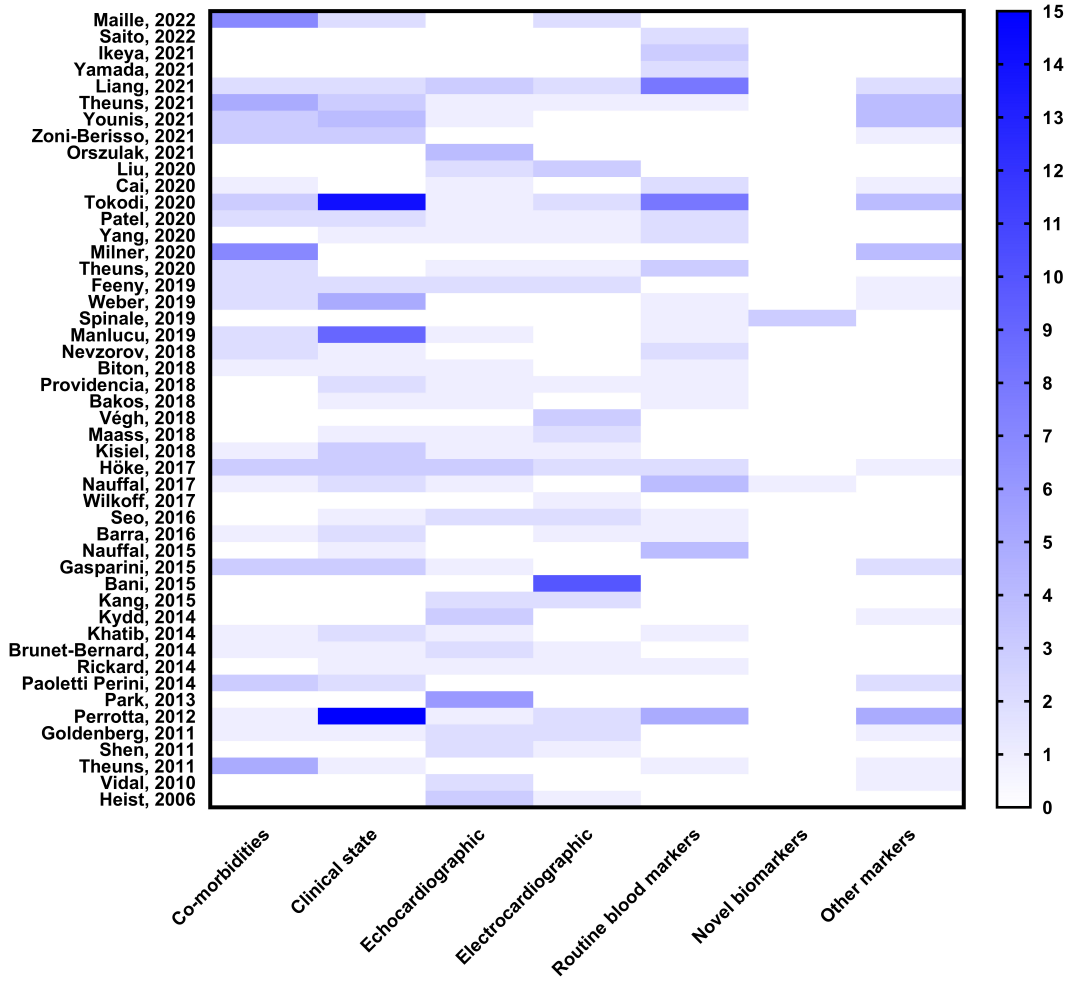

FIGURE 2
Heat map of the predictors used in the risk scores of cardiac resynchronization therapy.

Therapy (MADIT-CRT). The MADIT-CRT identified the most relevant routine clinical risk factors that affect mortality in CRT: gender, etiology of heart failure, the presence of left bundle-branch block and wide QRS, prior heart failure hospitalizations, and left ventricular and atrial dimensions. The MADIT-CRT score has been served as a gold standard and used as a reference in many validation studies (10–12).

The Seattle Heart Failure Model (SHFM) is a well-known risk estimation tool to predict the 1-, 2-, and 5-year mortality in chronic heart failure patients with conservative therapy (13). Perrotta et al. (14) applied the SHFM to patients who received a CRT, or a CRT-D and the model showed a good discrimination capacity in the mortality prediction. In the same year, the SHFM was validated in CRT populations by others as well (15, 16). Park et al. (17) were the first who developed a risk score, the EchoCG score, by using echocardiographic strain analysis to predict the reverse remodeling after CRT implantation. Strain analysis was included in many models later (11, 18–20). Similarly, to strain analysis, electrophysiologic modalities were also used in risk score development, such as sophisticated ECG analysis (21–23), vectorcardiography (24), or heart rate histogram analysis (25).

However, simplicity and availability are the keys to risk score development. The EAARN (26), the VALID-CRT (27), the HF-CRT (28), the CRT-SCORE (29), the AL-FINE (30), the ScREEN (31), the CRT-D Futility score (32), the MAGGIC (33), and many others can be calculated with routine laboratory and clinical parameters. Incorporating these principal concepts, machine learning algorithms can provide personalized risk predictions and online calculators are also available (34–36).

Conclusion

This is the first systematic review of risk scores in cardiac resynchronization therapy. The scores show a great diversity in terms of used predictors and endpoints. As we demonstrated, the number of the different scoring systems has drastically increased in the past few years and a very marked heterogeneity can be observed among them. Unfortunately, this makes their translation and transition into everyday clinical practice difficult. Furthermore, the majority of studies were conducted prior to the current era of quadruple HFrEF therapy. These limitations must be considered before the routine application of the score systems.

Rickard et al. have shown in a prior review that classic markers (native LBBB, non-ischemic etiology, wide QRS, female gender and sinus rhythm) predict outcomes after CRT-D (4). However,

there is growing evidence available on novel risk factors for CRT response, incorporated into the numerous risk score systems. The predictors can be categorized into the following different groups: co-morbidities, clinical state, echocardiographic, electrocardiographic, routine blood markers, and novel biomarkers as shown in the present review; the overlap of the markers in the various models is minimal. Some biomarkers are not yet incorporated into the daily routine clinical practice and their widespread use is therefore limited. Moreover, the lack of cross-validation across the risk scores limits the ability to objectively determine which of them should be incorporated into daily practice.

Although all the listed risk scores have the potential to predict outcomes after CRT, more data is required to enable us to select which will be appropriate to use in the daily clinical practice to predict the prognosis of severe heart failure patients, who undergo CRT. As the number of possible predictors and combinations is overwhelming, machine learning based algorithms or the help of artificial intelligence might be required to develop a uniform CRT risk score system.

It must be emphasized that, currently, the decision of CRT implantation is based on the ejection fraction, the width of the QRS, and the presence of LBBB; none of the guidelines do endorse any risk score to be applied in the process. Therefore, risk scores are useful to give information regarding the prognosis after implantation but should not influence the implantation itself.

Author contributions

AB and GS contributed to the conception and design of the study and wrote the first draft of the manuscript. GS and BM provided the institutional background to the study. AB and PP collected data and performed the statistical analysis. All authors contributed to manuscript revision, read, and approved the submitted version.

Conflict of interest

GS reports personal fees from Abbott, Bayer, Boston Scientific, and Johnson and Johnson Medical outside the submitted work.

The remaining authors declare that the research was conducted in the absence of any commercial or financial relationships that could be construed as a potential conflict of interest.

Publisher's note

References

1. Ponikowski P, Voors A, Anker S, Bueno H, Cleland J, Coats A, et al. 2016 ESC Guidelines for the diagnosis and treatment of acute and chronic heart failure: the task force for the diagnosis and treatment of acute and chronic heart failure of the European society of cardiology (ESC)developed with the special contribution of the heart failure association (HFA) of the ESC. *Eur Heart J.* (2016) 37: 2129–200.

2. McDonagh T, Metra M, Adamo M, Gardner R, Baumbach A, Böhm M, et al. 2021 ESC Guidelines for the diagnosis and treatment of acute and chronic heart failure. *Eur Heart J.* (2021) 42:3599–726.

3. Fornwalt B, Sprague W, BeDell P, Suever J, Gerritse B, Merlino J, et al. Agreement is poor among current criteria used to define response to cardiac resynchronization therapy. *Circulation.* (2010) 121:1985–91.

4. Rickard J, Michtalik H, Sharma R, Berger Z, Iyoha E, Green A, et al. Predictors of response to cardiac resynchronization therapy: a systematic review. *Int J Cardiol.* (2016) 225:345–52.

5. Heggermont W, Auricchio A, Vanderheyden M. Biomarkers to predict the response to cardiac resynchronization therapy. *Europace.* (2019) 21:1609–20.

6. Heist E, Taub C, Fan D, Arzola-Castaner D, Alabiad C, Reddy V, et al. Usefulness of a novel "response score" to predict hemodynamic and clinical outcome from cardiac resynchronization therapy. *Am J Cardiol.* (2006) 97:1732–6.

7. Charlson M, Pompei P, Ales K, MacKenzie CR. A new method of classifying prognostic comorbidity in longitudinal studies: development and validation. *J Chronic Dis.* (1987) 40:373–83.

8. Theuns D, Schaer B, Soliman O, Altmann D, Sticherling C, Geleijnse M, et al. The prognosis of implantable defibrillator patients treated with cardiac resynchronization therapy: comorbidity burden as predictor of mortality. *Europace.* (2011) 13:62–9.

9. Goldenberg I, Moss A, Hall W, Foster E, Goldberger J, Santucci P, et al. Predictors of response to cardiac resynchronization therapy in the multicenter automatic defibrillator implantation trial with cardiac resynchronization therapy (MADIT-CRT). *Circulation.* (2011) 124:1527–36.

10. Spinale F, Meyer T, Stolen C, Van Eyk J, Gold M, Mittal S, et al. Development of a biomarker panel to predict cardiac resynchronization therapy response: results from the SMART-AV trial. *Heart Rhythm.* (2019) 16:743–53.

11. Seo Y, Ishizu T, Machino-Ohtsuka T, Yamamoto M, Machino T, Kuroki K, et al. Incremental value of speckle tracking echocardiography to predict cardiac resynchronization therapy (CRT) responders. *J Am Heart Assoc.* (2016) 5:e003882.

12. Younis A, Goldberger J, Kutyifa V, Zareba W, Polonsky B, Klein H, et al. Predicted benefit of an implantable cardioverter-defibrillator: the MADIT-ICD benefit score. *Eur Heart J.* (2021) 42:1676–84.

13. Levy W, Mozaffarian D, Linker D, Sutradhar S, Anker S, Cropp A, et al. The Seattle heart failure model: prediction of survival in heart failure. *Circulation.* (2006) 113:1424–33.

14. Perrotta L, Ricciardi G, Pieragnoli P, Chiostri M, Pontecorboli G, De Santo T, et al. Application of the Seattle heart failure model in patients on cardiac resynchronization therapy. *Pacing Clin Electrophysiol.* (2012) 35:88–94.

15. Clemens M, Szegedi Z, Kardos L, Nagy-Baló E, Sándorfi G, Edes I, et al. The Seattle heart failure model predicts survival in patients with cardiac resynchronization therapy: a validation study. *J Card Fail.* (2012) 18:682–7.

16. Smith T, Levy W, Schaer B, Balk A, Sticherling C, Jordaens L, et al. Performance of the Seattle heart failure model in implantable defibrillator patients treated with cardiac resynchronization therapy. *Am J Cardiol.* (2012) 110:398–402.

17. Park J, Negishi K, Grimm R, Popovic Z, Stanton T, Wilkoff B, et al. Echocardiographic predictors of reverse remodeling after cardiac resynchronization therapy and subsequent events. *Circ Cardiovasc Imaging.* (2013) 6:864–72.

18. Kydd A, Khan F, Ring L, Pugh P, Virdee M, Dutka D. Development of a multiparametric score to predict left ventricular remodelling and prognosis after cardiac resynchronization therapy. *Eur J Heart Fail.* (2014) 16:1206–13.

19. Kang Y, Cheng L, Cui J, Li L, Qin S, Su Y, et al. A new score system for predicting response to cardiac resynchronization therapy. *Cardiol J.* (2015) 22:179–87.

20. Orszulak M, Filipecki A, Wróbel W, Berger-Kucza A, Orszulak W, Urbańczyk-Swić D, et al. Regional strain pattern index-a novel technique to predict CRT response. *Int J Environ Res Public Health.* (2021) 18:926.

21. Bani R, Checchi L, Cartei S, Pieragnoli P, Ricciardi G, Paoletti Perini A, et al. Simplified selvester score: a practical electrocardiographic instrument to predict response to CRT. *J Electrocardiol.* (2015) 48:62–8.

22. Végh E, Kandala J, Januszkiewicz L, Ren J, Miller A, Orencole M, et al. A new simplified electrocardiographic score predicts clinical outcome in patients treated with CRT. *Europace.* (2018) 20:492–500.

23. Liu X, Hu Y, Hua W, Yang S, Gu M, Niu H, et al. A predictive model for super-response to cardiac resynchronization therapy: the QQ-LAE score. *Cardiol Res Pract.* (2020) 2020:3856294.

24. Maass A, Vernooy K, Wijers S, van 'T Sant J, Cramer M, Meine M, et al. Refining success of cardiac resynchronization therapy using a simple score predicting the amount of reverse ventricular remodelling: results from the markers and response to CRT (MARC) study. *Europace.* (2018) 20:e1–10.

25. Wilkoff B, Richards M, Sharma A, Wold N, Jones P, Perschbacher D, et al. a device histogram-based simple predictor of mortality risk in ICD and CRT-D patients: the heart rate score. *Pacing Clin Electrophysiol.* (2017) 40:333–43.

26. Khatib M, Tolosana J, Trucco E, Borràs R, Castel A, Berruezo A, et al. EAARN score, a predictive score for mortality in patients receiving cardiac resynchronization therapy based on pre-implantation risk factors. *Eur J Heart Fail.* (2014) 16:802–9.

27. Gasparini M, Klersy C, Leclercq C, Lunati M, Landolina M, Auricchio A, et al. Validation of a simple risk stratification tool for patients implanted with cardiac resynchronization therapy: the VALID-CRT risk score. *Eur J Heart Fail.* (2015) 17:717–24.

28. Nauffal V, Tanawuttiwat T, Zhang Y, Rickard J, Marine J, Butcher B, et al. Predictors of mortality, LVAD implant, or heart transplant in primary prevention cardiac resynchronization therapy recipients: the HF-CRT score. *Heart Rhythm.* (2015) 12:2387–94.

29. Höke U, Mertens B, Khidir M, Schalij M, Bax J, Delgado V, et al. Usefulness of the CRT-SCORE for shared decision making in cardiac resynchronization therapy in patients with a left ventricular ejection fraction of =35. *Am J Cardiol.* (2017) 120:2008–16.

30. Kisiel R, Fijorek K, Sondej T, Pavlinec C, Kukla P, Czarnecka D, et al. Risk stratification in patients with cardiac resynchronisation therapy: the AL-FINE CRT risk score. *Kardiol Pol.* (2018) 76:1441–9.

31. Providencia R, Marijon E, Barra S, Reitan C, Breitenstein A, Defaye P, et al. Usefulness of a clinical risk score to predict the response to cardiac resynchronization therapy. *Int J Cardiol.* (2018) 260:82–7.

32. Maille B, Bodin A, Bisson A, Herbert J, Pierre B, Clementy N, et al. Predicting outcome after cardiac resynchronisation therapy defibrillator implantation: the cardiac resynchronisation therapy defibrillator futility score. *Heart.* (2022) 108:1186–93.

33. Manlucu J, Sharma V, Koehler J, Warman E, Wells G, Gula L, et al. Incremental value of implantable cardiac device diagnostic variables over clinical parameters to predict mortality in patients with mild to moderate heart failure. *J Am Heart Assoc.* (2019) 8:e010998.

34. Feeny A, Rickard J, Patel D, Toro S, Trulock K, Park C, et al. Machine learning prediction of response to cardiac resynchronization therapy: improvement versus current guidelines. *Circ Arrhythm Electrophysiol.* (2019) 12:e007316.

35. Tokodi M, Schwertner W, Kovács A, Tösér Z, Staub L, Sárkány A, et al. Machine learning-based mortality prediction of patients undergoing cardiac resynchronization therapy: the SEMMELWEIS-CRT score. *Eur Heart J.* (2020) 41: 1747–56.

36. Liang Y, Ding R, Wang J, Gong X, Yu Z, Pan L, et al. Prediction of response after cardiac resynchronization therapy with machine learning. *Int J Cardiol.* (2021) 344:120–6.

37. Vidal B, Delgado V, Mont L, Poyatos S, Silva E, Angeles Castel M, et al. Decreased likelihood of response to cardiac resynchronization in patients with severe heart failure. *Eur J Heart Fail.* (2010) 12:283–7.

38. Shen X, Nair C, Aronow W, Holmberg M, Reddy M, Anand K, et al. A new baseline scoring system may help to predict response to cardiac resynchronization therapy. *Arch Med Sci.* (2011) 7:627–33.

39. Brunet-Bernard A, Maréchaux S, Fauchier L, Guiot A, Fournet M, Reynaud A, et al. Combined score using clinical, electrocardiographic, and echocardiographic parameters to predict left ventricular remodeling in patients having had cardiac resynchronization therapy six months earlier. *Am J Cardiol.* (2014) 113:2045–51.

40. Rickard J, Cheng A, Spragg D, Cantillon D, Baranowski B, Varma N, et al. A clinical prediction rule to identify patients at heightened risk for early demise following cardiac resynchronization therapy. *J Cardiovasc Electrophysiol.* (2014) 25:278–82.

41. Paoletti Perini A, Bartolini S, Pieragnoli P, Ricciardi G, Perrotta L, Valleggi A, et al. CHADS2 and CHA2DS2-VASc scores to predict morbidity and mortality in heart failure patients candidates to cardiac resynchronization therapy. *Europace.* (2014) 16:71–80.

42. Barra S, Looi K, Gajendragadkar P, Khan F, Virdee M, Agarwal S. Applicability of a risk score for prediction of the long-term benefit of the implantable cardioverter defibrillator in patients receiving cardiac resynchronization therapy. *Europace.* (2016) 18:1187–93.

43. Nauffal V, Zhang Y, Tanawuttiwat T, Blasco-Colmenares E, Rickard J, Marine J, et al. Clinical decision tool for CRT-P vs. CRT-D implantation: findings from PROSE-ICD. *PLoS One.* (2017) 12:e0175205. doi: 10.1371/journal.pone.0175205

44. Nevzorov R, Goldenberg I, Konstantino Y, Golovchiner G, Strasberg B, Souleiman M, et al. Developing a risk score to predict mortality in the first year after implantable cardioverter defibrillator implantation: data from the Israeli ICD Registry. *J Cardiovasc Electrophysiol.* (2018) 29:1540–7.

45. Biton Y, Costa J, Zareba W, Baman J, Goldenberg I, McNitt S, et al. Predictors of long-term mortality with cardiac resynchronization therapy in mild heart failure patients with left bundle branch block. *Clin Cardiol.* (2018) 41:1358–66.

46. Bakos Z, Chatterjee N, Reitan C, Singh J, Borgquist R. Prediction of clinical outcome in patients treated with cardiac resynchronization therapy - the role of NT-ProBNP and a combined response score. *BMC Cardiovasc Disord.* (2018) 18:70. doi: 10.1186/s12872-018-0802-8

47. Theuns D, Van Boven N, Schaer B, Hesselink T, Rivero-Ayerza M, Umans V, et al. Predicting early mortality among implantable defibrillator patients treated with cardiac resynchronization therapy. *J Card Fail.* (2019) 25:812–8.

48. Weber D, Koller M, Theuns D, Yap S, Kühne M, Sticherling C, et al. Predicting defibrillator benefit in patients with cardiac resynchronization therapy: a competing risk study. *Heart Rhythm.* (2019) 16:1057–64.

49. Cai M, Hua W, Zhang N, Yang S, Hu Y, Gu M, et al. A prognostic nomogram for event-free survival in patients with atrial fibrillation before cardiac resynchronization therapy. *BMC Cardiovasc Disord.* (2020) 20:221. doi: 10.1186/s12872-020-01502-4

50. Patel D, Trulock K, Moennich L, Kiehl E, Kumar A, Toro S, et al. Predictors of long-term outcomes greater than 10 years after cardiac resynchronization therapy implantation. *J Cardiovasc Electrophysiol.* (2020) 31:1182–6.

51. Yang S, Liu Z, Hu Y, Jing R, Gu M, Niu H, et al. A novel risk model for mortality and hospitalization following cardiac resynchronization therapy in patients with non-ischemic cardiomyopathy: the alpha-score. *BMC Cardiovasc Disord.* (2020) 20:205. doi: 10.1186/s12872-020-01460-x

52. Milner A, Braunstein ED, Umadat G, Ahsan H, Lin J, Palma E. Utility of the modified frailty index to predict cardiac resynchronization therapy outcomes and response. *Am J Cardiol.* (2020) 125:1077–82.

53. Theuns D, Schaer B, Caliskan K, Hoeks S, Sticherling C, Yap S, et al. Application of the heart failure meta-score to predict prognosis in patients with cardiac resynchronization defibrillators. *Int J Cardiol.* (2021) 330:73–9.

54. Zoni-Berisso M, Martignani C, Ammendola E, Narducci M, Caruso D, Miracapillo G, et al. Mortality after cardioverter-defibrillator replacement: results of the DECODE survival score index. *Heart Rhythm.* (2021) 18:411–8.

55. Yamada S, Kaneshiro T, Yoshihisa A, Nodera M, Amami K, Nehashi T, et al. Albumin-bilirubin score for prediction of outcomes in heart failure patients treated with cardiac resynchronization therapy. *J Clin Med.* (2021) 10:5378.

56. Ikeya Y, Saito Y, Nakai T, Kogawa R, Otsuka N, Wakamatsu Y, et al. Prognostic importance of the controlling nutritional status (CONUT) score in patients undergoing cardiac resynchronisation therapy. *Open Heart.* (2021) 8:e001740.

57. Saito Y, Nakai T, Ikeya Y, Kogawa R, Otsuka N, Wakamatsu Y, et al. Prognostic value of the MELD-XI score in patients undergoing cardiac resynchronization therapy. *ESC Heart Fail.* (2022) 9:1080–9.

frontiers | Frontiers in Physiology

TYPE Review
PUBLISHED 26 January 2023
DOI 10.3389/fphys.2023.1054095

OPEN ACCESS

EDITED BY
Maciej M. Sterlinski,
National Institute of Cardiology, Poland

REVIEWED BY
Laura Perrotta,
Careggi University Hospital, Italy
Richard Gary Trohman,
Rush University, United States

*CORRESPONDENCE
Nadeev Wijesuriya,
nadeev.wijesuriya@kcl.ac.uk

SPECIALTY SECTION
This article was submitted to Cardiac Electrophysiology, a section of the journal Frontiers in Physiology

RECEIVED 26 September 2022
ACCEPTED 17 January 2023
PUBLISHED 26 January 2023

CITATION
Wijesuriya N, Elliott MK, Mehta V, De Vere F, Strocchi M, Behar JM, Niederer SA and Rinaldi CA (2023), Pacing interventions in non-responders to cardiac resynchronization therapy. *Front. Physiol.* 14:1054095. doi: 10.3389/fphys.2023.1054095

Pacing interventions in non-responders to cardiac resynchronization therapy

Nadeev Wijesuriya[1,2]*, Mark K. Elliott[1,2], Vishal Mehta[1,2], Felicity De Vere[1,2], Marina Strocchi[1], Jonathan M. Behar[1,2], Steven A. Niederer[1] and Christopher A. Rinaldi[1,2]

[1]School of Biomedical Engineering and Imaging Sciences, King's College London, London, United Kingdom, [2]Department of Cardiology, Guy's and St Thomas' NHS Foundation Trust, London, United Kingdom

Non-responders to Cardiac Resynchronization Therapy (CRT) represent a high-risk, and difficult to treat population of heart failure patients. Studies have shown that these patients have a lower quality of life and reduced life expectancy compared to those who respond to CRT. Whilst the first-line treatment for dyssynchronous heart failure is "conventional" biventricular epicardial CRT, a range of novel pacing interventions have emerged as potential alternatives. This has raised the question whether these new treatments may be useful as a second-line pacing intervention for treating non-responders, or indeed, whether some patients may benefit from these as a first-line option. In this review, we will examine the current evidence for four pacing interventions in the context of treatment of conventional CRT non-responders: CRT optimization; multisite left ventricular pacing; left ventricular endocardial pacing and conduction system pacing.

KEYWORDS

CRT, CRT non-response, endocardial pacing, leadless cardiac resynchronization therapy, conduction system pacing

Introduction

Cardiac Resynchronization Therapy (CRT), in addition to optimal medical therapy, is a widespread and successful treatment for patients with dyssynchronous heart failure (HF) (Glikson et al., 2021). Conventionally, CRT involves transvenous systems delivering biventricular (BiV) pacing from leads in the right ventricle (RV), and a cardiac vein via the coronary sinus (CS) to achieve epicardial left ventricular (LV) stimulation. There is strong evidence that CRT improves HF symptoms whilst reducing HF hospitalisations and improving mortality in indicated patients (McAlister et al., 2007).

Unfortunately, there is a subgroup of high-risk patients who have a poor therapeutic response to CRT, so-called "CRT non-responders" representing between 30% and 50% of CRT patients (Young et al., 2003). Several factors have been proposed to contribute to this limited efficacy. Cardiac venous anatomy significantly restricts the pacing location of the LV lead, which may lead to difficulty in targeting optimal sites, and avoiding areas of transmural scar (Wouters et al., 2021). LV scar is present in up to 40% of CRT candidates, and predicts poor response (BLEEKER et al., 2006; Chalil et al., 2007; Leyva et al., 2011; Wong et al., 2013). In addition, modelling studies demonstrate that conventional CRT does not replicate physiological activation across the endocardium and in some instances may be pro-arrhythmic (Mendonca Costa et al., 2019).

Treatment of CRT non-responders is extremely difficult, and this cohort of patients is known to have poor outcomes (Vijayaraman et al., 2022a). In recent years, several novel pacing

interventions have been investigated to assess whether these therapies can provide benefit when clinical improvement does not occur despite BiV or when conventional transvenous implantation was not successfully achieved. These interventions include: optimisation of atrioventricular (AV) and interventricular (VV) delays; multisite LV pacing; LV endocardial pacing and conduction system pacing (CSP).

In this review, we will examine the current data for these four pacing interventions in the treatment of CRT non-responders, discuss the limitations of the current body of evidence, and provide opinions on future directions in this field.

Optimisation of atrioventricular (AV) and interventricular (VV) delays

Delay optimisation has been the subject of investigation since the advent of CRT, arising from the theory that optimisation of both passive and active filling will maximise cardiac output, thereby improving outcomes. Observational studies have reported acute haemodynamic and electrical benefits of AV/VV optimisation in patients receiving CRT (Jansen et al., 2006; AlTurki et al., 2019), however, clinical trials have not consistently reported long term benefits (Brabham and Gold, 2013). The SMART-AV (Ellenbogen et al., 2010) trial which randomised 980 patients in a 1:1:1 ratio to CRT with an empirical AV delay of 120 ms, echocardiographically optimised AV delay, or AV delay optimised with SmartDelay, an electrogram-based algorithm. This study demonstrated no significant improvements in either AV optimisation arm over empirical settings based on LV end systolic volume improvement or clinical improvement at 6 months.

There are several reasons why acute mechanistic data examining haemodynamic benefits of AV delay optimisation do not translate to improve outcomes in clinical trials. The intrinsic PR interval is variable, especially in response to factors such as autonomic tone and exercise (Lee et al., 1995). As such, the optimal AV delay programmed in clinic may not reflect the patient's real-world physiology.

Another reason that AV optimisation has not shown significant positive results may be because the majority of patients respond very well to empirical BiV pacing. Thus, the beneficial effect will likely be small in an unselected CRT population. There may however be a role for optimisation in a selected CRT non-responder group. Brown et al. reported that in 32 echocardiographic CRT non-responders, CRT optimization significantly improved LV ejection fraction from 31.8% ± 4.7% to 36.3% ± 5.9% ($p < .001$) and LV end-systolic volume from 108.5 ± 37.6 to 98.0 ± 37.5 mL ($p = .009$). Additionally, speckle-tracking measures of LV strain significantly improved by 2.4% ± 4.5% (transverse; $p = .002$) and 1.0% ± 2.6% (longitudinal; $p = .017$) and aortic to pulmonic valve opening time, a measure of interventricular dyssynchrony, significantly ($p = .040$) decreased by 14.9 ± 39.4 ms (Brown et al., 2022). Similar conclusions were reached by Naqvi et al., who reported improved echo-derived strain measures of dyssynchrony in a series of 8 clinical non-responders receiving AV and VV optimisation (Naqvi et al., 2006). Whilst these results appear promising, they have not been consistently replicated. Another small study, in 8 patients classified as both echocardiographic and clinical non-responders, reported no improvements in echo outcomes after receiving CRT optimisation (Sepši et al., 2013). Larger randomised studies specifically targeting a non-responder population are needed to provide more definitive answers to this potentially practice changing intervention.

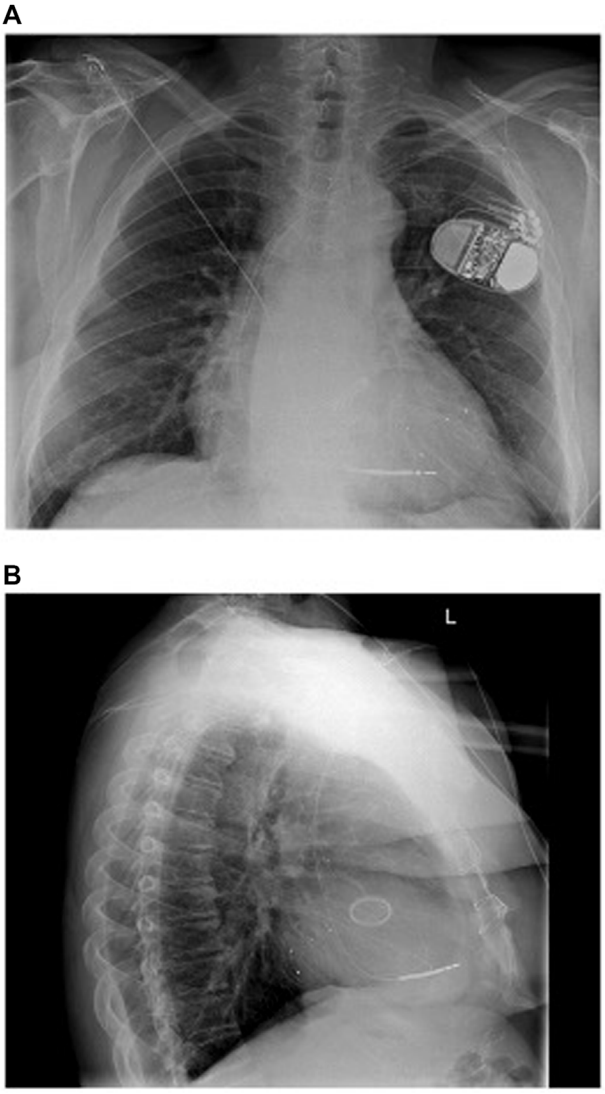

FIGURE 1
(A) Anteroposterior and **(B)** Lateral chest radiograph views 1 day post implant of triventricular CRT system with one LV lead in posterolateral vein and another in a lateral vein. Reproduced from reference 23, Gould et al., with permission.

Multi-point and multi-lead pacing

Multi-point pacing (MPP) and multi-lead pacing, such as "triventricular" (TriV) pacing is a well-studied area in the field of CRT non-response. Pacing the LV from multiple locations is an attractive concept as it potentially addresses the problems caused by ischaemic scar or other areas of slow conduction velocity that reduce the efficacy of CRT by affecting the LV paced wavefront. Several studies testing the efficacy of these interventions have been performed in non-responder populations. In the SMART-MSP trial, 102 patients who had an unchanged or worsened clinical composite score, (composed of all-cause mortality; HF events; patient global

assessment; and NYHA HF classification) at 6 months post-CRT had LV MPP turned on (Saba et al., 2022). They found that 51% of these patients became clinical responders at 12 months follow up, and concluded that LV MPP is beneficial in the treatment of non-responders. However, this trial did not include any echocardiographic data, as such the primary endpoint was a subjective measure. Furthermore, a criticism of this study was the lack of a control group, in particular, that a significant proportion of CRT non-responders at 6 months may have become responders at 12 months even in the absence of MPP. Indeed, this was demonstrated in Phase 1 of the MORE-CRT trial (Leclercq et al., 2019), which randomised 467 non-responders at 6 months post CRT to MPP-ON or MPP-OFF. This trial reported no significant difference in echo response between the groups at 12 months follow-up as evaluated in a blinded echo core lab. In both the MPP-ON (31.8%) and MPP-OFF (33.8%) groups a subset of non-responders converted into responders at follow-up. The authors suggested that there may be a delayed response to biventricular pacing beyond the initial 6 months owing to a myocardial substrate that needs more time to fully undergo reverse remodelling, or heart failure medication that continues to be up titrated-whether that be with MPP, MSP, or conventional CRT. A recently published meta-analysis by Mehta et al. reported that in randomised studies, there is no difference between MPP and conventional CRT (Mehta et al., 2021).

Multi-lead pacing, that is, the placement of an additional lead, most commonly in the LV to provide Triventricular (TriV) pacing (Figure 1), has also been evaluated in randomised control trials. The V3 trial (Bordachar et al., 2018) and STRIVE-CRT (Gould et al., 2022) are important negative trials which showed no significant difference in clinical or echocardiographic outcomes between standard of care and multi-lead pacing in unselected CRT populations. A meta-analysis of 415 patients by Elliott et al. (Elliott et al., 2022a) again reported no difference between TriV pacing and conventional BiV pacing.

Acute haemodynamic studies in both animals (Ploux et al., 2014; Heckman et al., 2020) and humans (Sohal et al., 2015) have reported that LV multi-lead pacing may provide acute haemodynamic benefits over BiV CRT in subjects who are "acute haemodynamic non-responders" to conventional CRT. These studies have yet to be replicated on a larger scale with robust outcome data. Until such time, it cannot be extrapolated that there is a significant benefit of implanting an additional LV lead in non-responders.

Left ventricular endocardial pacing

Endocardial pacing provides more physiological activation than epicardial pacing (Bordachar et al., 2012), and importantly, gives the benefit of unrestricted LV pacing locations, which can be vital in patients with factors including ischaemic scar or lack of suitable cardiac venous targets, through unfavourable anatomical characteristics such as difficult coronary sinus os access, a persistent left sided subclavian vein, or tributaries which are too small to support a lead. The emergence of LV endocardial pacing as a potential treatment for conventional CRT non-responders has been driven primarily by mechanistic studies which have consistently reported acute haemodynamic benefits for endocardial pacing versus conventional CRT (Derval et al., 2010; Ginks et al., 2012; Shetty et al., 2014; Sohal et al., 2014; Behar et al., 2016). The optimal LV pacing locations reported were highly variable, but in these studies, the endocardial site with the largest improvement in acute haemodynamic response (AHR) was consistently superior to conventional BiV pacing. Behar et al. (Behar et al., 2016) reported from a total of 135 sites tested in 8 patients that AHR was significantly greater when temporary pacing the same myocardial segment endocardially versus epicardially (15.2 ± 10.7% vs. 7.6 ± 6.3%; p = 0.014) and resulted in a shorter paced QRS duration (137 ± 22 ms vs. 166 ± 30 ms; $p < 0.001$). Interestingly, Sohal et al. (Sohal et al., 2014) reported an acute haemodynamic study of 10 patients with biventricular CRT devices. The optimal LV endocardial pacing site was at the same location as the existing epicardial LV lead in only four patients. An acute haemodynamic study performed by Padeletti et al. in 11 subjects also demonstrated that the optimal LV endocardial site in each patient significantly improved LV performance compared to conventional epicardial LV stimulation (Padeletti et al., 2012).

Mechanistic studies have also provided insight into which patients may benefit from endocardial pacing rather than epicardial LV pacing. Ginks et al. (Ginks et al., 2012) performed electroanatomical mapping to determine the intrinsic LV activation pattern and a haemodynamic study in 10 patients with LBBB referred for CRT. The authors reported that the majority (71%) of patients with non-ischemic heart failure and a line of conduction block causing LBBB responded to conventional CRT. In contrast, those with myocardial scar, and the absence of a line of conduction block, i.e. where LBBB was caused by homogenously slow conduction from the LV septum to the lateral wall, often required endocardial or multisite pacing to achieve CRT response. Non-responders have also specifically been studied in this setting. Gelder et al. (van Gelder et al., 2016) performed an acute haemodynamic study in 24 clinical CRT non-responders. They found that the initially implanted system generated an AHR ≥15% in five patients after A-V and V-V optimisation. Among these 5, three with posterolateral transvenous epicardial leads had no significant AHR increase with LV endocardial pacing. One of the two other patients with transvenous apical epicardial leads had an AHR rise from 19.7% to 66% with LV endocardial pacing. Nine of the 19 remaining patients had an increase in AHR to ≥15% at the optimal endocardial LV pacing position.

Initial systems delivering permanent LV endocardial pacing were lead-based. ALSYNC (Morgan et al., 2016) was a prospective clinical investigation of 118 patients who received a trans-septal (inter-atrial) LV endocardial pacing lead. Ninety patients (76.2%) had a failed epicardial lead or suboptimal cardiac venous anatomy and 28 (23.8%) were non-responders to previous CRT. At 6 months, the New York Heart Association (NYHA) class improved in 59% of patients, and 55% had LV end-systolic volume (LVESV) reduction of 15% or greater. Those patients enrolled after CRT non-response showed similar improvement, with 47% of patients having an improvement in LVESV of ≥15%, and 5% having an improvement ≥30%. Unfortunately in this study, 14 transient ischaemic attacks (9 patients, 6.8%) and five non-disabling strokes (5 patients, 3.8%) were observed. This prohibitively high embolic risk and the requirement for lifelong anticoagulation has motivated the development of novel leadless LV endocardial pacing systems.

Delivering CRT via leadless LV endocardial pacing has several potential advantages compared to lead-based systems. Complete device endothelialisation reduces the stroke risk and anticoagulation requirement (Echt et al., 2010), and devices can be implanted in patients where venous access or infection issues preclude both conventional and lead-based endocardial CRT. (Gamble et al.,

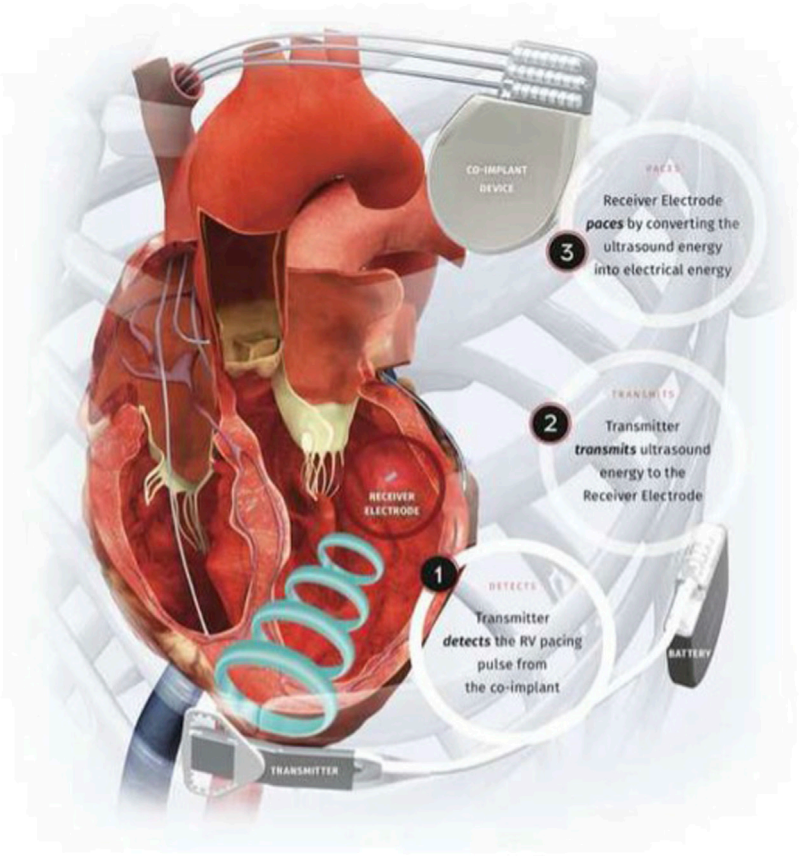

FIGURE 2
Components of the WiSE-CRT System. Reproduced from reference 64, Elliott et al., with permission.

2016). In addition, leadless pacing can avoid the numerous long-term complications associated with transvenous leads including: insulation breach, fracture (1%–4%); venous obstruction (8%–21%); and infection (1%–2%) (Bernard, 2016) which often result in the need for high risk extraction procedures.

The WiSE-CRT system (EBR Systems Inc., Sunnyvale CA) is the only commercially available leadless LV pacing system (Auricchio et al., 2014). The system consists of a battery connected to an ultrasound transmitter, which is implanted subcutaneously at the 4th, 5th, or 6th intercostal place, and the receiver electrode, which is implanted in the LV cavity via aortic or trans-septal access (Figure 2). The system requires the patient to have a "co-implant" *in situ* capable of producing continuous RV pacing, which can be either a conventional device, such as a pacemaker or implantable cardiac defibrillator (ICD), or a leadless pacemaker such as MICRA™ (Medtronic, Minneapolis MN). The transmitter and battery detect an RV pacing pulse emitted by the co-implant. Within 10 ms of detection of the RV pacing spike, the transmitter emits a number of ultrasound pulses to locate the receiver electrode. Once the transmitter is electronically optimally aligned, a longer ultrasound wave is emitted, which is detected and converted to a pacing stimulus by the receiver electrode. This results in LV pacing, and thereby BiV pacing.

Several observational studies have demonstrated that treatment with WiSE-CRT can deliver echocardiographic CRT response (Auricchio et al., 2014; Reddy et al., 2017; Sieniewicz et al., 2020; Okabe et al., 2022). A recent meta-analysis of these studies (Wijesuriya et al., 2022a) reported that in a total of 181 patients, there was a mean increase in LVEF of 6.3% (Mean difference 6.3, 95% Confidence Interval (4.35, 8.19) $p < 0.001$, with low heterogeneity ($p = 0.84$, $I^2 < 0.001\%$). The echocardiographic response rate (variably defined between studies as either a reduction in LVESV of >15%, an improvement in LVEF>5%, or an improvement in LVEF>10%) was 54% in a population where 22% were non-responders to conventional CRT.

A sub-analysis of the non-responder population of the WiSE-CRT registry was performed by Sidhu et al. (2020) The authors reported that in 18 patients, endocardial pacing resulted in a significant reduction in QRS duration compared with intrinsic QRS duration (26.6 ± 24.4 ms; $p = .002$) and improvement in left ventricular ejection fraction (LVEF) (4.7 ± 7.9%; $p = .021$). Overall, 55.6% of patients had improvement in their clinical composite score (consisting of number of hospitalizations with decompensated heart failure; survival to follow-up; improvement of ≥1 NYHA functional class; or improvement in their global assessment) and 66.7% had a reduction in LVESV ≥15% and/or absolute improvement in LVEF ≥5%. These results, albeit in a small patient cohort, provide preliminary favourable feasibility data of WiSE-CRT in treatment of non-responders. The ongoing SOLVE-CRT trial (NCT02922036) (Singh et al., 2021), a multicentre interventional study, will provide further valuable information about the efficacy of this new treatment modality.

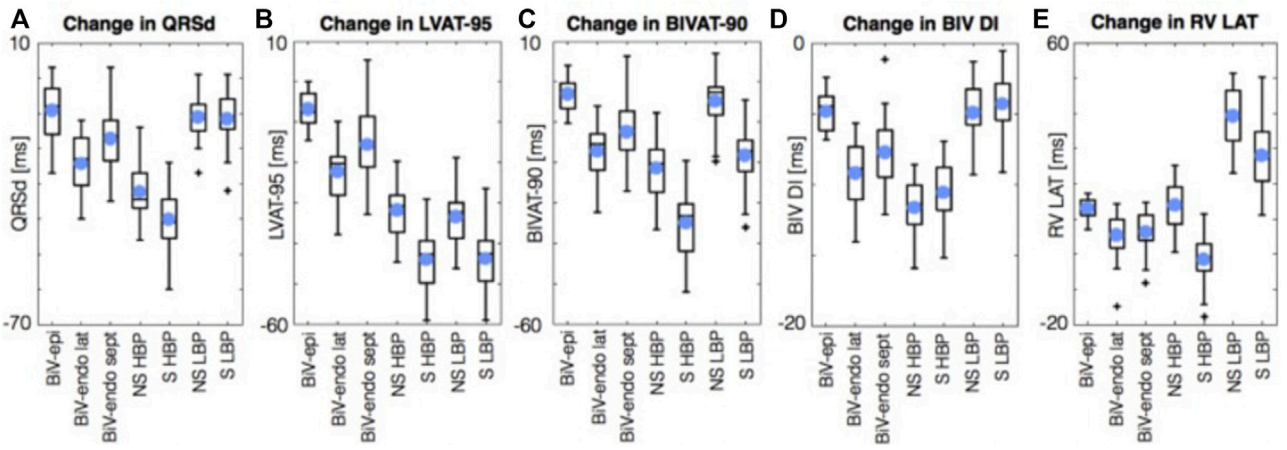

FIGURE 3
Simulations results using 24 four chamber heart meshes. Boxplots of the change in QRSd, **(A)** LVAT-95, **(B)** BIVAT-90, **(C)** BIV DI **(D)**, and RV LAT **(E)** from baseline with BiV-epi pacing at the optimal location, BiV-endo lateral pacing at the optimal location, BiV-endo septal pacing (BiV-endo sept), S- and NS-HBP, and S- and NS-LBP. *Light blue circles* represent mean values. *Plus symbols* represent outliers. BiV, biventricular; BIV DI, biventricular dyssynchronous index; BIVAT-90, 90% biventricular activation time; endo, endocardial; epi, epicardial; HBP, His-bundle pacing; LAT, lateral; LBP, left bundle pacing; LV, left ventricle; LVAT-95, 95% left ventricular activation time; NS, non-selective; QRSd, QRS duration; RV LAT, right ventricular latest activation time; S, selective; sept, septal. Reproduced from reference 55, Strocchi et al., with permission.

Conduction system pacing

Conduction system pacing (CSP) is an area of rapidly growing interest, built upon the attractive concept of restoring completely physiological ventricular activation. Initial studies in lead-based CSP focused on His Bundle Pacing (HBP). HBP achieves excellent cardiac resynchronization, but implantation can be difficult with success rates varying from 56%–95% (Bhatt et al., 2018; Sharma et al., 2018; Vijayaraman et al., 2018). Concerns about ventricular under-sensing and rising thresholds have emerged during long-term follow up (Lustgarten et al., 2019; Zanon et al., 2019). Left Bundle Branch Area Pacing (LBBAP) is a novel form of CSP which involves screwing a pacing lead deep into the interventricular septum from the RV in order to capture the left bundle system (Huang et al., 2019; Zhang et al., 2019). This technique has produced encouraging results from observational studies, with reported success rates of 80%–94%, (Padala and Ellenbogen, 2020), and significant improvements in LV systolic function (Zhang et al., 2019). Robust data from randomised control trials, however, is currently lacking. Current evidence, especially with regards to the role of CSP in non-response, is limited to *in silico* studies and observational studies.

Strocchi et al. (2020) performed an *in silico* study examining ventricular activation times on 24 four chamber heart meshes in the presence of simulated left bundle branch block (LBBB). They simulated BiV epicardial and BiV endocardial pacing, as well as HBP and LBBAP. They reported that HBP was superior ($p < .05$) to BiV endocardial and conventional BiV pacing with regards to reduction in LV activation time (AT) and interventricular dyssynchrony, (Figure 3). LBBAP reduced LV activation times but not interventricular dyssynchrony compared to conventional CRT and BiV endocardial pacing, due to late RV activation. The RV latest AT was higher with LBP than with HBP (141.3 ± 10.0 ms vs. 111.8 ± 10.4 ms). Optimizing AV delay during LBP reduced RV latest AT (104.7 ± 8.7 ms) and led to comparable response to HBP. These results suggest that CSP provides an electrical benefit over conventional CRT in unselected LBBB patients. We may extrapolate from this that CSP might be beneficial in patients who have not responded to conventional CRT.

Data from observational trials comparing conventional CRT with CSP in both unselected patients and non-responders has had variable outcomes. Non-randomised observational studies by Chen et al. and Vijayaraman et al. (Vijayaraman et al., 2022b; Chen et al., 2022) demonstrated improvements in QRS duration and echocardiographic outcomes with CSP compared to conventional BiV pacing in *de novo* implant patients, but this has not been consistently replicated (Upadhyay et al., 2019a; Toding Labi et al., 2022). Interestingly, Vijayaraman et al. performed a further observational study of 200 patients who underwent LBBAP for either inability to place a transvenous LV epicardial lead (Group 1, $n = 156$), or CRT non-response (Group 2, $n = 44$) (Vijayaraman et al., 2022a). QRS duration, LVEF and NYHA class improved in both groups, but more so in group 1. At mean 12 months follow-up the primary endpoint of death or HF hospitalisations was significantly lower in group 1 than group 2 (13% vs. 30%; HR 0.357; $p = .007$). The incidence of clinical and echocardiographic improvements in Group 1 was similar to those observed in patients undergoing conventional CRT in clinical trials. The authors concluded that LBBAP is a reasonable alternative to BiV CRT but more work is needed to assess its efficacy in non-responders.

An emerging field is the potential improvement in electrical synchronisation obtained through optimising conventional CRT with sequential CSP-LV pacing, known as His-Optimised CRT (HOT-CRT) or LBP-Optimised CRT (LOT-CRT). A mechanistic study of 11 patients showed that pressure-volume derived stroke volume was optimal when LV pacing was combined with HBP, suggesting that sequential CSP-LV activation provides benefit by preserving intrinsic RV activation (Padeletti et al., 2016). A 25 patient feasibility study of HOT-CRT (Vijayaraman et al., 2019) demonstrated that QRS duration at baseline was 183 ± 27 ms and significantly narrowed to 162 ± 17 ms with biventricular pacing ($p = 0.003$), to 151 ± 24 ms during HBP ($p < 0.0001$), and further to 120 ±

TABLE 1 Summary of different pacing options for CRT non-responders.

Pacing option	Evidence summary for CRT non-responders
AV/VV delay optimisation	Small observational studies—conflicting data Jansen et al., 2006; Ellenbogen et al., 2010; Brabham and Gold, (2013); AlTurki et al., 2019
Multi-point pacing (MPP)	MORE-CRT RCT—no benefit in MPP Leclercq et al., 2019
Multi-site pacing (MSP)	Mechanistic studies—Acute haemodynamic benefit in of MSP in acute haemodynamic non-responders to conventional CRT. Ploux et al., 2014; Sohal et al., 2015; Heckman et al., 2020 No larger studies as yet.
LV endocardial pacing	Small observational studies—Lead-based and leadless endocardial pacing may achieve echocardiographic and clinical response in a significant proportion of non-responders. (van Gelder et al., 2016; Sidhu et al., 2020 SOLVE-CRT study ongoing
Conduction system pacing	Observational studies—HBP, LBP, HOT-CRT and LOT-CRT may give potential improvements in electrical resynchronisation obtained by preserving intrinsic RV activation, yet to be demonstrated in a non-responder population. Vijayaraman et al., 2019; Vijayaraman et al., 2022b; Jastrzębski et al., 2022; Toding Labi et al., 2022

16 ms during HOT-CRT ($p < 0.0001$). During a mean follow-up of 14 ± 10 months, LV ejection fraction improved from 24 ± 7% to 38 ± 10% ($p < 0.0001$), and NYHA functional class changed from 3.3 to 2.04. Twenty-one of 25 patients (84%) were clinical responders while 23 of 25 (92%) demonstrated an echocardiographic response. A LOT-CRT feasibility study (Jastrzębski et al., 2022) reported a clinical response rate of 76% in 91 patients. Although performed in small cohorts with no control groups, the high CRT response rates seen in these studies raise the question of whether addition of CSP to BiV pacing in CRT non-responders will be efficacious in a significant number of patients. Larger studies of non-responder patients will of course be needed in this regard, and it will be important to consider safety outcomes as well as heart failure outcomes, given both the additional infection risk associated with upgrade procedures, as well as long-term risks of lead-lead interaction, thrombosis and tricuspid regurgitation which increase with implantation of additional transvenous leads (Bernard, 2016). This is particularly pertinent as while CSP is becoming more widespread worldwide, (Performance Reports | Medtronic CRHF, 2022), extraction of CSP leads remains a low-volume procedure with a very small evidence base (Wijesuriya et al., 2022b).

Recent advances in WiSE-CRT implantation have brought about the ability to perform CSP via a leadless LV endocardial approach, potentially circumventing long-term lead related issues (Elliott et al., 2021; Elliott et al., 2022b; Wijesuriya et al., 2022c). The endocardial receiver electrode component of the WiSE-CRT system has traditionally been implanted at the LV lateral wall using a retrograde femoral arterial approach, however the emergence of a trans-septal implant technique gives the operator the ability to find a stable delivery sheath position on the LV septal wall using deflectable sheaths such as the FlexCath (Medtronic, Minneapolis MN). Initially the LV septum is mapped using a decapolar catheter, enabling the electrode to be targeted to the site of a pre-systolic potential, with the aim of capturing the His-Purkinje system. In a case series of 8 patients, the implant success rate was 100% (Elliott et al., 2022b), with a significant reduction in QRS duration (187.1 ± 33.8 ms vs. 149.5 ± 15.7 ms; $p = .009$). One of these 8 patients was a CRT non-responder, with the remainder being transvenous LV epicardial lead failures. Further data in this regard will come with time-LV septal implants are projected to increase in view of an improved safety profile of trans-septal compared to large-bore aortic access, and historically, around 1 in 5 patients receiving WiSE-CRT have been conventional CRT non-responders (Wijesuriya et al., 2022a). Much work is required before this are progresses towards randomised trials-in the first instance electroanatomical mapping data determining the ventricular activation pattern of a WiSE-CRT septal implant will shed light on questions such as whether His-Purkinje tissue is captured, and whether this is electrically superior to LV endocardial pacing from alternative sites.

Discussion

We now have several new and/or emerging CRT options which all theoretically have the potential to treat non-responders to conventional BiV epicardial CRT (Table 1). Whilst there have been some positive outcomes reported from observational studies, these have not been consistently replicated in larger trials. We believe that there are several reasons for these inconsistencies.

The foremost issue is that conventional biventricular CRT is an excellent treatment option for HF. In appropriately selected candidates, response rates are 60%–70% (Young et al., 2003). Observational studies tend to report at most a fairly mild improvement in indices such as AHR[29] [44] in head-to-head comparisons between novel CRT therapies and conventional CRT in *de novo* patients. Because of relatively small projected impact on measurable parameters, it will always be very difficult for the novel therapies to demonstrate superiority compared to conventional CRT in an unselected group of patients. In particular, there is generally attenuation of effect size in larger clinical trials compared to observational studies. In small single-centre trials, there may be a degree of recruitment bias, possibly by avoiding subjects with unfavourable CRT characteristics such as atrial fibrillation or right bundle branch block. The influence of bias is less likely to be prominent in larger multicentre studies. As such, therapies which initially sound promising, such as AV/VV optimisation (Brabham and Gold, 2013) and multipoint/multi-lead pacing (Elliott et al., 2022a) have lost momentum due to negative results in clinical trials of unselected patients. In actuality, their primary benefit could have been demonstrated by specifically targeting a non-responder population, where the potentially larger impact on measurable parameters may be adequate to power randomised trials at a reasonable sample size.

This brings us to the point of patient selection. Mechanistic studies have generally shown that there is significant variability in the optimal pacing site between individuals (Shetty et al., 2014; Sohal et al., 2014; Behar et al., 2016). This may be due to factors such as scar location, phenotype of conduction disturbance and aetiology of heart failure.

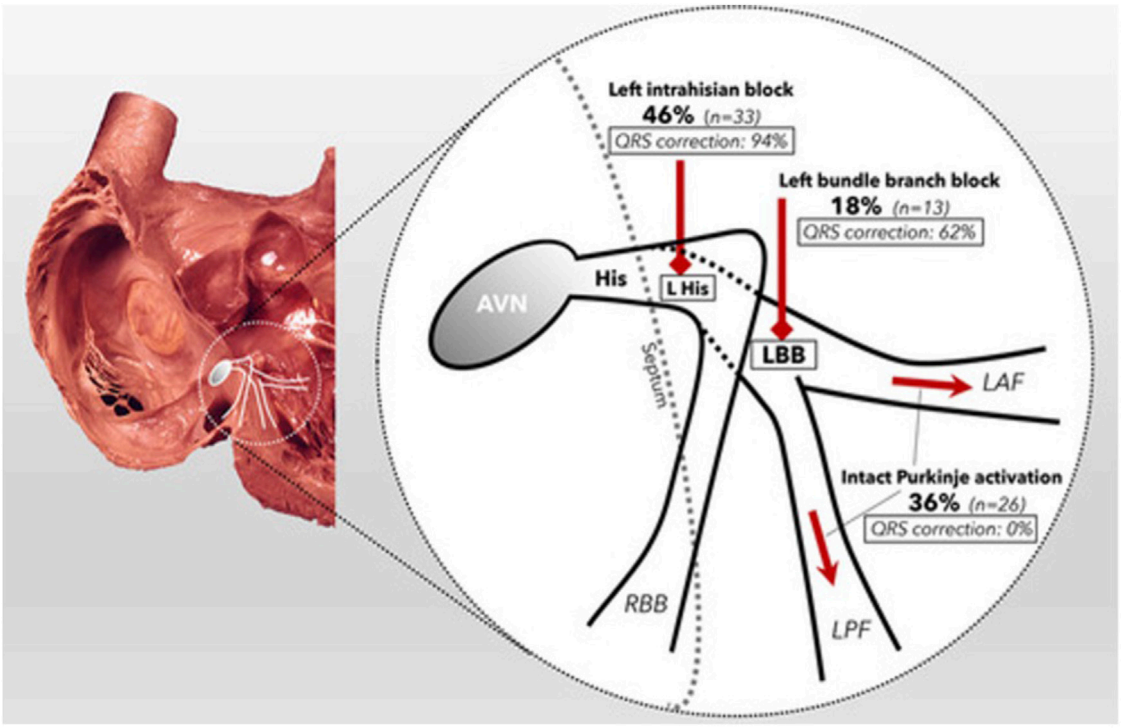

FIGURE 4
Schematic of the proximal conduction system, demonstrating the prevalence of each form of conduction disorder within the cohort (bold) and the percentage of patients whose QRSd was corrected by HBP (italic). Reproduced from reference 68, Upadhyay et al., with permission.

TABLE 2 Variations in definition of CRT response across trials.

Study	Definition of CRT response	Intervention
Vijayaraman et al., 2022a	CRT non-response was defined as improvement of LVEF <5% and either worsening or unchanged patient functional status	LBBAP
Brown et al., 2022	Non-responders had an improvement in LV ejection fraction (LVEF) by <5%, and incomplete responders had an improvement in LVEF by >5% with final LVEF <40% at least 3 months post-CRT	CRT optimisation
Naqvi et al., 2006	Symptoms of heart failure post-CRT	CRT optimisation
Sepši et al., 2013	Patients who have developed increase in LVEF >5% and those who had improvement of NYHA class during follow up were classified as responders. Patients who have developed drop in LVEF >5%	CRT optimisation
	and have decreased the NYHA class during the follow up were classified as non-responders. All between were classified as unchanged	
Saba et al., 2022	Non-response defined as unchanged or worsened clinical composite score at 6 months post-CRT.	Multi-site pacing
Leclercq et al., 2019	Response defined as <15% reduction in left ventricular end-systolic volume (LVESV) at 6 months post-CRT.	Multisite pacing
Bordachar et al., 2018	Non-response defined as unchanged or worsened clinical composite score 6 months post-CRT.	Multisite pacing
van Gelder et al., 2016	Non-response defined as remaining NYHA class 3 or 4 at least 6 months post-CRT.	Endocardial pacing
Sidhu et al., 2020	Non-response defines as unchanged or worsening of symptoms or New York Heart Failure (NYHA) functional class after at least 6 months post-CRT.	Leadless endocardial pacing
Chun et al., 2020	Decrease in (LV) end-systolic volume > 15% on echocardiography 6 months after implantation	Sacubitril-Valsartan
Giaimo et al., 2018	Non-response defined as previously treated with CRT for at least 6 months and remained classified as New York Heart Association (NYHA) functional class III or IV despite optimal medical therapy; the echocardiographic assessment showed lack of decrease of the left ventricular end-systolic volume (LVESV) of at least 10% and residual moderate-to-severe or severe FMR.	Mitraclip

(Ginks et al., 2012) For example, Upadhyay et al. (Upadhyay et al., 2019b) demonstrated in a temporary pacing and electroanatomical mapping study of 72 subjects with LBBB that whilst CSP overcame proximal block in 64% of patients, 36% of their cohort displayed "intact Purkinje activation" where conduction disturbance is caused by more distal diffuse disease (Figure 4). In these patients, the QRS duration was not corrected by HBP.

Lastly, CRT non-responders are a highly heterogenous group of patients where failure of conventional CRT may occur for a number of reasons. There may be an optimal pacing site for each patient, but currently, our pre-assessment procedures do not aim to identify this as part of standard clinical practice. Whilst prediction of optimal pacing sites has been demonstrated in a research setting (Duckett et al., 2011; Sieniewicz et al., 2018; Sohal et al., 2021) making this operational in a non-invasive, cost-effective manner will be more difficult. Further work involving pre-procedural imaging such as MRI and CT to define scar may yield positive results in this regard moving forward. Until such time as this personalised treatment can be delivered, it seems unlikely that any one alternative pacing modality will demonstrate superiority over a successful treatment like conventional CRT in larger clinical trials.

An additional issue in this field is difficulty in interpreting the current evidence base due to the lack of a standardised definition of CRT response. The most widely accepted definition involves an assessment of left ventricular reverse remodelling 6 months after implantation, with reductions in LV end-systolic volume (LVESV) of greater than 15% being the most useful measure (Picard et al., 2012). However, as shown in Table 2, studies examining CRT response use varied definitions, including echocardiographic (LVESV or LVEF), and clinical (NYHA class or clinical composite score). These definitions capture a broad group of patients. The causes of echocardiographic non-response are likely to be completely different from the causes of clinical non-response. For example, whilst sub-optimal LV lead position may lead to echocardiographic non-response, prevalent issues in heart failure such as anaemia, arrhythmia and sub-optimal medical therapy can lead to clinical non-response in the absence of persistent mechanical dyssynchrony (Sieniewicz et al., 2019). As such, the optimal second-line of treatment for these individual patients is also likely to vary, thus providing another cause of the lack of consistency in current studies.

Ultimately, determining the optimal second-line pacing intervention in CRT will require well designed clinical trials examining a standardised population of patients, with strict non-response inclusion criteria. Whilst early studies including WiSE-CRT (Sieniewicz et al., 2020), HOT-CRT (Vijayaraman et al., 2019) and LOT-CRT (Jastrzębski et al., 2022) may give us cause for optimism, it is important to avoid extrapolating these results from an unselected population to non-responder groups. For example, no studies have yet shown that the addition of CSP to conventional CRT non-responders will improve outcomes. Indeed, the observational study performed by the LBBAP collaborative study group (Vijayaraman et al., 2022a) suggested that whilst rescue LBBAP was a good alternative treatment for inability to place an epicardial lead via the CS, the response rate of LBBAP in CRT non-responders was poor, with a 30% rate of death or HF hospitalisation within 12 months. It may be that a significant proportion of non-responders are not patients who are receiving inadequate CRT, but rather patients who have an aggressive HF phenotype combined with other co-morbidities, in whom improvement will be challenging to achieve through novel pacing therapies alone. Improvements in outcomes for CRT non-responders have been demonstrated for therapies such as initiation of sacubitril-valsartan (Chun et al., 2020) and transcatheter mitral valve intervention for those with residual moderate/severe mitral regurgitation (Giaimo et al., 2018). These studies highlight the importance of a holistic approach to treating an unwell and high-risk HF population.

In summary, the heterogeneity of the dyssynchronous HF population and the high success rates of empirical conventional CRT mean that generating robust evidence for the optimal pacing alternatives for CRT non-responders is extremely challenging. There is likely a significant subgroup of CRT non-responders who have a superior alternative pacing location, in particular those who have problems with conventional LV lead implantation, or poor LV lead performance due to issues such as high capture thresholds and phrenic nerve stimulation. The plethora of novel therapies including endocardial and conduction system pacing may enable physicians to deliver tailored CRT for individual patients. Further study concentrating on patient selection will ultimately pave the way for this form of precision medicine.

Author contributions

NW performed literature review and manuscript preparation. ME, VM, FD, MS, JB, SN, and CR provided internal peer-review.

Funding

The authors are supported by the Wellcome/EPSRC Centre for Medical Engineering [WT203148/Z/16/Z]. ME and VM have received fellowship funding from Abbott. SN acknowledges support from the United Kingdom Engineering and Physical Sciences Research Council (EP/M012492/1, NS/A000049/1, and EP/P01268X/1), the British Heart Foundation (PG/15/91/31812,PG/13/37/30280, SP/18/6/33805), US National Institutes of Health (NIH R01-HL152256), European Research Council (ERC PREDICT-HF 864055) and Kings Health Partners London National Institute for Health Research (NIHR) Biomedical Research Centre. JB receives research funding and/or consultation fees from Abbott, Siemens Healthcare, EBR Systems, Biosense Webster outside of the submitted work. CAR receives research funding and/or consultation fees from Abbott, Medtronic, Boston Scientific, Spectranetics and MicroPort outside of the submitted work.

Conflict of interest

NW, ME, VM, FD, JB, and CR were employed by the Guy's and St Thomas' NHS Foundation Trust.

The remaining authors declare that the research was conducted in the absence of any commercial or financial relationships that could be construed as a potential conflict of interest.

Publisher's note

References

AlTurki, A., Lima, P. Y., Garcia, D., Montemezzo, M., Al-Dosari, A., Vidal, A., et al. (2019). Cardiac resynchronization therapy reprogramming to improve electrical synchrony in patients with existing devices. *J. Electrocardiol.* 56, 94–99. doi:10.1016/J.JELECTROCARD.2019.07.008

Auricchio, A., Delnoy, P. P., Butter, C., Brachmann, J., Van Erven, L., Spitzer, S., et al. (2014). Feasibility, safety, and short-term outcome of leadless ultrasound-based endocardial left ventricular resynchronization in heart failure patients: Results of the Wireless Stimulation Endocardially for CRT (WiSE-CRT) study. *Europace* 16 (5), 681–688. doi:10.1093/europace/eut435

Behar, J. M., Jackson, T., Hyde, E., Claridge, S., Gill, J., Bostock, J., et al. (2016). Optimized left ventricular endocardial stimulation is superior to optimized epicardial stimulation in ischemic patients with poor response to cardiac resynchronization therapy: A combined magnetic resonance imaging, electroanatomic contact mapping, and hemodynamic study to target endocardial lead placement. *JACC Clin. Electrophysiol.* 2 (7), 799–809. doi:10.1016/J.JACEP.2016.04.006

Bernard, M. L. (2016). Pacing without wires: Leadless cardiac pacing. *Ochsner* 16, 238–242.

Bhatt, A. G., Musat, D. L., Milstein, N., Pimienta, J., Flynn, L., Sichrovsky, T., et al. (2018). The efficacy of his bundle pacing: Lessons learned from implementation for the first time at an experienced Electrophysiology center. *JACC Clin. Electrophysiol.* 4 (11), 1397–1406. doi:10.1016/J.JACEP.2018.07.013

Bleeker, G. B., Schalij, M. J., van der Wall, E. E., and Bax, J. J. (2006). Postero-lateral scar tissue resulting in non-response to cardiac resynchronization therapy. *J. Cardiovasc Electrophysiol.* 17 (8), 899–901. doi:10.1111/j.1540-8167.2006.00499.x

Bordachar, P., Gras, D., Clementy, N., Defaye, P., Mondoly, P., Boveda, S., et al. (2018). Clinical impact of an additional left ventricular lead in cardiac resynchronization therapy nonresponders: The V3 trial. *Heart rhythm.* 15 (6), 870–876. doi:10.1016/J.HRTHM.2017.12.028

Bordachar, P., Grenz, N., Jais, P., Ritter, P., Leclercq, C., Morgan, J. M., et al. (2012), Left ventricular endocardial or triventricular pacing to optimize cardiac resynchronization therapy in a chronic canine model of ischemic heart failure, *Am. J. Physiol. Heart Circ. Physiol.*, 303, 207–215. doi:10.1152/AJPHEART.01117.2011/ASSET/IMAGES/LARGE/ZH40131204580005

Brabham, W. W., and Gold, M. R. (2013). The role of AV and VV optimization for CRT. *J. Arrhythm.* 29 (3), 153–161. doi:10.1016/J.JOA.2013.02.001

Brown, C. D., Burns, K. v., Harbin, M. M., Espinosa, E. A., Olson, M. D., and Bank, A. J. (2022). Cardiac resynchronization therapy optimization in nonresponders and incomplete responders using electrical dyssynchrony mapping. *Heart rhythm.* 19, 1965–1973. Published online August 5, 2022. doi:10.1016/J.HRTHM.2022.07.016

Chalil, S., Foley, P. W. X., Muyhaldeen, S. A., Patel, K. C. R., Yousef, Z. R., Smith, R. E. A., et al. (2007). Late gadolinium enhancement-cardiovascular magnetic resonance as a predictor of response to cardiac resynchronization therapy in patients with ischaemic cardiomyopathy. *EP Eur.* 9 (11), 1031–1037. doi:10.1093/EUROPACE/EUM133

Chen, X., Ye, Y., Wang, Z., Jin, Q., Qiu, Z., Wang, J., et al. (2022). Cardiac resynchronization therapy via left bundle branch pacing vs. optimized biventricular pacing with adaptive algorithm in heart failure with left bundle branch block: A prospective, multi-centre, observational study. *Europace* 24 (5), 807–816. doi:10.1093/EUROPACE/EUAB249

Chun, K. H., Oh, J., Yu, H. T., Lee, C. J., Kim, T. H., Uhm, J. S., et al. (2020). The role of sacubitril/valsartan in the management of cardiac resynchronization therapy non-responders: A retrospective analysis. *Esc. Heart Fail* 7 (6), 4404–4407. doi:10.1002/EHF2.12988

Derval, N., Steendijk, P., Gula, L. J., Deplagne, A., Laborderie, J., Sacher, F., et al. (2010). Optimizing hemodynamics in heart failure patients by systematic screening of left ventricular pacing sites: The lateral left ventricular wall and the coronary sinus are rarely the best sites. *J. Am. Coll. Cardiol.* 55 (6), 566–575. doi:10.1016/J.JACC.2009.08.045

Duckett, S. G., Ginks, M., Shetty, A. K., Bostock, J., Gill, J. S., Hamid, S., et al. (2011). Invasive acute hemodynamic response to guide left ventricular lead implantation predicts chronic remodeling in patients undergoing cardiac resynchronization therapy. *J. Am. Coll. Cardiol.* 58 (11), 1128–1136. doi:10.1016/J.JACC.2011.04.042

Echt, D. S., Moore, D., Cowan, M., Valli, V. E., Whitehair, J. G., and Willis, N. P. (2010). Chronic implantation of leadless pacing electrodes in the left ventricle of a goat model. *Heart rhythm.* 7, S451–S452.

Ellenbogen, K. A., Gold, M. R., Meyer, T. E., Fernndez Lozano, I., Mittal, S., Waggoner, A. D., et al. (2010). Primary results from the SmartDelay determined AV optimization: A comparison to other AV delay methods used in cardiac resynchronization therapy (SMART-AV) trial: A randomized trial comparing empirical, echocardiography-guided, and algorithmic atrioventricular delay programming in cardiac resynchronization therapy. *Circulation* 122 (25), 2660–2668. doi:10.1161/CIRCULATIONAHA.110.992552

Elliott, M. K., Jacon, P., Sidhu, B. S., Smith, L. J., Mehta, V. S., Gould, J., et al. (2021). Technical feasibility of leadless left bundle branch area pacing for cardiac resynchronization: A case series. *Eur. Heart J. Case Rep.* 5 (11), ytab379. doi:10.1093/EHJCR/YTAB379

Elliott, M. K., Mehta, V., Wijesuriya, N., Sidhu, B. S., Gould, J., Niederer, S., et al. (2022). Multi-lead pacing for cardiac resynchronization therapy in heart failure: A meta-analysis of randomized controlled trials. *Eur. Heart J. Open* 2 (2), oeac013. doi:10.1093/EHJOPEN/OEAC013

Elliott, M. K., Vergara, P., Wijesuriya, N., Mehta, V. S., Bosco, P., Jacon, P., et al. (2022). Feasibility of leadless left ventricular septal pacing with the WiSE-CRT system to target the left bundle branch area: A porcine model and multicenter patient experience. *Heart rhythm.* 19, 1974–1983. Published online August 5. doi:10.1016/J.HRTHM.2022.07.017

Gamble, J. H. P., Herring, N., Ginks, M., Rajappan, K., Bashir, Y., and Betts, T. R. (2016). Procedural success of left ventricular lead placement for cardiac resynchronization therapy: A meta-analysis. *JACC Clin. Electrophysiol.* 2 (1), 69–77. doi:10.1016/J.JACEP.2015.08.009

Giaimo, V. L., Zappulla, P., Cirasa, A., Tempio, D., Sanfilippo, M., Rapisarda, G., et al. (2018). Long-term clinical and echocardiographic outcomes of Mitraclip therapy in patients nonresponders to cardiac resynchronization. *Pacing Clin. Electrophysiol.* 41 (1), 65–72. doi:10.1111/PACE.13241

Ginks, M. R., Shetty, A. K., Lambiase, P. D., Duckett, S. G., Bostock, J., Peacock, J. L., et al. (2012). Benefits of endocardial and multisite pacing are dependent on the type of left ventricular electric activation pattern and presence of ischemic heart disease: Insights from electroanatomic mapping. *Circ. Arrhythm. Electrophysiol.* 5 (5), 889–897. doi:10.1161/CIRCEP.111.967505

Glikson, M., Nielsen, J. C., Kronborg, M. B., Michowitz, Y., Auricchio, A., Barbash, I. M., et al. (2021). 2021 ESC Guidelines on cardiac pacing and cardiac resynchronization therapy. *Eur. Heart J.* 42 (35), 3427–3520. doi:10.1093/eurheartj/ehab364

Gould, J., Claridge, S., Jackson, T., Sieniewicz, B. J., Sidhu, B. S., Porter, B., et al. (2022). Standard care vs. TRIVEntricular pacing in heart failure (STRIVE HF): A prospective multicentre randomized controlled trial of triventricular pacing vs. conventional biventricular pacing in patients with heart failure and intermediate QRS left bundle branch block. *EP Eur.* 24 (5), 796–806. doi:10.1093/EUROPACE/EUAB267

Heckman, L. I. B., Kuiper, M., Anselme, F., Ziglio, F., Shan, N., Jung, M., et al. (2020). Evaluating multisite pacing strategies in cardiac resynchronization therapy in the preclinical setting. *Heart Rhythm O2* 1 (2), 111–119. doi:10.1016/J.HROO.2020.03.003

Huang, W., Chen, X., Su, L., Wu, S., Xia, X., and Vijayaraman, P. (2019). A beginner's guide to permanent left bundle branch pacing. *Heart rhythm.* 16 (12), 1791–1796. doi:10.1016/J.HRTHM.2019.06.016

Jansen, A. H. M., Bracke, F. A., van Dantzig, J. M., Meijer, A., van der Voort, P. H., Aarnoudse, W., et al. (2006). Correlation of echo-Doppler optimization of atrioventricular delay in cardiac resynchronization therapy with invasive hemodynamics in patients with heart failure secondary to ischemic or idiopathic dilated cardiomyopathy. *Am. J. Cardiol.* 97 (4), 552–557. doi:10.1016/J.AMJCARD.2005.08.076

Jastrzębski, M., Moskal, P., Huybrechts, W., Curila, K., Sreekumar, P., Rademakers, L. M., et al. (2022). Left bundle branch–optimized cardiac resynchronization therapy (LOT-CRT): Results from an international LBBAP collaborative study group. *Heart rhythm.* 19 (1), 13–21. doi:10.1016/J.HRTHM.2021.07.057

Leclercq, C., Curnis, A., Delnoy, P. P., Rinaldi, C. A., Sperzel, J., Lee, K., et al. (2019). Cardiac resynchronization therapy non-responder to responder conversion rate in the more response to cardiac resynchronization therapy with MultiPoint pacing (MORE-CRT MPP) study: Results from phase I. *Eur. Heart J.* 40 (35), 2979–2987. doi:10.1093/EURHEARTJ/EHZ109

Lee, J. U., Kim, K. S., Kim, J. H., Lim, H. K., Lee, B. H., and Lee, C. K. (1995). PR interval behavior during exercise stress test. *Korean J. Intern Med.* 10 (2), 137–142. doi:10.3904/KJIM.1995.10.2.137

Leyva, F., Foley, P. W. X., Chalil, S., Ratib, K., Smith, R. E. A., Prinzen, F., et al. (2011). Cardiac resynchronization therapy guided by late gadolinium-enhancement cardiovascular magnetic resonance. *J. Cardiovasc. Magnetic Reson.* 13 (1), 29–9. doi:10.1186/1532-429X-13-29

Lustgarten, D. L., Sharma, P. S., and Vijayaraman, P. (2019). Troubleshooting and programming considerations for His bundle pacing. *Heart rhythm.* 16 (5), 654–662. doi:10.1016/J.HRTHM.2019.02.031

McAlister, F. A., Ezekowitz, J., Hooton, N., Vandermeer, B., Spooner, C., Dryden, D. M., et al. (2007). Cardiac resynchronization therapy for patients with left ventricular systolic dysfunction: A systematic review. *JAMA* 297 (22), 2502–2514. doi:10.1001/jama.297.22.2502

Mehta, V. S., Elliott, M. K., Sidhu, B. S., Gould, J., Porter, B., Niederer, S., et al. (2021). Multipoint pacing for cardiac resynchronisation therapy in patients with heart failure: A systematic review and meta-analysis. *J. Cardiovasc Electrophysiol.* 32 (9), 2577–2589. doi:10.1111/JCE.15199

Mendonca Costa, C., Neic, A., Kerfoot, E., Porter, B., Sieniewicz, B., Gould, J., et al. (2019). Pacing in proximity to scar during cardiac resynchronization therapy increases local dispersion of repolarization and susceptibility to ventricular arrhythmogenesis. *Heart rhythm.* 16 (10), 1475–1483. doi:10.1016/J.HRTHM.2019.03.027

Morgan, J. M., Biffi, M., Geller, L., Leclercq, C., Ruffa, F., Tung, S., et al. (2016). ALternate site cardiac ResYNChronization (ALSYNC): A prospective and multicentre study of left ventricular endocardial pacing for cardiac resynchronization therapy. *Eur. Heart J.* 37 (27), 2118–2127. doi:10.1093/EURHEARTJ/EHV723

Naqvi, T. Z., Rafique, A. M., and Peter, C. T. (2006). Echo-driven V-V optimization determines clinical improvement in non responders to cardiac resynchronization treatment. *Cardiovasc Ultrasound* 4, 39. doi:10.1186/1476-7120-4-39

Okabe, T., Hummel, J. D., Bank, A. J., Niazi, I. K., McGrew, F. A., Kindsvater, S., et al. (2022). Leadless left ventricular stimulation with WiSE-CRT System – initial experience and results from phase I of SOLVE-CRT Study (nonrandomized, roll-in phase). *Heart rhythm.* 19 (1), 22–29. doi:10.1016/j.hrthm.2021.06.1195

Padala, S. K., and Ellenbogen, K. A. (2020). Left bundle branch pacing is the best approach to physiological pacing. *Heart Rhythm o2.* 1 (1), 59–67. doi:10.1016/J.HROO.2020.03.002/ATTACHMENT/2874B128-4D77-4217-B818-E7D7D6E38D33/MMC4

Padeletti, L., Pieragnoli, P., Ricciardi, G., Innocenti, L., Checchi, L., Padeletti, M., et al. (2016). Simultaneous his bundle and left ventricular pacing for optimal cardiac resynchronization therapy delivery: Acute hemodynamic assessment by pressure-volume loops. *Circ. Arrhythm. Electrophysiol.* 9 (5), e003793. doi:10.1161/CIRCEP.115.003793

Padeletti, L., Pieragnoli, P., Ricciardi, G., Perrotta, L., Grifoni, G., Porciani, M. C., et al. (2012). Acute hemodynamic effect of left ventricular endocardial pacing in cardiac resynchronization therapy: Assessment by pressure-volume loops. *Circ. Arrhythm. Electrophysiol.* 5 (3), 460–467. doi:10.1161/CIRCEP.111.970277

Performance reports | medtronic CRHF product performance eSource. 2022, Available at: https://wwwp.medtronic.com/productperformance/past-reports.html. Accessed June 16, 2022.

Picard, M. H., Park, M. Y., Altman, R. K., Kumar, P., Parks, K. A., Heist, K. E., et al. (2012). Characteristics of responders to cardiac resynchronization therapy: The impact of echocardiographic left ventricular volume. *Wiley Online Libr.* 35 (12), 777–780. doi:10.1002/clc.22043

Ploux, S., Strik, M., van Hunnik, A., van Middendorp, L., Kuiper, M., and Prinzen, F. W. (2014). Acute electrical and hemodynamic effects of multisite left ventricular pacing for cardiac resynchronization therapy in the dyssynchronous canine heart. *Heart rhythm.* 11 (1), 119–125. doi:10.1016/J.HRTHM.2013.10.018

Reddy, V. Y., Miller, M. A., Neuzil, P., Sogaard, P., Butter, C., Seifert, M., et al. (2017). Cardiac resynchronization therapy with wireless left ventricular endocardial pacing the SELECT-LV study. *J. Am. Coll. Cardiol.* 69 (17), 2119–2129. doi:10.1016/j.jacc.2017.02.059

Saba, S., Nair, D., Ellis, C. R., Ciuffo, A., Cox, M., Gupta, N., et al. (2022). Usefulness of multisite ventricular pacing in nonresponders to cardiac resynchronization therapy. *Am. J. Cardiol.* 164, 86–92. doi:10.1016/J.AMJCARD.2021.10.027

Sepši, M., Křivan, L., Kozá, K. M., Sebo, M., Poloczek, M., Jarkovsky, J., et al. (2013). Optimization of cardiac resynchronization therapy in non-responders. *Cor Vasa* 55 (4), e293–e300. doi:10.1016/J.CRVASA.2013.07.002

Sharma, P. S., Naperkowski, A., Bauch, T. D., Chan, J. Y. S., Arnold, A. D., Whinnett, Z. I., et al. (2018). Permanent his bundle pacing for cardiac resynchronization therapy in patients with heart failure and right bundle branch block. *Circ. Arrhythm. Electrophysiol.* 11 (9), e006613. doi:10.1161/CIRCEP.118.006613

Shetty, A. K., Sohal, M., Chen, Z., Ginks, M. R., Bostock, J., Amraoui, S., et al. (2014). A comparison of left ventricular endocardial, multisite, and multipolar epicardial cardiac resynchronization: An acute haemodynamic and electroanatomical study. *Europace* 16 (6), 873–879. doi:10.1093/europace/eut420

Sidhu, B. S., Porter, B., Gould, J., Sieniewicz, B., Elliott, M., Mehta, V., et al. (2020). Leadless left ventricular endocardial pacing in nonresponders to conventional cardiac resynchronization therapy. *Pacing Clin. Electrophysiol.* 43 (9), 966–973. doi:10.1111/PACE.13926

Sieniewicz, B. J., Betts, T. R., James, S., Turley, A., Butter, C., Seifert, M., et al. (2020). Real-world experience of leadless left ventricular endocardial cardiac resynchronization therapy: A multicenter international registry of the WiSE-CRT pacing system. *Heart rhythm.* 17 (8), 1291–1297. doi:10.1016/j.hrthm.2020.03.002

Sieniewicz, B. J., Gould, J., Porter, B., Sidhu, B. S., Behar, J. M., Claridge, S., et al. (2018). Optimal site selection and image fusion guidance technology to facilitate cardiac resynchronization therapy. *Expert Rev. Med. Devices* 15 (8), 555–570. doi:10.1080/17434440.2018.1502084

Sieniewicz, B. J., Gould, J., Porter, B., Sidhu, B. S., Teall, T., Webb, J., et al. (2019). Understanding non-response to cardiac resynchronisation therapy: Common problems and potential solutions. *Heart Fail Rev.* 24 (1), 41–54. doi:10.1007/s10741-018-9734-8

Singh, J. P., Walsh, M. N., Kubo, S. H., Auricchio, A., Delnoy, P. P., Gold, M. R., et al. (2021). Modified design of stimulation of the left ventricular endocardium for cardiac resynchronization therapy in nonresponders, previously untreatable and high-risk upgrade patients (SOLVE-CRT) trial. *Am. Heart J.* 235, 158–162. doi:10.1016/J.AHJ.2021.02.008

Sohal, M., Hamid, S., Perego, G., Della Bella, P., Adhya, S., Paisey, J., et al. (2021). A multicenter prospective randomized controlled trial of cardiac resynchronization therapy guided by invasive dP/dt. *Heart Rhythm O2* 2 (1), 19–27. doi:10.1016/J.HROO.2021.01.005

Sohal, M., Shetty, A., Niederer, S., Chen, Z., Jackson, T., Sammut, E., et al. (2014). Delayed trans-septal activation results in comparable hemodynamic effect of left ventricular and biventricular endocardial pacing insights from electroanatomical mapping. *Circ. Arrhythm. Electrophysiol.* 7 (2), 251–258. doi:10.1161/CIRCEP.113.001152

Sohal, M., Shetty, A., Niederer, S., Lee, A., Chen, Z., Jackson, T., et al. (2015). Mechanistic insights into the benefits of multisite pacing in cardiac resynchronization therapy: The importance of electrical substrate and rate of left ventricular activation. *Heart rhythm.* 12 (12), 2449–2457. doi:10.1016/J.HRTHM.2015.07.012

Strocchi, M., Lee, A. W. C., Neic, A., Bouyssier, J., Gillette, K., Plank, G., et al. (2020). His-bundle and left bundle pacing with optimized atrioventricular delay achieve superior electrical synchrony over endocardial and epicardial pacing in left bundle branch block patients. *Heart rhythm.* 17 (11), 1922–1929. doi:10.1016/J.HRTHM.2020.06.028

Toding Labi, D. N., Rampengan, P. S., and D Kandou dr, R. (2022). Comparison between his-bundle pacing and biventricular pacing as cardiac resynchronization therapy for heart failure patients: A systematic review and meta-analysis. *EP Eur.* 24. doi:10.1093/EUROPACE/EUAC053.479

Upadhyay, G. A., Cherian, T., Shatz, D. Y., Beaser, A. D., Aziz, Z., Ozcan, C., et al. (2019). Intracardiac delineation of septal conduction in left bundle-branch block patterns: Mechanistic evidence of left intrahisian block circumvented by his bundle pacing. *Circulation* 139 (16), 1876–1888. doi:10.1161/CIRCULATIONAHA.118.038648

Upadhyay, G. A., Vijayaraman, P., Nayak, H. M., Verma, N., Dandamudi, G., Sharma, P. S., et al. (2019). On-treatment comparison between corrective his bundle pacing and biventricular pacing for cardiac resynchronization: A secondary analysis of the his-SYNC pilot trial. *Heart rhythm.* 16 (12), 1797–1807. doi:10.1016/J.HRTHM.2019.05.009

van Gelder, B. M., Nathoe, R., and Bracke, F. A. (2016). Haemodynamic evaluation of alternative left ventricular endocardial pacing sites in clinical non-responders to cardiac resynchronisation therapy. *Neth. Heart J.* 24 (1), 85–92. doi:10.1007/s12471-015-0773-7

Vijayaraman, P., Herweg, B., Ellenbogen, K. A., and Gajek, J. (2019). His-Optimized cardiac resynchronization therapy to maximize electrical resynchronization: A feasibility study. *Circ. Arrhythm. Electrophysiol.* 12 (2), e006934. doi:10.1161/CIRCEP.118.006934

Vijayaraman, P., Herweg, B., Verma, A., Sharma, P. S., Batul, S. A., Ponnusamy, S. S., et al. (2022). Rescue left bundle branch area pacing in coronary venous lead failure or nonresponse to biventricular pacing: Results from International LBBAP Collaborative Study Group. *Heart rhythm.* 19 (8), 1272–1280. doi:10.1016/J.HRTHM.2022.04.024

Vijayaraman, P., Naperkowski, A., Subzposh, F. A., Abdelrahman, M., Sharma, P. S., Oren, J. W., et al. (2018). Permanent His-bundle pacing: Long-term lead performance and clinical outcomes. *Heart rhythm.* 15 (5), 696–702. doi:10.1016/J.HRTHM.2017.12.022

Vijayaraman, P., Zalavadia, D., Haseeb, A., Dye, C., Madan, N., Skeete, J. R., et al. (2022). Clinical outcomes of conduction system pacing compared to biventricular pacing in patients requiring cardiac resynchronization therapy. *Heart rhythm.* 19 (8), 1263–1271. doi:10.1016/j.hrthm.2022.04.023

Wijesuriya, N., Elliott, M. K., Mehta, V., Behar, J. M., Niederer, S., Wilkoff, B. L., et al. (2022). Transvenous lead extraction in conduction system pacing. *Front. Physiol.* 13, 993604. doi:10.3389/FPHYS.2022.993604

Wijesuriya, N., Elliott, M. K., Mehta, V., Sidhu, B. S., Behar, J. M., Niederer, S., et al. (2022). Leadless left ventricular endocardial pacing for cardiac resynchronization therapy: A systematic review and meta-analysis. *Heart rhythm.* 0 (0), 1176–1183. doi:10.1016/J.HRTHM.2022.02.018

Wijesuriya, N., Elliott, M. K., Mehta, V., Sidhu, B. S., Strocchi, M., Behar, J. M., et al. (2022). Leadless left bundle branch area pacing in cardiac resynchronisation therapy: Advances, challenges and future directions. *Front. Physiol.* 0, 898866. doi:10.3389/FPHYS.2022.898866

Wong, J. A., Yee, R., Stirrat, J., Scholl, D., Krahn, A. D., Gula, L. J., et al. (2013). Influence of pacing site characteristics on response to cardiac resynchronization therapy. *Circ. Cardiovasc Imaging* 6 (4), 542–550. doi:10.1161/CIRCIMAGING.111.000146

Wouters, P. C., Vernooy, K., Cramer, M. J., Prinzen, F. W., and Meine, M. (2021). Optimizing lead placement for pacing in dyssynchronous heart failure: The patient in the lead. *Heart rhythm.* 18 (6), 1024–1032. doi:10.1016/J.HRTHM.2021.02.011

Young, J. B., Abraham, W. T., Smith, A. L., Leon, A. R., Lieberman, R., Wilkoff, B., et al. (2003). Combined cardiac resynchronization and implantable cardioversion defibrillation in advanced chronic heart failure: The MIRACLE ICD trial. *JAMA* 289 (20), 2685–2694. doi:10.1001/jama.289.20.2685

Zanon, F., Abdelrahman, M., Marcantoni, L., Naperkowski, A., Subzposh, F. A., Pastore, G., et al. (2019). Long term performance and safety of his bundle pacing: A multicenter experience. *J. Cardiovasc Electrophysiol.* 30 (9), 1594–1601. doi:10.1111/JCE.14063

Zhang, W., Huang, J., Qi, Y., Wang, F., Guo, L., Shi, X., et al. (2019). Cardiac resynchronization therapy by left bundle branch area pacing in patients with heart failure and left bundle branch block. *Heart rhythm.* 16 (12), 1783–1790. doi:10.1016/J.HRTHM.2019.09.006

Frontiers in Physiology

Understanding how an organism's components work together to maintain a healthy state

The second most-cited physiology journal, promoting a multidisciplinary approach to the physiology of living systems - from the subcellular and molecular domains to the intact organism and its interaction with the environment.

Discover the latest Research Topics

See more →

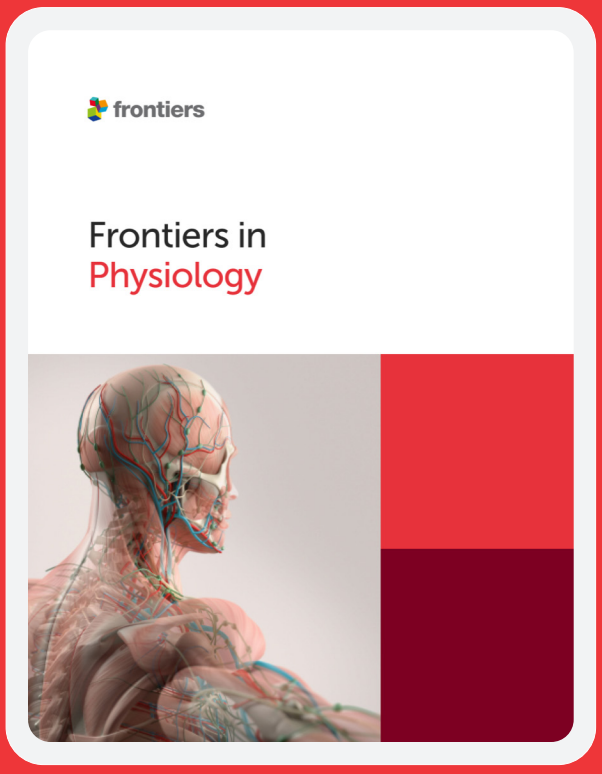

Frontiers

Avenue du Tribunal-Fédéral 34
1005 Lausanne, Switzerland
frontiersin.org

Contact us

+41 (0)21 510 17 00
frontiersin.org/about/contact